The Laboratory for Terrestrial Physics

2002 Annual Report

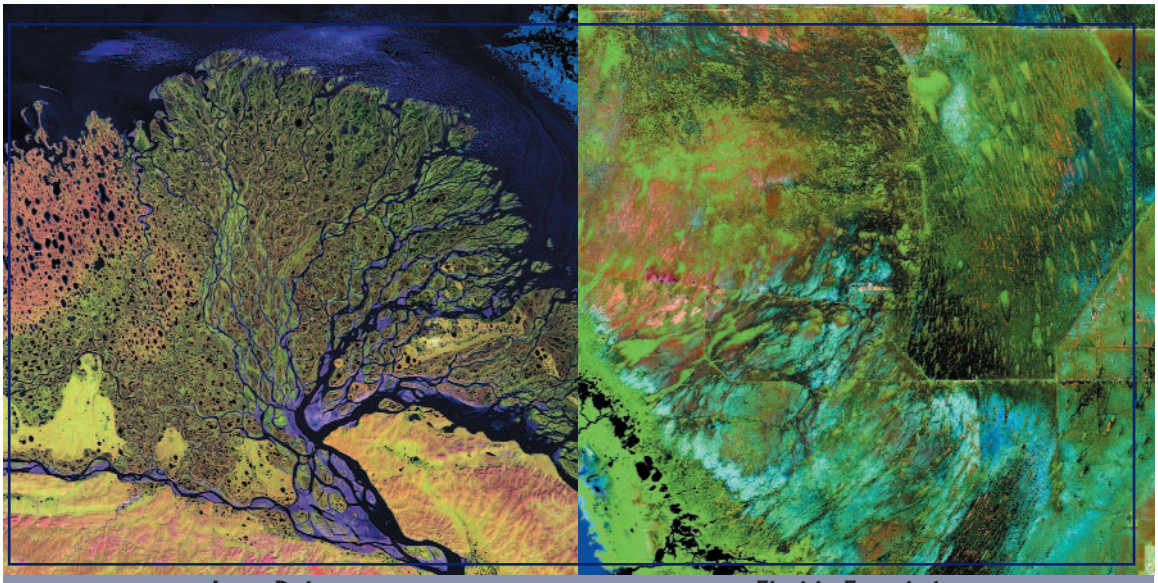

Lena Delta | Florida Everglades

Celebrating 30 Years of Continuous Landsat Global Coverage!

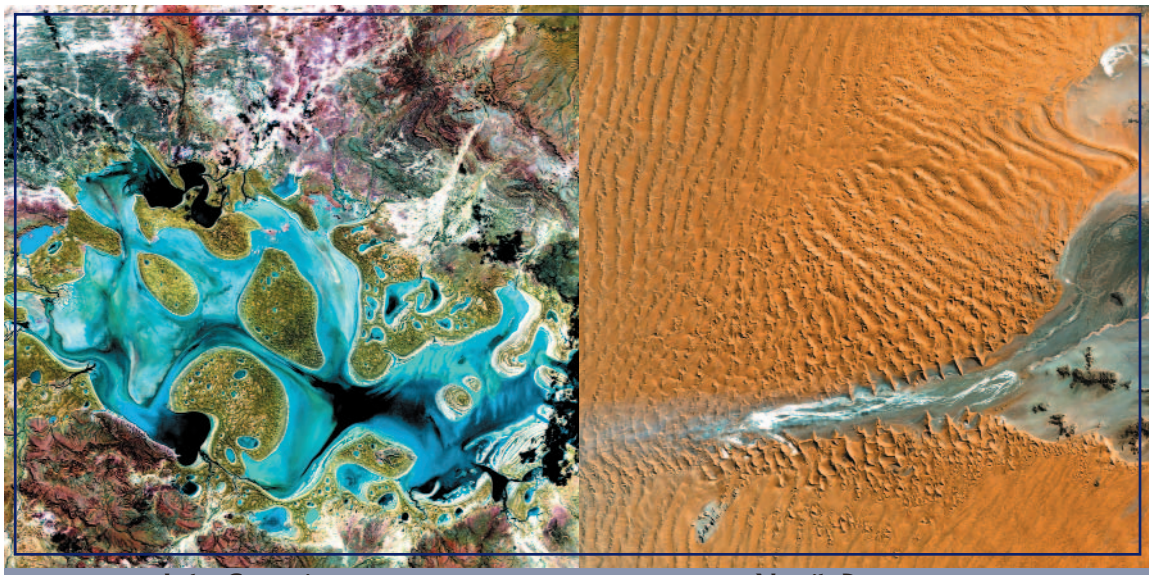

Lake Carnegie | Namib Desert

NASA Goddard Space Flight Center
Greenbelt, MD 20771

Laboratory for Terrestrial Physics
NASA Goddard Space Flight Center

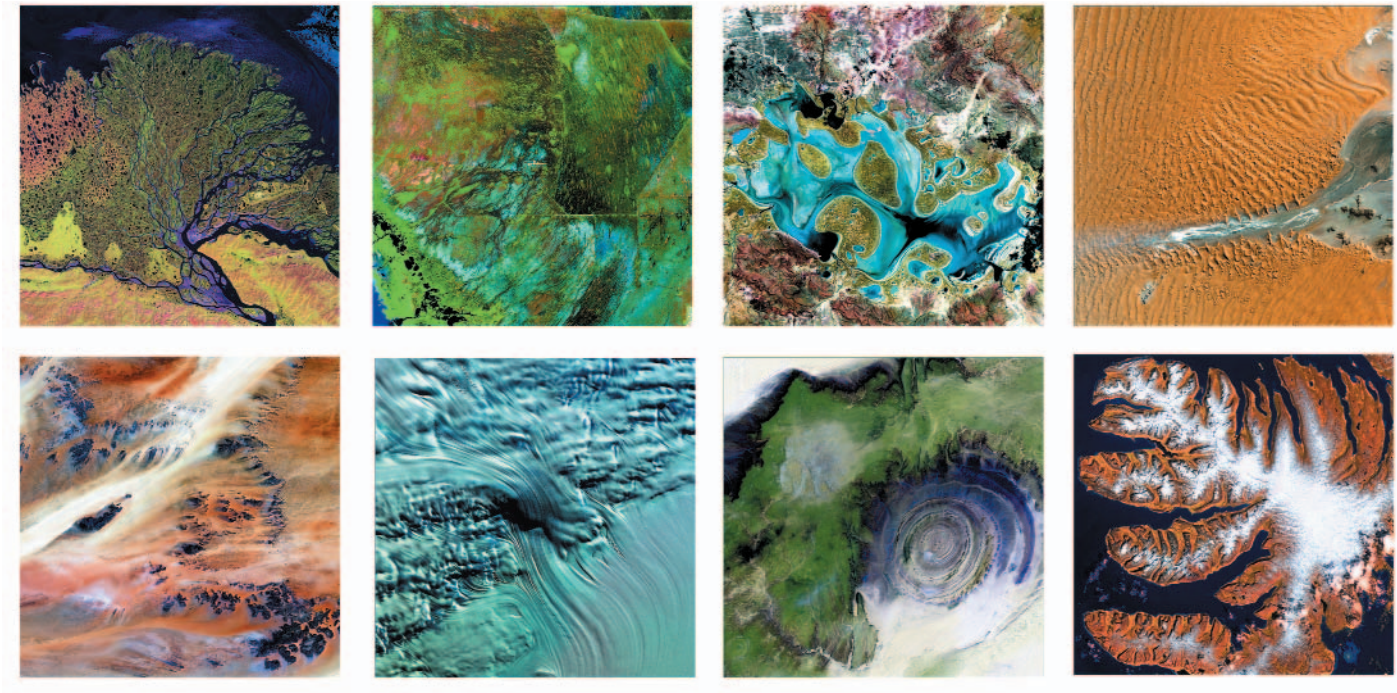

The cover of the Laboratory for Terrestrial Physics 2002 Annual Report honors the 30th Anniversary of Landsat! See the next page for a description of the proud role that LTP scientists have played in the history of Landsat!

The images on the front and back covers of this Report are a part of the Landsat-7: Earth as Art exhibit. This exhibit concept was initiated by the USGS EROS Data Center to commemorate the 30th anniversary of the Landsat program. It consists of approximately 40 images of different areas of the world - from deserts to lakes, from man-made features to natural ones, from ice and snow to cloud features. Various combinations of the Landsat 7 spectral bands were selected to create the vivid RGB (and often false color) composites. The images were selected on the basis of aesthetic appeal, and use the visceral avenue of art to convey the thrilling perspective of the Earth that Landsat provides to the viewer.

Members of the Laboratory for Terrestrial Physics worked with the USGS to reproduce and distribute the exhibit to high visibility areas. During 2002, the Earth as Art exhibit was on display at NASA Headquarters, the Library of Congress in Washington, DC, and at several other venues throughout the country. An on-line exhibit of the images can be viewed at http://landsat.gsfc.nasa.gov/earthasart/

All 8 cover images are shown above:

Top (L-R): The Lena Delta in Russia, the Florida Everglades in the United States, Lake Carnegie in Western Australia, and the Namib Desert in Namibia, Africa.

Bottom (L-R): The Terkezi Oasis in Chad, Africa, Lambert Glacier in Antarctia, the Richat Structure in Mauritania, Africa, and the West Fjords in Iceland.

The Lab for Terrestrial Physics Role in Landsat History

The Laboratory for Terrestrial Physics (LTP) has made significant contributions to the success of the Landsat Program, particularly in the area of ensuring the scientific integrity of the various missions. In the mid 1970s, Dr. Louis Walter, the Code 920 Division Chief at that time, was the Study Scientist leading the development of the specifications for the new Thematic Mapper instrument to improve upon the early successes realized with the original Multispectral Scanner instrument. Dr. Vincent Salomonson followed Dr. Walter as both the next 920 Lab Chief and as the Landsat Project Scientist overseeing the development of the Landsat 4 and 5 missions in the late 1970s and early 1980s. Drs. John Barker and Darrel Williams of the Biospheric Sciences Branch (BSB) supported Dr. Salomonson as Associate and Assistant Project Scientists, respectively. With the return of Landsat oversight to NASA in 1992, Dr. Williams, Head of the BSB at that time, was appointed Project Scientist for Landsat 7, with Dr. James Irons of the BSB serving as Deputy Project Scientist and Dr. Barker once again serving as Associate. Mr. Brian Markham of the BSB has substantially contributed to the calibration of the Landsat instruments and has served as the Calibration Scientist for Landsat 7. Dr. Irons is continuing the LTP and BSB tradition by serving as the Project Scientist for the next generation Landsat mission, known as the Landsat Data Continuity Mission or LDCM.

Contained In This Report...

Introduction 1

Biospheric Sciences 5

Geodynamics and Space Geodesy 65

Laser Remote Sensing & Technology 111

Education/Public Outreach 155

Appendices 163

Table of Contents

Table of Contents i

Introduction 1

Our Mission and Place within NASA 2

Organizational Structure 3

Staff 3

Biospheric Sciences 5

Biospheric Sciences Research 6

AERosol RObotic NETwork (AERONET) *6*

Carbon Cycle *8*

Interannual Variability in the Terrestrial Carbon Cycle 8

Measuring Human Impacts on Biodiversity and Carrying Capacity of Ecosystems 11

Forest Characterization *15*

Siberian Forest Cover and Disturbance 15

Forest Dynamics in Northeastern China 15

Siberian Forest Leaf Area Index 16

Tropical Forest Structure with Lidar 16

Delaware Forests Inventory Using an Airborne Laser 16

Verification and Evaluation of SRTM Data 17

BRDF Model Inversion Using Neural Networks 18

Radar-Lidar Fusion 19

Southern Africa Burned Area Mapping 19

Health Initiatives *21*

Pediatric Asthma Study 21

Satellite Remote Sensing of Ebola River Hemorrhagic Fever Outbreaks 22

Field and Airborne Research Experiments 25

The Vegetation Fluorescence Project 25

EOS Land Validation Core Sites and CEOS Land Product Validation 26

Flight Experiment for Carbon Sequestration Studies: Using Combined VHF SAR & Lidar for Biomass Measurement 30

An Inexpensive, Portable Airborne Laser System For Forest Mensuration 32

Biomass Measurements from Lidar Mapping 33

Data Processing 34

Global Data Processing for MODIS 34

MODIS Rapid Response System 35

Ozone Monitoring Instrument Science Investigator's Processing System 38

Satellite Programs 40

Flight Programs 40

Landsat and the Land Cover Satellite Project Science Office 40

The Earth Observing One (EO-1) Base Mission 43

EOS Terra Mission 46

Planned Programs 47

Landsat Data Continuity Mission (LDCM) 47

NPOESS Preparatory Project (NPP) 48

International Programs 50

The Large Scale Biosphere-Atmosphere Experiment in Amazonia (LBA) 50

The Northern Eurasia Earth Science Partnership Initiative (NEESPI) 52

Refereed Journal Publications 54

Proceedings Papers, NASA Technical Documents, etc. 59

Geodynamics and Space Geodesy 65

Geomagnetism 66

Understanding Geomagnetic Field Variation with Numerical Modeling 66

Comprehensive Field Modeling Paper Published 67

American Geophysical Union (AGU) Virtual Session Held 68

SWARM Constellation Selected by ESA 69

Four Attend Ørsted International Science Team Meeting 70

Magnetic Study of Rocks in the Kola and Krivoy Rog Deep Boreholes 71

Narrow-Scale Flow at Top of Earth's Core 71

Magsat, Ørsted and CHAMP Data Compared 72

Precise Orbit Determination, Gravity Field, and Terrestrial Reference Frame 74

Precision Orbit Determination Activities within The Space Geodesy Branch 74

Detection of a Large Scale Mass Redistribution in the Terrestrial System since 1998, and an Assessment of the Potential Causes. 77

Earth Geopotential Solutions from CHAMP Satellite Data 79

The NASA Geodetic/Astrometric VLBI Program 81

International VLBI Service (IVS) 83

Crustal Dynamics Data Information System (CDDIS) 84

Improved Mapping Functions for Atmospheric Corrections in Satellite Laser Ranging 85

Absolute Earth Scale from SLR Measurements 87

Kinematic GPS Activity within the Laboratory for Terrestrial Physics 89

Global Geophysical Fluids 90

Application of Core Dynamics Modeling to Geodetic Studies 90

Precise Atmospheric Loading Estimates for New Space Gravity Missions. 91

Crustal Deformation 92

Earth Anelasticity from Satellite Tracking and Altimetry 92

Invited Review Summary of South Central Alaska Crustal Deformation 93

Topography and Surface Change 95

Puget Sound Lidar Studies 95

Quantifying Plains Volcanism on the Eastern Snake River Plains and Mars 96

Planetary Geology and Geophysics 99

Buried Basins on Mars 99

Recent Studies of Mars Magnetic Anomalies 101

Atmospheric Rotational Effects on Mars Based on the NASA Ames General Circulation Model 101

Orbital-Rotational-Climatic Interaction 104

Orbital Noise and Climate Fluctuation 104

A Spin-Up for Asteroid 951 Gaspra 105

Refereed Journal Publications: 107

Conference Proceedings Papers: 109

Laser Remote Sensing and Technology 111

Spaceborne Lidars 111

Geoscience Laser Altimeter System (GLAS) on the ICESat Mission 111

Laser Pointing Angle Measurement for the Geoscience Laser Altimeter 115

GLAS Main Bench Checkout Equipment 117

Mercury Laser Altimeter (MLA) 118

The Mars Orbiter Laser Altimeter (MOLA) - Radiometry 119

Airborne and Ground Based Lidars 121

Laser Vegetation Imaging Sensor (LVIS) - Airborne Imaging Laser Altimetry 121

Airborne Multikilohertz Microlaser Altimeter (Microaltimeter) 122

Spectral Ratio Biospheric Lidar 123

Automatic Weather Station (AWS) Lidar 124

Laser Technology R&D 127

Vegetation Canopy Lidar: VCL Laser Transmitter Development 127

Diode Based Single Frequency 1064 nm Laser for Seeding High Power Nd:YAG Lasers 131

One Micron Testbed Program: Laser Risk Reduction 132

Fiber Amplifier Power Scaling/Frequency Doubling Effort 136

Laser Sounder Technique for Remotely Measuring Atmospheric CO2 Concentrations 137

Spaceborne Imaging Laser Altimetry Mission Concept and Technology Development 138

Investigation of Bose-Einstein Condensates for Advanced Gravity Gradiometer Designs 139

Satellite Laser Ranging 140

NASA Satellite Laser Ranging (SLR) Network 140

International Laser Ranging Service 141

SLR2000 Autonomous Satellite Laser Ranging Station 144

Calibration 145

EOS Calibration 145

Diffuser Calibration Facility (DCaF) 147

Calibration Facility 150

Refereed Journal Publications: 153

Proceedings Papers, NASA Technical Reports, etc. 153

Education/Public Outreach 155

The Global Learning and Observation to Benefit the Environment Program (GLOBE) 155

Baltimore Student Sun Photometer Network (BSSN) 157

The IMAGERS (Interactive Multimedia Adventures for Grade School Education Using Remote Sensing) Program 157

Earth as Art 159

Earth as History 160

MOLA: Models of Earth and Mars Topography for Classroom Use 161

Classroom Activity Development 163

Website Development 164

Other Projects 164

Acknowledgements 165

Appendices (Acronyms, Grants and Contracts) 166

Introduction

Thank you for taking the time to acquaint yourself with the Laboratory for Terrestrial Physics and our accomplishments for 2002!

The Laboratory advances NASA programs through the exploration of Earth and planetary solid-body physics. These explorations involve the physics and dynamics of the Earth, as well as of the planets and their satellites. The Lab's innovative and exciting programs study the global properties of the solid Earth, global and regional scale vegetation monitoring, biosphere-atmosphere interactions, and laser remote sensing.

The Laboratory's Biospheric Sciences program encompasses a broad range of basic and applied research to study terrestrial ecosystems and their interactions with the atmosphere using multi-scale remote sensing, modeling, and advanced analytical techniques. Experiments and investigations utilizing new techniques and capabilities enhance our understanding of global processes for Earth System Science.

The Laboratory's "geophysical and geodynamic" studies span a wide range of subjects in the research of both the Earth and solid planetary bodies, especially Mars. Present-day measurements using both surface and satellite data, models derived from these, and other observational and theoretical information, are used to help improve our understanding of the evolution of the core, mantle and crust, and their interactions with surface topography.

The Laboratory's laser measurement research studies new techniques based on analysis and tests with airborne and spaceborne instruments. Accordingly, this area links the scientific requirements to define, design, build, and demonstrate instruments for Earth and planetary remote-sensing science programs. The laser research itself is focused on improving the understanding of electro-optical sensor physics, and the propagation environment. Additional technological skills are employed in the development of advance techniques for defining subsystem performance through the development and engineering of flight instruments, and the calibration and characterization of these instruments in realistic environments.

The Laboratory's information processing research focuses on developing reliable, low-cost computing systems for the production, distribution, and analysis of regional and global data sets. The Laboratory's information technology improves the security and reliability of the computing environment.

Ultimately, our activities result in the advance of scientific knowledge. To this point, the Laboratory relies on its key personnel - its scientists and researchers - to report their results in conferences, symposia, and publications. Interaction with the national and international scientific community is essential, and integrally a part of our Laboratory's efforts.

This comprehensive report includes our philosophy, an overview of our dedicated staff, and descriptions of our projects, with synopses of the Laboratory's achievements and accomplishments for 2002. This report encompasses the Laboratory's dedication to human resources, their scientific interactions, and outreach activities with the outside community.

Please take some time to peruse this report, and contact me or my staff if you have any questions, concerns, or comments.

Sincerely,

David E. Smith
Chief, Laboratory for Terrestrial Physics

Our Mission and Place within NASA

Mission: The Laboratory for Terrestrial Physics is dedicated to the advancement of knowledge in Earth and planetary science, by conducting innovative research using space technology.

The Laboratory's mission and activities support the work and new initiatives at NASA's Goddard Space Flight Center (GSFC). The Laboratory's success contributes to the Earth Science Directorate as a national resource for studies of Earth from Space. The Laboratory is part of the Earth Science Directorate based at the GSFC in Greenbelt, MD. The Directorate itself is comprised of the Global Change Data Center (GCDC), the Space Data and Computing Division (SDCD), and four science Laboratories, including Laboratory for Terrestrial Physics, Laboratory for Atmospheres, and Laboratory for Hydrospheric Processes all in Greenbelt, MD. The fourth research organization, Goddard Institute for Space Studies (GISS), is in New York, NY.

Relevant to NASA's Strategic Plan, the Laboratory ensures that all work undertaken and completed is within the vision of GSFC. The philosophy of the Laboratory is to balance the completion of near term goals, while building on the Laboratory's achievements as a foundation for the scientific challenges in the future.

For your convenience, we have published this report on the Internet at the following link: http://ltpwww.gsfc.nasa.gov/

Organizational Structure

The Laboratory for Terrestrial Physics is one of 3 scientific divisions within the Earth Sciences Directorate, sharing research with the Laboratory for Hydrospheric Processes and Laboratory for Atmospheres, and the Goddard Institute for Space Studies.

Staff

The Laboratory hosts 72 civil servants (67 full-time permanent), and 243 supporting contractors, which are on site or near site. University grants and cooperative agreements draw 37 additional scientists and technologists. There are 3 additional employees from other government agencies who are long-term residents within the Laboratory. The average age of a Laboratory civil servant is 50, and the average age of all professionals is 51. Ages range from 26 (secretary) or 33 (researcher) to 76. For the civil servants within the Laboratory, the average length of government service is over 20 years; a majority of those have spent their entire time within the Laboratory. This may be taken as an indicator that the Laboratory is a "good place to work."

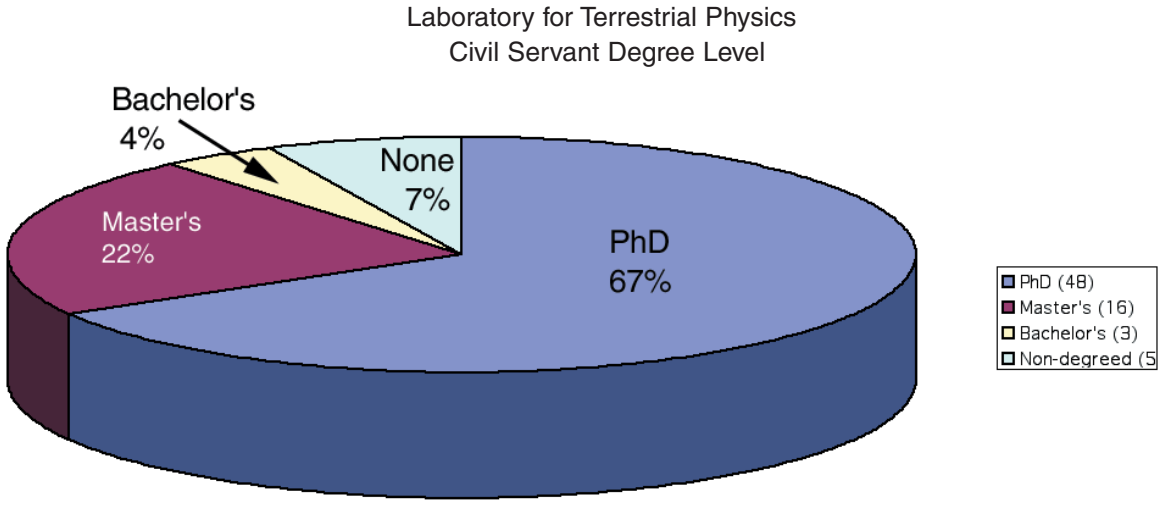

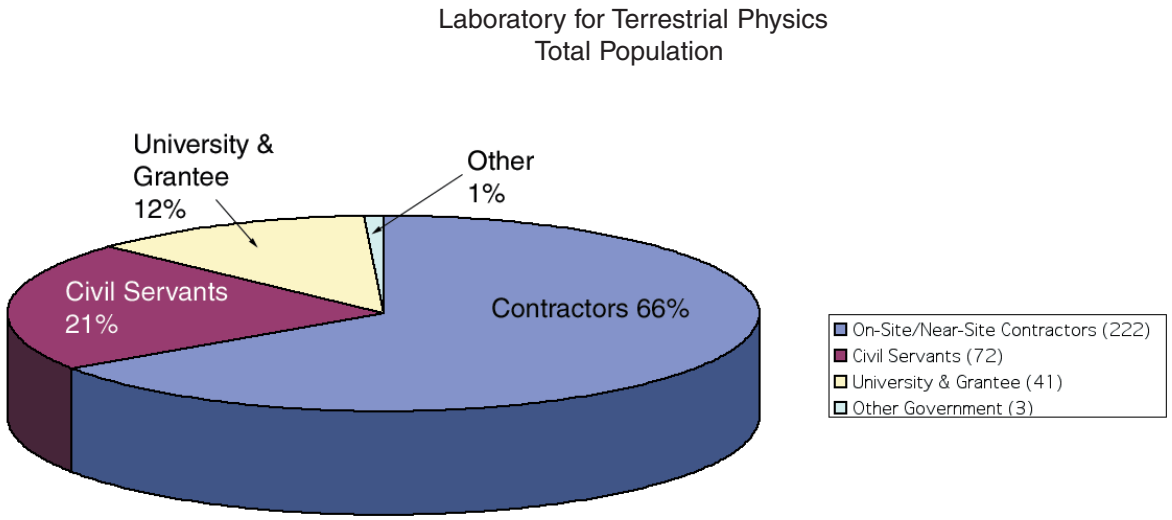

Organizational Structure

There are many different professional skills represented within the Laboratory. As a gross summary, there are 20 researchers in geo/planetary physics and dynamics; 19 in biospheric sciences; 9 in laser physics and development; and 7 each in instrument science and information science. Additionally, there are 10 employees who devote the majority of their time to administrative tasks, from project science to office administration.

Laboratory for Terrestrial Physics
Specializations

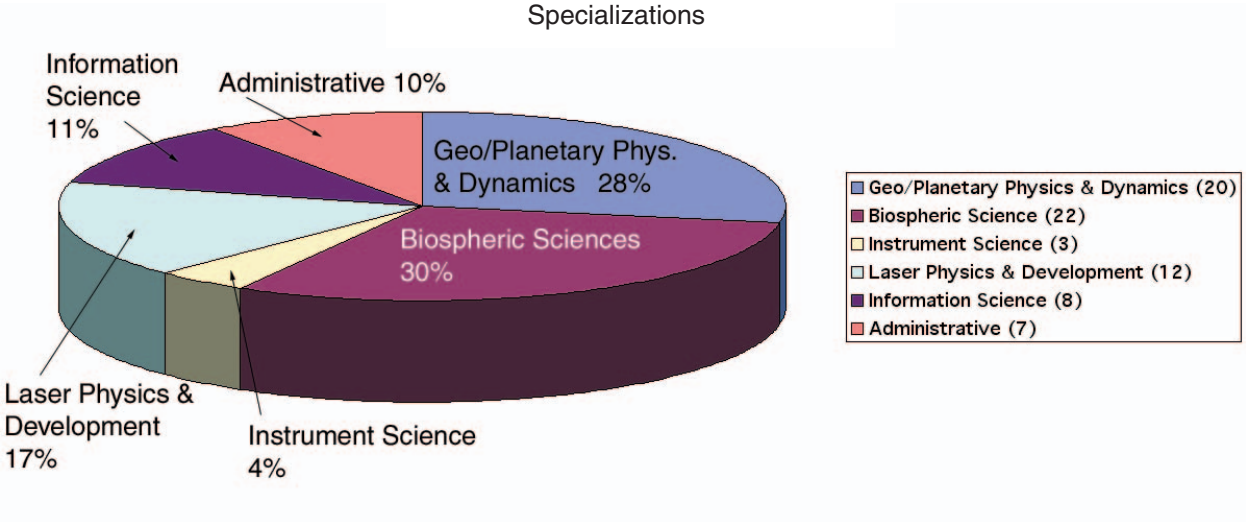

The Laboratory is composed of 5 branches, 2 offices, 4 staff scientists, and a large number of cooperating institutions. Particularly notable in the latter category are MIT, University of Maryland at College Park, University of Maryland Baltimore Campus; Scripps Institute of Oceanography (one Laboratory employee is permanently located there), the U.S. Geological Survey, and International Laser Ranging and Very Long Baseline Interferometer services. Branches range in size from 7 to 20 employees; offices from 3 to 5.

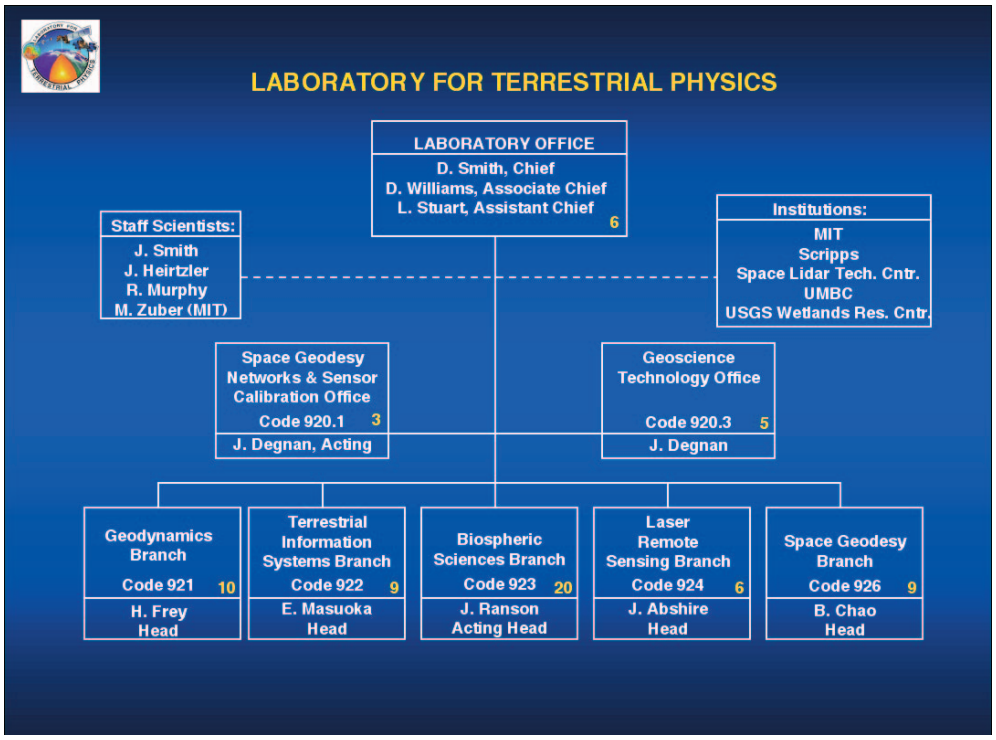

Biospheric Sciences

Biospheric Sciences, within the Laboratory for Terrestrial Physics, encompasses a broad range of basic and applied research to study terrestrial ecosystems and their interactions with the atmosphere using multi-scale remote sensing, modeling, and advanced analytical techniques. Experiments and investigations of a scientific nature utilizing Earth observations, new techniques and capabilities enhance our understanding of global processes for Earth System Science. For additional information see http://ltpwww.gsfc.nasa.gov/bsb/Home.html. Specifically, our Biospheric Sciences effort:

(1) Utilizes ground, aircraft, and satellite remote sensing instruments to measure variables that describe the temporal and spatial dynamics of natural ecosystems as well as human impacts on these systems, especially the vegetation condition (e.g., land cover, height, biomass, photo-synthetic capacity), soils (e.g., soil condition and type), and links to atmospheric constituents (e.g., aerosols, CO_2);

(2) Develops mathematical models which predict land surface conditions and processes related to rates of vegetation, soil, and atmosphere exchanges (e.g., radiation, heat, water, greenhouse gases, net primary productivity) as functions of remotely-sensed and ground-based observations;

(3) Acquires, produces, and distributes comprehensive, integrated land data sets incorporating ground, airborne, and/or satellite observations to facilitate model development and validation;

(4) Ensures the scientific integrity of new Earth remote sensing systems to improve space-based Earth observations by conducting calibration and validation studies and by serving as project managers and project and instrument scientists; and

(5) Performs basic research, which leads to the definition and development of new technologies, sensors, and missions to advance state-of-the art capabilities for monitoring global changes.

Through the above activities the Laboratory assesses and predicts environmental changes due to natural and anthropogenic processes at local to global scales to improve our understanding of global dynamics and processes occurring on the land, in the oceans, and in the lower atmosphere. Past studies include assessment of deforestation, desertification, land use, land cover, vegetation anomalies, primary productivity, famine early warning, biomass burning, ecologically-influenced pests and diseases, and the extent and impact of urbanization. In this report the Biospheric Sciences projects are organized under four sub-categories: **Research, Data Processing, Satellite Programs, and International Programs.**

Biospheric Sciences Research

The primary responsibility of the Biospheric Sciences discipline is to facilitate the use of remote sensing to measure, monitor and understand the ecology of the Earth through research into remote sensing techniques.

AERosol RObotic NETwork (AERONET)

Goddard's ground-based AERosol RObotic NETwork (AERONET) program provides measurements of column integrated aerosol optical, microphysical and radiative properties. The original program was developed from the requirement to remove aerosol effects on remotely sensed imagery of the surface. Over the past decade, the need shifted to validation of satellite retrievals of aerosol optical thickness and more recently aerosol characterization due to the advanced retrievals of climate sensitive particle size and absorption characteristics (single scattering albedo). The decadal growth to almost 150 permanent sites distributed on every continent and a variety of island sites provides a unique opportunity to characterize aerosol properties on several scales. Summarized below is a regional investigation of biomass burning aerosol as measured by AEROENT during the southern African biomass burning season of 2000, followed by the first global assessment of the climatically important single scattering albedo using the widely distributed AERONET sites over years of observations (Dubovik, et al., 2002).

Measurements of the column-integrated aerosol optical properties in the southern African region were made by AERONET sun-sky radiometers at several sites in August-September 2000 as a part of the SAFARI 2000 dry season field campaign. Fine mode biomass burning aerosols dominated in the northern part of the study region (Zambia), which is an active burning region. Other aerosols including fossil fuel burning, industrial, and aeolian coarse mode types also contributed the aerosol mixture in other regions (South Africa and Mozambique), which were not as strongly dominated by local burning. The large amount of smoke produced in the north lead to a north-south gradient in aerosol optical depth (τ_a) in September, with biomass burning aerosol concentrations reduced by dispersion and deposition during transport. Large average diurnal variations of τ_a(typical diurnal range of 25%) were observed at all sites in Zambia as a result of large diurnal trends in fire counts in that region that peak in mid-afternoon. However, for all sites located downwind to the south, there was relatively little (~5-10%) average diurnal trend observed as the aerosol transport is not strongly influenced by diurnal cycles. AERONET radiometer retrievals of aerosol single scattering albedo (ω_0) in Zambia showed relatively constant values as a function of τ_a, for τ_{a440} ranging from 0.4 to ~2.5. The wavelength dependence of ω_0 varied significantly over the region, with greater decreases for increasing wavelength at smoke dominated sites than for sites influenced by a significant coarse mode aerosol component. Retrievals of mid-visible ω_0 based on the fitting of Photosynthetically Active Radiation (PAR; 400-700 nm) flux measurements to modeled fluxes for smoke in Mongu, Zambia yielded an average value of 0.84. This is in close agreement with the estimated average of 0.85 derived from interpolation of the AERONET retrievals made at 440 and 675 nm, for August-September, 2000. The spectral dependence of ω_0 independently retrieved with the AERONET measurements and with diffuse fraction measurements in Mongu, Zambia was similar for both techniques, as a result of both methods retrieving the imaginary index of refraction (~0.030-0.035 on one day) with very little wavelength dependence. Constant imaginary refractive index as a function of wavelength is consistent with soot being the primary component of aerosol absorption.

Although the biomass burning aerosol optical properties measured at several sites in Zambia during August-September 2000 were relatively uniform, over the broader southern Africa region the observations suggest significant aerosol variability. The observed regional differences in aerosol single scattering albedo and size distributions, due to aerosol aging during transport and from con-

tributions by other aerosol sources (i.e. aeolian dust, fossil fuel combustion aerosols, etc.), need to be considered when assessing regional aerosol radiative forcings and retrieval of aerosol properties from satellite. Aerosol optical properties also change seasonally in some southern Africa locations and this aspect of regional aerosol dynamics is being examined in another study.

Dubovik used eight years of globally distributed data from AERONET to produce a climatology of aerosol optical properties. Using Dubovik and King's comprehensive inversion, these data resulted in the development of robust models of real undisturbed aerosol in the total atmospheric column and, for the first time, allowed quantitative differentiation of both the magnitude and spectral dependence of the absorption of aerosol in locations with varying emission sources and conditions. These reported data agree with known aerosol information in general; however they reveal several important differences for each type of aerosol.

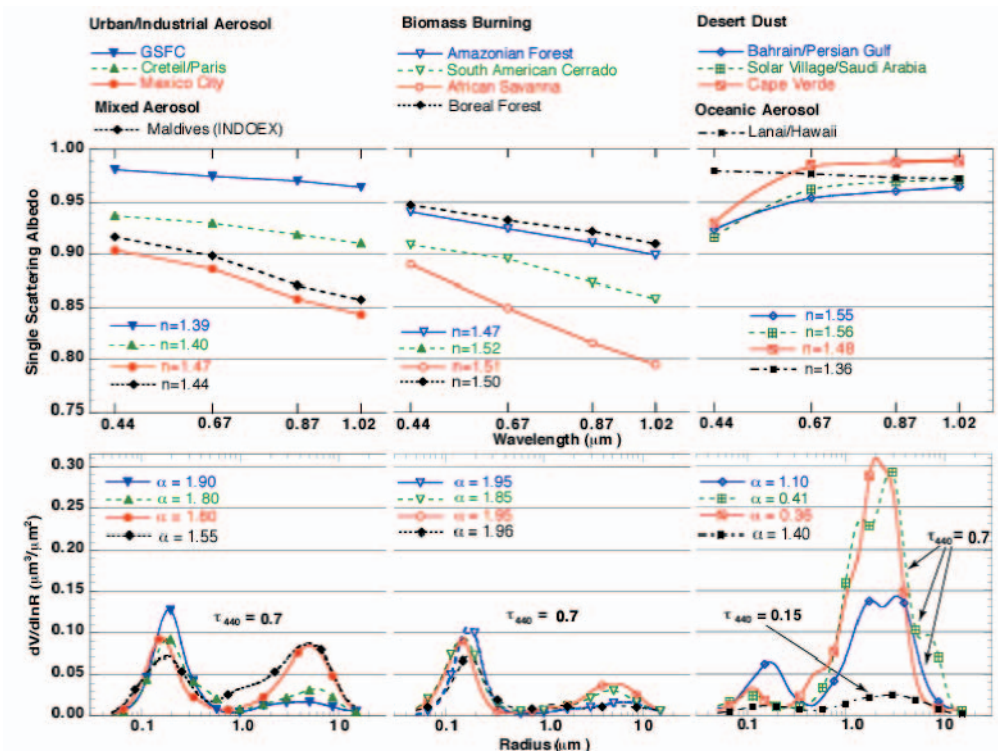

Figure 1. The averaged optical properties of different types of tropospheric aerosol retrieved from the global AERONET network of ground-based radiometers. Urban/industrial, biomass burning and desert dust aerosols are shown for $\tau_{ext}(440) = 0.7$. Oceanic aerosol is shown for $\tau_{ext}(440) = 0.15$ since oceanic background aerosol loading does not often exceed 0.15. Ångström parameter τ is estimated using optical thickness at two wavelengths, 440 and 870 nm.

For example, Dubovik et al. found that:

- In contrast to most aerosol models, and in agreement with analysis of satellite data, desert dust absorption of solar radiation is weak for wavelengths greater than 550 nm (ω_0 ~ 0.96 – 0.99). However dust exhibits a pronounced absorption in the blue spectral range ($\omega_0(440)$ ~ 0.92 – 0.93).

- Smoke absorption is related to the vegetation type burned and relative contribution of the flaming and smoldering combustion phases. Boreal and Amazonian forest fire smoke absorbs distinctly less ($\omega_0(440)$ ~ 0.94) than grassland dominated smoke from African savanna ($\omega_0(440)$ ~ 0.88) and mixed source smoke at South American cerrado sites ($\omega_0(440)$ ~ 0.91).

- Absorption for urban/industrial aerosol varies from almost no absorption ($\omega_0(440) \sim 0.98$) at GSFC (East Coast of U.S.) to significant absorption in places with high level of industrial pollution: $\omega_0(440) \sim 0.90$ in Mexico City and $\omega_0(440) \sim 0.89$ for near the Indian subcontinent. Aerosol over Paris shows an intermediate level of absorption ($\omega_0(440) \sim 0.93 – 0.94$).

References:

Dubovik, O., B.N. Holben, T.F. Eck, A. Smirnov, Y.J. Kaufman, M.D, King, D. Tanre, and I. Slutsker, Variability of absorption and optical properties of key aerosol types observed in worldwide locations, J. Atm. Sci., 59, 590-608, 2002

Eck, T.F., B.N. Holben, D.E. Ward, M.M. Mukelabai, O. Dubovik, A. Smirnov, J.S. Schafer, N.C. Hsu, S.J. Piketh, A. Queface, J. Le Roux, R.J. Swap and I. Slutsker, Variability of biomass burning aerosol optical characteristics in southern Africa during the SAFARI 2000 dry season campaign and a comparison of single scattering albedo estimates from radiometric measurements, J. Geophys. Res., accepted, 2003.

Contact: Brent Holben, Brent.N.Holben@nasa.gov

Carbon Cycle

Interannual Variability in the Terrestrial Carbon Cycle

Measurements of the concentration of CO_2 in the atmosphere show that fossil fuel burning is causing CO_2 to increase and also that significant CO_2 sinks (anthropogenic input exceeds observed atmospheric increases) exist which vary in magnitude from year to year. Given the scale of these changes in the composition of the atmosphere and the potential effects on climate the international science community has focused much attention on improving the understanding of the processes responsible for carbon sources and sinks (Intergovernmental Panel on Climate Change, 2001, Chapter 3).

On average about half of the CO_2 emitted to the atmosphere through fossil fuel burning and deforestation each year remains in the atmosphere. The oceans and land surfaces absorb the rest but large uncertainties exist as to the mechanisms responsible for this net sink. This sink varies from year to year between 0 to nearly all of the emitted CO_2. The relative contributions of ocean versus land processes can be disentangled using atmospheric $^{13}C/^{12}C$ measurements in conjunction with CO_2 measurements. This is because the important CO_2 exchange process on land is C_3 photosynthesis which discriminates strongly against $^{13}CO_2$ while air-sea CO_2 exchange is controlled by physical processes that produce less discrimination. Results from recent studies using this technique show that the land surface is responsible for about half the total sink and may be responsible for most of the interannual variability in the atmospheric CO_2 growth rate. However, the estimated magnitude of the land sink is sensitive to a number of assumptions, such as, 1) the contribution of C_4 plants to terrestrial production and 2) covariance in the response of plant productivity and $^{13}CO_2$ discrimination to drought.

In a collaborative effort between scientists from California Institute of Technology and Carnegie Institution of Washington, aspects of the interpretation of the atmospheric isotopic composition were addressed. In addition, this effort explored the role of fire in determining interannual variability in the atmospheric CO_2 growth rate.

Contributions of C_4 photosynthesis to terrestrial primary productivity and atmospheric $\delta^{13}C$

The global distribution of the fractional coverage of C_4 plants can be predicted from satellite derived vegetation classification maps, crop inventory data bases and models of climate controls on photosynthesis (Figure 2). C_4 plants naturally occur and are largely restricted to tropical and subtropical regions though C_4 crops such as corn are grown in more temperate climates. C_4 photosynthesis is almost completely restricted to herbaceous forms of vegetation and therefore, is less prominent in closed canopy forests such as tropical rain forests. Using the map and productivity models, it is estimated that C_4 photosynthesis is about1/3 of annual global C_3 photosynthesis. By including the impact of C_4 photosynthesis on the atmospheric $\delta^{13}C$, the estimated terrestrial carbon sink inferred from atmospheric measurements is 60% larger than if photosynthesis is neglected (Still et al., 2003). Longer term climate driven changes in the distribution of C_4 relative to C_3 plants will likely influence atmospheric $\delta^{13}C$.

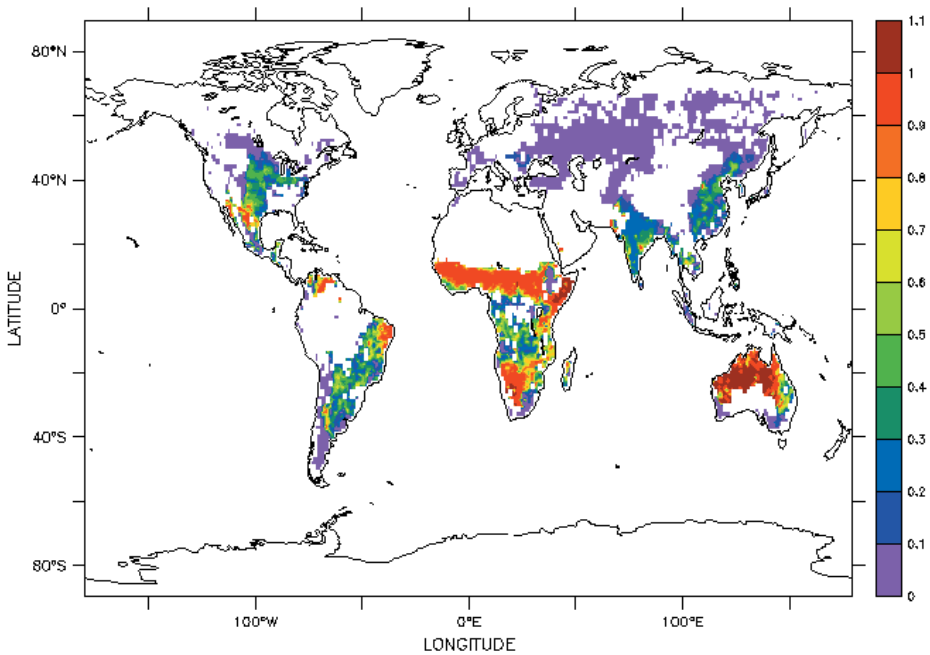

Figure 2. Map of the fraction of vegetation in each pixel that possesses the C_4 pathway.

Impacts of Drought on Estimating Land Sinks from Atmospheric $\delta^{13}C$

The strong discrimination by C_3 plants (the dominant type globally) against $^{13}CO_2$ produces a measurable signal in atmospheric $\delta^{13}C$ that is used to estimate the terrestrial contribution to the observed variations in atmosphere CO_2 concentrations. C_3 discrimination by individual plants has been shown to vary, however, in response to atmospheric humidity and drought. Global drought episodes associated with the ENSO cycle might be expected to affect inferences about the size of terrestrial carbon sink that are based on atmospheric $\delta^{13}C$ and CO_2 concentration measurements. Ecophysiological and biogeochemical models were used to estimate the magnitude of the impact of climate variability on inferred carbon sinks (see Randerson et al., 2002 on Refereed Publication list). Small changes in discrimination caused by drought were found to have a large impact on inferred terrestrial sinks because the decrease in discrimination caused by drought is associated with decreases in gross primary production. The results imply that previous analyses that ignored this effect overestimated interannual variability in global carbon sinks (Figure 3).

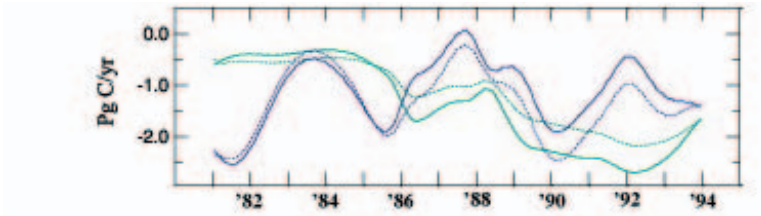

Figure 3. Interannual variability in the atmospheric carbon flux anomalies associated with the land and the ocean (negative denotes sink). Net fluxes from the land to the atmosphere are indicated in blue and from the ocean in green. Solid lines are for simulations in which the drought impacts are ignored and dotted lines for drought impacts included.

Fire

Analysis of the interannual variability in the rate at which global atmospheric CO_2 is increasing shows intriguing correlations with ENSO cycles. During El Nino phases the growth rate is larger than intervening periods. Other analyses indicate that this variability is largely a result of carbon fluxes associated with land processes. The explanations for these phenomena have for the most part focused on the impacts of climate on the balance between photosynthesis and respiration on land. For instance, the drier, warmer conditions in the tropics during El Nino causes inhibition of photosynthesis and/or stimulation of respiration producing a net sink anomaly at the global scale. Recently, it has been argued that much of the net land source is the result of increased wild fires associated with El Nino conditions. In particular during the strong El Nino of 1998 when the atmospheric sink was near zero large fires occurred in Indonesia and in northern boreal forests. These arguments are based on atmospheric observations and there are no published direct observations of the global distribution and magnitude of fire emissions.

Using fire counts from the VIRS instrument on board TRMM that were calibrated with burned area estimates from MODIS scenes, a time series of burned area has been constructed within the TRMM footprint (30S-38N, where 90% of global fires occur) for the period 1998 to the present. Figure 4 shows the % of area in each grid cell that burned per year averaged from 1998-2001. A biogeochemical model of biomass production and decomposition has been modified to include fire mortality and fuel consumption. Using the burned area maps as input to the model, seasonality and interannual variability in carbon emissions from fire can be predicted (van der Werf et al., 2003). Early results support the proposition that fires are largely responsible for the large increase in the growth rate of atmospheric CO_2 in 1998. Currently this analysis is being extended to the entire globe.

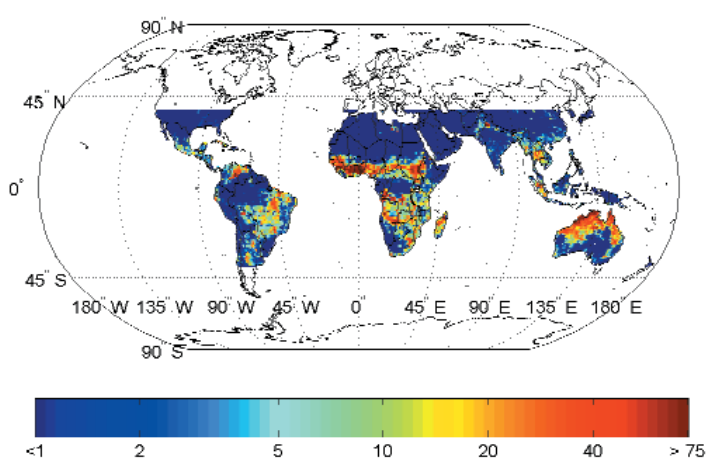

Figure 4. % of pixel area burned per year averaged for 1998-2001.

References:

Still, C. J., J. A. Berry, G. J. Collatz, and R. S. DeFries, Global distribution of C_3 and C_4 vegetation: Carbon cycle implications. Global Biogeochemical Cylces 17, 1006, doi:10.1029/2001GB001807, 2003

van der Werf, G. R., J. T. Randerson, G. J. Collatz, and L. Giglio, Carbon emissions from fires in tropical and subtropical ecosystems, Global Change Biology (accepted), 2003.

Contact: Jim Collatz, George.J.Collatz@nasa.gov

Measuring Human Impacts on Biodiversity and Carrying Capacity of Ecosystems

As we begin to recognize the scope of human influence on Earth's ecosystems, it is important to understand how specific forms of human induced land transformation affect the dynamics of Earth's biological systems. Scientists in the Biospheric Sciences Branch are working with conservation biologists from the World Wildlife Fund in a study using daytime and nighttime Earth observation data to quantify the impact of various forms of land use on biological biodiversity. This study is unique in two ways; 1) diurnal (day and night) satellite data are used, and 2) a carbon cycle approach was taken in the assessment of impact. The carbon-based approach focuses specifically on how the conversion of land to urban and other uses affects the net primary productivity (NPP) of the landscape. NPP is the amount of plant material added to the biosphere through photosynthesis and is measured in units of carbon (g C). NPP not only represents a specific amount of carbon removed from the atmosphere, it is also the primary source of food for Earth's food web supporting all heterotrophic organisms (organisms that require preformed organic compounds for food energy) including human beings.

Nighttime images of the Earth collected by the Defense Meteorological Satellite Program's Operational Linescan System (DMSP/OLS) showing a dramatic view of city lights were used to delineate urbanized areas across the globe. AVHRR data, collected during daylight hours, were used to examine the comparative health of vegetation within and around urbanized areas (Figure 5). The satellite data were then merged with an extensive biodiversity database of 76 ecoregions in the US with information on thousands of important species. Analyses were carried out focusing on: 1) the consequences of urbanization on NPP in the United States, and 2) the extent to which both urban and agricultural land use types are impinging on biologically diverse ecoregions.

Our results show that urbanization is taking place on the most fertile lands and hence has a disproportionately large overall negative impact on NPP. Urban land transformation in the US has reduced the annual NPP by 0.04 Pg C or 1.6% of its pre-urban value. The reduction is enough to offset the 1.8% gain made by the conversion of land to agricultural use, even though urbanization covers an area less than 3% of the land surface in the US and agricultural lands approach 29% of the total land area. At local and regional scales, urbanization increases NPP in resource-limited regions, and through localized warming "urban heat" contributes to the extension of the growing season in cold regions (Figure 6). In terms of biologically available energy, the loss of NPP due to urbanization of agricultural lands alone is equivalent to the caloric need of 16.5 million people annually, or about 6% of the US population (Figure 7).

a.

b.

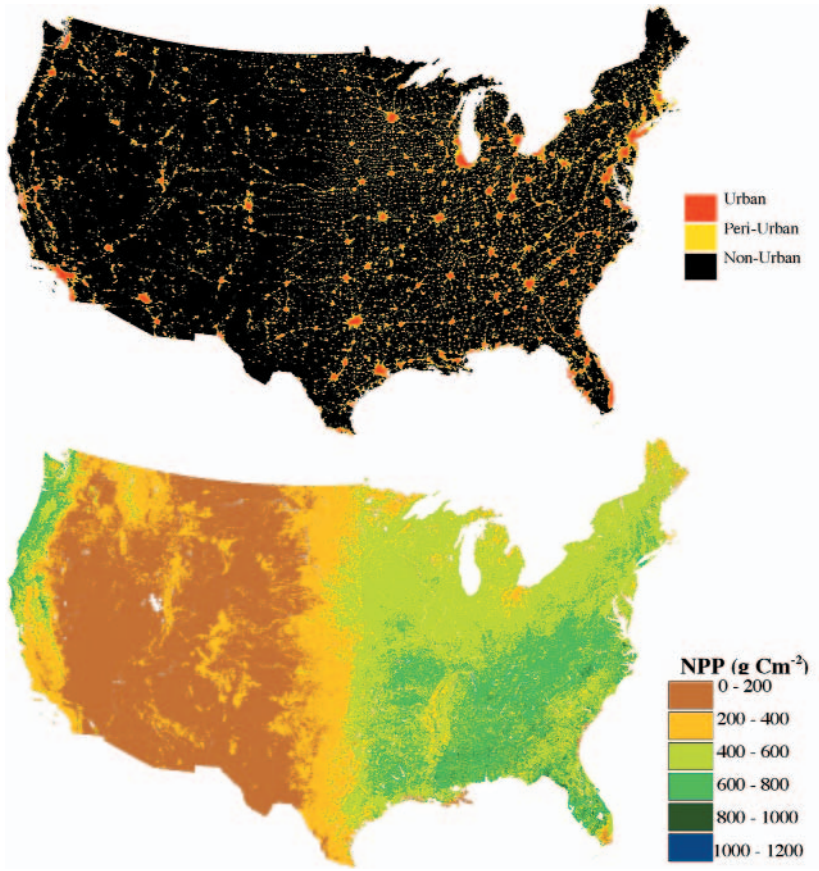

Figure 5. (a) Urbanization map generated from nighttime satellite images from the Defense Meteorological Satellite's Operational Linescan System (DMSP/OLS) collected from October 1994 to March 1995. Red (urban), Yellow (peri-urban), Black (non-urban). (b) Simulated total annual NPP for the U.S. at 1 km x 1 km horizontal resolution.

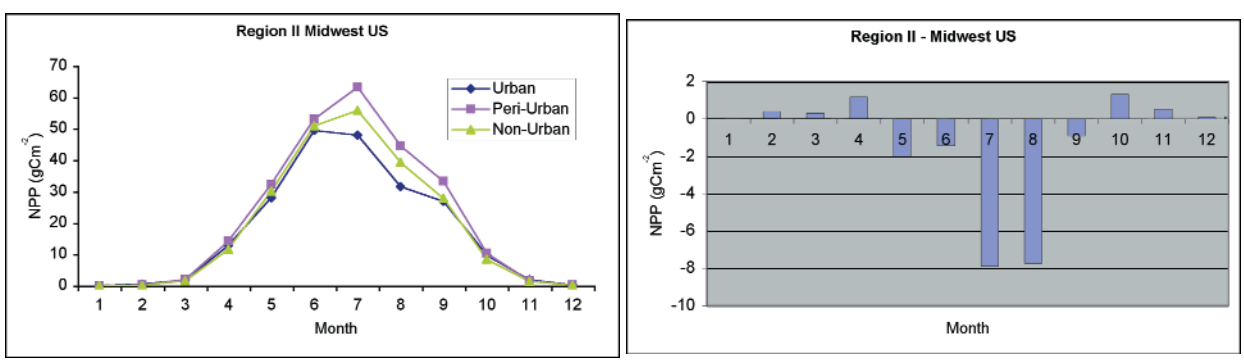

a. b.

Figure 6. Seasonal dynamics of the impact of urbanization on NPP for the Midwestern US. (a) Monthly mean NPP rates for urban (circles), peri-urban (squares), and non-urban (triangles) areas, (b) NPP difference showing the loss (negative) or gain (positive) in NPP rates (gm-2) resulting from urbanization (urban – non-urban). The growing season is extended due to urban heating but productivity is reduced overall compared to non-urbanized areas.

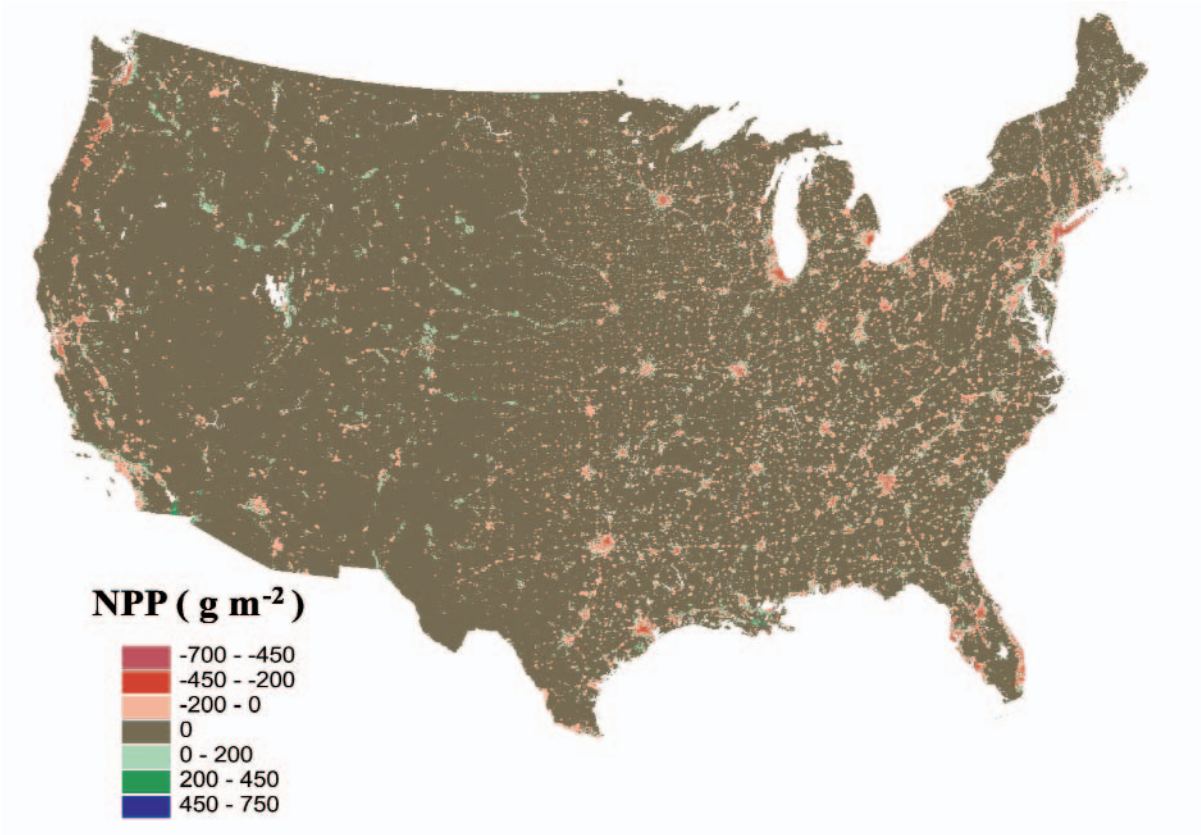

Figure 7. Difference in NPP showing the total annual reduction (negative) or gain (positive) in the rates of NPP(gm-2) (POST-urban – PRE-urban). The overall loss of NPP due to urbanization is 0.04 Pg C annually (about 1.6% of the total annual pre-urban NPP of the continental US) enough to off-set the gains in NPP realized by agriculture.

As part of this study we also combined our remotely-sensed measures of urbanization and agriculture with distributional data for eight major plant and animal taxa (comprising over 20,000 species) to assess conservation priorities among 76 terrestrial ecoregions in North America. We combined the species data into overall indices of richness and endemism and compared these indices against the percent cover of urbanization and agriculture in each ecoregion. The analyses yielded four "priority sets" of 6-16 ecoregions where high levels of biodiversity and human land use coincide. The most threatened ecoregions tend to be concentrated in the southeastern U.S., California, and, to a lesser extent, the Atlantic coast, southern Texas and the U.S. Midwest. Across all 76 ecoregions, urbanization is positively correlated to both species richness and endemism, emphasizing that human activities and biodiversity are on a collision course (Figure 8). These results indicate that conservation efforts in densely-populated areas are especially important and perhaps even more important than preserving remote parks in relatively pristine regions for safeguarding biological diversity on the North American continent.

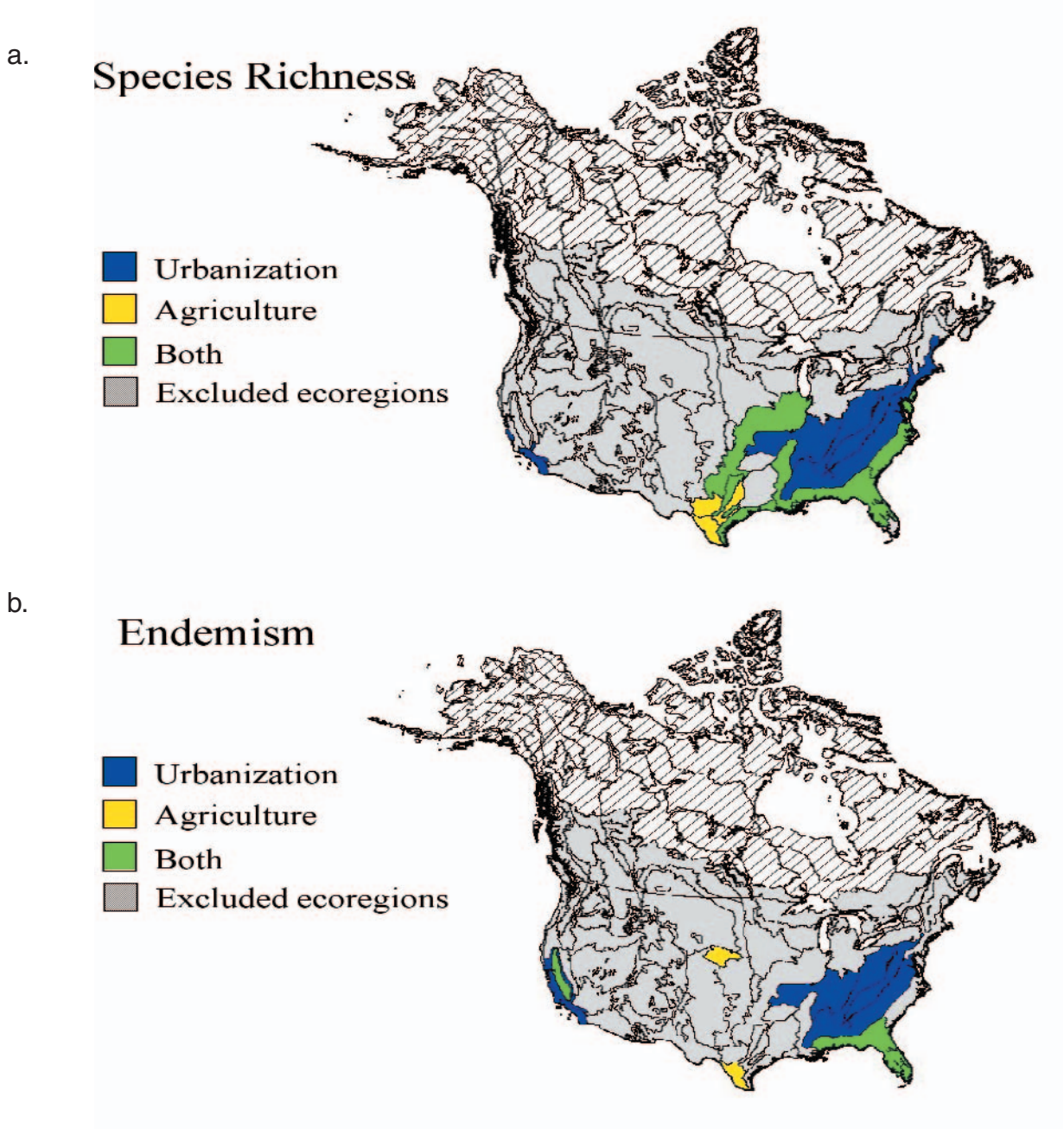

Figure 8. Maps of ecoregions in the top 66% quantile of biodiversity and land use indices. a) richness index versus urbanization, agriculture, or both. b) endemism index versus urbanization, agriculture, or both.

Contact: Marc Imhoff, Marc.L.Imhoff@nasa.gov

Forest Characterization

Forests cover approximately 30% of the Earth's land surface and are important to global energy, water and carbon cycles. In addition they provide habitat for animals, protection of soil resources and food and fiber for humans. The alteration of the forest landscape by natural and human factors results in changes in landcover, land use and forest ecosystems. It is imperative for scientists to know the location, amount and type of forests along with structure and productivity and to be able to track the changes in these attributes. Biospheric Sciences forest research covers tropical, temperate and boreal biomes and is multiscaled: from large area characterization of forests and forest change to local scale assessment of forest attributes such as biomass and leaf area. It is a goal of the Laboratory to develop and exploit new technologies that improve the ability to measure forests from space. (References to papers in this Forest Characterization subsection are given at the end of the subsection or, if published in 2002 by Laboratory staff, at the end of the Biospheric Sciences section)

Siberian Forest Cover and Disturbance

Siberian forests are an important source/sink of carbon with total carbon storage in Western Siberia estimated to be 4300 MT, and in Eastern Siberia about 12500 MT. Wildfire is the most important disturbance affecting Siberian forests. Insect invasions, logging, air pollution, and exploitation of mineral reserves are also present in significant amounts. Recent observations suggest that the taiga forests are expanding into the tundra, dark needle conifer (i.e., Siberian pine, spruce, fir) are appearing in larch dominated communities, and post-disturbance succession patterns are changing – all possible indicators of climate warming. Ground studies and remote sensing analysis are being conducted to develop techniques to identify and quantify these changes. Our recent efforts have reported on the use of coarse resolution satellite data (i.e., AVHRR) for forest characterization in central Siberia (Kharuk et al, 2003b) and have made progress toward using higher resolution optical and microwave satellite data for disturbance mapping (Ranson, et al, 2002a, 2003, Kharuk et al., 2002, 2003a). Radar backscatter modeling was used to develop a technique to compensate for the effect of terrain slopes on biomass estimation from SAR data (Sun et al. 2002a). Current work emphasizes on-ground measurements with data fusion to monitor impacts of forest disturbances using temporal and multisource satellite data (e.g., MODIS, MISR, Landsat and SAR).

Contact: Jon Ranson, Kenneth.J.Ranson@nasa.gov

Forest Dynamics in Northeastern China

Some 30% of China's forest resources are concentrated in the northeastern provinces of Liaoning, Jilin and Heilongjiang, and the northeastern part of the Inner Mongolia Autonomous Region. This area has seen tremendous change during the 20th century, ranging from widespread clearing for agriculture and timber in the early part of the century, to ambitious reforestation programs beginning in the 1970's. Terra MODIS and Landsat are being used to map the current extent of forests in Northeastern China, track the changes in forest cover during the 1990's, and initiate a GIS-based monitoring system to provide updated forest cover maps in the future. To date, new forest cover maps have been made from multi-temporal classification of MODIS NDVI data (Sun et al., 2002c). These maps agree with aggregate statistics provided by the Chinese Academy of Forestry. Landsat imagery from 1990 and 2000 were used to estimate rates of forest clearing and re-growth (Sun et al. 2002b). The results suggest that during the decade of the 1990's forest cover in Northeastern China remained roughly stable, possibly increasing by about 0.2% per year. Significant deforestation has occurred locally, however, as a result of agricultural conversion within foothills along the perimeter of the Manchurian plain.

Contact: Jeff Masek, Jeffery.G.Masek@nasa.gov

Siberian Forest Leaf Area Index

The goal of the Leaf Area Index for Fire Chronosequences in Siberian Boreal Forests study is to determine leaf area index (LAI) for four different post-fire age sites using both surface and remotely sensed data. There is a lack of data for this area of the world, and good information is needed for accurate global assessment of carbon storage potential. Field campaigns to collect surface data were conducted in 1999, 2000, and 2001, and Landsat, MODIS, and IKONOS imagery have been acquired. The past year was spent assembling, analyzing, and preparing the data for publication. LAI values for the sites roughly follow theoretical predictions. Total (and overstory) LAI values for each of the post-fire stand ages are as follows (LAI in units of m^2/m^2): 0-2 year site: 0.2-0.4 (0.0); 13 year: 1.4-3.0 (0-2.4); 25 year: 1.0-4.0 (0.8-2.8); and over 100 years: 5.5-9.1 (4.3-8.7). Variations occur due to heterogeneity across the site in both fire severity and vegetation regrowth patterns. Relationships between surface data and vegetation indices developed from satellite data are not strong which is hindering extrapolation of site values to broader scales. This work will continue in 2003.

Contact: Don Deering, Donald.W.Deering@nasa.gov

Tropical Forest Structure with Lidar

There were two important milestones in the efforts to develop global measurements of vegetation biomass from lidar published in 2002. The quality of lidar-derived estimates of aboveground biomass from La Selva Biological Station, based on data collected in 1998 using a Laboratory developed instrument, LVIS, have set a new standard for biomass remote sensing in tropical forests (Drake et al., 2002a). Simple functions of lidar waveforms explained more than 90% of the variation in field biomass data (89% in cross-validation tests). Also performed was a basic validation of vertical distributions of intercepted surfaces from lidar, showing that differences between distributions in lidar waveforms and those reconstructed from simple tree crown geometry were smaller than those characterizing land-cover type differences (e.g., primary versus secondary tropical forest) within the same data source (Drake et al., 2002b). Together with results from the temperate zone, and work in review reporting good results estimating biomass from lidar in semi-deciduous tropical forest, these findings confirm that lidar can be a vital tool for research on the global carbon budget. No other remote sensing method does as well at resolving biomass differences among very tall, dense forests.

Contact: Bob Knox, Robert.G.Knox@nasa.gov

Delaware Forests Inventory Using an Airborne Laser

Forest inventory estimates of volume and biomass and acreage estimates of various forest height-canopy cover classes were generated from a single set of airborne laser profiling data acquired during the summer of 2000. The stratum, county and statewide estimates of above-ground dry biomass may be converted directly to estimates of standing carbon. A portable, inexpensive lidar called PALS (Profiling Airborne Lidar Sensor) was used to inventory forests statewide; in addition, the systematic laser measurements were used to identify and map mature forest stands which might support the Delmarva Fox Squirrel (Sciurus niger cinereus), an endangered species previously endemic on the Eastern Shore of the Chesapeake Bay. Merchantable volume estimates were within 14% of US Forest Service estimates at the county level and within 4% statewide. Total above-ground dry biomass estimates were within 19% of USFS estimates at the county level and within 16% statewide. The laser heights and the biomass estimates derived from those measurements demonstrate the utility of an airborne laser for forest characterization and mensuration. See Figure 9.

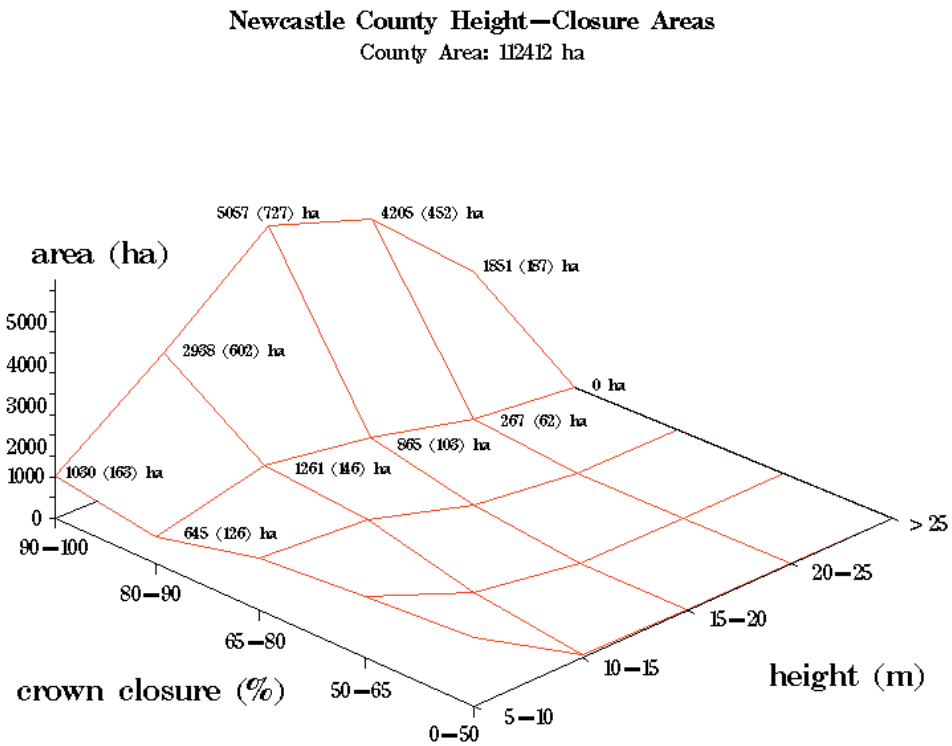

Figure 9. 3-D surface of forest height - crown cover classes in Newcastle County, Delaware. The numbers in parentheses are the associated standard errors of estimate.

Contact: Ross Nelson, Ross.F.Nelson@nasa.gov

Verification and Evaluation of SRTM Data

Efforts continued towards validating Shuttle Radar Topography Mission (SRTM) digital elevation models (DEMs). SRTM is expected to improve on existing DTED-1 DEMs (Figure 10). SRTM data has lower vertical accuracy but higher horizontal resolution and accuracy than satellite lidar data (such as Shuttle Laser Altimeter (SLA) and the recently launched Geosciences Laser Altimeter System (GLAS)), and the vertical accuracy of the SRTM data is less affected by the local slope. Cross-verification of surface height from these instruments is critical for technique advancement and applications. Field work in Russia was conducted in August 2002 by U.S. and Russian investigators. The forests near or within SLA-02 footprints were sampled for tree diameter at breast height (dbh), height and stem density along with GPS location. It was found that the land cover types and forest structures match the SLA-02 waveforms. The surface height profiles measured by SLA-02 and SRTM are highly correlated (R2 > 0.95). The surface height discrepancies between SRTM and SLA-02 are random at open areas and are correlated to tree heights (for details see Sun et al 2002d). SRTM provides improved elevation data, which will be essential for co-registration of satellite images from different platforms, and reduction of terrain effects on SAR (synthetic aperture radar) data. Figure 10 shows SRTM Digital elevation data for a portion of central Siberia. Further studies will be conducted when the GLAS data becomes available.

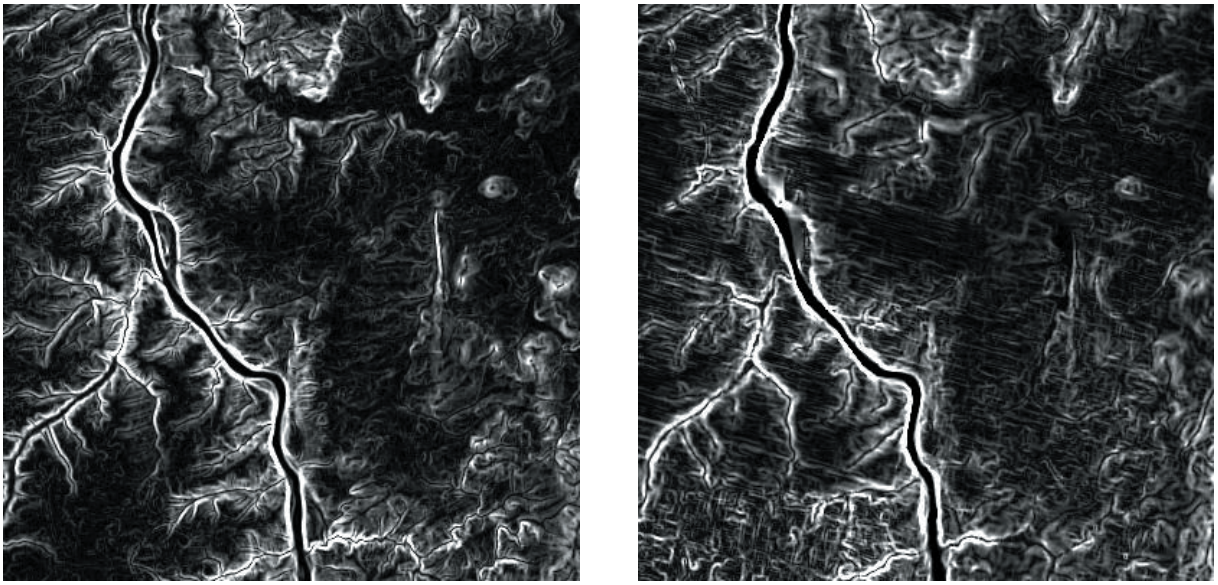

Figure 10. Local slope calculated from SRTM DEM (left) and DTED-1 DEM (right) of the Yenisei River Valley in Central Siberia. Note the greater detail in drainage basin topography of the SRTM DEM, and the noisy stripes from the DTED-1 data.

Contact: Guoqing Sun, Guoqing.Sun.1@gsfc.nasa.gov

BRDF Model Inversion Using Neural Networks

Radiative transfer models for forest canopies serve as a basis for extracting forest characteristics using directional/spectral data from satellite sensors (e.g. MODIS, MISR, POLDER, SeaWiFS). Only recently have there been significant efforts made to provide operational algorithms to invert these models. These efforts have exposed a need to significantly improve the efficiency and accuracy of traditional efforts for inverting these physically based models. In an effort to overcome the limitations of traditional inversion methods, a neural network method was designed and tested. Neural networks provide a computational structure which allows it to learn complex nonlinear relationships that cannot be envisioned by a researcher. In this study a complex 3D model (Discrete Anisotropic Radiative Transfer, DART) developed by Dr. J. Gastellu-Etchegorry and others from CESBIO, France, was inverted using POLDER-like data. The model was inverted to recover forest characteristics such as forest cover, leaf area index, and soil reflectance. The neural network method was significantly more accurate than the traditional methods. By using only a few directional view angles as opposed to only a nadir view the accuracy of recovering forest canopy characteristics was significantly improved (Kimes, et al, 2002). This neural network approach can provide an accurate, efficient, and stable inversion method for radiative transfer models using directional/spectral data from satellite-borne sensors.

Contact: Dan Kimes, Daniel.S.Kimes@nasa.gov

Radar-Lidar Fusion

Derivation of forest structure is vital for understanding forest state and change and the implications of the carbon cycle information retrieval from lidar and radar data. Radar backscatter and lidar waveform models, which are based upon a common three-dimensional forest stand structure, were parameterized using realistic forest physical stands to produce a data set of forest structural parameters and lidar/radar responses. Both radar backscatter and lidar waveform models are three-dimensional, and were parameterized using forest attributes simulated from a forest succession model, ZELIG, developed at the University of Virginia. The radar backscattering and lidar waveforms were calculated for a number of stands. This approach allows comparison of radar and lidar interaction with forest canopies and is useful for investigating the data characteristics of these active sensors and the relationships between these new data (Sun and Ranson 2002). Further studies on the definition and retrieval of potential parameters or indices from lidar waveforms will be done, so the commonality and complementarily of lidar and radar data can be better understood, and the critical structural variables driving the signature be identified.

Contact: Jon Ranson, Kenneth.J.Ranson@nasa.gov

Southern Africa Burned Area Mapping

Southern Africa is subjected to some of the most extensive biomass burning in the world. Fires occur due to both natural and anthropogenic causes, primarily lightening and land management. Information on the timing and spatial extent of fire is required to allow managers, planners, and policy makers the opportunity to understand fires in their environmental, economic, and social contexts and to formulate their responses accordingly. At regional to global scales this information is required to estimate trace gas and particulate emissions associated with natural and anthropogenic fires, important for understanding loss of biomass and release of carbon and greenhouse gases to the atmosphere and their associated radiative forcing on the climate.

Satellite remote sensing provides the only practical means to monitor biomass burning over areas as extensive as southern Africa. Active fire locations have been derived systematically by hotspot detection algorithms applied to orbital satellite data. However, these data do not provide reliable information on the spatial extent and timing of burning as clouds preclude hotspot detection and because the satellite may not overpass when burning occurs. Algorithms that use multi-temporal satellite data to map the areas affected by the passage of fire, often called burned areas, are less subject to these constraints. A new approach to change detection, applicable to high-temporal frequency satellite data, that maps the location and approximate day of change occurrence, has been developed. The algorithm has been used to generate southern Africa burned area maps for 2000 – 2002 from daily MODIS 500m land surface reflectance data.

Figure 11 illustrates the 500m MODIS burned area product (colored pixels) and validation data (vectors) over the Okavango delta, Botswana, in the 2001 dry season. The correspondence between these independently derived burned area data sets and the coherent spatio-temporal progression of burning is evident. The validation data were derived from multi-temporal Landsat Enhanced Thematic Mapper Plus (ETM+) data following a protocol implemented by members of the Southern Africa Fire Network (SAFNet) in Namibia, Botswana, Zimbabwe, Malawi, South Africa, and Mozambique. The MODIS burned area product is now being considered for global implementation and to feed SAFNet local and regional resource management and environmental assessment applications in addition to regional greenhouse gas emission inventories.

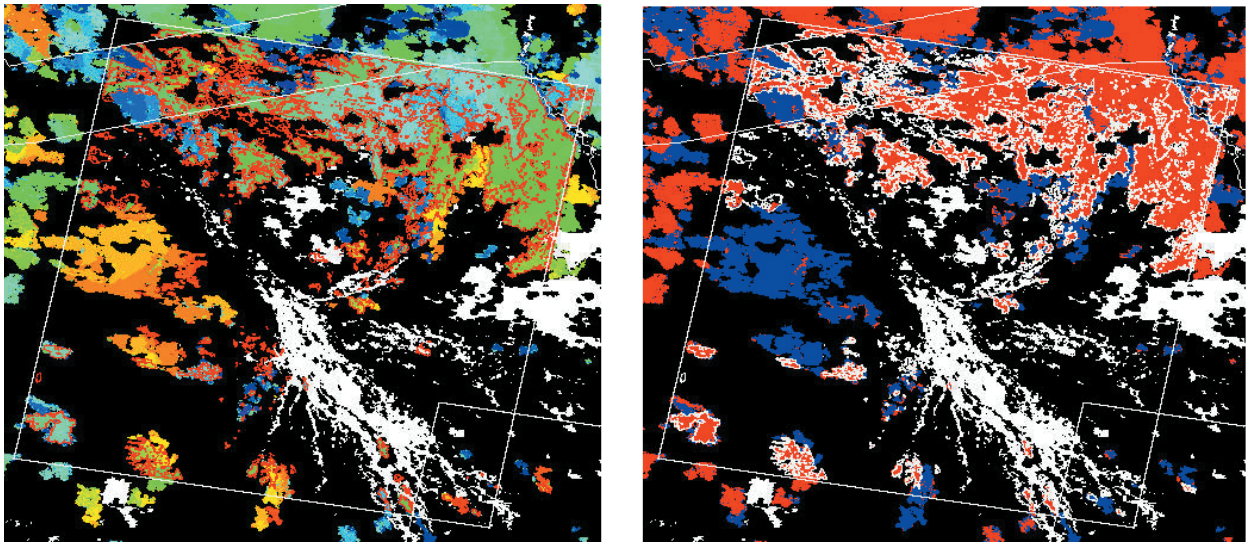

Figure 11. MODIS 500m burned area product and Landsat ETM+ independent burned area validation data, Okavango delta, Botswana. Vectors show independent burned area data mapped in the period between two ETM+ acquisitions 6 August and 23 September 2001 (left- red vectors, right- white vectors). Colored pixels show the burned areas detected by MODIS over 105 days from 20 July to 1 November 2001 (left- colored with a rainbow scale to indicate the approximate day of burning, bottom- right to indicate burned areas detected within the Landsat ETM+ acquisition period, blue to indicate MODIS burned areas detected before or after the ETM+ acquisition period). Black pixels indicate no burning detected by MODIS, white pixels indicate areas that could not be mapped due to persistent cloud. The 185 X 170 km Landsat ETM+ scene boundary and the borders of Botswana, Namibia (Caprivi Strip) and Angola are also shown (white vectors, top and bottom).

Contact: David Roy, droy@kratmos.gsfc.nasa.gov

References for Forest Characterization:

Kharuk V. I., Ranson K. J., Kuz'michev V. V., Im S. T. 2003a. Landsat based analysis of insect outbreaks in southern Siberia, In Press, Canadian J. Remote Sensing

Kharuk V.I., Ranson K.J., Burenina T.A., Fedotova E.V.2003b. NOAA/AVHRR data in mapping of Siberian forest landscapes along the Yenisey transect, International J. Remote Sensing, in press.

Nelson, R.F., G. Parker, and M. Hom. 2003. A Portable Airborne Laser System for Forest Inventory. Photogrammetric Engineering and Remote Sensing, accepted for publication.

Nelson, R.F., A. Short, M. Valenti, and C. Keller. 2003. A Multiple Resource Inventory of Delaware Using Airborne Laser Data. submitted to BioScience.

Ranson, K. J., K. Kovacs G. Sun, V. I. Kharuk. 2003. Disturbance recognition in the boreal forest using radar and Landsat 7, In press, Canadian J. Remote Sensing

Health Initiatives

Pediatric Asthma Study

The problem of pediatric asthma in Baltimore, Maryland is serving as a prototype for the development of tools that would contribute to decision support systems being used within the medical and public health communities. An epidemic of pediatric asthma is underway in the US in that the number of children with asthma has more than doubled in the last 15 years. National data also show that poor, minority children are disproportionately affected, requiring higher rates of hospitalization for asthma and incurring higher mortality rates. In Baltimore City, asthma is the most common chronic illness of children accounting for up to 20% of pediatric hospital admissions, with rates more than double the national rate.

Temporal and spatial trends in hospital admissions and emergency room visits within Baltimore show some relationship to environmental and socioeconomic trends. However, the number of possible variables involved and the complex, non-linear relationships between these variables makes it extremely difficult to understand. In order to handle the large and diverse data sets to identify environmental causes of childhood asthma, the following tools have been developed: data collection, data integration with GIS, data manipulation, visualization and scenario building, and applied mathematical modeling and prediction.

Accomplishments to date include

1. The development of a robust tool for data integration and manipulation which includes:

- Input of multidisciplinary data
- Encapsulation of complex and diverse data sets into a common format
- Conversion between spatial and temporal units (e.g. census to zip code)
- Spatial and temporal integration of inputted data in a GIS structure
- Graphical user interface for easy access to data and tools
- Clipping tool for choosing locations or areas for graphical or digital output
- Graphical output including thematic maps (State, county, zip code, census tract, and others), multiple graphing for displaying data
- Prediction capabilities using adaptive non-linear techniques (e.g. neural networks)
- Output of integrated data sets based on overlaying spatial or temporal criteria
- Data manipulation (e.g. weighting, adding, subtracting, multiplication, division, etc.) for query and decision making

2. Collection of a comprehensive set of environmental, clinical, and socioeconomic data including:

- Clinical data
- Socio-Economic data
- School data
- Weather Air Quality
- Water Quality
- Environmental (pollen, molds, brownfields, soil properties, topography, etc.)
- Land Use and Boundaries (roads, cities, traffic, major industrial areas, agricultural etc.)
- Remote Sensing (Landsat, AVHRR, Ikonos, SPOT, Aeronet, MODIS, ASTER, etc.)

3. Production of remote sensing products including:

- Land cover classification and land use change (for vegetation type, amount, cropland, and urban extent) from Landsat

• Urban characteristics for Baltimore City (Landsat)
• Animation of timing of greenness (SPOT, 1KM, 1998-2002) (for relating vegetation phenology, and agricultural activity to asthma trends)
• Pollution maps derived from Landsat (NO_2, SO_2,CO) (in development)
• Key landmark features overlaid on 1m IKONOS base map
• Particulate matter load, size, and characterization from Aeronet

4. Preliminary Research Results:

• Asthma rates are high in Baltimore City, Maryland, compared with national rates, with 5-14 year olds disproportionately affected.
• There is a strong seasonal pattern in pediatric asthma hospital admissions in Baltimore City with peaks in spring and fall and lows in summer and winter.
• The same seasonal pattern and timing of peak admissions is observed throughout the State of Maryland.
• This seasonal pattern supports relationships between asthma and certain classes of environmental triggers and contradicts relationships previously linked with asthma (e.g. high atmospheric ozone).
• Predictions of temporal asthma hospital admissions in Baltimore City can be made with relatively high accuracy based solely on historical trends (r^2 = .80).
• Highly accurate spatial predictions of asthma hospital admissions were made in Baltimore City using satellite based information (Landsat) combined with socio-economic data (r^2 = .95). The characteristics of zip codes areas with high pediatric asthma hospitalization rates were:
  ▪ Highest proportion of families headed by single parent
  ▪ Highest levels of poverty
  ▪ Highest proportion of built-up areas
  ▪ Lowest vegetation cover
  ▪ Highest thermal IR radiant temperatures
• Schools with the highest prevalence of asthma were identified (based on data from school nurses) and chosen for further study of indoor triggers. Results showed that allergens found indoors within the Baltimore City Public schools do not appear to be high enough to be the primary trigger of pediatric asthma in Baltimore City.

Contact: Elissa Levine, Elissa.Levine@nasa.gov

Satellite Remote Sensing of Ebola River Hemorrhagic Fever Outbreaks

Ebola hemorrhagic fever, named after the Ebola River in equatorial Africa, first appeared in June 1976, during an outbreak of 284 cases in Nzara and Maridi, Southern Sudan with a fatality rate of 53%. In September 1976, another outbreak of 318 cases occurred in Yambuku, Democratic Republic of the Congo (DRC), in which 88% of the affected died. One fatal case was identified in Tandala, DRC, in June 1977, followed by an outbreak involving 34 cases with 20 deaths, again in Nzara, Sudan, in July 1979 (a residual outbreak).

Ebola River hemorrhagic fever was not reported again until the end of 1994, when three outbreaks occurred within a relatively short time. In October, an outbreak was identified in a chimpanzee group in Tai, Cote d'Ivoire (12 chimpanzee cases, all chimps died) with one human infection that was not fatal. Forty-nine cases (59% fatal) were reported the following month in northeast Gabon in the gold panning camps of Mekouka, Andock, and Minkebe. Later that same month, 315 cases (77% were fatal) were reported at Kikwit, DRC, through unknown initial exposure thought to have occurred to men working in a charcoal pit. In Gabon, two subsequent outbreaks were report-

ed in February and July 1996, respectively, in Mayibout II, a village 40 km south of the original outbreak in the gold panning camps (31 cases, 68% of whom died), and a logging camp between Ovan and Koumameyong, near Booue (60 cases and 40 deaths); these cases are thought to be residuals from the initial Gabon November 1994 outbreaks.

The emergence of Ebola hemorrhagic fever in equatorial Africa is enigmatic. It is thought to result from, or to be facilitated by, human intrusion into previously uninhabited tropical areas, changes in the ecology of the Ebola virus or its natural reservoir(s), mutation of the Ebola virus, and possibly severe climatic conditions, which could serve as a "trigger" event. No reservoir or vector has yet been found. The work is described in more detail in Tucker et al. (2002).

All known outbreaks of Ebola have been linked to tropical forests. A study of environmental conditions associated with Ebola hemorrhagic fever was conducted after preliminary reports strongly suggested that simultaneous outbreaks occurred, during two limited time periods in the 1970s and 1990s, immediately following a sudden shift from a very dry to a wet period. The study investigated climatic conditions associated with the documented outbreaks and the degree of human intrusion in the outbreak areas using satellite data in the 1981 to 2000 time period. No time-series satellite data are available for the 1970s; thus the satellite time series analysis is restricted to outbreaks in the 1990s. Work is continuing to extend the analysis from 2000 through to early 2003.

Ebola hemorrhagic fever outbreaks were identified from documented, clinically described, and serologically confirmed cases. The date of the first documented Ebola case was used to define the start of each outbreak. The assumption was made that the first or index case had come into contact with Ebola virus up to 25 days prior to the onset of the illness. This includes an incubation period of 21 days plus additional time spent between onset of symptoms and subsequent appearance at a clinic.

Landsat multispectral scanner [MSS] (80 m spatial resolution) and thematic mapper [TM] (30 m spatial resolution) data were acquired for the outbreak times and locations to determine the ecological setting. The respective vegetation associations ranged from primary tropical forest in a continuum of tropical forest (Gabon and Zaire sites), isolated primary tropical forest surrounded by human activities (Cote d'Ivoire site), or gallery tropical forest in a savanna matrix (Sudan sites).

Data from the Advanced Very High Resolution Radiometer (AVHRR) instrument carried on board the National Oceanic and Atmospheric Administration's (NOAA) polar orbiting series of satellites was used to create monthly normalized difference vegetation index (NDVI) mapped to 8 km resolution grid for all of Africa. NDVI is used as a surrogate for photosynthetic capacity, which is directly influenced by rainfall. The NDVI is computed from the red (550-700 nm) and near infrared (730-1100 nm) channels of the AVHRR according to:

(1) $$NDVI = (r_{nir} - r_r) / (r_{nir} + r_r)$$

where r_{nir} and r_r are the surface reflectances in the 730-1000 nm and 550-700 nm regions of the electromagnetic spectrum, respectively.

Maximum value compositing was performed to minimize the effects of cloud contamination, atmospheric effects, scan angle and solar zenith angle effects without having to resort to an explicit atmospheric correction. A time and latitude varying atmospheric correction was applied for the El Chichon (1982-1984) and Mt. Pinatubo (1991-1993) stratospheric aerosol periods. Data were inter-calibrated between different satellites periods and corrected for sensor degradation. Nearly two decades of data were processed from four NOAA satellites, NOAA-7 (1981-1985), NOAA-9 (1985-1988), NOAA-11 (1988-1994), NOAA-9 (1994-1995, descending node 0900 hour local solar overpass time), and NOAA-14 (1995-1999). The composite images were visually checked for navigation accuracy, tested for spatial coherence and then assembled into time series.

Monthly mean NDVI images were derived from the time series by computing the respective 18 year mean images, taking care not to include outlier or missing data values in the mean. Monthly NDVI anomaly images were then computed by taking the difference between the monthly NDVI and that of the respective monthly mean.

The NDVI anomaly images were then analyzed to reveal spatial patterns and temporal persistence of above normal and below normal NDVI. NDVI time series profiles of anomalies were developed for outbreak locations in Tai, Cote d'Ivoire; Mekouka, Gabon; and Kikwit, DRC.

A threshold algorithm was applied to the NDVI time series to identify regions in the tropical forest stratum experiencing a change from persistently below-normal NDVI to persistently above-normal NDVI conditions. A tropical forest stratum mask was constructed based on NDVI values between 0.4 and 0.8 in the computed 18-year annual mean NDVI image. Geographic areas associated with major negative-to-positive NDVI anomaly changes were calculated using criteria of anomaly severity, persistence, and clustering: (1) two months of persistent negative ΔNDVI < -0.025 followed by one month ΔNDVI >0.025; (2) three months of persistent negative ΔNDVI < -0.025 followed by two months Δ NDVI >0.025 and only selecting pixels surrounded by similarly-affected pixels; (3) three months of persistent negative ΔNDVI < -0.05 followed by two months ΔNDVI >0.05 with no test for similarly-affected pixels; and (4) three months of persistent negative ΔNDVI < -0.05 followed by two months ΔNDVI >0.05 and only selecting pixels surrounded by similarly-affected pixels (Figure 12). Distances from the nearest group of anomaly pixels were then calculated for each of the documented outbreak sites.

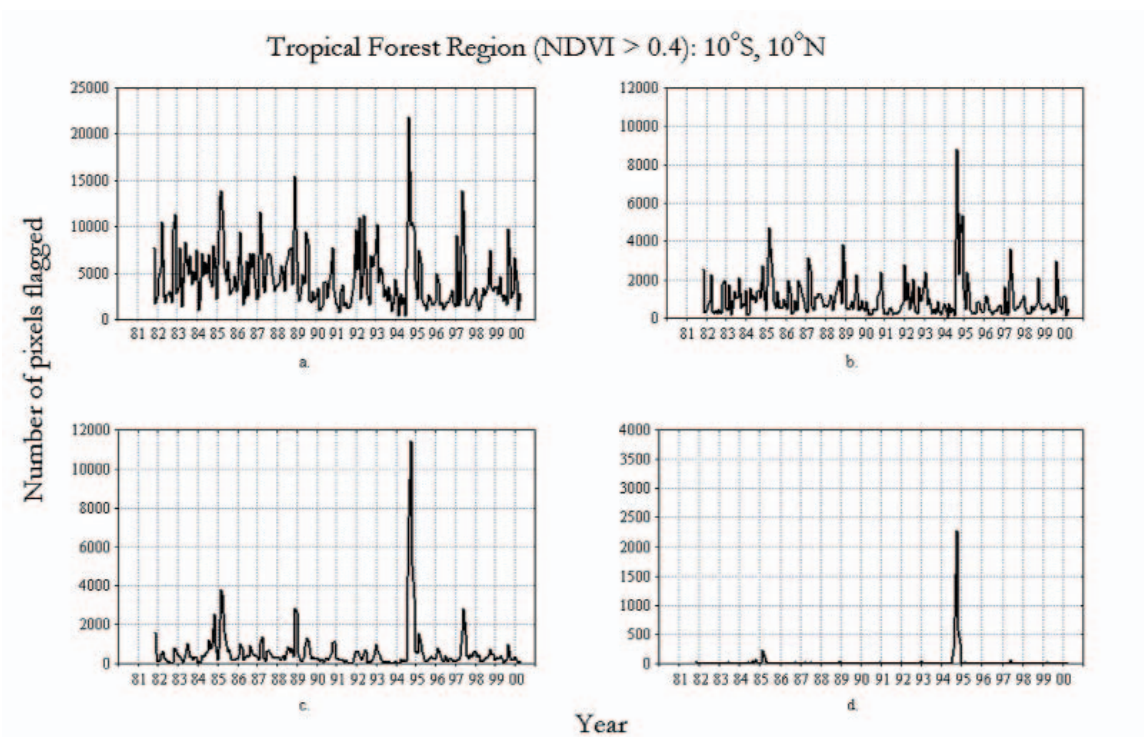

Figure 12. Using the NDVI profiles, the number of pixels in the tropical forest stratum of Africa were computed where possible NDVI "trigger" events occurred. These were summed and plotted vs. time. (a) a ΔNDVI of 0.025 with 2 months <0.025 followed by 1 month > 0.025; (b) a ΔNDVI of 0.025 with 3 months <0.025 followed by 2 months > 0.025; (c) a ΔNDVI of 0.05 with 3 months <0.05 followed by 2 months > 0.05 without any pixels "filtered"; and (d) a ΔNDVI of 0.05 with 3 months <0.05 followed by 2 months > 0.05 where only those pixels surrounded by similar flagged pixels are included.

Analysis of time series profiles of NDVI anomalies developed for the 1994-1996 outbreak locations showed a common feature for all three locations (Tai, Mekouka, and Kikwit): a significant change from below average NDVI values to above average NDVI within a short period of time. The relative change was on the order of 0.2-0.3 NDVI units within a four-month period.

Large areas of marked NDVI changes existed for the Gabon and Congo 1994 Ebola outbreak areas. These marked NDVI changes preceded the 1994 outbreaks by 1 to 4 months and occurred within 60 km from the documented outbreak locations. The situation for Tai, Ivory Coast does not follow this pattern and indicates an Ebola antecedent outbreak >200 km distant. Because local rainfall data reported very high precipitation at this location in October 1994, it is unclear if the remote sensing analysis is too conservative for the Tai outbreak or if introduction of the virus occurred with a highly mobile species.

Distances of up to 220 km would need to be traversed if the Ebola virus outbreak at Tai, Ivory Coast was associated with the rainfall and hence NDVI anomaly which we mapped for tropical Africa. The 60 km distances found for the 1994 Gabon and Congo Ebola outbreak sites are plausible for a combination of arthropod, vertebrate, and/or "infected person" transmission, ultimately to people in the documented outbreak areas.

This analysis is limited by the occurrence of only one Ebola outbreak during our 1981-1999 satellite record. Work is continuing to complement the NDVI time series with a companion time series of satellite-derived surface temperature and the addition of NDVI data for 2000-2001. Recent advances in satellite remote sensing will also provide retrievals of near-surface humidity and precipitation, in addition to improved normalized difference vegetation index time series which is being continued by several different instruments flying on several different satellites.

Contact: Compton Tucker, Compton.J.Tucker@nasa.gov

Field and Airborne Research Experiments

The Vegetation Fluorescence Project

The Vegetation Fluorescence Project is a joint NASA and USDA project conducted at the Agricultural Research Service in Beltsville, MD. The major focus of this project is to understand the interaction of the nitrogen (N) and carbon (C) cycles affecting plant productivity. This interaction was researched through optical, physiological, and morphological measurements related to C and N uptake and photosynthetic function of vegetation included in controlled N application experiments. Three essential state-of-the art instruments to augment the measurement capabilities of this study were used: a spectrofluorometer (Fluorolog-3); a leaf chamber capable of simultaneously obtaining chlorophyll fluorescence and photosynthesis; and a solar simulator.

In 2001, this project focused on laboratory measurements of field grown corn that were provided four levels of nitrogen fertilizer application. Preliminary results from the 2000 and 2001 growing seasons were presented in four IGARSS'02 papers (Toronto, Canada, June 23-27, 2002); a SPIE paper (9th International Symposia on Remote Sensing, Crete, Greece, September 22-27, 2002); a paper presented at a workshop entitled "Remote Sensing for Agriculture and the Environment" sponsored by the Organization for Economic Cooperation and Development (OECD) in Kifissia, Greece (Sept 17-20, 2002); a poster included in the 2002 BARC Poster Day (April 18, 2002); and a poster/presentation (Oct. 3, 2002) for the USDA Deputy Under-Secretary for Research, Education and Economics, Dr. Rodney Brown. Results from these years were also included in a journal paper submitted to Remote Sensing of Environment (Corp et al.).

Due to the 2002 drought, additional data on field corn was not acquired this year. Instead, a controlled N experiment was undertaken, which is expected to continue for three years. Funded by the NASA Terrestrial Ecology Program, the study researches the effects of excess N that might occur in riparian forests due to either pollution inputs from the atmosphere or land runoff, for seedlings of three tree species (red maple, sweet gum, tulip poplar). Beginning in early June, N was applied bi-weekly at four dose levels. Week-long measurements campaigns were conducted at three different times during the growing season (mid July, early September, early October) on a sample of 60 (out of 200) trees.

Experiments were also conducted in 2002, sponsored by the Defense Threat Reduction Agency (DTRA), on several species (corn, soybean, pigweed) to determine whether fluorescence was altered in the foliage of plants exposed to trinitrotoluene (TNT) in the substrate. Optimal N or TNT was applied in four dose levels weekly to potted plants held in a cold frame with removable covers. Three week-long measurement campaigns were conducted in June, July, and September. Preliminary results of these experiments were presented at a joint NASA/National Institute of Justice meeting held at GSFC in November.

A standard set of measurements made on individual leaves has been established. Spectral measurements acquired from both upper and lower leaf surfaces included: 1) emission images acquired in four bands (blue, green, red, far-red bands, 10-20 nm wide), induced by broadband UV/VIS excitation, with the in-house Fluorescence Imaging System; 2) high spectral (5 nm) fluorescence emission spectra, resulting from single wavelength excitations at 532, 350, and 280 nm, acquired with the Fluorolog-3 spectrofluorometer; 3) high spectral resolution (<3 nm; ~400 - 2500 nm) optical properties (reflectance, transmittance, absorptance) acquired with a spectroradiometer (Analytical Spectral Devices, Inc., ASD) and an integrating sphere; and 4) the percent of "apparent reflectance" in the red edge spectrum (650 - 750 nm) due to chlorophyll fluorescence, calculated from ASD optical spectra acquired at 1 s intervals (for 2 min) with/without a Schott RG 665 long pass filter, after exposure of dark-adapted leaves to simulated solar irradiance. Some measurement sets also included 3-D fluorescence excitation matrices for fixed emission wavelengths (e.g., solar Fraunhofer lines, 677 and 745 nm). Also determined were photosynthetic parameters, chlorophyll fluorescence kinetics, pigment content, N and C content; and specific leaf mass, chlorophyll fluorescence kinetics, and pigment content.

The NASA participants are associated with the Biospheric Sciences Branch: Dr. Elizabeth Middleton , Dr. Petya K. Entcheva Campbell, UMBC/JCET; and SSAI employees, Larry A. Corp, L. Maryn Butcher, Phillip Padden, and Emmett Chappelle (formerly 923). The USDA participant is James E. McMurtrey, III of the Hydrology and Remote Sensing Laboratory at BARC.

Contact: Elizabeth Middleton, Elizabeth.M.Middleton@nasa.gov

EOS Land Validation Core Sites and CEOS Land Product Validation

Based on lessons learned from the previous generation of global land imaging systems (Justice and Townshend, 1994), NASA considers product validation to be an integral component in the production of global land products. For each product derived from satellite data there needs to be field data, or ground reference, to ensure that the information in the satellite product is accurate. For global products produced in the 250m to 1km spatial resolution range, high-resolution (4 to 30m) airborne or satellite data provide a useful intermediate point from which to relate ground measurements to the course resolution global products. To facilitate validation efforts over a network of field sites, the MODIS land team continues to develop an online infrastructure of data and information for the EOS Land Validation Core Sites, including the systematic collection of remote sensing data from other missions. Using the EOS/MODIS land product validation experience, research at GSFC has led land product validation efforts within the international com-

munity. The EOS Core Sites and participation in the CEOS Land Product Validation subgroup are a joint activity between the Terrestrial Information Systems and Biospherics Sciences Branches, within the Laboratory for Terrestrial Physics.

EOS Land Validation Core Site: update

The EOS Land Validation Core Site system was initiated by the MODIS Land Validation Team to coincide with the launch of Terra. One of the primary goals of Goddard and the MODIS Land Team's efforts in support of the EOS Land Validation Core Sites was to provide easy access to EOS data for research sites around the world. Although their development was primarily for the validation of EOS data, the Core Site infrastructure can and has been used for validation of many satellite sensors (Morisette, et al., 2002).

Currently there are 26 Core Sites, with free ftp access available for most of the Core Site data sets. These data include ETM+, ASTER, and 200 x 200 km subsets of MODIS and SeaWiFS data. Many of the Core Sites are already part of existing science data networks, such as the FLUXNET network http://daacl.esd.ornl.gov/FLUXNET/), AERONET (http://aeronet.gsfc.nasa.gov:8080/), and the Long Term Ecological Research site network (LTER: http://www.lternet.edu). High-resolution IKONOS data are also available for the Core Sites (NASA Scientific Data Purchase program registration required). In August 2002, the EOS Land Validation Core Site WWW pages reached the 1000 link milestone, where each link points to a unique satellite data set. The EOS Land Validation Core Site system continues to serve validation of global land products from MODIS Terra and Aqua, as well as other multi-resolution science research at these sites.

CEOS LPV

In an attempt to leverage off of the infrastructure and experience from MODIS Land validation, researchers at GSFC have helped establish the Committee on Earth Observing Satellites (CEOS) "Land Product Validation" (LPV) Subgroup. Since the LPV subgroup's inception in late 2000, Goddard scientists have chaired the subgroup and have also organized several outreach workshops.

The mission of the subgroup is to foster quantitative validation of high-level land products derived from remote sensing data in the solar reflective and thermal infrared wavelengths. It will pursue this mission through the following objectives:

- To define uncertainty objectives with product users

- To identify and support global test sites for both systematic and episodic measurements

- To develop consensus "best practice" protocols for data collection, description, scaling, and comparison with satellite products

- To identify needs and opportunities for coordinating collaboration among space agencies, industry, academia, and scientific organizations and networks.

- To develop procedures for validation, data exchange, and management (with the Working Group on Information System and Services, WGISS)

These objectives are being achieved through a series of topical workshops, international product intercomparison activities, and a transition from the EOS to CEOS Land Validation Core Sites. The topical workshops are co-chaired by community experts, focusing on specific land product validation issues. The initial programmatic focus will be on the Global Observation of Forest and Land Cover Dynamics (GOFC/GOLD) priorities of Fire/Burn Scar products, Land Cover/Land

Cover Change products, and Biophysical products (such as Leaf Area Index, LAI and Albedo). Collaboration with industry, data centers, satellite product developers, and other CEOS working groups and their subgroups, will be sought. The initial LAI workshop has resulted in the "CEOS LAI-Intercomparison Activity", where several separate international efforts are being combined to provide independently-derived high-resolution LAI maps for over 20 sites (see Figure 13). These maps can then be compared to the MODIS (or other) global LAI products, thus providing more validation sites than any one agency alone could develop. To transition from EOS to CEOS Land Validation Core Sites, LPV has led a joint activity between its parent working group (the Working Group on Calibration and Validation) and the other working group of CEOS (the Working Group on Information System and Services). This "Test Facility" will be similar to the EOS Core Site infrastructure but will provide access beyond NASA's EOS satellite data sets, and look to include any global land product that is produced by a CEOS member (see Figure 14).

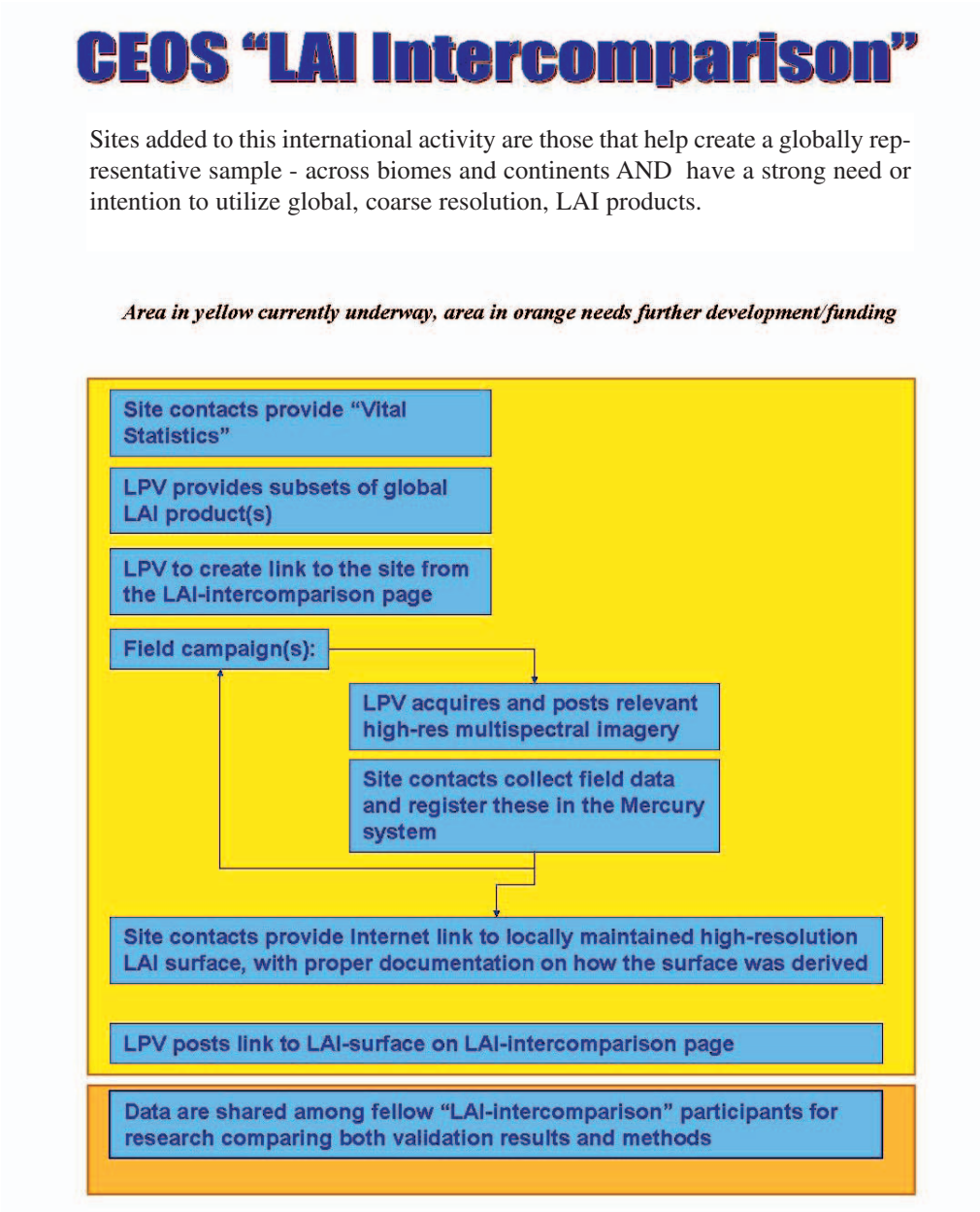

Figure 13. Strategy and flow diagram for LAI intercomparison effort.

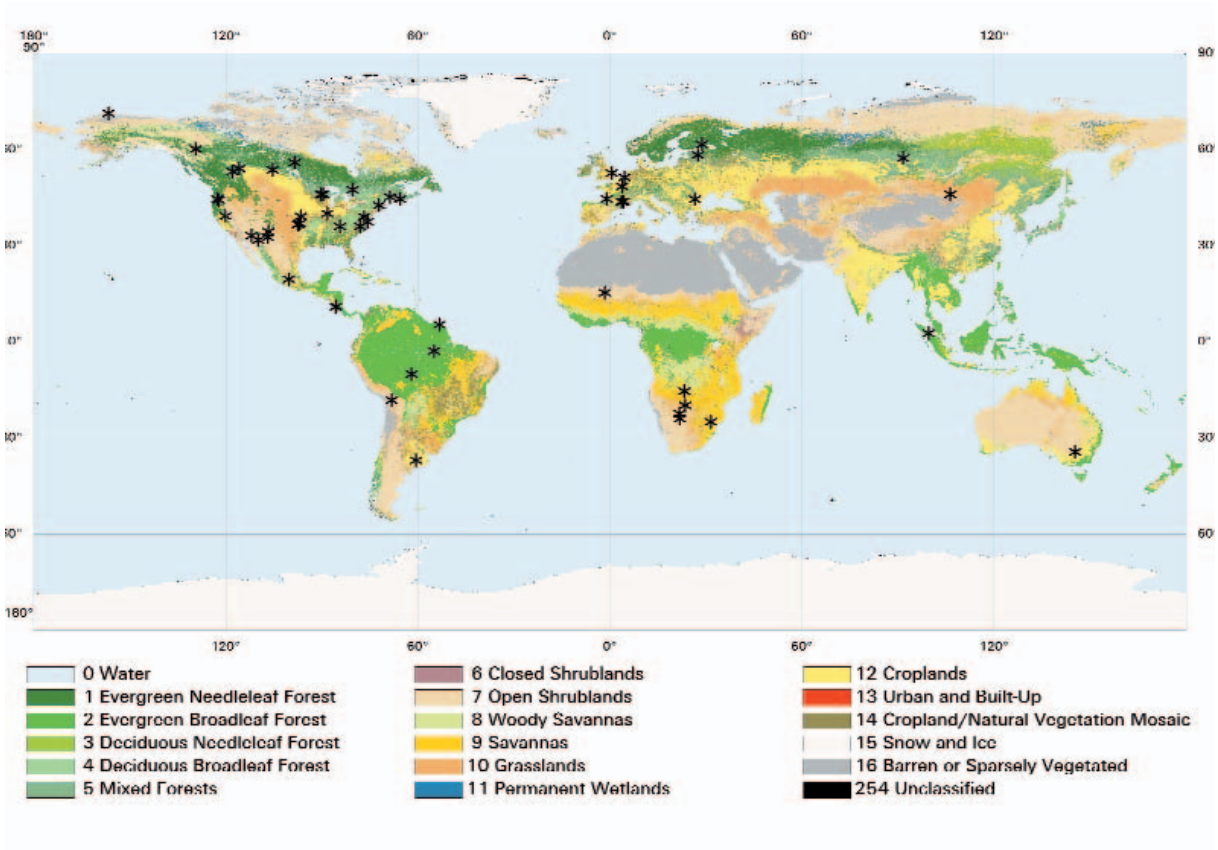

Figure 14. Proposed CEOS Land Validation Core Sites, shown on the MODIS land cover product (image provided courtesy of Boston University).

Future plans

MODIS land validation activities will continue to focus on the EOS Core Sites for validation in the MODIS/Aqua time frame. Additionally, the National Polar-orbiting Operational Environmental Satellite System Preparatory Project (NPOESS NPP) has included the EOS Land Validation Core Sites in their validation plans as primary targets for land product validation. GSFC will continue to play a leadership role in the CEOS Land Product Validation subgroup, looking to convene additional topical meetings and continuing the CEOS Land Product Validation Core Site and Intercomparison activities

References:

Justice, C.O. and Townshend, J.R.G. 1994. Data sets for global remote sensing: lessons learnt. International Journal of Remote Sensing. 15(17):3621-3639.

Morisette, J. Privette, J, and Justice, C., 2002, "A framework for the validation of MODIS land products", Remote Sensing of Environment, 83 (1-2) 77-96.

Contact: Jeffrey T. Morisette, Jeffrey.T.Morisette@nasa.gov

Flight Experiment for Carbon Sequestration Studies: Using Combined VHF SAR & Lidar for Biomass Measurement

Forest biomass represents a significant pool of carbon recently removed from the atmosphere. The remote measurement of the above ground component of forest biomass is a primary goal of scientists interested in Earth's carbon cycle and, more recently as a consequence of international environmental treaties, a goal for both policy makers and commodity traders. The remote sensing of biomass using radar requires a balance between sensitivity to the vegetation and the ability to penetrate the vegetation. For this reason, the use of radar, which probes vegetation, is being explored as a means of measuring forest biomass. However, the majority of the currently available SAR systems use frequencies above 1000 MHz which saturate at relatively low forest biomass densities thereby missing most of Earth's standing biomass. To address this problem, the Biospheric Sciences Branch has developed a VHF (80-108MHz) radar system (BioSAR) designed specifically to measure the biomass of forest stands above 100 tons/ha. The instrument had its first flight test in 1997 over Big Thicket Forest Preserve in eastern Texas, and a full deployment to Central America in 1998 where it successfully produced biomass estimates of dense tropical forests within ± 10% of the field measured values (Figure 15).

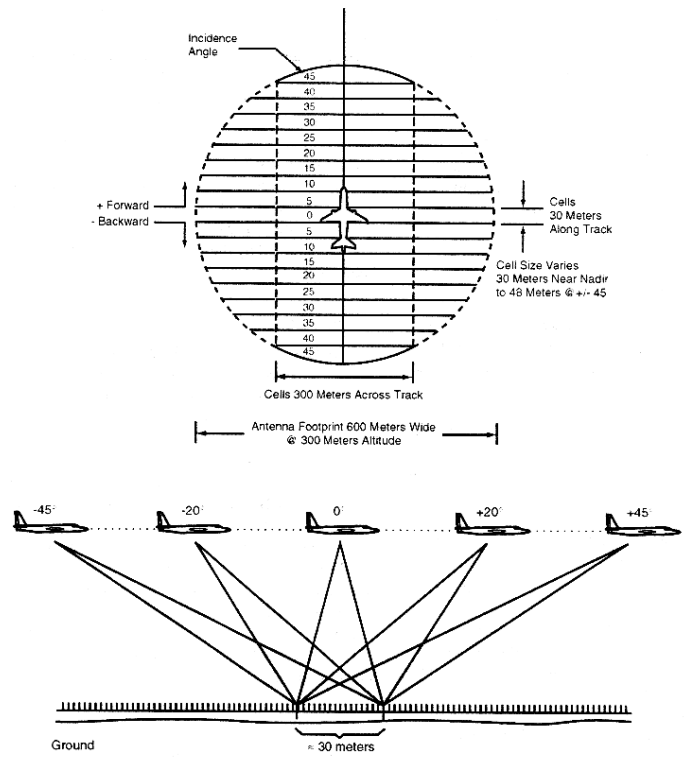

Figure 15. Top; BioSAR™ ground geometry - planar view. The antenna points straight down. As shown here, Doppler sorting is used to achieve 20 different look angles between +45° and –45° from the nadir in the along-track dimension. The resolution cell, after SAR processing, is approximately 30 meters in the along-track dimension, and 300 meters in the across-track dimension. While the actual across-track pattern of dimension of 600 meters (illuminated) is determined by the beam width and aircraft altitude it is nominally range gated to 300 meters for data collection. Bottom; BioSAR™ ground geometry - a single cell in cross-section. In this conceptual mode, a cell (30 m along track) is pulsed repeatedly using all six frequencies as the sensor flies over that point on the ground. The fore and aft angles can be logged separately or averaged together to make incidence angle bins in 5° intervals. Each cell has radar data for 6 frequencies acquired at multiple incidence angles.

As a result of this remarkable progress, a joint experiment has been implemented between the Biospheric Sciences Branch and the DoE's Oak Ridge National Laboratory to fly the BioSAR sensor along with a Profiling Airborne Lidar Sensor (PALS) in a series of flights designed to fully test the new combined system for carbon sequestration studies. The addition of the PALS system, which was also developed by the Biospheric Sciences Branch, will provide accurate forest height measurements (Figure 16). Please see the next article, titled "An Inexpensive, Portable Airborne Laser System For Forest Mensuration" for information about PALS. The data from PALS will be added to BioSAR's volumetric measurement capability and the combined data tested for making accurate forest stand biomass determinations in varying terrain conditions. The BioSAR and PALs sensors will be mounted on the Twin Otter aircraft leased by NASA and fly at least two forest sites with an established biomass/carbon cycle science research heritage. The effort benefits from a cost-sharing arrangement with the Department of Energy.

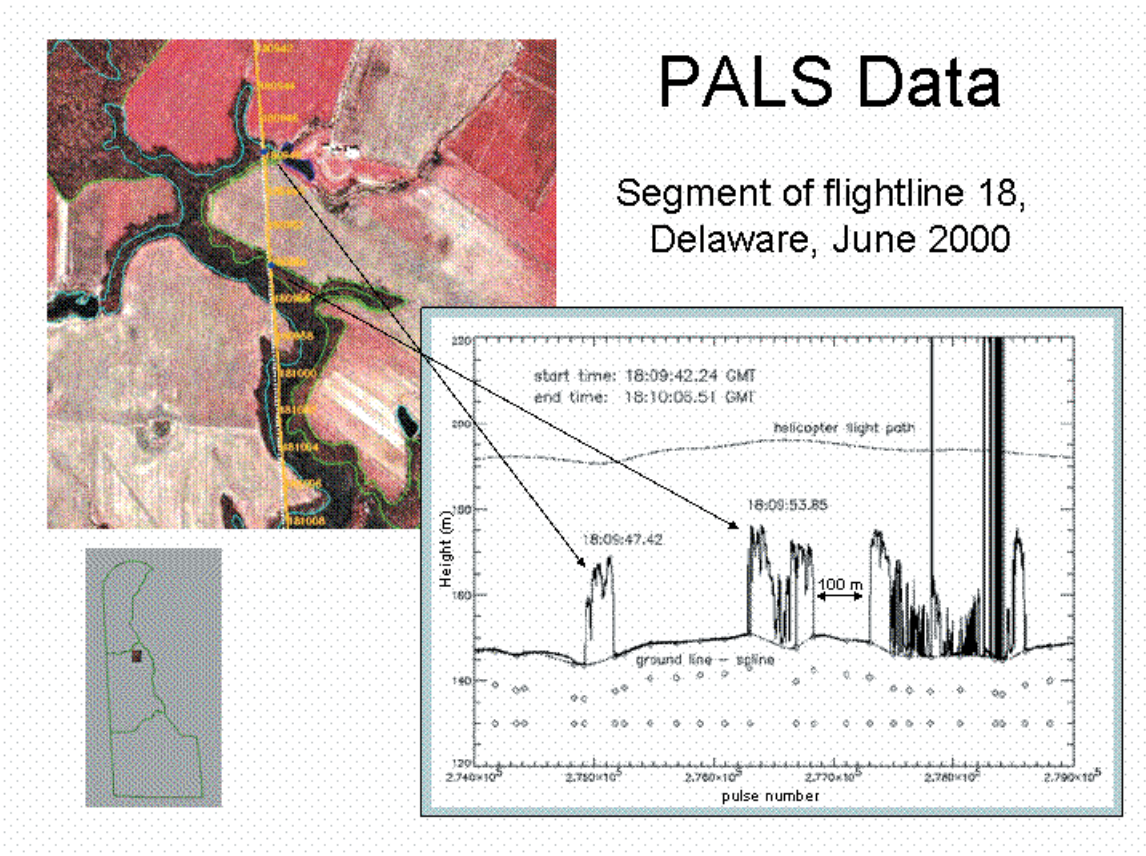

Figure 16. Laser profiling measurements will be acquired coincidently with the BioSAR measurements along the aircraft flight path. The laser is eyesafe in flight. The laser footprint directly beneath the aircraft will be 0.70m at a flight altitude of 300m AGL coincident temporally an spatially with the BioSAR footprint. PALS measures forest canopy height, height variability, and canopy density.

Contact: Marc Imhoff, Marc.L.Imhoff@nasa.gov

An Inexpensive, Portable Airborne Laser System For Forest Mensuration

A simple, lightweight, inexpensive, portable airborne laser profiling system has been assembled from off-the-shelf, commercially available components. The system, which costs approximately $30,000 USD, is designed to fly aboard small helicopters and single or two-engine high-wing aircraft without airframe modification. The system acquires first-return range and amplitude measurements at data rates up to 2000 hz (operator-controlled) and has an operational envelope up to 300m above terrain. The airborne laser profiling system includes the laser transmitter/receiver, differential GPS, a CCD video camera and recorder, and a laptop computer, which interleaves and records the GPS and laser range/amplitude data. The portable airborne laser system - PALS - was designed to acquire forest height measurements along linear flight transects in order to conduct regional or subcontinental forest inventories worldwide. Height measurement accuracy is illustrated in Figure 17. This economical laser system now puts airborne laser mensuration within reach of operational foresters and researchers interested in making rapid forest structure and/or timber surveys in remote areas. PALS has been used to acquire over 5000 km of flight transect data over the state of Delaware.

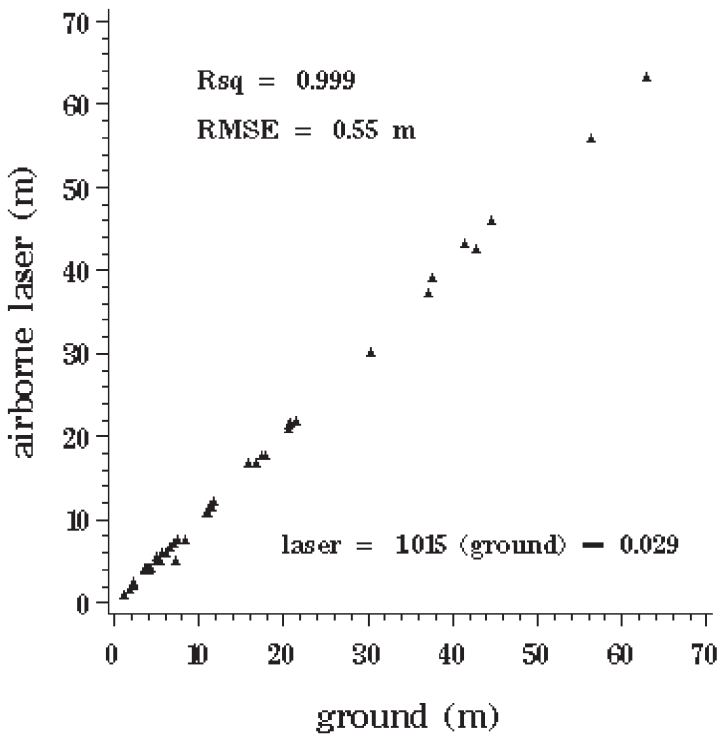

Figure 17. Comparison of building heights as measured by PALS and measured on the ground using a laser range/angle finder.

Reference:

Nelson, R.F., G. Parker, and M. Hom. 2003. A Portable Airborne Laser System for Forest Inventory. Photogrammetric Engineering and Remote Sensing, accepted for publication.

Contact: Ross Nelson, Ross.F.Nelson@nasa.gov

Biomass Measurements from Lidar Mapping

In addition to providing a method to measure topography beneath vegetation cover, laser altimetry enables measurements of forest canopies that cannot be achieved by other remote sensing techniques. David Harding and collaborators at Oregon State University, the USDA Forest Service Pacific NW Research Station, and the Smithsonian Environmental Research Center, have published a series of articles that document this capability. Using field observations of forest properties and data acquired by the airborne Scanning Lidar Imager of Canopies by Echo Recovery (SLICER), methods were developed to predict forest attributes from the laser backscatter signal. As a first step, two properties of forest canopies important to ecosystem function are obtained from the backscatter signal: vertical transmittance of light (Parker et al., 2001) and height distribution of plant area (Harding et al., 2001).

Height indices derived from the plant area distributions have previously been shown to be an accurate predicator of above ground forest biomass for specific forest types (reviewed in Lefsky et al., 2002a). Lefsky et al (2002b) show that a single predictive relationship is equally applicable to three different closed-canopy forest biomes: temperate deciduous, temperate coniferous, and boreal coniferous (Figure 18). Based on regression of height indices and field observations of above ground biomass, mean height of the canopy squared (a proxy for height x stem diameter; a measure of volume) is the best laser-based predictor. The relationship is linear to high biomass levels and accounts for the observed variance to a high degree (80% to 90%). The generality of this result, at least for these three biomes, suggests that laser backscatter data for closed-canopy forests can be used to predict biomass without knowing the specific forest cover type sampled. The forest canopy measurement capabilities developed using airborne SLICER data will be applied on a global basis to laser altimeter data acquired by the Ice, Cloud and Land Elevation Satellite (ICESat).

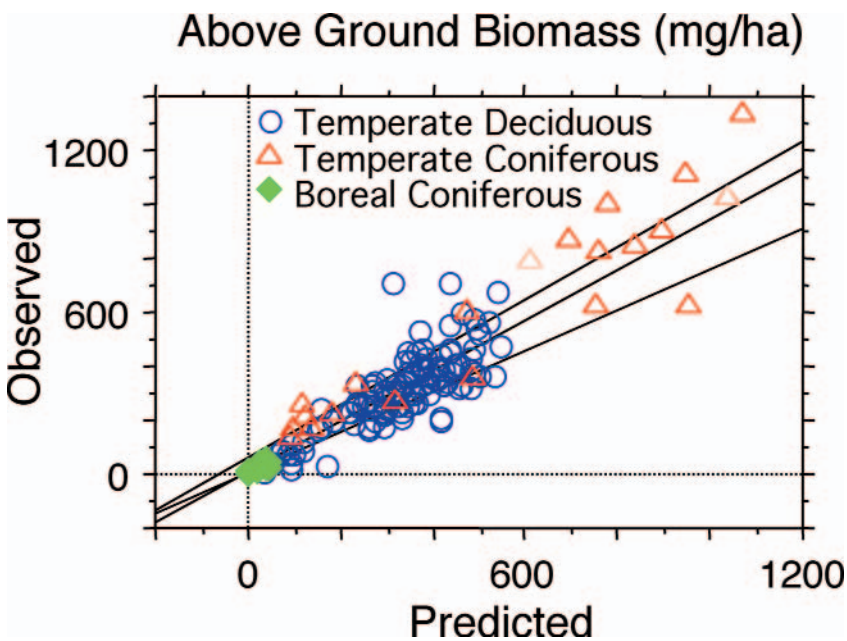

Figure 18. Relationship for three forest biomes between observed biomass and that predicted from laser backscatter height indices.

References:

Harding, D.J., M.A. Lefsky, G.G. Parker, and J.B. Blair, Laser altimeter canopy height profiles: Methods and validation for deciduous, broadleaf forests, Remote Sensing of Environment, 76(3): 283-297, 2001.

Lefsky, M.A., W.B. Cohen, G.G. Parker, and D.J. Harding, Lidar remote sensing for ecosystem studies, Biosciences, 52(1), 19-30, 2002a.

Lefsky, M.A., W.B. Cohen, D.J. Harding, G.G. Parker, S.A. Acker, and S.T. Gower, Lidar remote sensing of aboveground biomass in three biomes, Global Ecology and Biogeography, 11(5): 393-399, 2002b.

Parker, G.G., M.A. Lefsky, and D.J. Harding, Light transmittance in forest canopies determined using airborne laser altimetry and in-canopy quantum measurements, Remote Sensing of Environment, 76(3): 298-309, 2001.

Contact: David Harding, harding@core2.gsfc.nasa.gov

Data Processing

Another responsibility of the Laboratory is the development of new data processing techniques, and the development of new data sets. This is largely done in the Terrestrial Information Systems Branch, often in cooperation with the Biospheric Sciences Branch.

Global Data Processing for MODIS

MODIS (MODerate-resolution Imaging Spectroradiometer) instruments, launched on the EOS Terra and EOS Aqua spacecraft in December 1999 and June 2002, image the Earth in 36 spectral bands in visible through thermal wavelengths (459nm – 9.58µm) with spatial resolution of 250meters, 500meters and 1 kilometer. From an initial 70GB of raw instrument data, 44 global science products are produced with an average daily volume of 850GB from each MODIS instrument. These products extend the data record of products from heritage sensors, such as land surface reflectance, sea surface temperature and NDVI from AVHRR and ocean color from SeaWiFS, and offer finer spatial resolution, better calibration and more precise Earth-location of pixels.

In 2002, the MODIS team focused its efforts on improving science quality, completing a global validation of EOS Terra products and modifying formats to make land products easier to use by the community. Before the first major reprocessing of MODIS products began, over 170 changes were made to the 60 science applications programs that create global land, ocean and atmosphere products. During the reprocessing a 64 processor Silicon Graphics Origin 3000 supercomputer and a 200 processor Linux cluster were used to reprocess the 3 year data record from Terra at the rate of 8 data days per day. Over 3 TB (trillion bytes) of data products produced daily were distributed to MODIS quality assessment teams, the MODIS science team and to Distributed Active Archive Centers (DAACs), which archive the products and distribute them to the public. Two globally validated products that were highlights of the 2002 reprocessing campaign are sea surface temperature (SST) products achieving accuracies to within 0.3^{o}K (a significant improvement over SST from precursor instruments) and atmospherically corrected land surface reflectance with absolute accuracies to better than 3%. SST is an important parameter for models of global climate and weather prediction, and the land surface reflectance product is the foundation for all land products that deal with vegetation, such as vegetation indices, land cover type and change, leaf area index and net primary production.

An essential component in improving the quality of MODIS products has been a rigorous process of product quality assurance involving unit testing of science software, large scale science tests on all software and a program of continuous product quality monitoring and validation. Figure 19 below summarizes this process. The numbers in colored ovals in the left hand side of the figure represent software changes. Note slightly more than a third of the software changes submit-

ted by the science team survive the testing process and run in the production system.

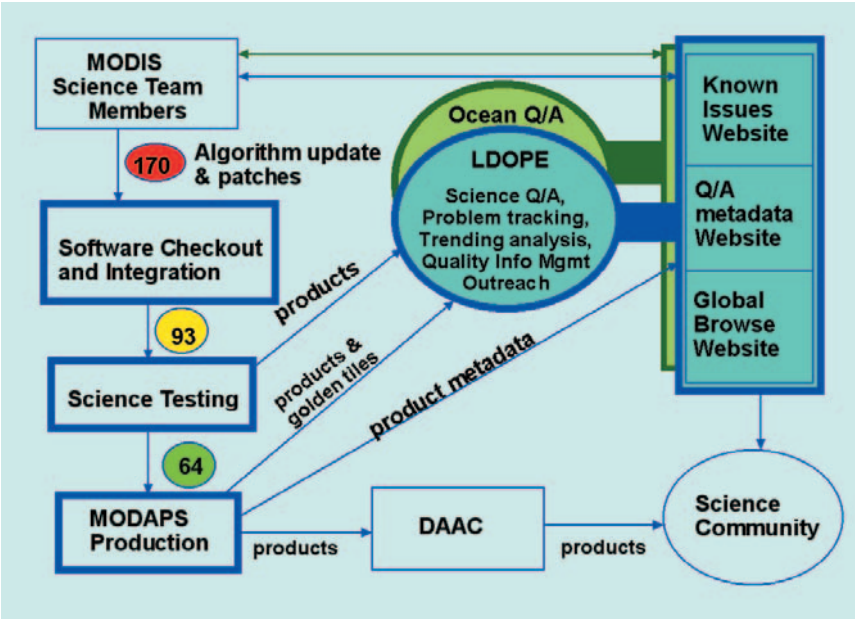

Figure 19. Quality Assurance

Contact: Ed Masuoka, Edward.J.Masuoka@nasa.gov

MODIS Rapid Response System

A collaboration between NASA, the University of Maryland, and the USDA Forest Service led to the development of a processing system capable of generating near-real-time products from MODIS data to support the Forest Service in its effort to better allocate firefighting resources across the United States. The Rapid Response System (http://rapidfire.sci.gsfc.nasa.gov/), located at NASA/GSFC in the Terrestrial Information Systems Branch, started operating in 2001. 2002 represented a continuation of the effort undertaken in 2001, and was mostly focused on streamlining the activities prototyped during the first year, on augmenting the system with new products, and on developing new application partnerships.

The Rapid Response System now generates a fire detection product, a corrected reflectance product, and a vegetation index product in near-real-time for most of the Earth's land surfaces, from both the Terra/MODIS and the Aqua/MODIS instruments. The Rapid Response System receives MODIS level-0 data from NOAA's MODIS Near-Real-Time System from the entire Earth within 4 hours of data acquisition. The subset of the data containing continents and major islands is processed upon reception.

Fire locations are retrieved using a fire detection algorithm. Those fire locations are immediately communicated to the USDA Forest Service Remote Sensing Center in Salt Lake City. The Forest Service incorporates fire locations into a Geographic Information System (GIS) and generates regional fire maps twice daily. These maps represent the fires detected by MODIS overlaying various geographic layers (see Figure 20). Fire maps are made available to the fire managers and are used to provide a synoptic view of the fire situation and help determine the best strategy to allocate fire fighting

resources. The process is all automated from the data acquisition to the generation of fire maps.

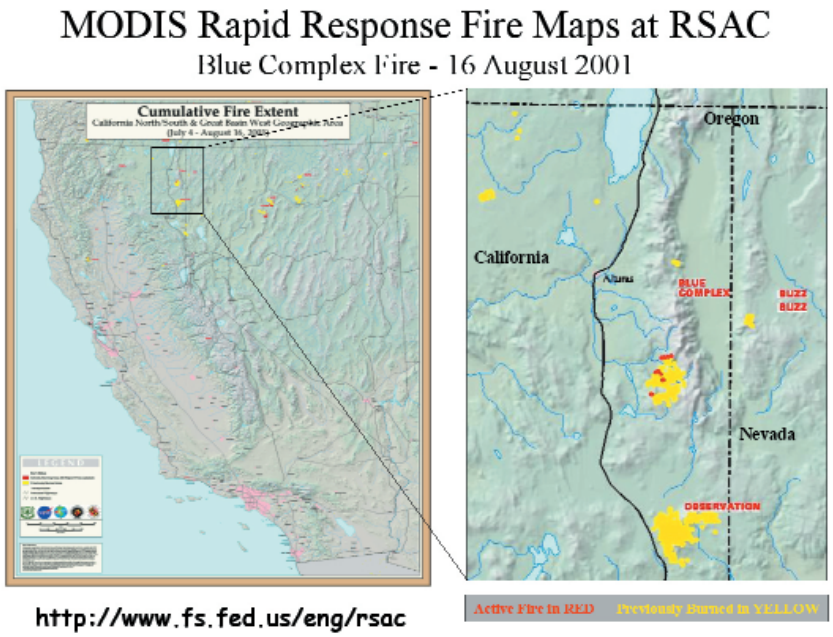

Figure 20. MODIS Rapid Response Fire Maps at RSAC.

MODIS has now become a tool recognized at the highest level of the national firefighting community. It is advertised by the National Interagency Fire Center (NIFC) as one of the main sources of fire data (http://www.nifc.gov/firemaps.html). The MODIS Rapid Response fire data is now integrated in the Geospatial Multi-Agency Coordination (GEOMAC) system, the main web-based mapping tool offered to the fire managers (http://geomac.usgs.gov/).

The Rapid Response Team packaged and delivered a version of the processing software working with MODIS Direct Broadcast data. The Forest Service began operating two Direct Broadcast receiving stations in 2002 (Remote Sensing Applications Center, Salt Lake City, UT, and Fire Sciences Lab, Missoula, MT) and now runs the Rapid Response software in both locations, and operationally generates fire locations and corrected reflectance within minutes of data acquisition in the region covered by the receiving range of each dish.

The Rapid Response System also communicates the fire locations detected by MODIS to the University of Maryland where the data are ingested by a Web-GIS system and made available to the public and the fire community through a web interface. In particular the University of Maryland has developed a collaboration with the Global Observation of Forest Cover (GOFC) fire partners, regrouping a number of regional fire groups across the world.

Another key product of the Rapid Response System is the corrected reflectance product. The MODIS top-of-the-atmosphere calibrated radiances are corrected for various atmospheric effects to produce this corrected reflectance, from which it is possible to generate images of the Earth. High-resolution imagery from all the data processed by the Rapid Response System is automatically made available on the Rapid Response web site (http://rapidfire.sci.gsfc.nasa.gov/realtime/). That near-real time imagery is used by the fire community in addition to the fire locations to help interpret fire situations, determine the presence of smoke, evaluate the burned area, etc. The near-real-time imagery is also used by other science communities. For example, it is now

used routinely by the Dartmouth Flood Observatory to map flooded areas (http://www.dartmouth.edu/artsci/geog/floods/).

Hand-picked imagery is also posted in the Rapid Response Image Gallery (http://rapidfire.sci.gsfc.nasa.gov/gallery/). 1600 gallery images were generated in 2002. A large number of the Rapid Response gallery images cover newsworthy events related to natural hazards (see Figures 21, 22, and 23). The Rapid Response System provides the backbone of the Earth Observatory's Natural Hazards section (http://earthobservatory.nasa.gov/NaturalHazards/) and is also the main MODIS contributor to the Visible Earth image database (http://visibleearth.nasa.gov/). More than fifty images were posted as image of the day by the Earth Observatory. Twenty-five images from the Rapid Response system were featured on the GSFC web page in 2002.The Rapid Response System counted a number of successes in the media in 2002, with each time many appearances on major TV stations and newspapers: Sydney fires in January, Colorado fires in mid-June, Arizona fires in end-June, Quebec fires in July, Mt. Etna eruption in October. Almost 900,000 images were downloaded from the Rapid Response web site by approximately 45,000 different visitors in 2002.

Figure 21. (Left) Eruption of Mt. Etna in Sicily (10/28/02). (Right) Dust Storm off West Africa (03/02/03).

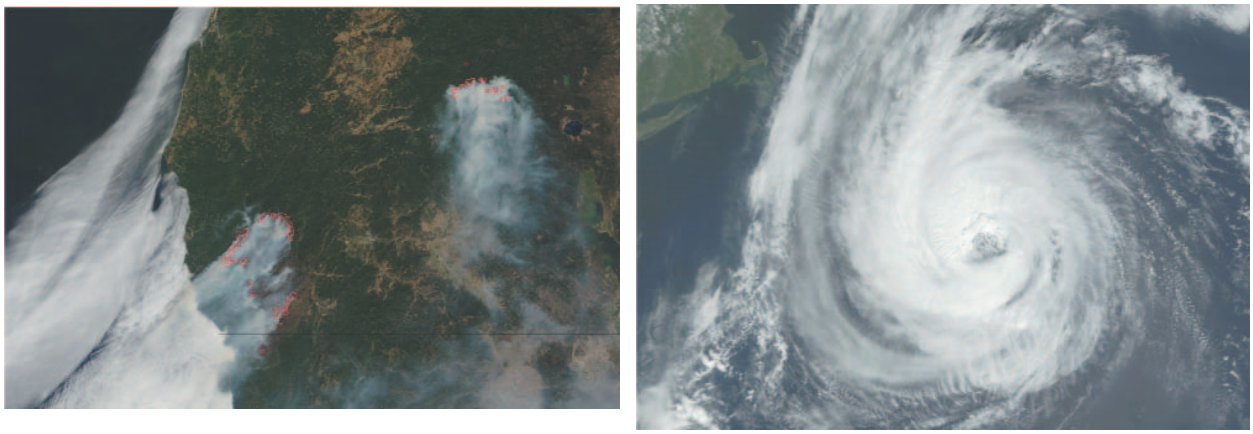

Figure 22. (Left) Biscuit and Tiller Fires in California and Oregon (08/14/02). (Right) Example of 250m Corrected Reflectance Product, Hurricane Erin (09/11/01).

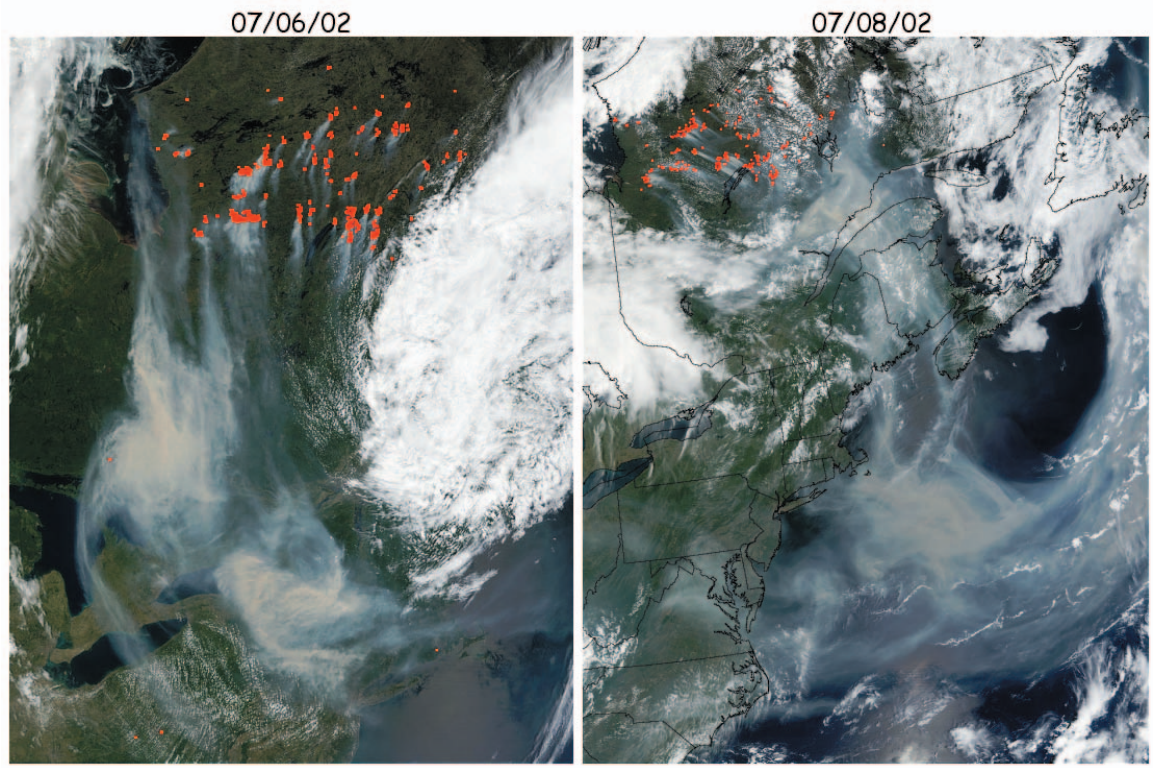

Figure 23. Fires and smoke across Quebec and Northeast US.

Contact: Jacques Descloitres, jack@ltpmail.gsfc.nasa.gov

Ozone Monitoring Instrument Science Investigator's Processing System

Rapidly evaluating possible improvements to algorithms for measuring ozone, aerosol, and other products is now possible. The OMI Science Investigator's Processing System, OSIPS, developed by the Terrestrial Information Systems Branch (Code 922) provides both high speed processing and rapid data delivery to the scientist's desktop computers. The OMI DAta Processing System, OMIDAPS, combines multiple Intel processors in a next generation system based on the MODis Adaptive Processing System, MODAPS. With the power of OMIDAPS it is possible to process twenty-two years of data from the Total Ozone Mapping Spectrometer in less than three days instead of the three months it used to take. The OSIPS and the scientists in the Atmospheric Chemistry Branch (Code 916) share access to a newly installed high speed Fibre Channel disk. Data sets are reprocessed with evolving algorithms in the OSIPS and then pushed onto the shared disk and immediately available to scientists evaluating them in a different building. This shared disk will also support the adaptation of the algorithms for the Ozone Monitoring Instrument (OMI) after it is launched on the EOS Aura spacecraft in 2004.

One tool now available allows scientists to examine the effect of a small change in an algorithm by viewing a movie of the difference between outputs of the two algorithms for every day in the twenty-two year period. Figure 24 illustrates this with total ozone and surface reflectivity data from the TOMS instrument on the Earth Probe satellite. The top left and right images show the new values of the total ozone and the surface reflectivity for the first day of 1998. The bottom two images show the relative difference between two candidate algorithms. Examining the images for the entire period revealed a small problem confined to the Polar Regions. Subsequent

analysis identified the cause of the difference and a revised algorithm has been developed and tested to process data from the upcoming Ozone Measuring Instrument, OMI, to be flown on the AURA spacecraft in 2004.

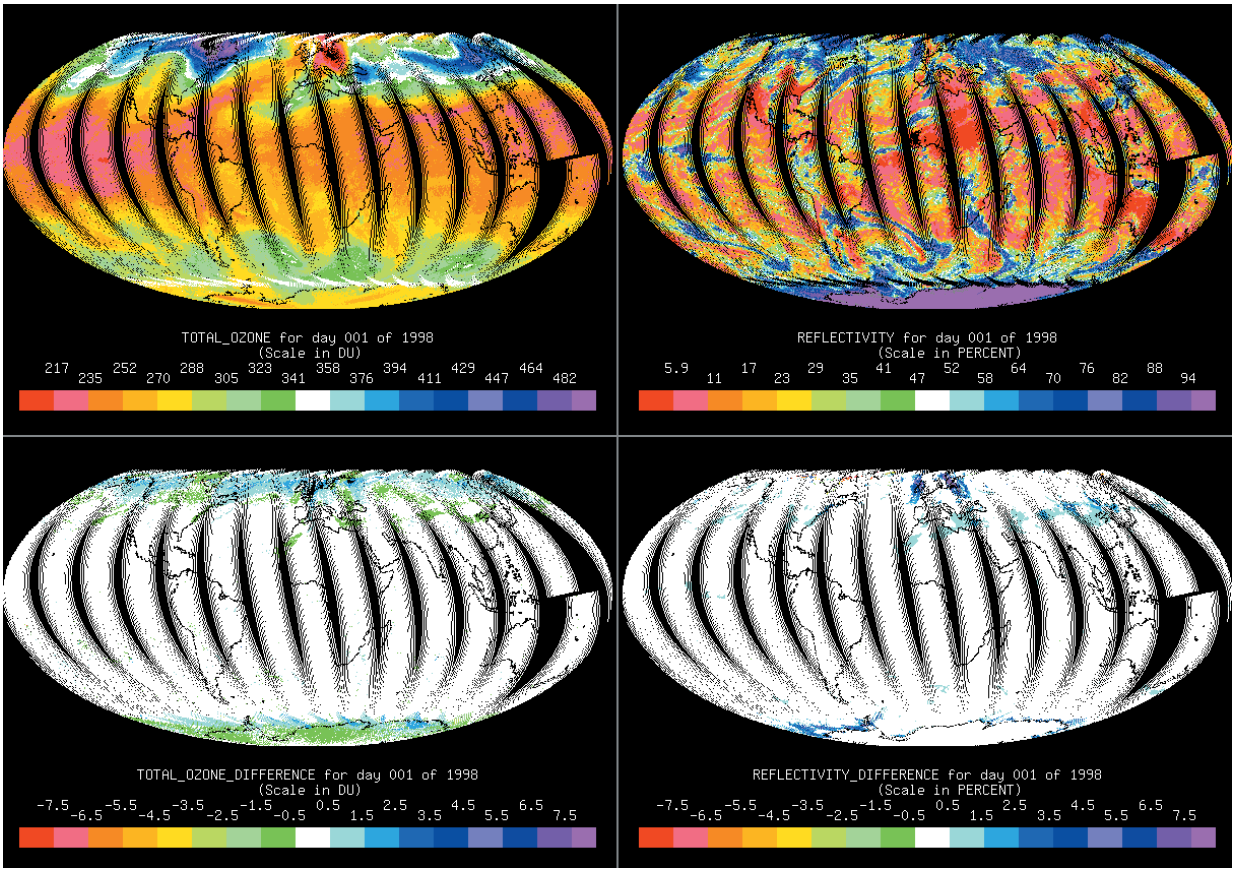

Figure 24. Total ozone and surface reflectivity data from the TOMS instrument.

Contact: Al Fleig, afleig@ltpmail.gsfc.nasa.gov

Satellite Programs

A major activity in Biospheric Sciences concerns management of present and future satellite missions, either as Project Manager, Project Scientist, and Instrument Scientist or in the calibration and validation of the data. Following are descriptions of such activities, ranging from currently orbiting satellites to planned missions.

Flight Programs

Landsat and the Land Cover Satellite Project Science Office

Thirty years ago, on July 23, 1972, NASA launched the first Landsat satellite, beginning what is now the longest record of the Earth's continental surfaces as seen from space. It is a record unmatched in quality, detail, coverage and value. Today, both Landsat-5 and Landsat-7 continue to operate, routinely gathering multispectral imagery of the globe for environmental assessments, land-cover mapping, and commercial applications. Since launch in April 1999, some 291,000 Landsat-7 ETM+ scenes had been archived at the USGS EROS Data Center (EDC) in Sioux Falls, South Dakota, which also holds an archive of over 500,000 Landsat-5 TM scenes.

At NASA GSFC, the Land Cover Satellite Project Science Office (LPSO) is responsible for long-term calibration/validation of Landsat-7 ETM+ data, and ensuring the scientific success of the Landsat-7 mission. Working jointly with personnel from the USGS (which is responsible for mission operations), the LPSO team tracks the radiometric and geometric character of acquired data, and makes recommendations to enhance their quality and scientific utility. As described in other sections of this document, the LPSO is also actively involved in the NMP Earth Observing-1 mission, and in formulating the Landsat Data Continuity Mission, the designated follow-on to Landsat-7.

Key Landsat-related accomplishments during 2002 included:

Landsat On-Orbit Performance and Calibration: The Landsat-7 ETM+ on-orbit performance and calibration is evaluated and maintained through the cooperative efforts of LPSO at Goddard Space Flight Center and USGS via the Landsat-7 Image Assessment System (IAS) at the EROS Data Center. NASA contributes primarily radiometric expertise and analyses, and funds and coordinates the acquisition and processing of vicarious radiometric calibrations via an RTOP under the Land Cover and Land Use Change program. USGS operationally maintains and updates the calibrations and processing systems, conducts the operational processing and provides primarily geometric expertise and analyses. Vicarious radiometric calibration efforts are conducted by the University of Arizona (K. Thome), Rochester Institute of Technology (J. Schott), NASA/Jet Propulsion Laboratory (F. Palluconi) and South Dakota State University (D. Helder). The results reported at recent meetings have shown that: (1) the ETM+ reflective calibration continues to be excellent with accuracy to better than 5%, (2) the stability of the bands is better than 0.5% per year, (3) the ETM+ thermal band has an accuracy compared to ground measurements of better than 0.6 degrees K and (4) the stability of the thermal band is better than 0.1% per year. The teams have recommended that the current calibration be retained for the reflective and thermal bands as the significance of the currently reported trends is unclear.

A new effort to develop an atmospheric correction tool for the ETM+ single thermal band was initiated in 2002. This methodology accesses the global National Centers for Environmental Prediction (NCEP) atmospheric profiles and can calculate atmospheric correction parameters for any Landsat-5 or Landsat-7 thermal band image for which there is a coincident atmospheric profile. This tool can be accessed via the Landsat web site (http://landsat.gsfc.nasa.gov/).

The LPSO and the USGS EDC have also been involved in an effort to reconstruct the 19-year radiometric calibration history of the Landsat-5 Thematic Mapper. The team listed above, as well as P. Teillet from the Canada Center for Remote Sensing, are involved. The reflective band record has been reconstructed from the data from the best-behaved TM internal calibration lamp combined with an absolute anchoring to the Landsat-7 ETM+ calibration during simultaneous imaging of the two instruments in June 1999. The new procedure will replace the scene-by-scene use of the internal calibrator data from all three lamps. EDC expects to have the new calibration processing methodology in place by Spring 2003. Data processed after this point in time will be tied to the Landsat-7 calibration and will provide a radiometrically consistent data set for Land Cover Studies since 1984.

Landsat Team Receives Pecora Award: Darrel Williams, Landsat Project Scientist from NASA GSFC, and RJ Thompson, Director of the USGS EROS Data Center were chosen to jointly receive the William T. Pecora Award for 2001 on behalf of the entire Landsat-7 Team at the biannual Pecora Conference which was held in Denver, Colorado in mid-November, 2002. The Pecora Award is presented annually by the Department of the Interior (DoI) and NASA to recognize outstanding contributions by individuals or groups toward the understanding of the Earth by means of remote sensing. The Pecora Award was established in 1974 to honor the memory of Dr. William T. Pecora, former Director of the U.S. Geological Survey and DOI Under Secretary, whose early vision and support helped establish what we know today as the Landsat satellite program.

Validation of the Landsat-7 Long-term Acquisition Plan: Unlike coarse-resolution sensors like MODIS and AVHRR, Landsat sensors do not acquire data at all times, but instead are switched on to acquire particular scenes of interest. The Landsat-7 Long-term Acquisition Plan (LTAP) specifies where and when Landsat-7 ETM+ data are to be acquired, in order to create a scientifically optimal global archive. In general, the LTAP seeks to avoid cloud contamination in Landsat imagery by "looking ahead" using NOAA cloud predictions, and seeks to acquire a seasonally-refreshed global archive, concentrating on particular intervals when local vegetation shows greatest change (dynamics) as derived from AVHRR NDVI data.

Although anecdotal evidence has suggested that the Landsat-7 LTAP is a success, 2002 marked the first rigorous validation of its performance. Dr. Samuel Goward (U. Maryland) and Terry Arvidson (Lockheed-Martin) led the validation activities, and were supported by LPSO personnel Darrel Williams, Brian Markham, Richard Irish, Jeffrey Masek, as well as personnel from the Landsat Mission Operations Center (MOC) and USGS EDC. The group concluded that the LTAP was generally doing an excellent job of providing seasonal, global coverage. However, too few scenes were acquired for the northern boreal forests, while too many scenes were acquired of desert environments (North Africa, Arabia). A boreal acquisition campaign for 2003 will attempt to remedy this situation. The validation activity also concluded that cloud avoidance was working well (a 25% decrease in archive cloud contamination compared to a non-avoidance scenario), and that there was no scientific need to gather data for which the predicted cloud-cover was greater than 80% outside of the United States. This change was implemented in the Landsat-7 MOC during 2002. A separate validation of the Landsat Automated Cloud Cover Assessment (ACCA) system indicated that cloud cover figures calculated from acquired images were accurate to within 10%, 95% of the time.

Earth As Art: In celebration of the 30th anniversary of the first Landsat launch, NASA and the USGS created an exhibit called "Landsat: Earth as Art." The exhibit highlighted images that were selected on the basis of aesthetic appeal, and also served to introduce the public to Landsat data. The exhibit opened July 17 at the Library of Congress in Washington, D.C. A selection of the "Landsat: Earth as Art" images was on display in the Russell Office Building Rotunda in Washington, D.C., July 20 - 26, and throughout the fall at the Arizona Science Center in Phoenix, Ariz. Another exhibit was recently on display in Rapid City, S.D., at the Children's Science Center. During December,

2002, the exhibit received considerable media attention, with coverage by CNN, CBS, Newsday, and others, resulting in numerous downloads of imagery from the "Earth as Art" website.

Australian Greenhouse Office Use of Landsat Data: Dr. Darrel Williams served on the review panel for the Australian Greenhouse Office's "Carbon Accounting Team" in May 2002. The Greenhouse Office has created a multi-temporal Landsat data base for the entire continent of Australian to assess the extent and productivity of vegetation communities within Australia since the early 1970's, in support of the United Nations Framework Convention on Climate Change (UNFCCC) and the Kyoto Protocol. This multitemporal data set may be the most robust continental scale Earth observation data set of its type ever assembled, and sets a new standard for scientific and policy use of the Landsat archive.

NSLRSDA Archive Advisory Committee: The U.S. Geological Survey's (USGS) National Satellite Land Remote Sensing Data Archive (NSLRSDA) was established in 1992 to maintain a permanent, comprehensive Government archive of global Landsat and other land remote sensing data. Drs. Darrel Williams of NASA GSFC and Samuel Goward, University of Maryland have served on the Archive Advisory Committee (AAC) for several years, and in 2002, they focused their attention on assessing the robustness of the annual global Landsat MSS and TM coverage available in the Archive at EDC. Their activities will continue in 2003, and working in concert with the Chief Archivist at EDC, John Faundeen, they plan to identify geographic "gaps" in the EDC archives and to approach appropriate International Ground Stations to determine if they have coverage in their respective archives that may be used to fill these gaps.

Landsat Global Data Working Group: Drs. Jeffrey Masek and Darrel Williams (NASA GSFC) participated in the Landsat Global Data Working group, chaired by Dr. Anthony Janetos (Heinz Institute), which was charged with developing an acquisition and analysis strategy for the Year 2000 Landsat global data purchase. This dataset will provide global, orthorectified Landsat coverage for the globe for the year 2000, providing a complement to the existing 1990 GeoCover product.

Additional Outreach Activities: During 2002, the LPSO group undertook a variety of outreach activities to educators, policy-makers, and the general public, including:

- GSFC Colloquium on Landsat's 30th Anniversary with Darrel Williams, Vincent Salomonson, and David Skole (U. Michigan)

- Production of "zoom in" visualizations for The Super Bowl and Winter Olympics

- Presentations to high school science teachers on optical remote sensing and Landsat

- Preparation of visual displays for NASA HQ for Congress

- Presentation to Native American students using Landsat data for habitat analysis

Contact: Jeffrey Masek, Jeffrey.G.Masek@nasa.gov

The Earth Observing One (EO-1) Base Mission

The Earth Observing One (EO-1) Base Mission met all of its proscribed goals by the end of calendar year 2002. The original intent of this mission was to validate the onboard technologies through one year of data collection followed by an additional year of analysis. EO-1 was launched from Vandenberg Air Force Base in November 2000. The satellite was tasked to collect data for validation by the Science Validation Team (SVT) during 2001. Early in 2002, processing and distribution of EO-1 data was turned over to the USGS EROS Data Center (EDC) as part of the EO-1 "Extended Mission." The analysis phase of the Base Mission continued through 2002, culminating in the final SVT meeting, held in November 2002.

The SVT completed their analyses of the data gathered during the entire Base Mission period from December 2001 through January 2002 at the end of 2002. The emphasis of the validation is on characterizing the performance of the EO-1 instruments in acquiring remotely sensed measurements contributing to a variety of important earth science applications. The results of many of these studies were presented at IGARSS-2002 EO-1 sessions in June 2002. A special issue of the IEEE Transactions on Geoscience and Remote Sensing (TGARS), devoted to the SVT EO-1 validation results, will appear in early 2003.

The EO-1 Extended Mission offers users in various government agencies, the commercial sector and general research community the opportunity to investigate the potential of applying technology and techniques developed for EO-1 to solving problems in their own areas of interest. With the demise of the Lewis and Orbview-4 spacecrafts, EO-1 uniquely offers a space-borne spectral imaging capability that is not currently available from any other source. The EO-1 Mission requirements specified 1000 acquisitions to yield 200 scene comparisons with Landsat 7. At the end of 2002, EO-1 had acquired almost 7000 scenes. Researchers wishing to schedule acquisitions during the Extended Mission or order data acquired by others during all phases of the mission should access the EDC website at http://eo1.usgs.gov/.

The EO-1 Mission has proven to be highly successful in identifying technologies and techniques to be employed in future earth observing missions. It has provided a test-bed for refining specifications and expectations in the Landsat Data Continuity Mission (LDCM). It has provided a powerful platform for investigating the power of space borne spectral imaging for extracting information about surface processes. The SVT conducted a substantial effort to explore and exploit the uses of spectral imaging and vastly improved multispectral radiometric resolution for earth science applications during the last half of 2002.

Since EO-1 was pointable, it proved to be a valuable tool for monitoring catastrophic events. In addition, the inherent band-to-band registration, due to the ALI chip design and platform yaw steering capability, facilitates the creation of pan-enhanced color composites. Figures 25 through 28 show examples of these capabilities.

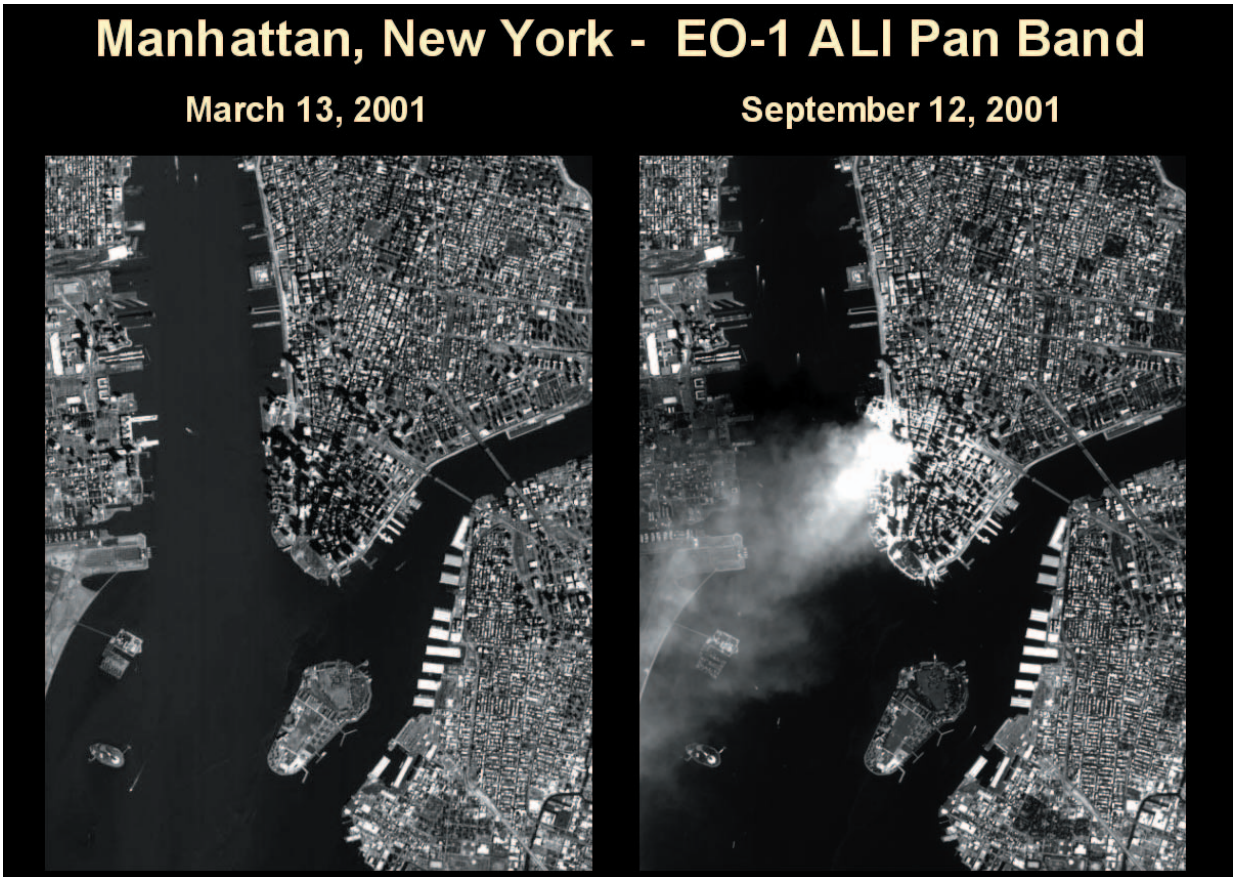

Figures 25. World Trade Center, before and after September 11th attack.

Figure 26. World Trade Center, after September 11th attack. Color Composite.

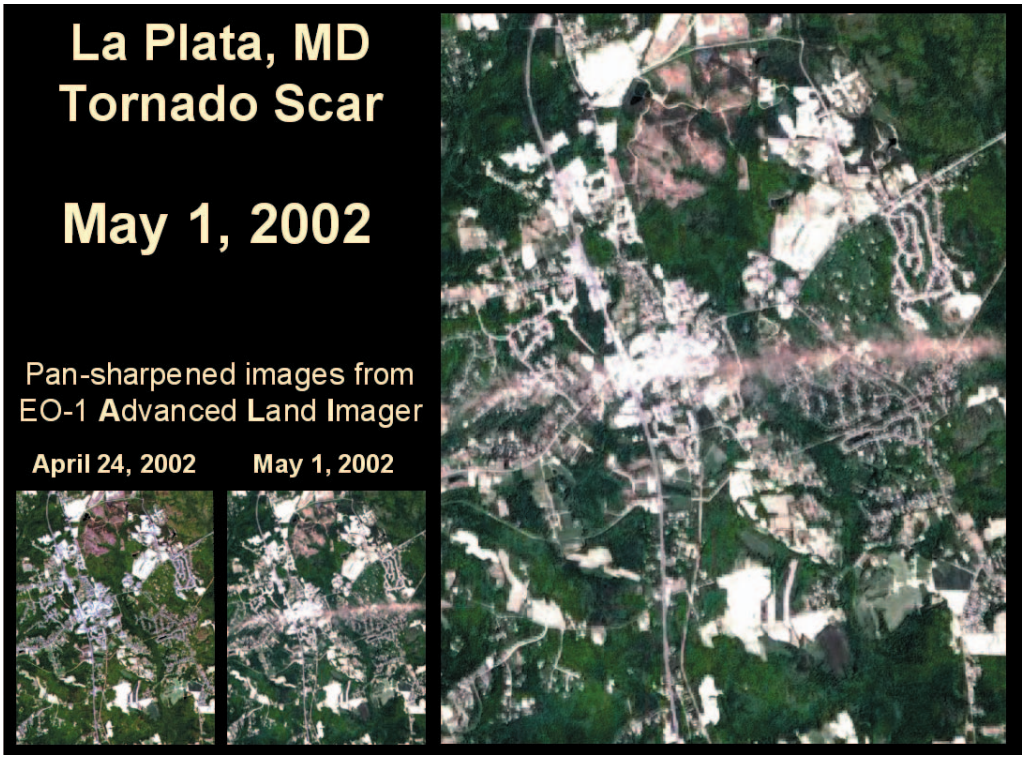

Figure 27. La Plata, Maryland tornado track.

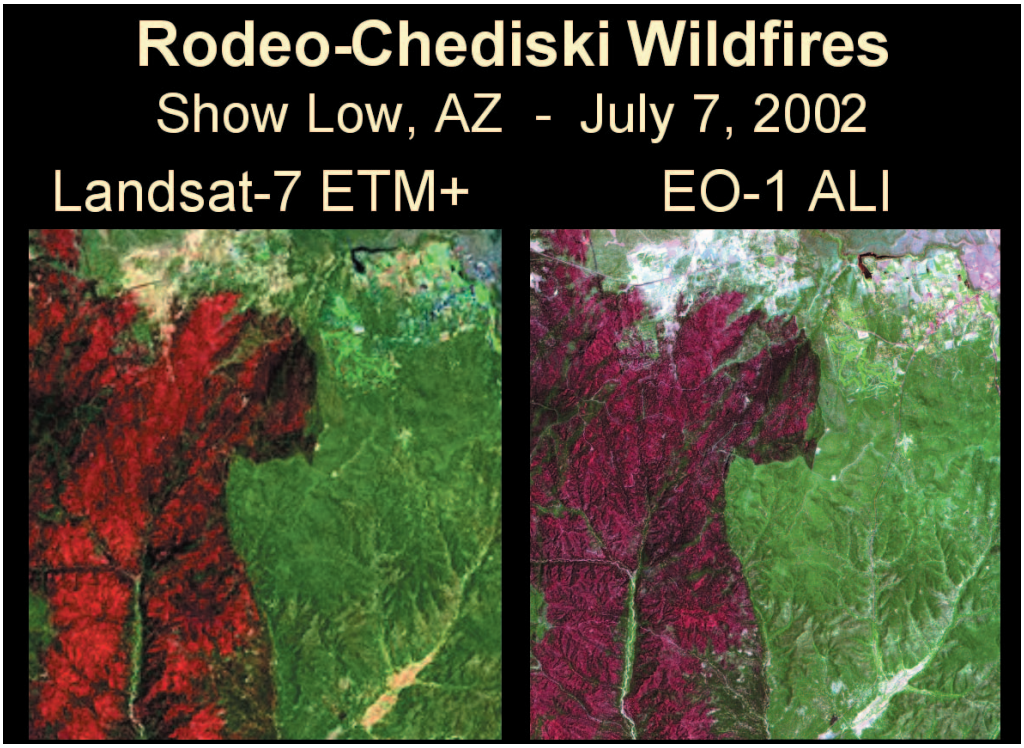

Figure 28. EO-1 / Landsat wildfire delineation. Red coloration indicates burned areas

Contact: Steve Ungar, Stephen.G.Ungar@nasa.gov

EOS Terra Mission

Terra was launched in December 1999, and is the flagship spacecraft for NASA's Earth Observing System Program. The five Terra Spacecraft instruments have been providing scientific data since the instrument doors were opened on February 24, 2000. As of January 2003, all Terra systems were nominal and all instruments were collecting science data. During 2002, the Terra equator crossing time was adjusted to be 10:30 am + 5minutes, through a series of inclination adjust maneuvers. A few instrument anomalies were dealt with this past year. The MODIS instrument scientific formatting equipment was experiencing a problem with frequent resets. Switching to the redundant side system alleviated this problem. MODIS has experienced no other significant problems since this anomaly was resolved. MOPITT experienced a brief cooler malfunction in December. Despite these and earlier problems MOPITT is acquiring science data for both carbon monoxide and methane. MISR and CERES operated throughout the year with no significant problems.

The year 2002 highlights include release of several important scientific data sets. ASTER nearly completed their first global acquisition data set. Through a new agreement with Japan, U.S. Geologic Survey's Eros Data Center (EDC) is now able to process level 1B data. ASTER now charges $55 a scene through EDC. However, NASA investigators do not have to pay this fee. CERES continued to produce validated ERBE like products and is preparing to release new data products. MISR released global cloud, surface and aerosol products. MODIS released validated data sets for several science products, including surface albedo, vegetation leaf area index, sea surface temperature, and aerosol optical depth. MOPITT is producing carbon monoxide data products and releasing them through the Langley DAAC. Terra product definitions and status of Terra Data Products are found on the Internet at:

http://eosdatainfo.gsfc.nasa.gov/eosdata/terra/terra_dataprod.html

The MODIS direct broadcast system continues to provide critical wildfire data to U.S. and foreign fire services. The Terra Flight Operations group was able to successfully negotiate a waiver from NASA's Deep Space Network to allow direct broadcast data over the Canberra, Australia antenna during the recent and severe fire season. Previous agreements stated that Terra must cease direct broadcasting while over the DSN antennae thus severely restricting use of MODIS for fire fighting activities. MODIS is also being used extensively, along with Landsat and other higher resolution instruments, to assess post-fire forest conditions by the U.S. Forest Service Burned Area Emergency Rehabilitation Project.

A new "Natural Hazards" site was opened by the Earth Observatory Web site. This site highlights the use of satellite data for monitoring floods, volcanoes, storms, wild fires and other observable events. For the first time, MOPITT was able to release image data to support news events on the Earth Observatory Web site. In addition the Earth Observatory was awarded a 2002 Webby Peoples Choice Award by The International Academy of Digital Arts and Sciences. The site can be viewed at http://earthobservatory.nasa.gov/

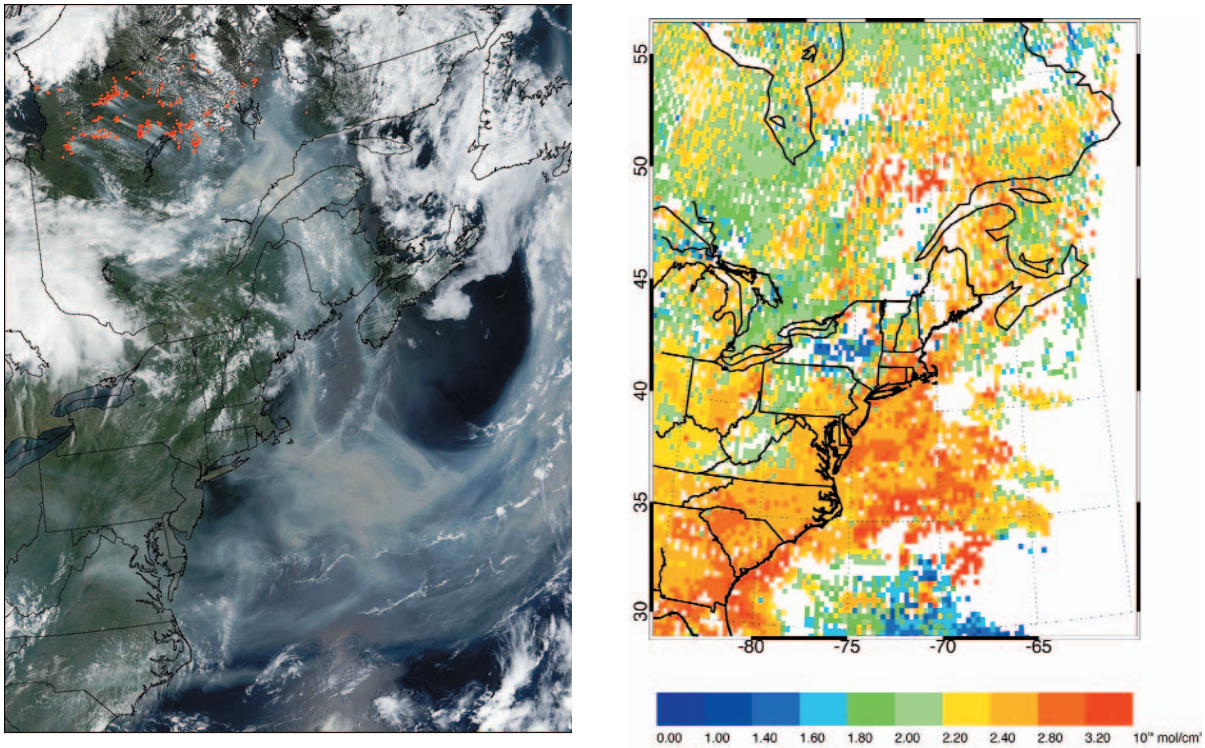

Figure 29. Left, Terra Moderate Resolution Imaging Spectroradiometer (MODIS) image from July 8, 2002, shows smoke from wildfires (red dots) in Québec, Canada, drifting southward over the eastern United States (image courtesy of Terra MODIS Science Team). Right, MOPITT total column Carbon Monoxide image for July 1-8, 2002 period (image courtesy of Terra MOPITT Science Team).

Contact: K.J. Ranson, Kenneth.J.Ranson@nasa.gov

Planned Programs

Landsat Data Continuity Mission (LDCM)

The Landsat Data Continuity Mission (LDCM) will be the follow-on mission to Landsat 7 and will begin providing data by March 2007. NASA traditionally specifies the design of the spacecraft, instruments, and ground systems acquiring data for its Earth science mission. Landsat 7, for example, is a government specified, owned, and operated satellite system. In contrast NASA will procure LDCM data from a privately-owned and commercially-operated remote sensing satellite system. NASA has specified the content, quantity, and characteristics of LDCM data to be delivered by a commercial system operator. A NASA-selected commercial operator will deliver specification-compliant data to NASA's partner in the Landsat Program, the United States Geological Survey (USGS). The USGS will archive the LDCM data at its EROS Data Center (EDC) in Sioux Falls, South Dakota and will distribute Level 1 data products (that is, radiometrically corrected data registered to cartographic projections) to the general public on request. LDCM data will be available from the EDC no later than March 2007. The objective of this new procurement approach is to not only ensure Landsat data continuity for Earth science, but to also foster growth of the commercial remote sensing market place. The hope is that the commercial operator will share the cost and risk of the LDCM with the government and that ultimately Landsat like data will be available from purely commercial sources.

NASA is taking a two-step approach to the LDCM data procurement. The first step, a formulation phase, was conducted in 2002. NASA released a Request for Proposals for formulation phase studies on November 01, 2001. Proposals were received on December 19 and proposal evaluations were performed during early 2002. On March 15 NASA announced the selection of two private companies, Resource 21 of Engelwood, Colorado and DigitalGlobe of Longmont, Colorado, to perform trade studies, develop preliminary designs, and develop business plans. The formulation phase culminated in November with a preliminary design review conducted by each company. NASA worked with each company during the period of performance to refine LDCM data specifications, define calibration requirements, and craft a data policy that protects both the scientific mission and commercial interests. NASA at the same time used the formulation phase results to help write an RFP for the second step of the procurement process, the implementation phase.

The implementation phase RFP was release on January 06, 2003. Following the receipt and evaluation of proposals, NASA will select a single commercial operator to deliver LDCM data to the USGS for a period of five yeas beginning in March 2007. The contract will include a costed option for an additional five years of data. The LDCM Project Science Office within the LTP has worked closely with the GSFC Landsat Project Office on all phases and aspects of the LDCM data procurement process. In particular, LTP scientists were heavily involved in the definition of the LDCM data specifications, the calibration and validation requirements, and the data policies. This involvement will continue through the implementation phase.

Contact: Jim Irons, James.R.Irons@nasa.gov

NPOESS Preparatory Project (NPP)

The NPOESS Preparatory Project (NPP) will launch in 2006 to maintain continuity of certain environmental data sets that were initiated with NASA's Terra and Aqua satellites. It also provides risk reduction for the operational National Polar-Orbiting Operational Environmental Satellite System (NPOESS) scheduled for launch in 2009. NPOESS is designed to supply weather forecasting data to the nation's operational agencies (NOAA and the U.S. Air Force), and is managed by the Interagency Program Office (IPO, a joint agency office composed of NOAA, NASA and the U.S. Air Force members).

The NPP satellite will carry four sensors, including the Visible Infrared Imaging Radiometer Suite (VIIRS), the Cross-track Infrared Sounder (CrIS), the Advanced Technology Microwave Sounder (ATMS) and the Ozone Mapping and Profiler Suite (OMPS). See Figure 26. The addition of a fifth sensor, the Clouds and Earth's Radiant Energy System (CERES), is under consideration. The VIIRS sensor is a 22-band wide field-of-view imaging sensor similar to EOS MODIS. The CrIS and ATMS sensors will work together to provide atmospheric temperature and moisture profiles. The OMPS system, with both nadir and limb-looking sensors, will provide both the ozone total column and vertical profiles.

NPP will launch in late 2006 into an 824 km orbit with a 10:30 equator crossing time at the descending node. The spacecraft will provide direct-to-ground transmission of stored mission instrument data, and also provide direct broadcast of real-time instrument data. Spacecraft flight operations and the spacecraft operations control center will be managed by Northrop Grumman, the NPOESS Shared System Performance Responsibility (SSPR) contractor.

The NPP operational products are designed to meet the needs of NASA, NOAA and the Air Force. The NPOESS Interface Data Processing Segment (IDPS), also provided by IPO/SSPR, will provide pseudo-operational processing of NPP instrument data for the user agencies. The products directly address 12 of the 23 NASA Earth Science Enterprise key research questions, and provide

16 of the 24 key EOS long-term measurements. NASA will provide additional ground processing capability to the research community for generation of additional research products, such as calibration/validation products and higher-level climate data records. Short- and long-term archive and distribution capabilities to support funded research will also be provided.

NASA currently supports NPP science through its Project Science Group (PSG) and through participation on IPO's Operational Algorithm Teams. In early 2003, NASA will solicit an NPP Science Team to help with sensor and product testing, and to evaluate research needs for additional products. Later, a second team may be solicited to develop climate data records.

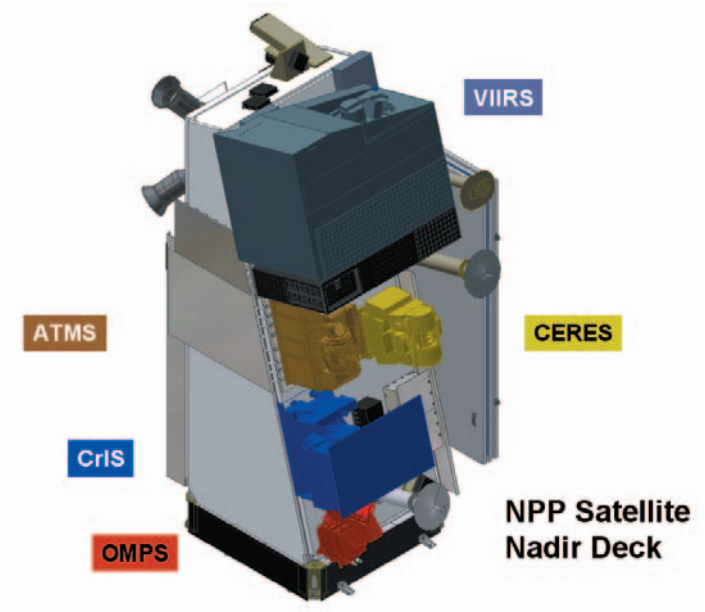

Figure 30. NPP Instruments

Contact: Jeff Privette, Jeffrey.L.Privette@nasa.gov

International Programs

Laboratory personnel over the past ten or more years have taken on management or coordination roles in major international field campaigns. These field campaigns involve interdisciplinary scientists from NASA, other federal agencies, universities, and international partners performing in-depth research into various ecosystems such as grassland prairies in Kansas (FIFE), northern hardwoods in Maine (FED), and boreal forest in Canada (BOREAS). Web sites: http://boreas.gsfc.nasa.gov/ and http://fedwww.gsfc.nasa.gov/. Below are two such activities: LBA (tropical forest in Amazonia) and a new project, the Northern Eurasia Earth Science Partnership Initiative (NEESPI)

The Large Scale Biosphere-Atmosphere Experiment in Amazonia (LBA)

The Large Scale Biosphere-Atmosphere Experiment in Amazonia or LBA Project is led by the Ministry of Science and Technology in Brazil with international cooperation from NASA and the European Union. The LBA Project is composed of various independently funded components. NASA currently funds the LBA-ECO and LBA-HYDROMET components, which are both managed at the Goddard Space Flight Center. LBA-ECO activities have been continuing since a formal agreement was signed in 1998 and field infrastructure was put in place to start field activities in 1999 (see Figure 31 and 32).

Figure 31. Both triangular radio towers (as shown) and walk-up platform towers have been erected at numerous sites within the forests in the Amazon basin to facilitate measurements of atmospheric gas profiles, water vapor, etc. These measurements of seasonal and interannual variation effects on biosphere-atmosphere fluxes will run for 3 to 5 years.

Since the completion of the implementation phase in 2001, the LBA-ECO Field Operations Team has taken on a stronger role in terms of logistical, administrative, and technical support for the investigators working in the field in Brazil. The high level of scientific activity made it necessary to open a new support office in Santarem. The emphasis of this new office is to support long-term researchers and students. In 2002, a new flux tower was put into operational use in a recently logged area. Data from this new tower will be used to compare fluxes with a neighboring tower in an undisturbed forested area. The Project Office also continues to maintain the various tower sites, base camps, and office facilities for the LBA-ECO researchers, as well as a large fleet of vehicles and other support equipment.

After three years of data collection, LBA is maturing and the collaboration in the project between American and Brazilian scientists is producing excellent scientific results. The LBA-ECO Project Office at Goddard provided extensive help in organizing the Second International LBA Science Conference in Manaus, Brazil (July 7-10, 2002). Staff members created a web site to facilitate conference registration, information dissemination, as well as abstract submission, review, and acceptance. The meeting was attended by hundreds of participants, including prominent scientists reporting results from their LBA research. The Project Office at Goddard worked with their Brazilian

counterparts to provide logistical support during the meeting and participated in the LBA press and media support group to help disseminate conference results to media outlets.

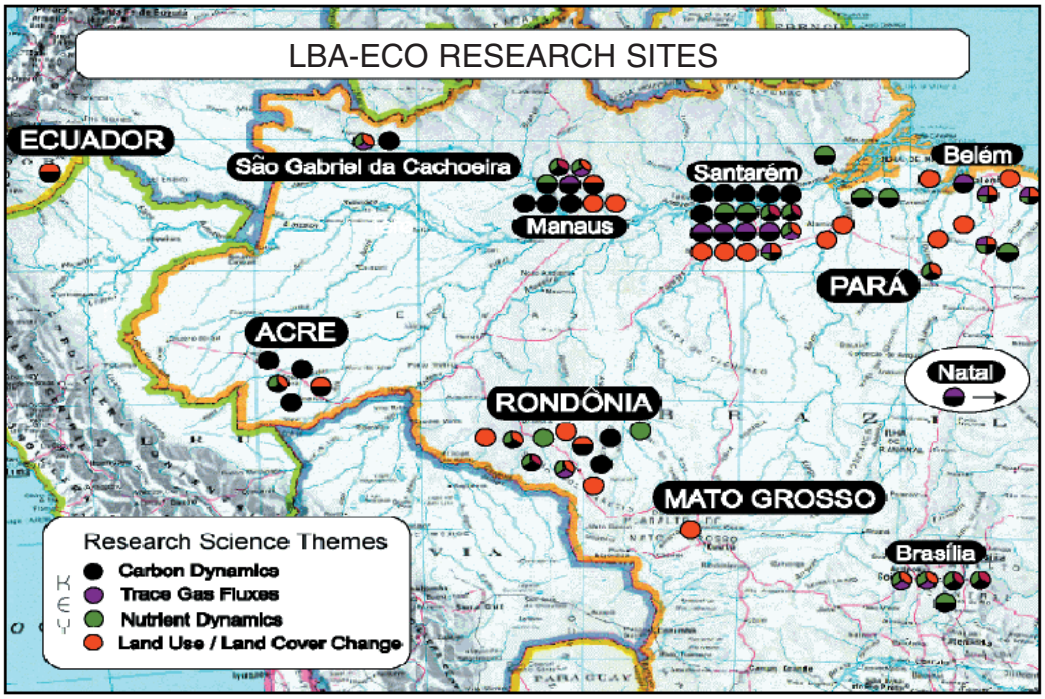

Figure 32. The geographical distribution of LBA-ECO research sites throughout the Amazon basin is illustrated in this map, along with a summary of the range of research themes being conducted at each location.

Some of the results presented at the conference indicate that fires in the Amazon region produce an overabundance of aerosols that serve as condensation nuclei, reducing the amount of condensed water on individual nuclei and inhibiting rain events in the Amazon region. Results from a study in a wetland area suggest that a greater amount of carbon is released from rivers than previously thought. New research proposed in Phase 2 at Ilha Bananal will provide further evidence on the nature and origin of wetland fluxes.

In 2002, the LBA-ECO Project Office prepared comprehensive reports of the LBA-ECO Phase 2 proposals for reviewers to make preliminary selections. The selected proposals strike a good balance between continuing data collection at existing sites in order to build up long-term data sets and starting new lines of research in other environments in the Amazon where new instrumentation will be installed.

The LBA-Air-ECO science teams have made significant progress in planning their flights and preparing for their campaigns in 2003. However, the lack of a signed implementing agreement for LBA-Air-ECO has hampered efforts to prepare for the Air-ECO activities in Brazil.

The LBA-ECO Project Office created a new website, coinciding with the start of Phase 2. The organization and layout of the website were greatly improved, making it easier for the science team to communicate with LBA-ECO logistics support staff, the LBA-ECO Project Office, the LBA Central Office, NASA program managers, and Brazil's Ministry of Science and Technology. As a result of adopting open-source software using Linux and mySQL, the cost savings to NASA was estimated to be $50,000 per year.

LBA-ECO collaborated with Brazil's Ministry of Science and Technology and other Brazilian agencies to support the LBA Student Conference in Belém (March 16-21, 2002). The conference

gave students that support LBA research the opportunity to present the results of their work to LBA investigators and other students.

As Phase 1 of LBA-ECO has ended, progress has been made in getting data sets registered into the LBA data system. From November 2001 to December 2002, total registrations (data sets and posters) in Beija-flor (the metadata search and data retrieval system for LBA) increased from 323 to 586, an increase of 81% -- 73% of which were contributed by LBA-ECO funded investigations. Furthermore, registration of actual data sets (excluding posters) increased from 231 to 379 data sets: an increase of 148 data sets -- 91% of which were contributed by LBA-ECO funded investigators. This number is particularly significant given that LBA-ECO investigation teams compose only about half of all LBA investigation teams.

During the past year, communications between the LBA-ECO Project Office and the LBA Central Office in Brazil have improved significantly. The two offices have bi-weekly teleconferences to discuss issues related to LBA-ECO activities in Brazil and how to work with the Central Office by openly sharing information to resolve problems mutually.

Contact: Darrel Williams, Darrel.L.Williams@nasa.gov

The Northern Eurasia Earth Science Partnership Initiative (NEESPI)

Various NASA funded investigations and others in recent years have shown that the circumboreal region of the Earth has been warming up. One of the results has been a gradual increase in vegetation lushness and growing season in parts of the Northern Hemisphere. However, Eurasia appears to be especially impacted and greening even more than North America, with more lush vegetation for longer periods of time. Evidence continues to mount that the northern latitude warming during the past few decades has been affecting the structure and function of terrestrial ecosystems in high-latitude regions and may be affecting regional and global climate systems.

Northern Eurasia is also a major player in the global carbon budget, particularly the boreal forests and peatlands, as circumpolar boreal forest systems alone contain more than 5 times the carbon of temperate forests and almost double the amount of carbon in the World's tropical forests. Climate warming induces natural terrestrial processes to release more carbon dioxide and methane, a particular concern in the boreal zone where more than 60% of the carbon exists as peat. Much of the peat is imbedded in permafrost, which may be melting. Additionally, a warmer boreal zone climate is resulting in more frequent and larger fires in all of the terrestrial ecosystems. Reasonable models speculate that these effects could eventually lead to a "runaway greenhouse" scenario. Aforestation and reforestation may not help either, as recent research has shown that in large parts of northern Eurasia, the decrease in surface albedo by forestation is as important as carbon sequestration in its forcing of climate. As a result, forest carbon sinks in these regions could exert a much smaller cooling influence than expected, or even exert an overall warming influence.

As a result, interest within the global change research community has grown dramatically in the past decade. Northern Eurasia is a vast area about which relatively little is known in the Western scientific world, and as the region where temperature rise is expected to be the greatest, feedbacks to the atmosphere are potentially large. These effects coupled with the dramatic political shifts throughout this region in the early 1990's and the attendant potential for rapid economic development, create the possibility for large and significant biological, climatic and socioeconomically coupled land use changes throughout this region.

Science issues for northern Eurasia are growing in global importance not only in relation to climate change and carbon, but also for aquatic, arid, and agricultural systems, snow and ice dynam-

ics, and human health issues among others. For example, these changes have substantial implications for human livelihoods in high-latitude regions and elsewhere through effects on subsistence resources (e.g., reindeer populations and their movements), commercial fisheries resources, infrastructure, and industrial activity; and they may have consequences for the functioning of the entire Arctic System. Some of the potential effects include the way that water and energy are exchanged with the atmosphere, radiatively active gases are exchanged with the atmosphere, and freshwater is delivered to the Arctic Ocean. Socioeconomic changes during the past 10 years are found in the death rate of men increasing by more than six times and of women by nineteen times with the current average life expectancy of 37 years for the native peoples in the Russian part of northern Eurasia.

The International Geosphere Biosphere Program (IGBP) reported this year that the circumboreal region containing northern Eurasia is one of the critical "Switch and Choke" points in the Earth system, and proposed that what is needed for this region is a "glue" to fit multidisciplinary pieces of research together into a fully integrated, regional program. Generally, small and/or "detached" research projects are conducted in this huge, biologically, hydrologically, and climatically diverse and complicated region, and the countries and institutions in this region generally do not have the expertise and/or resources to independently conduct and coordinate the needed research.

At the 12th Meeting of the U.S.-Russian Earth Science Joint Working Group (ESJWG) held in Moscow in October 2002, NASA and the Russian Academy of Sciences formally agreed to work together to develop a program of research that is called the Northern Eurasia Earth Science Partnership Initiative, or the NEESPI. The mission of the NEESPI is to ". . . identify the critical science questions and establish a program of coordinated research on the state and dynamics of terrestrial ecosystems in northern Eurasia and their interactions with the Earth's climate system to enhance scientific knowledge and develop predictive capabilities to support informed decision-making and practical applications."

The agreement followed more than two years of informal discussions and planning between U.S. and Russian scientists and administrators across Russia and in the U.S. These discussions culminated in the first formal NEESPI Workshop, which was held at the Presidium of the Russian Academy of Sciences in Moscow in February 2002; and involved more than 50 participants from many Russian governmental agencies and private organizations as well as representatives from the U.S. and Canada.

The NEESPI provides a framework for currently funded NASA Earth Science investigations (>20 studies during the past 3 yrs.) to improve their sharing of resources and data and information, and to facilitate research collaborations and resolving Russian bureaucratic issues, and to promote study integration and planning. The NEESPI currently assists in seeking and providing funding for short term research projects (over the next 1-2 yrs) and seeks to provide the "glue" (longer term, multi-source funding) for developing an integrated understanding of the Earth system for this part of the globe.

The NEESPI leadership is working with other U.S. agencies/scientists and international partners to develop a formal NEESPI Science Plan for an integrated, interdisciplinary Earth science project that will be viable for securing funding from multiple NASA programs and other national and international partner organizations to subsequently implement a program of research to address key science questions of global significance in Northern Eurasia. The first NEESPI Science Plan Workshop is scheduled for April 2003 in Suzdal, Russia, and the publication of the NEESPI Science Plan is expected in the first quarter of 2004 – just prior to the first Northern Eurasia Earth Science Conference to be held in Ann Arbor, Michigan in May 2004. The goal is to have a full NEESPI Project Implementation in two, three-year phases to begin in CY2005.

Contact: Donald W. Deering, Donald.W.Deering@nasa.gov

Refereed Journal Publications

Amr, S., M.B. Bollinger, M. Myers, R.G. Hamilton, S.Weiss, M. Rossman, L. Osborne, S. Timmins, **D.S. Kimes**, **E.R. Levine**, C.J. Blaisdell. Asthma and its environmental triggers in Baltimore City Public Schools., Annals of Asthma, Allergy, and Immunology, 90:34-44, 2002

Anyamba, A., K.J. Linthicum, **R. Mahoney,** and **C.J. Tucker**, Mapping Potential Risk of Rift Valley fever outbreaks in African Savannas using Vegetation Index Time Series Data, *Photogrammetic Engr. & Remt.Sens., 68*, No. 2, 137-145, 2002.

Anyamba, A., **C.J. Tucker,** and **R. Mahoney**, From El Niño to La Niña: Vegetation response patterns over East and Southern Africa during 1997-2000 period, *J. Climat,15, 3096-3103, 2002.*

Birkett, C.M., L.A.K. Mertes, T. Dunne, M. Costa, and M. Jasinski,, Altimetric Remote Sensing of the Amazon: Application of Satellite Radar Altimetry, *J. Geophys.Res.,* 107 (D20), 10.1029/2001JD000609, 4th September, 2002.

Blaisdell, C., M.B. Bollinger, S. Timmins, **D. Kimes, E. Levine**, M. Myers, and S. Weiss. Temporal and Spatial Trends in Pediatric Asthma Hospitalization in Maryland. *J. of Asthma*, 39(7):567-575, 2002**.**

Bogaert J., Zhou L., **Tucker C.J.,** Myneni R.B., and Ceulemans R., Evidence for a persistent and extensive greening trend in Eurasia inferred from satellite vegetation index data. *J.Geophys. Research-Atmospheres*_107(D11): DOI 10.1029/2001JD001075, 2002.

Bounoua L., R. S. DeFries, **G. J. Collatz**, P. S. Sellers, H. Khan, Effects of land cover conversion on climate, *Climate Change 52*, 29-64, 2002.

Chang CI, Chiang SS, **Smith JA**, et al., Linear spectral random mixture analysis for hyperspectral imagery, IEEE T GEOSCI REMOTE 40 (2): 375-392 FEB 2002

Chin, M., P. Ginoux, **S. Kinne**, O. Torres, **B. N. Holben**, B. N. Duncan, R. V. Martin, J. A. Logan, A. Higurashi, and T. Nakajima, Tropospheric aerosol optical thickness from the GOCART model and comparisons with satellite and sunphotometer measurements*, J. Atmos. Sci., 59*, 461-483, 2002.

Christopher, S.A., J. Zhang, **B.N. Holben**, and S.-K. Yang, GOES-8 and NOAA-14 AVHRR retrieval of smoke aerosol optical thickness during SCAR-B, *Int. J. Remote Sensing, 23*, 4931-4944, 2002.

Coe, M.T., M.H. Costa, A. Botta, and **C.M. Birkett**, Long-term simulations of discharge and floods in the Amazon Basin, *J. Geophys. Res*., 107 (D20), 10.1029/2001JD000740, 4th September, 2002.

DeFries R. S., **L. Bounoua**, **G. J. Collatz**, Human modification of the landscape and surface climate in the next 50 years. *Global Change Biology 8,* 438-454, 2002

Dickinson R. E., J. A. Berry, G. B. Bonan, **G. J. Collatz**, C. B. Field, I. Y. Fung, M. Goulden, W. A. Hoffman, R. B. Jackson, R. Myneni, P. J. Sellers, M. Shaikh, Nitrogen Controls on climate model evapotranspiration, *Journal of Climate 15*, 278-295, 2002.

Drake, J.B., R.O. Dubayah, D.B. Clark, **R.G. Knox, J.B. Blair,** M.A. Hofton, R.L. Chazdon, J.F. Weishampel, and S.D. Prince, Estimation of tropical forest structural characteristics using large-footprint lidar, *Remote Sensing of Environment 79:* 305 - 319, 2002.

Drake, J.B., R.O. Dubayah, **R.G. Knox,** D.B. Clark, and **J.B. Blair**, Sensitivity of large-footprint lidar to canopy structure and biomass in a neotropical rainforest, *Remote Sensing of Environment 81:* 378 - 392, 2002.

Dubovik, O., **B.N.Holben**, **T.F.Eck**, **A.Smirnov**, Y.J.Kaufman, M.D.King, D.Tanre, and **I.Slutsker**, Variability of absorption and optical properties of key aerosol types observed in worldwide locations, *J.Atm.Sci*., *59*, 590-608, 2002.

Dubovik, O., B. N. Holben, **T. Lapyonok**, A. Sinyuk, M. I. Mishchenko, P. Yang and **I. Slutsk**er, Non-spherical aerosol retrieval method employing light scattering by spheroids, *Geophys. Res. Lett.*, 10.1029/2001GL014506,24 May 2002.

Guillevic P., R. D. Koster, M. J. Suarez, **L. Bounoua, G. J. Collatz**, S. O. Los, S. P. P. Mahanama, Influence of the interannual variability of vegetation on the surface energy balance - A global sensitivity study, *Journal of Hydrometeorology 3*, 617-629, 2002

Hicke J.A., Asner G.P., Randerson J.T., **Tucker C.J., Los S.O**., Birdsey R., Jenkins J.C., Field C., Holland E., Satellite-derived increases in net primary productivity across North America, 1982-1998, *Geophysical Research Letters* 29(10):10.1029 2001GL013578, 2002.

Hicke J.A., Asner G.P., Randerson J.T., **Tucker C.J., Los S.O**., Birdsey R., Jenkins J.C., Field C., Trends in North American net primary productivity derived from satellite observations, 1982-1998 *Global Biogeochemical Cycles* 16(2): 10.1029/2001GB001550, 2002.

Ichoku, C., R. Levy, Y.J., Kaufman, L.A. Remer, R.-R. Li, V.J. Martins, **B.N. Holben**, N. Abuhassan, **I. Slutsker, T.F. Eck**, C. Pietras, Analysis of the performance characteristics of the five-channel Microtops II Sun photometer for measuring aerosol optical thickness and precipitable water vapor, *J. Geophys. Res*., 10.1029/2001JD001302, 12 July 2002.

Ichoku, C., D. A. Chu, S. Mattoo, Y. Kaufman, L.A. Remer, D. Tanre, **I. Slutsker** and **B.N. Holben**, A spatio-temporal approach for global validation and analysis of MODIS aerosol products, Geophys. Res. Lett., 29, No 12, 10.1029/2001GLO13206,2002.

Justice, C. O., **Giglio, L**., Korontzi, S., Owens, **J., Morisette**, **J. T., Roy, D., Descloitres**, J., Alleaume, S., Petitcolin, F., & Kaufman, Y., The MODIS Fire Products. *Remote Sensing of Environment., 83*, 244–262, 2002.

Justice C. O., J. R. G. Townshend, **E. F. Vermote**, **E. Masuoka**, **R. E. Wolfe**, **N. Saleous**, **D.**

P. Roy, **J. T. Morisette**, An overview of MODIS Land data processing and product status, *Remote Sensing of Environment, 83* (1-2), 3-15 2002.

Kaufman, Y.J., **O.Dubovik**, **A.Smirnov**, and **B.N.Holben**, Remote sensing of non-aerosol absorption in cloud free atmosphere, *Geophys. Res. Lett., 29*(18), 1857, doi:10.1029/2001GL014399, 2002.

Kaufman, Y.J., D. Tanre, **B.N. Holben**, S. Mattoo, L.A. Remer, **T.F. Eck**, J. Vaughan, and B. Chatenet, Aerosol radiative impact on spectral solar flux at the surface, derived from principal-plane sky measurements, *J. Atmos. Sci., 59*, 635-646, 2002.

Kharuk V.I., **K.J Ranson**., V.V Kuzmichev., T.A. Burenina, A. Yu. Tikhomirov, and S.T. Im, An analysis of temporal dynamics of the Siberian silkmoth outbreaks, *Russian J. of Remote Sensing*, 4: 1-12, 2002.

Kimes, D., J. Gastellu-Etchegorry, and P. Esteve, 2002, "Recovery of Forest Canopy Characteristics Thorough Inversion of a Complex 3D Model", *Remote Sensing of Environment, 79*:320-328.

Little, E.E., R.D. Calfee, D.L. Fabacher, C. Carey, V.S. Blazer, and **E.M. Middleton**, Effects of ultraviolet-B radiation on toad early life stages, Environmental Science and Pollution Research, online electronic publication, 10 pp., 6/30/2002

Lefsky, M.A., W.B. Cohen**, D.J. Harding**, G.G. Parker, S.A. Acker, and S.T. Gower, Lidar remote sensing of aboveground biomass in three biomes, *Global Ecology and Biogeography*, 11(5): 393-399, 2002.

Lefsky, M.A., W.B. Cohen, G.G. Parker, and **D.J. Harding**, Lidar remote sensing for ecosystem studies, *Biosciences*, 52(1), 19-30, 2002.

Lobell D.B., Hicke J.A., Asner G.P., Field C.B., **Tucker C.J., Los S.O.** Satellite estimates of productivity and light use efficiency in United States agriculture, 1982-98, *Global Change Biology* 8(8):722-735, 2002.

Los, S. O., **C. J. Tucker**, **A. Anyamba**, M. Cherlet, **G. J. Collatz**, **L. Giglio**, **F. G. Hall** and J. Kendall, *The Biosphere: A Global Perspective***,** Chapter 5, **In** A. K. Skidmore (Editor) Environmental Modelling with GIS and Remote Sensing, pp. 70-96, Taylor & Francis, New York, 2002.

Morisette, J.T.. Privette, J.L., and Justice, C.O., A framework for the validation of MODIS land products, *Remote Sensing of Environment*, 83 (1-2) 77-96, 2002

Myneni, R.B., Y. Knyazikhin, **J.L. Privette**, J. Glassy, Y. Tian, Y. Wang, S. Hoffman, X. Song, Y. Zhang, G.R. Smith, A. Lotsch, M. Friedl, **J.T. Morisette**, P. Votava, R.R. Nemani, and S.W. Running, Global products of vegetation leaf area and fraction absorbed PAR from year one of MODIS data, *Remote Sensing of Environment*, 83 (1-2) 214 - 231, 2002.

O'Neill, N.T., **T.F.Eck**, **B.N.Holben**, **A.Smirnov**, A.Royer, and Z.Li, Optical properties of boreal forest fire smoke derived from Sun photometry, *J. Geophys. Res., 107(D11)*, 10.1029/2001JD000877, 2002.

Otter, L.B., R.J. Scholes, P. Dowty, **J.L. Privette**, K. Caylor, S. Ringrose, M. Mukelabai, P. Frost, O. Totolo, E.M. Veenendaal, The SAFARI 2000 wet season campaigns, *S. African J. Sci*., *98(3/4),* 131-137, 2002

Otterman, J., A. Karnieli, **T. Brakke**, D. Koslowsky, H.-J. Bolle, D. Starr, and H. Schmidt, Desert scrub optical density and spectral-albedo ratios of impacted-to-protected areas by model inversion, *Int. J. Remote Sensing, 23*, 3959-3970, 2002.

Petitcollin F. and **Vermote E. F**., 2002, Land Surface Reflectance, Emisivity and Temperature from MODIS Middle and Thermal Infrared data, Remote Sensing Of Environment, 83,1-2,112-134.

Privette, J.L., R.B. Myneni, Y. Knyazikhin, M. Mukelabai, Y. Tian, Y. Wang, G. Roberts and S. Leblanc, Early spatial and temporal validation of MODIS LAI in the Southern Africa Kalahari, *Remote Sens. Environ*., *83*, 232-243, 2002.

Qin, Wenhan, S.A.W. Gerstl, **D.W. Deering** and N.S.Goel, Characterizing leaf geometry for grass and crop canopies from hotspot observations: A simulation study. *Remote Sens. Environ.* 80 (1), 100-113, 2002.

Ouaidrari, H., Goward, S.N. , Czajkowski, K.P. , Sobrino, J.A**., Vermote, E.F.**, 2002, Land Surface Temperature Estimation from AVHRR Thermal Infrared Measurements: An Assessment for the AVHRR Land Pathfinder II Data Set, Remote Sensing of Environment, 81, 114-128.

Randerson J. T., **G. J. Collatz**, J.E. Fessende, A. D. Muno, C. J. Still, J. A. Berry, I. Y. Fung, N. Suits, A. S. Denning, A possible global covariance between terrestrial gross primary production and 13C discrimination: Consequences for the atmospheric 13C budget and its response to ENSO, *Global Biogeochemical Cycles , 16*, 1136, doi:10.1029/2001GB001845, 2002.

Remer, L.A., D.Tanre, Y.J.Kaufman, C.Ichoku, S.Mattoo, R.Levy, D.A.Chu, **B.N. Holben**, **O.Dubovik**, **A.Smirnov**, J.V.Martins, R.-R.Li, Z.Ahmad, Validation of MODIS aerosol retrieval over ocean*, Geophys.Res.Lett*., *29(12)*, 10.1029/2001GL013204, 2002.

Rogers, D.J, Myers, M. F**., Tucker, C.J.,** Smith, P.F., White, D. J., Backenson, P.B., Eidson, M., Kramer, L.D., Baaker, B., and Hay, S**.,** Predicting the distribution of West Nile Fever in North America using satellite sensor data. *Photogram. Eng. Remote Sens.* 68:112-136, 2002.

Rosenqvist, Å., **C.M. Birkett**, E. Bartholomé, and G. De Grandi, Using satellite altimetry and historical gauge data for validation of the hydrological significance of the JERS1 SAR (GRFM) mosaics in Central Africa*, Int. J. Rem. Sens.*, 23 (7), 1283-1302, 2002.

Roy D. P., **J. S. Borak**, **S. Devadiga**, **R. E. Wolfe**, **M. Zheng**, **J. Descloitres**, The MODIS Land

product quality assessment approach, *Remote Sens. Environ., 83* (1-2), 62-76, 2002.

Sabol, D. E., Gillespie, A. R., Adams, J. B., Smith, M. O., and **Tucker, C. J.,** Structural stage in Pacific Northwest forests estimated using simple mixing models of multispectral images. *Remote Sens. Environ.* 80:1-16, 2002.

Schaaf, C.B., Gao, F., Strahler, A.H., Lucht, W., Li, X., Tsang, T., Strugnell, N.C., Zhang, X., Muller, J-P., Lewis, P., Barnsley, M., Hobson, P., Disney, M., Roberts, G., Dunderdale, M., Doll, C., d'Entremont, R, P., Hu, B., **Privette, J.L.,** and **Roy, D**., The at-launch MODIS BRDF and albedo science data product, *Remote Sens. Environ.*, *83*, 135-148, 2002.

Schafer, J.S., T. F. Eck, B. N. Holben, P. Artaxo, M. A. Yamasoe, and A. S. Procopio, Observed reductions of total solar irradiance by biomass-burning aerosols in the Brazilian Amazon and Zambian Savanna, *Geophys. Res. Lett., 29*, 1823, doi:10.1029/2001GL014309, 2002.

Schafer , J.S., B.N. Holben, T.F. Eck, M.A. Yamasoe and P. Artaxo, Atmospheric effects on insolation in the Brazilian Amazon: Observed modification of solar radiation by clouds and smoke and derived single scattering albedo of fire aerosols, *J. Geophys. Res*., 107, 8074, doi:10.1029/2001JD000428, 2002.

Shabanov, N.V., Zhou, L., Knyazikhin, Y., Myneni, R.B. and **Tucker, C.J.,** Analysis of interannual changes in northern vegetation activity observed in AVHRR data from 1981 to 1994. *IEEE Trans. Geosci. Remote Sens.* 40:115-130, 2002.

Smirnov, A., **B.N.Holben**, **T.F.Eck**, **I.Slutsker**, B.Chatenet, and R.T.Pinker, Diurnal variability of aerosol optical depth observed at AERONET (Aerosol Robotic Network) sites, *Geophys. Res. Lett.* , *29* (23), 2115, doi:10.1029/2002GL016305, 2002.

Smirnov, A., B.N.Holben, Y.J.Kaufman, **O.Dubovik**, **T.F.Eck**, **I.Slutsker**, C.Pietras, and R.Halthore, Optical properties of atmospheric aerosol in maritime environments, *J.Atm.Sci*., *59*, 501-523, 2002.

Smirnov, A., **B.N.Holben**, **O.Dubovik**, **N.T.O'Neill**, **T.F.Eck**, D.L.Westphal, A.K.Goroch, C.Pietras, and **I.Slutsker**, Atmospheric aerosol optical properties in the Persian Gulf region, *J. Atm. Sci., 59*, 620-634, 2002**.**

Sun, G., K.J. Ranson and V.I. Kharuk, Radiometric slope correction for forest biomass estimation from SAR data in the Western Sayani Mountains, Siberia. *Remote Sensing of Environment*, 79: 279-287, 2002.

Swap, R.J., H. Annegarn, J.T. Suttles, J. Haywood, M.C. Helmlinger, C. Hely , P.V. Hobbs, **B.N. Holben** , J. Ji , M.D. King , T. Landmann , W. Maenhaut, L. Otter, B. Pak , S.J. Piketh , S. Platnick, **J.L. Privette**, et al., The SAFARI 2000 dry season campaigns, *S. African J. Sci., 98(3/4)*, 125-130, 2002

Takamura, T, T. Nakajima, O **Dubovik, B. Holben, S. Kinne**., Single-Scattering albedo and

radiative forcing of various aerosol species with a global three-dimensional model, *J. of Climate*, 15,4, 333-352, 2002.

Tian, Y., C.E. Woodcock, Y. Wang, **J.L. Privette**, et al., Multiscale analysis and validation of the MODIS LAI product. I. Uncertainty Assessment, *Remote Sens. Environ.*, *83*, 414-430, 2002.

Tian, Y., C.E. Woodcock, Y. Wang, **J.L. Privette**, et al., Multiscale analysis and validation of the MODIS LAI product over Maun, Botswana. II. Sampling Strategy, *Remote Sens. Environ.*, *83*, 431-441, 2002.

Tucker, C. J., Wilson, J. M., **Mahoney, R., Anyamba, A**., Linthicum, K. J., and Myers, M., 2002. "Climatic and Ecological Context of Ebola Outbreaks". *Photogrammetric Engineering and Remote Sensing*, (2002) 68, N0. 2,147-152.

Ungar, S., Overview of the Earth Observing One (EO-1) Mission, *IEEE Geosci. & Remote Sens. Newsletter, v. 123*, 3-6.

Vermote, E. F. and **Roy, D.P**.,2002, Land Surface Hot-Spot observed by MODIS over Central Africa, *International Journal of Remote Sensing*, Cover Letter, (11): 2141-2143.

Vermote E.F., **El Saleous N**, Justice C, 2002, Atmospheric correction of the MODIS data in the visible to middle infrared: First results, Remote Sens. Environ., 83, 1-2, 97-111.

Wolfe R. E., M. Nishihama, A. J. Fleig, J. R. Kuyper, D. P. Roy, J. C. Storey, F. S. Patt, Achieving sub-pixel geolocation accuracy in support of MODIS land science, *Remote Sensing of Environment, 83* (1-2), 31-49, 2002.

Zhao, T.X.-P., L.L.Stowe, **A. Smirnov**, D. Crosby, J. Sapper, and C.R.McClain, Development of a global validation package for satellite oceanic aerosol retrieval based on AERONET sunphotometer observations and its application to NOAA/NESDIS operational aerosol retrievals, *J.Atm.Sci*., *59*, 294-312, 2002.

Proceedings Papers, NASA Technical Documents, etc.

Arvidson, T., **R. Irish, B. L. Markham, D. L. Williams**, J. Feuquay, J. Gasch, and S. N. Goward, Validation of the Landsat 7 Long Term Acquistion Plan, In Proc of the Pecora 15, Held 10-15 November 2002, Denver, CO, ASPRS, Bethesda, MD, 2002.

Campbell, P.K.E., **E.M. Middleton**, **L.A. Corp**, J.E. McMurtrey III, M.S. Kim, **E.W. Chappelle**, and **L.M. Butcher**, Contribution of chlorophyll fluorescence to the reflectance of corn foliage, Proceedings, International Geoscience and Remote Sensing Symposium, IGARSS 2002, Toronto, Canada, 3 pp., CD-ROM 6/24/2002.

Corp, L.A., **E.M. Middleton**, J.E. McMurtrey, **P.K. Entcheva Campbell**, M.S. Kim, **E.W. Chappelle,** and **L.M. Butcher**, Fluorescence imaging techniques for monitoring vegetation, Proceedings, International Geoscience and Remote Sensing Symposium, IGARSS 2002, Toronto,

Canada, 3 pp., CD-ROM 6/24/02.

Descloitres, J., R. Sohlberg, J. Owens, **L. Giglio**, C. Justice, M. Carroll, **J. Seaton**, M. Crisologo, M. Finco, K. Lannom, and T. Bobbe, 2002: The MODIS Rapid Response Project. Proceedings of the IEEE International Geoscience and Remote Sensing Symposium (IGARSS'02).

Dorofeev F.V., D.M.Kabanov, M.V.Panchenko, S.M.Sakerin, **A.Smirnov**, S.A.Turchinovich, **B.N.Holben**, and N.N.Shchelkanov, AROSIBNET: preliminary results and prospective, Symposium on Aerosols in Siberia, Tomsk, Russia, November 24-27, 2002.

Holben, B. N., O. Dubovik, T. F. Eck, A. Smirnov, A. Vermeulen, I. Slutsker, AERONET: Ground-based aerosol characterization, Proceedings of a Workshop: "Air Pollution as a Climate Forcing", East-West Center, Honolulu, April 29-May 3, 2002, pp. 77-78.

Kharuk V. I. and **K.J. Ranson**, Landsat-7 in evaluation of oilfield exploitation impact on the south Evenkiya larch dominant communities. In Proceedings of SPIE's Symposium "Remote Sensing of the Atmosphere, Ocean, Environment, and Space". Vol. 4898. 23-27 October 2002, Hangzhou, China, 2002.

Kharuk, V.I.**K. J. Ranson**, V. Tret'yakova, and A. Shashkin, 2002. Reaction of the larch dominated communities on climate trends //In: Proceedings of an International Symposium "Improvement of Larch (Larix sp) for better growth, stem form and wood quality". France, Gap September 16-21. INRA, ed. L.E. Paques. Pp. 289-295.

Le Moigne, J., A. Cole-Rhodes, R. Eastman, T. El-Ghazawi, K. Johnson, S. Kaewpijit, N. Laporte, **J. Morisette**, N. Netanyahu, H. Stone and I. Zavorin, Multiple Sensor Image Registration, Image Fusion and Dimension Reduction of Earth Science Imagery, Proceeding of FUSION'2002, pp 999-1006, 2002.

Le Moigne, J., A. Cole-Rhodes, R. Eastman, K. Johnson, **J. Morisette**, N. Netanyahu, H. Stone and I. Zavorin, 2002, " Multi-Sensor Image Registration for On-the-Ground or On-Board Science Data Procesisng," Science Data Processing Workshop, SDP'2002, Greenbelt, January 2002, pp. 961-966.

Levine, E. and **D. Kimes**. Assessing Links between Ecosystem Health and Childhood Asthma. Proceedings of the Healthy Ecosystems, Healthy People Conference, Washington, DC., 2002.

Levine, E., J. Robin, and S. Riha, Using Satellite Imagery and GLOBE data to Model Soil Dynamics, Proc. 6th Annual GLOBE meeting, Chicago, IL., 2002.
http://www.globe.gov/fsl/html/templ.cgi?model_soil&lang=en&nav=1

Levine, E., J. Robin, and N.Owe. Effects of Acid Rain on Soil pH, Proc. 6th Annual GLOBE meeting, Chicago, IL, 2002. http://www.globe.gov/fsl/html/templ.cgi?acid_soil&lang=en&nav=1

Levine, E. and J. Robin, Understanding Soil Color Patterns across the Globe", Proc. 6th Annual

GLOBE meeting, Chicago, IL, 2002.
http://www.globe.gov/fsl/html/templ.cgi?soilcolor_paterns&lang=en&nav=1

Lindsay, F.E. and **Masek, J**. (2002). A Tale of Two Cities: Characterizing Urban Growth Using Variable Resolution Remote Sensing Data. Proceedings for the Third International Symposium Remote Sensing of Urban Areas. Istanbul, Turkey. Vol.2, pp.591-599.

Markham, B. L., J.L. Barker, J.A. Barsi, **E. Kaita**, K.J. Thome, D.L. Helder, F. D. Palluconi, J.R. Schott, and P. Scaramuzza, Landsat-7 ETM+ radiometric stability and absolute calibration, In Proc. of SPIE/Europe, Held 23-27 September 2002, Crete, Greece, SPIE, Bellingham, WA, 2002.

Marshall, C.H., R.A. Pielke, Sn., **L.T. Steyaert**, T.M. Cronin, D.A. Willard, J.W. Jones, T.J. Smith III, and **J.R. Irons**, Impact of land-use management practices in Florida on the regional climate of South Florida, Conference Paper Presented at the 13th Symposium on Global Change and Climate Variations (online AMS Web Proceedings, Session J8.6, 3 pp.), 82nd Annual Meeting of the American Meteorological Society, Orlando FL, January 13-17, 2002.

McClain, C.F., **F.G. Hall, G.J. Collatz,** S.R. Kawa, W.W. Gregg, J.C. Gervin, **J.B. Abshire**, A.E. Andrews, C.D. Barnet, M.J. Behrenfeld, P.S. Caruso, A.M. Chekalyuk, L.D. Demaio, A.S. Denning, J.E. Hansen, F.E. Hoge, **R.G. Knox, J.G. Masek,** K.D. Mitchell, J.R. Moisan, T.A. Moisan, S. Pawson, M.M. Rienecker, S.R. Signorini, **C.J. Tucker**, *Science and Observation Recommendations for Future NASA Carbon Cycle Research,* National Aeronautics and Space Administration, Goddard Space Flight Center, Greenbelt, Maryland, NASA/TM - 2002 - 210009, 2002.

McMurtrey, J.E., **E.M. Middleton**, **L.A. Corp**, **P.K. Entcheva Campbell**, **L.M. Butcher**, **E.W. Chappelle**, and W.B. Cook, Fluorescence responses from nitrogen plant stress in 4 Fraunhofer band regions, Proceedings, International Geoscience and Remote Sensing Symposium, IGARSS 2002, Toronto, Canada, 3 pp., CD-ROM 6/24/02.

Middleton, E.M., **P.K. Entcheva Campbell**, J.E. McMurtrey, **L.A. Corp**, **L.M. Butcher**, and **E.W. Chappelle**, 'Red Edge' optical properties of corn leaves from different nitrogen regimes, Proceedings, International Geoscience and Remote Sensing Symposium, IGARSS 2002, Toronto, Canada, 3 pp., CD-ROM 6/24/02.

Middleton, E.M., J.E. McMurtrey, **P.K.E. Campbell**, **L.A. Corp**, **L.M.Butcher**, and **E.W. Chappelle,** Optical and fluorescence properties of corn leaves from different nitrogen regimes, Proceedings, 9th International Symposium on Remote Sensing (Remote Sensing 2002), SPIE- the International Society for Optical Engineering. Crete, Greece, Sept.23-27, 12 pp.

Nishihama M., **R. E. Wolfe**, **J. Kuyper**, **A. J. Fleig**, MODIS Geolocation Error Analysis Developments, IGARSS 2002: IEEE International Geoscience and Remote Sensing Symposium and 24th Canadian Symposium On Remote Sensing, Vols I-VI, Proceedings - Remote Sensing: Integrating Our View Of The Planet, 3661-3663, 2002.

Panchenko M.V., S.A.Terpugova, V.S.Kozlov, V.N.Uzjegov, S.M.Sakerin, D.M.Kabanov, B.D.Belan, M.Yu.Arshinov, T.M.Rasskazchikova, P.P.Anikin, G.I.Gorchakov, A.A.Isakov, V.M.Kopeykin, M.A.Sviridenkov, E.G.Semutnikova, **B.N.Holben**, and **A.Smirnov**, Echo of the Moscow region fires in the atmosphere of West Siberia, Symposium on Aerosols in Siberia, Tomsk, Russia, November 24-27, 2002.

Pedelty, J.A., Morisette, J.T., and Smith, J.A., "A Comparison of Landsat-7 ETM+ and EO-1 ALI Images Over Rochester, NY", SPIE, Aerosense Conference, Orlando FL, April 1-5, vol. 4725, p. 357-365, 2002.

Pinheiro, A.C., **J.L. Privette**, **R. Mahoney** and **C.J. Tucker** (2002), Directional effects in AVHRR Land Surface Temperature over Africa, Recent Adv. Quantitative Remote Sens. [J.A. Sobrino, ed.], Univ. of Valencia Publ., Spain, pp. 971-978.

Pinzón, J. E.,. "Using HHT to successfully uncouple seasonal and interannual components in remotely sensed data." SCI 2002 Proceedings, July 14 - 18, Orlando, FL, p. 78-83, 2002.

Privette, JL, Crystal B. Schaaf, Alan Strahler, Rachel T. Pinker, Michael J. Barnsley and **Jeffrey T. Morisette**, Summary of the International Workshop on Surface Albedo Product Validation, *EOS Earth Observer, 14(2),* 17-18, 2002

Ranson, K.J., K. Kovacs and G. Sun, Accounting for Topographic Slope Effects on Radar Backscatter in Siberian Forests, IGARSS02, Toronto, Canada, 2002.

Ranson, K.J., G. Sun, K.Kovacs and V.I. Kharuk, Utility of SARs for mapping forest disturbance in Siberia. IGARSS02, Toronto, Canada, 2002.

Sato, M., J. Hansen, **O. Dubovik, B. N. Holben**, Black carbon global climate forcing inferred from AERONET, Proceedings of a Workshop: "Air Pollution as a Climate Forcing", East-West Center, Honolulu, April 29-May 3, 2002, pp.106-108.

Schafer, J.S., T.F. Eck, B.N. Holben, P. Artaxo, M.A. Yamasoe, A.S. Procopio, Atmospheric Attenuation Of Total Solar Flux By Clouds and Aerosols At Six Amazonian Sites: 1999-2001, Second LBA International Scientific Conference, Manaus, Brazil, July 7-10, 2002.

Smid, J., **B. Markham**, P. Svzcek and P. Volf, Calibration, regression models and the web, In Proc. of SPIE/Europe, Held 23-27 September 2002, Crete, Greece, SPIE, Bellingham, WA, 2002.

Smirnov, A., **B.N.Holben**, **O.Dubovik**, L.Remer, **T.F.Eck**, and **I.Slutsker**, Atmospheric aerosol optical properties during PRIDE, PRIDE Data Workshop, Miami, FL, February 12-14, 2002.

Smirnov, A., **B.N.Holben**, R.Frouin, G.Fargion, **O.Dubovik**, **T.F.Eck**, and **I.Slutsker**, Atmospheric aerosol optical properties at the SIMBIOS/AERONET sites, SIMBIOS Science Team Meeting, Baltimore, MD, January 15-17, 2002.

Steyaert, L.T. and R.A. Pielke, Sr., Using Landsat-derived land cover, reconstructed vegetation, and atmospheric mesoscale modeling in environmental and global change research, Paper pre-

sented at the 53rd International Astronautical Congress (12 pp.), World Space Congress, Houston, Texas, October 10-19, 2002.

Sun, G., L. Rocchio, J. Masek, D. Williams, and K. J. Ranson, Chracterization of Forest recovery from fire using Landsat and SAR data, Proceedings of IGARSS'02, June 24-28, 2002, Toronto, Ontario, Canada.

Sun. G., K. J. Ranson, Modeling lidar and radar returns of forest canopies for data fusion, Proceedings of IGARSS'02, June 24-28, 2002, Toronto, Ontario, Canada.

S**un, G., J. Masek, D. Williams, L. Rocchio, and K. J. Ranson**, Forest and land-use mapping from temporal MODIS Data, Proceedings of IGARSS'02, June 24-28, 2002, Toronto, Ontario, Canada.

Sun, G. and K. J. Ranson, V. I. Kharuk, and **K. Kovacs**, Preliminary results in verification and evaluation of SRTM data, Proceedings of Advanced Workshop on InSAR Applications, pp. 7-13, Dec. 16-17, 2002, Hong Kong.

Ungar, S., Overview of the Earth Observing One (EO-1) mission, Proceedings of IGARSS'02, June 24-28, 2002, Toronto, Ontario, Canada., 568-571.

Geodynamics and Space Geodesy

The "Geo" sciences in the Laboratory of Terrestrial Physics largely reside in the Geodynamics Branch and the Space Geodesy Branch. Together these groups study a wide range of subjects in the broad disciplines of geophysics, geology, geodesy and geodynamics for both the Earth and solid planetary bodies, especially Mars. Present-day measurements using both surface and satellite data, models derived from these, and other observational and theoretical information are used to help improve our understanding of the evolution of the core, mantle and crust, and their interactions with the fluid envelopes at and above the surface. Major areas of work are described in more detail below, and examples of major accomplishments in the last year are provided in the following sections.

Geodynamics includes studies of the surface and interior of the Earth and planets: their current state, including dynamics, and the processes which operate to produce the observed state and motions. Specific areas of research and study include the following:

(1) Core fluid motions and how it relates to changes in the Earth's magnetic field;

(2) Motions of the Earth's crust and the relationship with earthquake hazard, especially in areas of active subduction;

(3) Vertical rebound of paleolakes and the constraints it provides on lower crustal and upper mantle properties;

(4) Long term orbital-rotational evolution and its relationship to long term climate change;

(5) Magnetic properties of the Earth's crust and the nature of the sources of magnetic anomalies not just on the Earth but on Mars as well;

(6) Topographic characterization of the surface of the Earth and Mars, in the former case to understand landforms associated with active faulting, in the latter case to understand volcanic and tectonic structures and the origin of the fundamental crustal topographic dichotomy, and how large scale impacts affect early crustal evolution.

Space geodesy involves positional studies of the Earth's surface and its orientation in space, the Earth's gravity field, and the use of their time evolution to understand fundamental Earth processes. The latter include mantle convection, plate motion, and fluid mass transports both on the surface (e.g., ocean and atmospheric circulation, land hydrology, icesheets) and in the core. Active areas of work incorporate the following:

(1) Determination of the precise orbits for Earth satellites and planetary spacecraft and determination of the Earth's fundamental reference frame;

(2) Gravity field model development for Earth and other planets, both the static and time-varying components;

(3) Oceanic and solid body tidal processes and the resultant deformation of the Earth;

(4) The effects of redistribution of geophysical fluids (air, water, ice) on the Earth and their manifestation in, for example, the time-variable gravity field and Earth rotation parameters;

(5) Analysis and modeling of space-geodetic Very-Long-Baseline Interferomettry measurements and applications to Earth's rotation studies: and

(6) Development of space techniques that enable precise measurement of the above- mentioned geodetic observables.

Brief descriptions of each of the major areas of work are provided below. Individual significant highlights of the past year are provided, along with contact information for the relevant author.

Background for each of these areas can be found in the 2001 Annual Report. Additional progress and ongoing work for this year is indicated by papers given at national and international meetings during the year.

Geomagnetism

Understanding Geomagnetic Field Variation with Numerical Modeling

Surface and space geomagnetic observations identify that the Earth's magnetic environment varies on a wide spectrum of time scales, from seconds to millions of years. While external sources (e.g. electromagnetic processes in ionsphere and magneosphere) contributes to small and fast varying disturbances near the Earth's surface, the most significant changes arise from the dynamical processes in the Earth's liquid outer core. The outer core is in vigorous convection, driven by gravitational energy released from secular cooling of the Earth. This turbulent convection generates and maintains a strong core field (accounting for 97% of the total magnetic energy observed at the surface of the Earth) that varies on time scales up to millions of years.

The Modular, Scalable, Self-consistent, Three-dimensional (MoSST) numerical model, under constant development in our Laboratory, is able to explain qualitatively the physics of the geomagnetic field generation (geodynamo), and to model possible force balances in the core, such as the Taylor's constraint that governs torsional oscillations on decadal time scales. Advances in this model, together with new geomagnetic observations (from e.g. Ørsted, Champ, Ørsted-2/SAC-C),are making feasible the assimilation of observational data to numerical dynamo simulation. With this research, it could be able to predict long-time geomagnetic secular variation, and to constrain numerical core dynamics modeling via observational results.

In 2002, a new algorithm was introduced to the model that could reduce Computing Processor Unit (CPU) time by one order of magnitude, greatly speeding up the simulation process. The initial testing confirmed the expectation. Further testing and benchmarking are in process prior to fully implementing the algorithm. In addition, activities were advanced on geomagnetic data assimilation. Researchers from Code 921, Code 926 and Data Assimilation Office (DAO) are examining the discrepancies between the MoSST dynamo results, observed geomagnetic field (derived from NASA Comprehensive model that utilizes surface and satellite data from Magsat, Ørsted and Champ, and appropriate assimilation algorithms to produce analysis states for assimilation. These initial results are very encouraging: while there is no correlation between the two results in the absence of any data assimilation, it was found that with a very crude (non-optimized) data insertion (to the modeling results), certain correlation is shown between the two results, as shown in Figure 1.

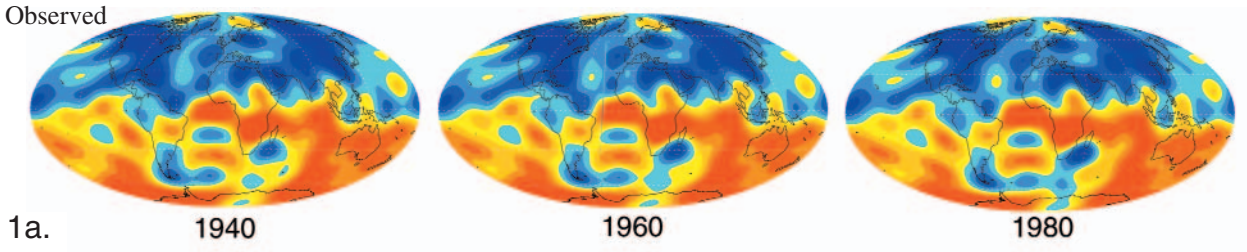

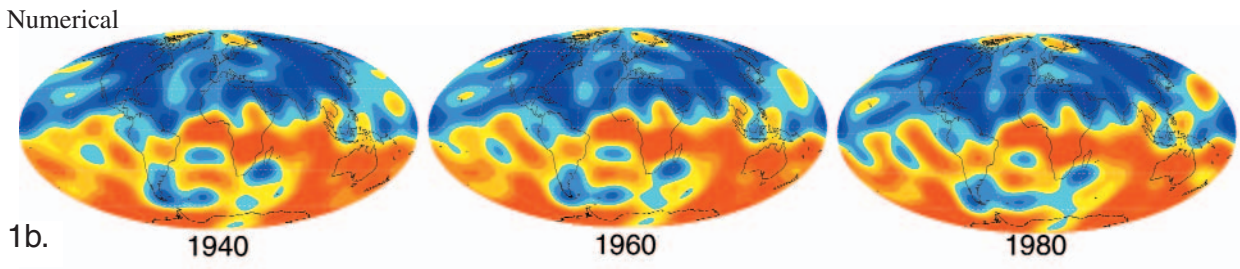

Figure 1. Examples of geomagnetic data assimilation. 1a, (see bottom of previous page) is three snapshots of the observed geomagnetic field morphology at the core-mantle boundary (CMB). 1b (above) is the results from MoSST numerical modeling, in which the analysis state (initial solution) is obtained by inserting the observed field in 1940 to a numerical dynamo solution. The assimilated results are similar to observations, in particular the large-scale features, such as the south Atlantic anomaly.

Contact: Contact: Weijia Kuang, Weijia.Kuang-1@nasa.gov

Comprehensive Field Modeling Paper Published

Ongoing improvements in the development of the GSFC Comprehensive Model reached a milestone with the recent publication of a major paper by Sabaka et al. (2002). This model, based on data from POGO, Magsat, and ground-based observations, represents the state-of-the-art in main field models, and includes parameterized components for the external fields and the lithospheric fields as well as the core field. This same year has seen further refinements in comprehensive modeling (CM) efforts, led by Terry Sabaka, which were reported on at the 4th Ørsted International Science Team meeting in Copenhagen, Denmark in September (see below). The latest improvements include additional data from the most recent magnetic mapping missions, the Danish Ørsted and German CHAllenging Mini-Satellite Payload (CHAMP) satellites. These push the model envelope from an earlier 1960-1985 to a period covering 1960-mid 2002. In addition to extension of the main field secular variation model, a much lower noise lithospheric field was derived (Figure 2). In-situ currents through which Ørsted flies are now modeled in continuous diurnal time.

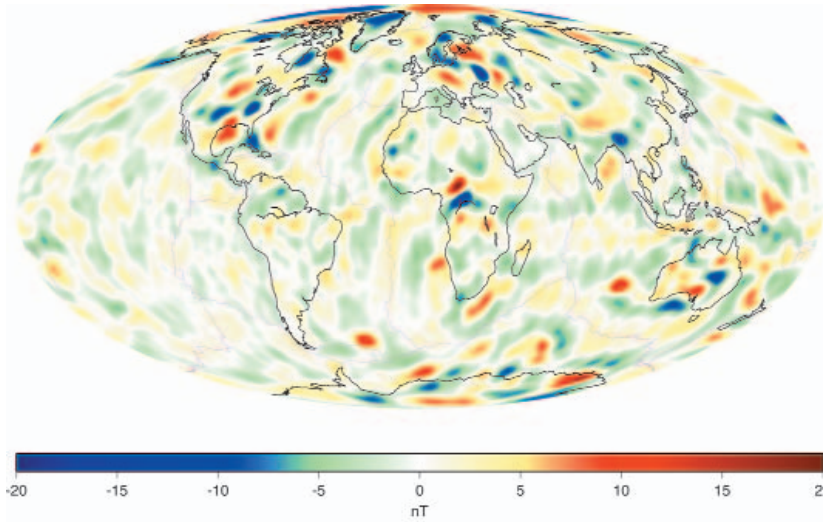

Figure 2. Lithospheric anomalies from the latest Comprehensive Model, including Ørsted and CHAMP data. These have much less noise than in earlier models.

Goddard's comprehensive models are now being used for a variety of applications. For example, the model will be used as the basis for removal of contamination from long-wavelength and diurnal variations in the planned USGS High Altitude Magnetic Mapping (HAMM) mission (an aeromagnetic survey). They have also been used by several research groups and in industry. Current and future programs using the Comprehensive Models include multi-satellite in-flight calibration efforts (Olsen et al., 2002) and mission simulation studies for the proposed SWARM (constellation) mission. Because of the increasing demand for these models, a website is being developed that will offer the latest models, codes and documentation. As part of this outreach effort, Sabaka has developed a versatile forward code available in ANSI Fortran, which computes magnetic and electric current density fields at positions in space and time, and also returns model coefficients in various forms.

References:

Olsen, N., L. Toffner-Clausen, T. Risbo, P. Brauer, J. Merayo, F. Primdahl and T. Sabaka, In-flight calibration methods used for the Ørsted mission, Earth Planets and Space, 2002 (accepted).

Sabaka, T.J., N. Olsen and R.A. Langel, A comprehensive model of the quiet-time, near-Earth magnetic field: phase 3, Geophys. J. Int., 151, 32-68, 2002.

Contact: Terry Sabaka, Sabaka@geomag.gsfc.nasa.gov

American Geophysical Union (AGU) Virtual Session Held

In what may be a template for the future, AGU conducted a "virtual session" during its Spring Meeting, using a web-based protocol to bring together participants from around the world. Mike Purucker was one of the chief organizers of session GP21A, which discussed analysis of selected, previously posted, data from the "mini-constellation" of magnetic field satellites Ørsted, CHAMP and SAC-C. 27 authors and co-authors from nine different countries were involved.

Figure 3. Michael Purucker and 26 other authors from nine countries engaged in a "virtual" session as part of the Spring 2002 AGU Meeting.

One of the main topics discussed was the apparently forced decay of the Earth's dipolar field, which is occurring 10 times faster than would happen if the core dynamo (which generates the field) were suddenly switched off. Growing patches of reversed polarity field are believed responsible. If these continue to grow they could lead to a new reversal of the Earth's field as has occurred in the past.

In preparation for this unique event, 19 days of common satellite data were selected and posted on a dedicated web site, in order that different analysis methods could be applied to the same data. The community was alerted to the virtual session through e-mail with a link provided to the web site. The data became available in January and February, and abstracts submitted and posted in March. Authors submitted their presentations in early May which were made available on the web site. The "live" session was actually held in 2-hour periods on May 28th and 29th.

Following the actual "live" session, discussions were appended in June and a CD with papers and data was distributed to the authors. This follow-up is another unique aspect of the virtual session method of holding international meetings. A meeting report appeared in the August 20 issue of EOS (v.83, p. 368, 2002) in the "About AGU" section.

Contact: Mike Purucker, purucker@geomag.gsfc.nasa.gov

SWARM Constellation Selected by ESA

In May of 2002, the European Space Agency (ESA) selected three new Earth Opportunity Mission candidates for possible launch in the 2007-2009 time frame. One of those missions, SWARM, is a multi-satellite mission designed to study the multitude of magnetic fields encountered in near-Earth space. Mike Purucker is one of several U.S. co-investigators (3 are from GSFC!) on the SWARM science team, and is the only U.S. participant asked by ESA to serve on the Mission Advisory Group (MAG) during the 1.5 year Phase A Study period. At the end of this time a decision will be made as to whether or not SWARM continues on to launch. The main function of the MAG is to formulate the detailed scientific requirements for the new mission and to draft a Mission Requirements Document.

SWARM is to provide the best description yet of the Earth's magnetic environment, including its particles, fields and currents, and how these change over time. These are important to our understanding of the interior of the Earth as well as the likely vulnerability of the Earth to periods of low magnetic field intensity. For example, it is now known that the Earth's main field is decaying at a rate faster than would be expected if the fluid motions in the core were suddenly switched off. This "forced decay" may be leading to a major reversal of the Earth's field.

SWARM will provide important new knowledge of the expanding, deepening South Atlantic Anomaly, with its serious implications for low-Earth satellite operations. Geographically, the recent decay of the Earth's magnetic dipole is largely due to changes in the field in that region. The geomagnetic field models resulting from this mission will have practical applications in many different areas, such as space weather and radiation hazards and understanding of atmospheric processes related to climate and weather.

The SWARM concept consists of a constellation of four satellites in two different polar orbits between 400 and 550 km altitude. Each satellite will provide high-precision and high-resolution measurements of the magnetic field. Together they will provide the necessary observations for the geomagnetic field that is needed to model its various sources.

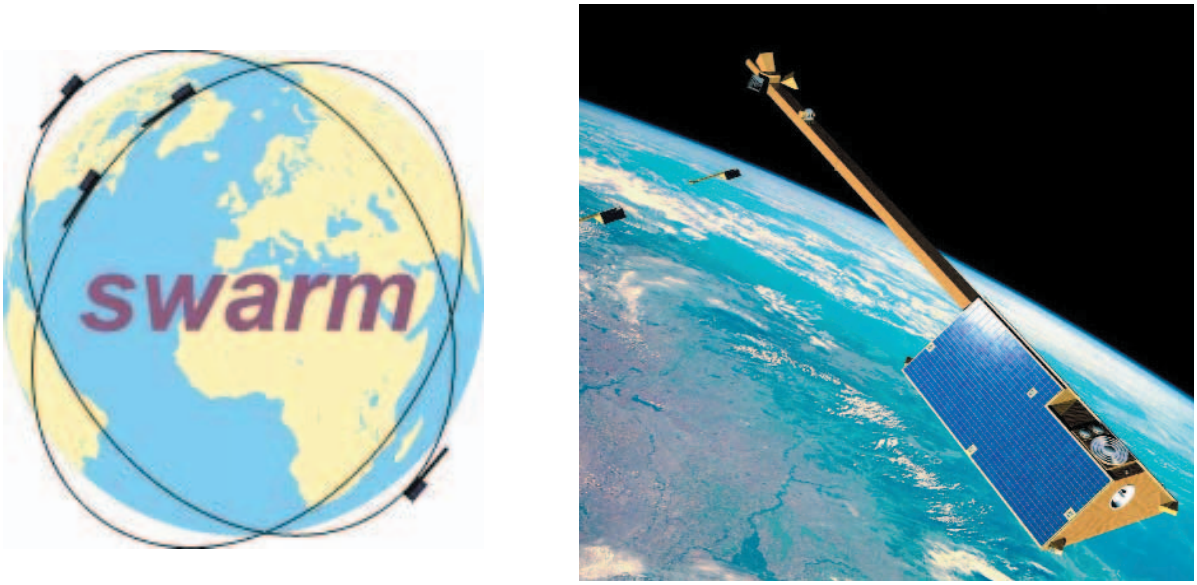

Figure 4. Left: SWARM logo. Right: Artist's concept of the SWARM constellation.

Contact: Mike Purucker, purucker@geomag.gsfc.nasa.gov

Four Attend Ørsted International Science Team Meeting

Figure 5.

In a strong show of the strength of the Goddard Geomagnetics Program, four members of the Lab for Terrestrial Physics (LTP) presented papers at the 4th Ørsted International Science Team meeting in Copenhagen, Denmark on 23-27 September 2002.

Pat Taylor (with co-authors Kim, Potts, von Frese and Frawley) gave a poster on "Satellite altitude geopotential study of the Kursk Magnetic Anomaly (KMA)" and was a co-author on a paper by Kim, von Frese, Park and Taylor "Utility of satellite magnetic observations for estimating near surface magnetic anomalies." Coerte Voorhies had a paper "Narrow scale, weak field flow at the top of Earth's core: evidence from Ørsted, Magsat and secular variation."

Mike Purucker presented along with Sabaka, Olsen and Maus his paper "How have Ørsted, CHAMP, and SAC-C improved our knowledge of the oceanic regions?" Terry Sabaka chaired a session and also gave a paper with Olsen on the "Comprehensive Modeling of the Earth's magnetic field: current status and future prospects". A paper on the most recent field model was published this year (see above).

In addition, Benoit Langlais, a post-doc from France working in the LTP, was a co-author on the paper by Hulot, Eymin, Langlais, Mandea and Olsen, "Small scale structure of the geodynamo inferred from Ørsted and Magsat satellite data", which was presented by Hulot.

Contact: Herb Frey, Herbert.V.Frey@nasa.gov

Magnetic Study of Rocks in the Kola and Krivoy Rog Deep Boreholes

In order to constrain the possible origin of satellite altitude crustal magnetic anomalies, information of the magnetic properties of rocks from the likely source regions is needed. Magnetic properties of rocks from two different boreholes, the Kola superdeep borehole and Krivoy Rog deep borehole, have recently been compared. Highly magnetic serpentinized peridotites and sedimentary rocks affected by sulfide mineralization were recovered at the Kola borehole at a depth interval of 1540-1940 m. The Krivoy Rog borehole recovered highly magnetic iron quartzites of Banded Iron Formations at depths of 1853-2040 m. Extremely high values of remanent magnetization (NRM), magnetic susceptibility (K) and Konigsberger ratio (Qn) are found at approximately the same depths of about 2000 m from both boreholes. There is no obvious reason why high magnetizations should occur at the same depth in two boreholes with such different lithologies. Magnetic surveys and surface sampling in the nearby Krivoy Rog and Kursk Magnetic Anomaly areas have revealed iron quartzites with high magnetization, similar to values given here. AF demagnetization tests suggest that a magnetically hard and stable NRM component, likely caused by hematite, occurred in iron quartzites in different forms and grain sizes ranges.

The data for this study can be found on the Goddard Magnetic Petrology Database now being compiled at the Geodynamics Branch of NASA/Goddard Space Flight Center and published on the web at: http://core2.gsfc.nasa.gov/research/terr_mag/php/MPDB/frames.html

A paper on this work has been submitted to Earth and Planetary Science Letters.

Contact: Katharine Nazarova, nazarova@geom.gsfc.nasa.gov

Narrow-Scale Flow at Top of Earth's Core

In previously published work [Voorhies, 1993, 1995], slow changes of the geomagnetic field were fitted in terms of broad-scale fluid flow by the top of Earth's liquid ferro-metallic outer core. These conditional core surface flow estimates indicate that the molten metal moves at about 8 km/yr. Analysis of magnetic changes from 1945 to 1980 revealed evidence for time-dependent flow by the top of the core, including a curious acceleration of fluid upwelling in an area 2900 km beneath Bermuda. If this acceleration were to continue past 1980, the intense upwelling would tend to blow away magnetic field line footpoints, weakening the magnetic field in this region. As it turned out, the greatest change in geomagnetic field intensity here on Earth's surface between the epoch 1980 Magsat mission and the epoch 2000 Ørsted mission was the 2400 nT (5%) drop in intensity centered on Bermuda.

Further work on the spectra of the main geomagnetic field and of its slow secular variation has revealed some evidence for narrow scale flow across a dynamically weak field. To test this hypothesis against observation, the Ørsted Initial Field Model is used to estimate the radius of Earth's core by spectral methods. The theoretical spectrum tested is obtained from the hypotheses of narrow scale flow across a dynamically weak magnetic field near the top of Earth's core. This describes a low degree, core-source magnetic energy range. Core radius c and amplitude K are estimated by fitting log-theoretical to log-observational spectra at low degrees. Estimates of c for degrees 4 through 12 are 3441 to 3542 km, which do not differ significantly from the seis-

mologic core radius (3480 km). Significant differences do occur if N exceeds 12, which is consistent with appreciable non-core source fields at degrees 13 and above (crustal fields). Similar results are obtained from the 1980 epoch Magsat model CM3. Also used was an expectation spectrum for low degree secular variation (SV) induced by narrow scale flow by the top of the core. The value of c obtained by fitting this form to the mean observational SV spectrum from model GSFC 9/80 is 3470 + 91 km, also in accord with seismologic estimates. This test of the narrow scale flow hypothesis is independent of the weak field hypothesis.

The results were summarized at the 2002 meeting of the Ørsted International Science Team and have been submitted to the Journal of Geophysical Research in the paper "Narrow scale, weak field flow by the top of Earth's core: Evidence from Magsat, Ørsted, and secular variation."

Contact: Coerte Voorhies, voorhies@geomag.gsfc.nasa.gov

Magsat, Ørsted and CHAMP Data Compared

Crustal magnetic anomaly signals are far weaker than either the Earth's main magnetic dipole field or the omnipresent time-varying external fields. In order to establish that these small amplitude, time-invariant magnetic signatures truly represented crustal units and therefore are useful in regional geologic and tectonic studies, it is useful to make satellite magnetic anomaly maps over well known magnetic features. Alternatively, upward-continued ground-based or aeromagnetic surveys can be compared with satellite data. When Magsat was launched in 1979, a satellite altitude (350 km) magnetic anomaly map over the well-known Kursk Magnetic Anomaly (KMA) region of Russia was produced by Taylor and Frawley (1987). The KMA (510 N, 370 E) has long been recognized as one of the largest magnetic anomalies on Earth. It is associated with massive quartz iron-ore formations (the largest known iron-ore deposits on Earth). In February 1999, the Ørsted satellite was launched (Neubert et al., 2001) into a much higher orbit (850 by 613 km) than Magsat. It was assumed by some that crustal magnetic anomalies would not be resolved. Taylor et al. (2000) showed, however, there was a distinct and similar crustal magnetic signal recoverable from Ørsted over this region (Figure 6). Following the launch of CHAMP into a circular 454 km orbit in July 2001, the initial data from this most recent mission was used to make yet another crustal anomaly map of the KMA (Figure 7).

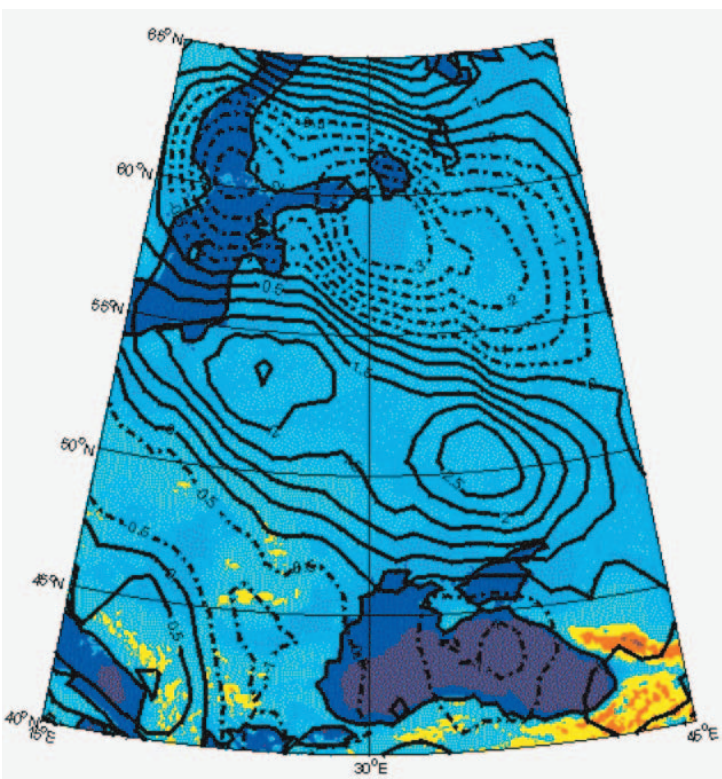

Figure 6. Anomaly maps of Magsat and CHAMP data plotted together over the KMA. Magsat contours are in a gray shade and the CHAMP contours are bolder. Contour interval is 3 nT with zero contour dotted and positive and negative values given by solid and dashed contours respectively.

Figure 7 shows the superposition of both the Magsat and CHAMP magnetic anomaly maps. Note that these anomaly contours over the KMA are very similar, having a generally northwest-southeast trend across this region and mirroring the iron-ore formations.

Differences between these anomaly fields are due to the greater number of orbit profiles from the CHAMP data set and different ranges of altitude and orbital eccentricities between these two satellites. Both the currently operating Ørsted and CHAMP geopotential satellites are able to record magnetic anomalies from sources within the Earth's crust and therefore can be used for geologic and tectonic studies. CHAMP is also recording the gravity field, so future studies will be able to incorporate the magnetic measurements with these gravity data to add another parameter to aid in our modeling of the crustal features of the Earth.

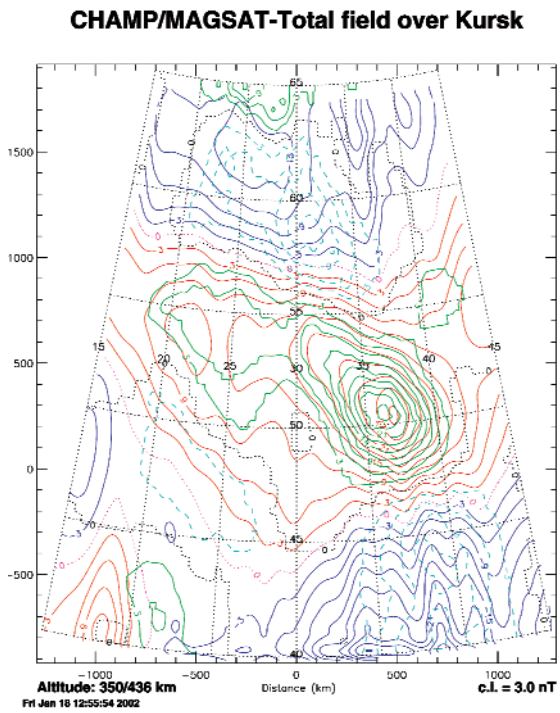

Figure 7. Anomaly maps of Magsat and CHAMP data plotted together over the KMA. Positive Magsat contours are green and positive CHAMP contours are red. Negative contours are blue, solid for CHAMP and dashed for Magsat. Contour interval is 3 nT with zero contour dotted.

[Report taken from: P. Taylor, H. Kim, R. von Frese, L. Potts and J. Frawley, Satellite-Altitude Geopotential Study of the Kursk Magnetic Anomaly (KMA), First CHAMP Mission Results for Gravity, Magnetic and Atmospheric Studies, edited by Ch. Reigber, H. Luehr and P. Schwintzer, Springer-Verlag, Heidelberg, in press, 2003]

References:

Neubert, T. et al. (2001): Ørsted Satellite Captures High-Precision Geomagnetic Field Data, Eos, Transactions, American Geophysical Union, 82, 81 and 87-88.

Taylor, P. T. and J. J. Frawley (1987): Magsat anomaly data over the Kursk region, USSR, Phys. Earth Planet. Interiors, 45, 5-15.

Taylor, P.T., R.R.B. von Frese and H. R. Kim (2000): Ørsted and Magsat: A comparison over the Kursk magnetic anomaly, Proceedings, 3rd Internantional Science Meeting, Grasse, France

Contact: Patrick Taylor, Geodynamics Branch, Patrick.Taylor@nasa.gov

Precise Orbit Determination, Gravity Field, and Terrestrial Reference Frame

Precision Orbit Determination Activities within The Space Geodesy Branch

Precise orbit determination (POD) is a major area of activity and expertise in the Lab for Terrestrial Physics (LTP). For some applications, as with satellite altimetry, POD enables science objectives such as the study of ocean, ice and land topography and surface change. In other applications, for example, reference frame and gravity field determination, science is derived directly from the precise determination of satellite orbits. Highlights below are some of the POD achievements of the LTP for the year 2002.

Jason-1 and TOPEX/Poseidon POD, Achieving the 1 cm Radial Orbit Accuracy Goal: Jason-1, launched on December 7, 2001, continues the time series of centimeter level ocean topography observations as the follow-on to the highly successful TOPEX/Poseidon (T/P) mission. The POD is critical to meeting the ocean topography goals of the mission. Fortunately, Jason-1 POD can rely on four independent tracking data types available including near continuous tracking data from the dual frequency codeless BlackJack Global Positioning System (GPS) receiver. Highly accurate orbit solutions have been computed using individual and various combinations of GPS, Satellite Laser Ranging (SLR) and Doppler Orbitography by Radio Positioning Integrated on Satellite (DORIS) data types from over 240 days of Jason-1 tracking data.

For nearly a decade NASA GSFC has computed the Precise Orbit Ephemerides (POEs) for the T/P mission based on SLR and DORIS tracking data. Building upon these capabilities, models and standards we have computed nearly 24 cycles (10-day repeat orbits) of Jason-1 POEs. Results from the recent Jason-1 Science Working Team meeting (Oct. 2002, New Orleans, LA) indicate these SLR/DORIS POEs are of the highest quality and show excellent agreement with high-fidelity POEs computed at other centers (e.g. JPL, CSR, CNES) and with other data types (e.g. our GPS computed orbits). Several improvements have been made in the SLR/DORIS POD including the calibration of the SLR tracking point offset with respect to the spacecraft center of mass and the development of an SLR/DORIS reduced dynamic solution strategy.

Also computed were highly precise orbits based on GPS data alone and in combination with SLR and DORIS tracking. Performance of the dynamic GPS based orbit solutions is excellent and suggests the 1 cm radial orbit accuracy mission goal is likely being achieved. Radial orbit overlap difference RMS is on the order of 7.3 mm (Figure 8) and independent high elevation SLR fit is 14 mm (Figure 9). The high elevation independent SLR residual performance is a good metric to gauge radial orbit accuracy, but the result does contain error sources other than radial orbit error. These orbit performance metrics alone indicate the GPS dynamic orbit solutions are highly precise and do not possess any significant systematic errors. Another valuable orbit performance test is to difference the SLR+DORIS orbit solutions with

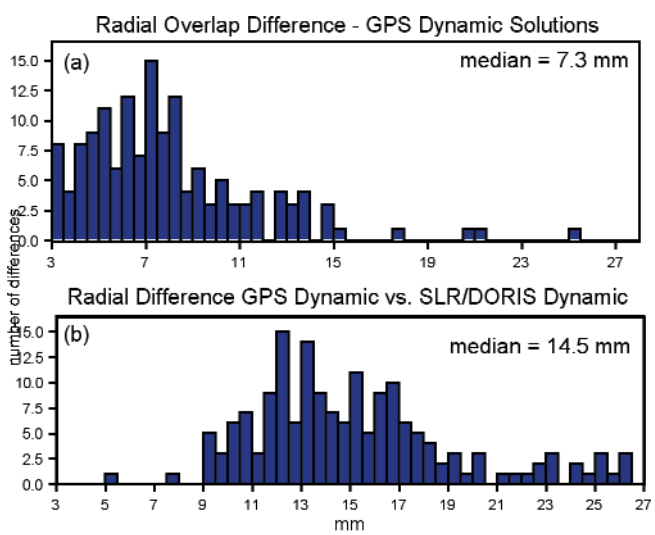

Figure 8. Jason-1 GPS dynamic solutions (30-hr. arc) (a) radial overlap difference and (b) radial difference with SLR/DORIS solutions.

the GPS based orbit solutions. This test can reveal tracking data and solution strategy dependent systematic orbit error. The orbits computed from the two sets of independent tracking data and orbit solution strategies show remarkable radial orbit agreement at the 14.5 mm level over the 190 days of orbit solutions compared (Figure 8). Ongoing analysis has shown further improvement in the GPS based orbit solutions has been obtained by employing a more aggressive reduced dynamic solution strategy (highly empirical parameterization).

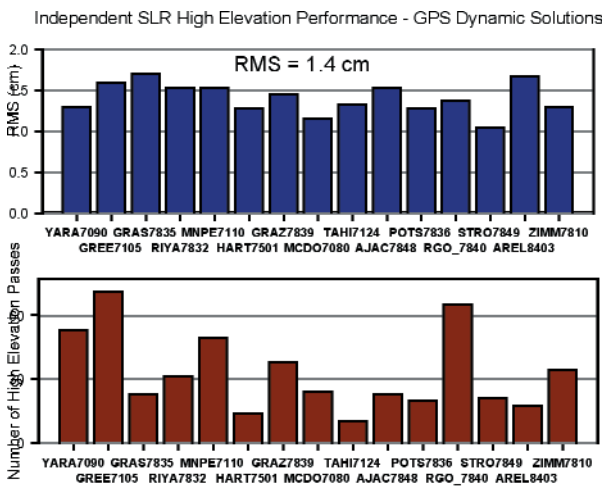

Figure 9. Jason-1 GPS dynamic orbit solutions (190, 30-hr. arcs) high elevation independent SLR performance

Although, Jason-1 will replace T/P it is important to continue to compute T/P precise orbit ephemerides as long as its altimeter remains active. Therefore, a tie between the Jason-1 and T/P missions can be established and a continuous history of ocean topography can be established. The LTP continues to compute the precise orbit ephemerides that are used on the geophysical data records (GDRs) of the T/P mission. T/P has been returning altimeter data almost continuously since October of 1992. Since then the Space LTP has computed more than 330 ten-day "cycles" of T/P orbits each with an accuracy of better than 3 cm radially and better than 15 cm in total position. The routine production of these highly accurate orbits has been a major factor in the success of the T/P mission.

POD for Earth Gravity Modeling (CHAMP and GRACE): The Laboratory has a very long history of extracting Earth gravity information from the analysis of satellite motion. With the launch of the German CHAMP (The Challenging Mini-satellite Payload) in 2000 and the launch of the US-German GRACE (The Gravity Recovery and Climate Experiment), the techniques by which gravity information is recovered from tracking data has dramatically changed and the LTP will help shape that change. These next generation gravity missions combine a new generation of GPS receivers, a high-precision three-axis accelerometer, and star cameras for the precision attitude determination. Accelerometer data is used to separate gravity perturbations from non-gravity perturbations after on-orbit calibration of the accelerometer. For the CHAMP mission, precision orbit determination based on GPS and SLR tracking data isolates the orbit perturbations, while GRACE includes inter-satellite ranging. We have processed over 90 days of CHAMP GPS, SLR and accelerometry data and has employed much of this data into new gravity solutions (see Gravity Model Development section). The state-of-the-art GPS and SLR tracking data analysis is complemented by the innovative accelerometer data analysis capabilities which are being applied to the on-orbit calibration of

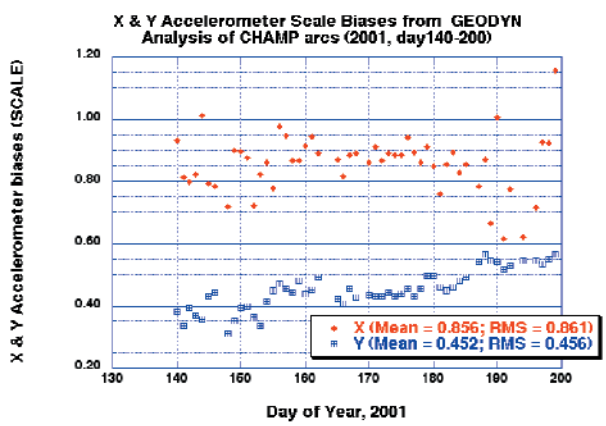

Figure 10. Calibration of CHAMP X and Y scale biases per each 30-hr. arc.

the CHAMP accelerometer. Figure 10 illustrates CHAMP accelerometer scale bias calibrations based on 30-hr. arc solutions. Figure 11 shows the CHAMP post-fit GPS double difference ionosphere-free carrier phase residuals for each 30-hr. arc processed (5025811 observations; median RMS = 0.83 cm). Figure 12 presents histograms of CHAMP radial overlap RMS (median = 0.82 cm) and independent SLR fit RMS (median = 4.1 cm) for each 30-hr. arc solution.

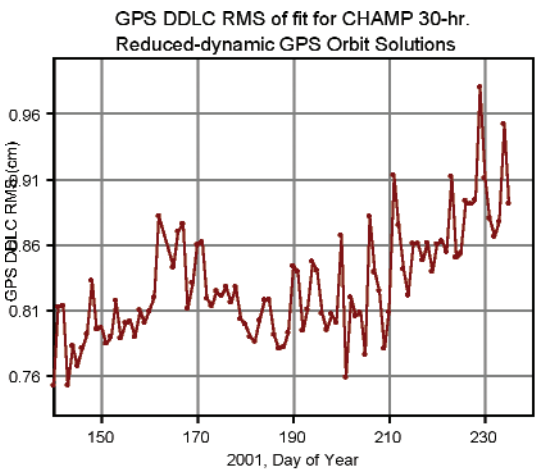

Figure 11. Champ GPS DDLC post-fit RMS per 30-hr. arc.

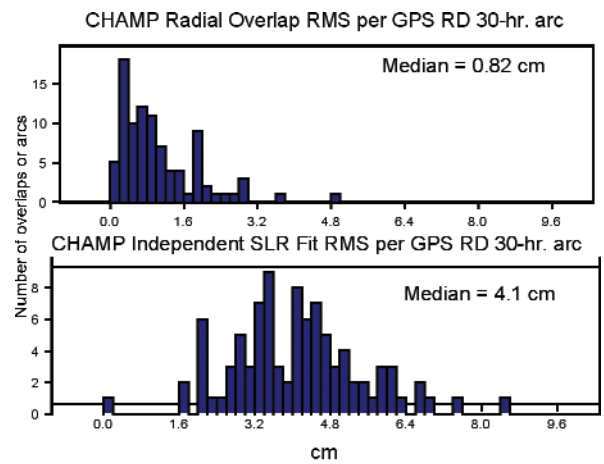

Figure 12. Radial overlap performance (top) and independent SLR fit RMS per 30-hr. arc (bottom)

POD for Laser Altimetry (SLA, MGS, ICESat): Orbit determination for laser altimeter satellites brings with it a unique set of challenges and possibilities. Laser altimeters require on-orbit calibration of instrument parameters such as pointing and ranging biases. The Laboratory has developed an approach that simultaneously determines the orbit of a satellite along with the laser altimeter instrument parameters from a combined reduction of navigation tracking and laser altimeter range data. These capabilities have been applied to Mars Global Surveyor orbit determination and altimetric calibration and was an integral part of Mars topographic mapping and geopotential development. In preparation for future earth observing space-based laser altimeter missions, this approach has been successfully applied to the reduction of Shuttle Laser Altimeter (SLA-01 and SLA-02) mission tracking and altimeter ranging data significantly improving the orbits and geolocation. In 2002, the focus was on refining these capabilities and developing and assessing POD and geolocation calibration and validation strategies in preparation for the January 12, 2003 ICESat launch.

GEOSAT Follow On (GFO): GFO is a radar altimeter satellite. The satellite belongs to the Navy, but the data is available to the scientific community. By an agreement with the Department of the Navy and the National Oceanic and Atmospheric Administration (NOAA), the Laboratory is funded to compute the precise orbit ephemeredes for GFO. The GPS receivers on GFO have not been performing at a usable level and we are one of the very few groups capable of achieving near TOPEX/Poseidon level accuracy for GFO without GPS tracking. This is in part due to the dynamic crossover capability. GFO-GFO dynamic crossovers are routinely used in our GFO orbit solutions and were also used to "tune" a gravity field for GFO. In 2002, the Laboratory continued to routinely produce the GFO precision orbits that have enabled scientific research across government agencies.

Contact: David Rowlands, David.D.Rowlands@nasa.gov

Detection of a Large Scale Mass Redistribution in the Terrestrial System since 1998, and an Assessment of the Potential Causes.

The recent results of Cox and Chao [2002] identified a significant departure from the otherwise linear post-glacial rebound (PGR) dominated drift in the Earth's J_2 zonal harmonic. That analysis included Satellite Laser Ranging (SLR) data from a total of 10 different satellites, covering the period from 1979 up to 2002, and has since been extended through 2002. The recovered series includes J2 through J4, as well as some sectorial and tesseral signals describing longitudinal gravity variations.

Figure 13 shows the complete data series. With the exception of the additional data in 2002, it is similar to Figure 2 of Cox and Chao [2002]. In addition to the J_2 zonal, the time series for J_3 was also estimated. The J_3 zonal, which describes north-south mass distribution, does not show any significant anomalies corresponding to the timing of the J_2 event. There are indications that J_2 is returning to the nominal values and long-term trend dictated by post-glacial rebound. Consequently, the deviation may be interannual in nature, and therefore does not necessarily represent a departure from the long-term trend.

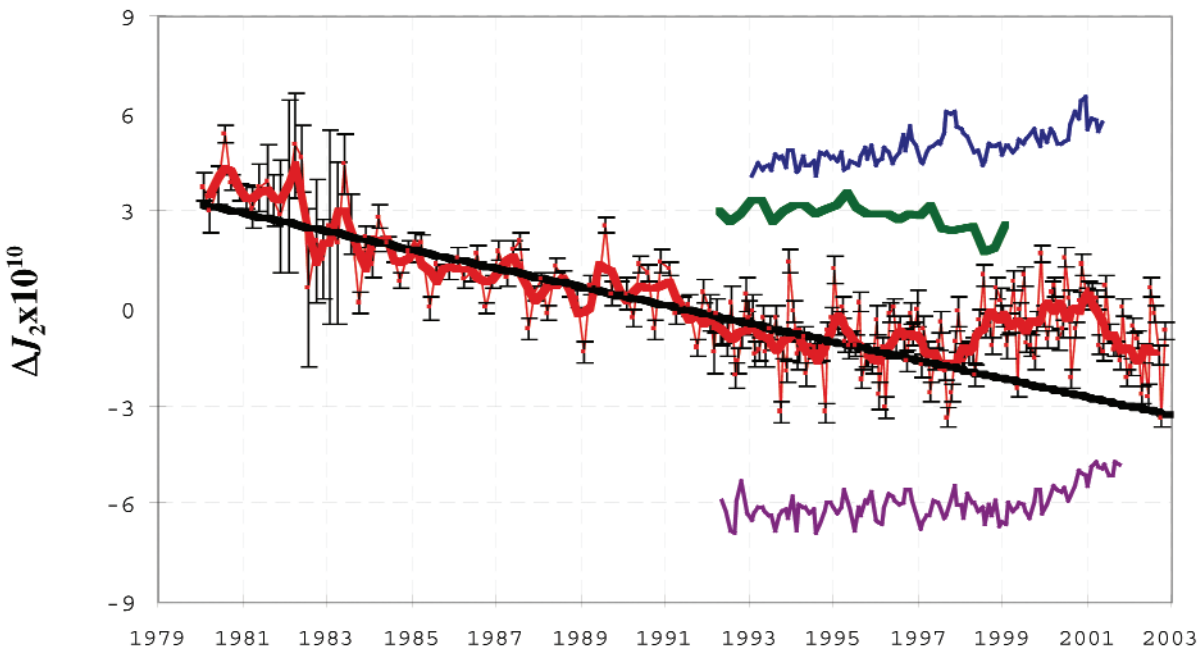

Figure 13. Observed ΔJ_2, after subtraction of the IB corrected atmospheric signal and an empirical annual term, before (thin red line with error bars) and after an annual filter has been applied (heavy red line). Error bars are the observed J_2, uncertainties. The heavy black line is a weighted fit to the (unfiltered) pre-1997 data. The slope is $-2.8x10^{-11}$ year^{-1}. The offset green line (second from top) is the J_2 implied by the Greenland + W. Antarctic ice heights derived from ERS-1/2 altimetry data. Also shown are the J_2 implied by the T/P uniform Global Sea Level change (blue, offset, top), and that considering the geographic distribution of the sea height changes (purple, offset, bottom). Neither sea height derived estimate includes steric effects. Sampling intervals are 90-days in 1979, 60-days from 1980 through 1991, and 30-day afterwards. No detrending of rates has been performed. Units are 10^{-10}.

The atmospheric gravity correction applied to the data in Figure 13 was computed from the monthly National Center for Environmental Predictions (NCEP) reanalysis pressure grids assuming a two-dimensional approximation. While the atmosphere explains a good portion of the variation from the monthly to annual periods, it does not explain the anomaly. The maximum difference between the two-dimensional and three-dimensional computations amounts to ~$0.5x10^{-10}$

change in the annual amplitude, with no significant effect on the interannual variation.

Ice melting scenarios large enough to explain this deviation produce a large Global Sea Level change (~2 mm/yr above the pre 1998 rate), which simply has not been observed. Likewise, the apparent recent turn in J_2 would then imply a recent accumulation of ice mass, which, while not impossible, is unlikely. Terrestrial water impoundment is another possible factor. Large dams can individually cause a jump of ~0.2×10^{-10} in J_2, however, the cumulative effect since 1998 is far too small to explain the observed J_2 changes. Regrettably there is insufficient reliable data at the moment to make any assessment about the role of hydrology. Review of geodynamo model output showed that under some assumptions rates as large as ~$0.5\text{-}1.0 \times 10^{-11}$ per year are possible. While the core signal may be larger than previously assumed, it still does not explain the J_2 anomaly.

There is evidence that some component of the cause of the J_2 anomaly lies within the oceans. The timing corresponds to changes in the primary empirical orthogonal function (EOF) modes for the sea surface temperature (SST) and sea surface height (SSH) in the extra-tropic regions (See Figure 14a and 14b). The primary SST EOF mode corresponds to the Pacific Decadal Oscillation (PDO), which is generally correlated with the J_2 series. The timing also corresponds to changes in the primary EOF modes of the ECCO ocean model [Stammer et al., 1999] bottom pressure (Figure 14c and14d). Analysis of the ECCO assimilation run output shows that the most influential region is the Southern Pacific, although some effects are also seen in the other regions. However, the ECCO ocean model bottom pressure data can only explain about 25% of the observed magnitude of the J_2 change. Nonetheless, the good overall agreement in the timing and nature of the event with the ocean activity warrants more detailed analysis of the ocean's role.

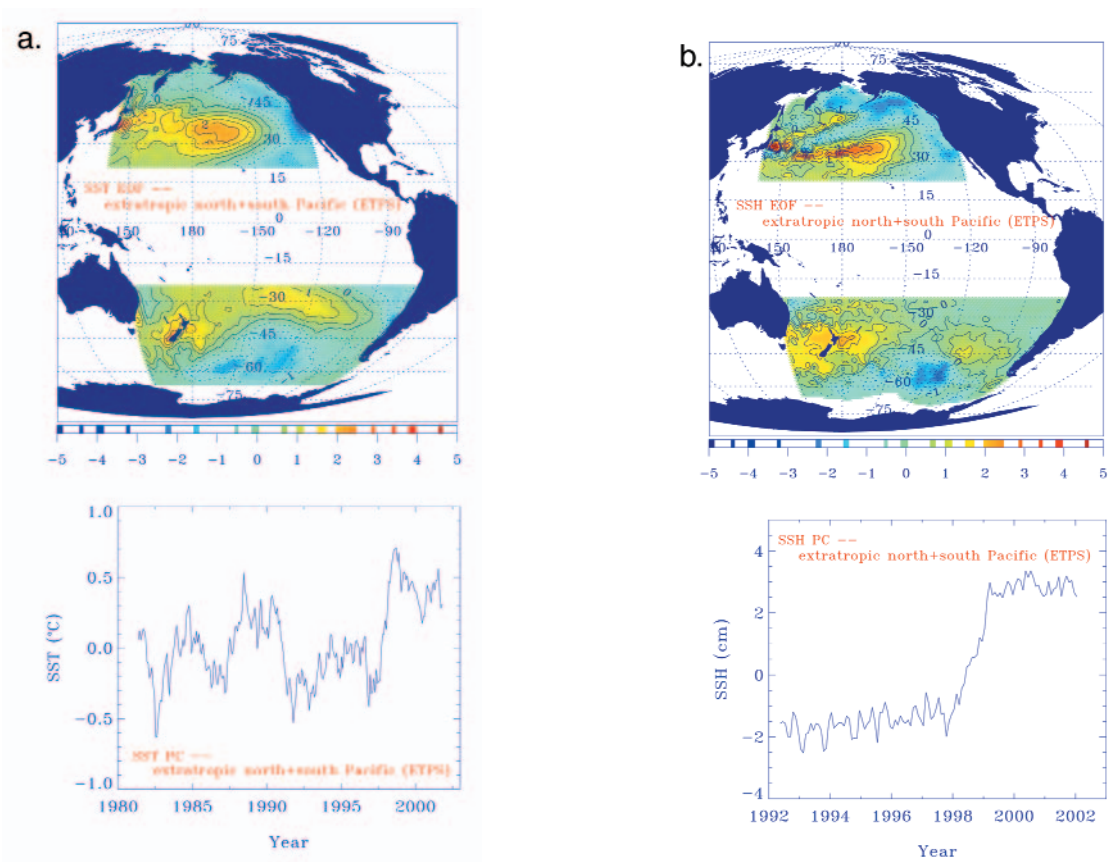

Figure 14. Primary modes of EOF/PC analyses of the (a) Reynold's Sea Surface Temperature, (b) T/P Sea Surface Height for the extratropic regions of the Pacific Ocean.

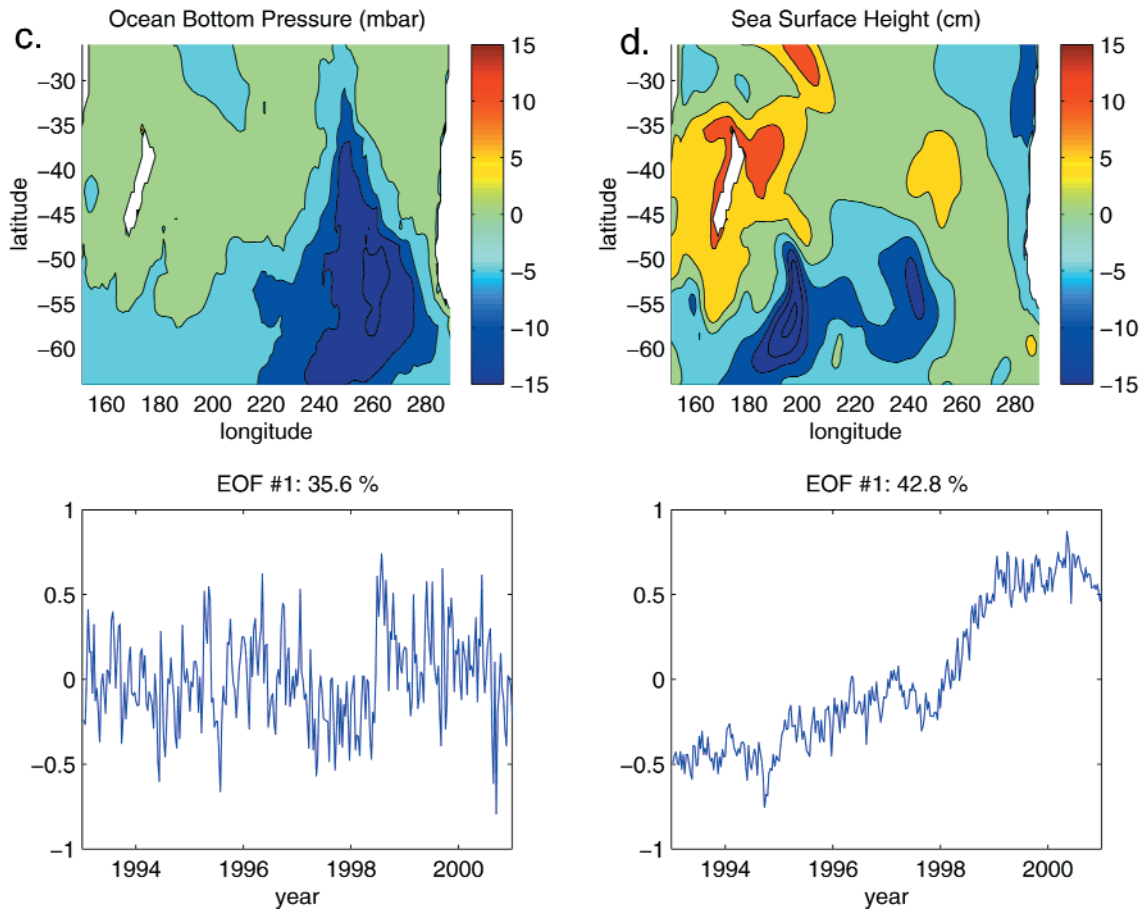

Figure 14. (c) ECCO ocean bottom pressure, and (d) ECCO sea surface height from the assimilation model for the South Pacific. For each panel, the top figure shows the spatial component of the mode, while the bottom panel shows the time series of the scalar component.

Contact: Christopher Cox, ccox@stokes.gsfc.nasa.gov

Earth Geopotential Solutions from CHAMP Satellite Data

The CHAMP (CHAllenging Minisatellite Payload) spacecraft, launched in July 2000, is the first in a series of missions that will revolutionize the ability to model the Earth's geopotential. The CHAMP mission, managed by the GeoForschungsZentrum (GFZ), Potsdam, Germany, orbits the Earth at altitudes of 400 – 450 km at a near polar inclination. The spacecraft is equipped for precision tracking with the global positioning system (GPS), and satellite laser ranging (SLR). In addition, CHAMP carries a precision accelerometer to measure the nonconservative forces acting on the spacecraft. More than ninety days of CHAMP GPS, SLR, and accelerometry data (from days 140 to 230 of 2001) has been processed using our GEODYN orbit determination software. These data have been used to estimate solutions for the Earth's geopotential that are a substantial improvement over earlier solutions based on pre-CHAMP data (for example, EGM96, JGM-2, JGM-3).

The processing of the CHAMP data involves several steps. First, is to determine the best possible orbits using a reduced-dynamic technique for a series of 30-hr arcs. Second, is the calibration of the accelerometer to determine the appropriate scale and absolute biases. Velocity impulses are estimated to account for the numerous attitude maneuvers experienced by the CHAMP spacecraft, which have no expression in the smoothed accelerometer data provided by GFZ. Normal

equations are created to 120 x 120 in spherical harmonics on the Cray SV1 and the HP/Compaq SC45 supercomputers at NASA GSFC's National Center for the Computational Sciences. So far, we estimated test solutions to 90x90 using between 10 and 40 days of data.

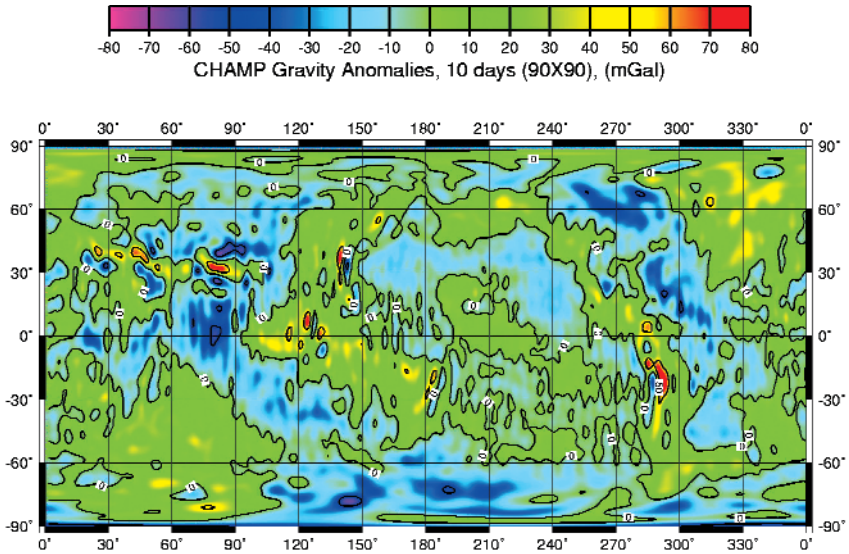

Figure 15: Gravity Anomalies to 90x90 from ten days of CHAMP data.

Figure 15 illustrates the anomalies from a 90 x 90 solution based on CHAMP data from May 20-30, 2001. This solution was based on only 368,814 GPS double difference observations. While the solution will not have as much detail as a high degree solution that includes altimetry or surface gravity (such as EGM96), a fair amount of detail is discernible from only ten-days of CHAMP data.

Figure 16 illustrates the degree variances from two satellite-only geopotential solutions: EGM96S, based solely on pre-CHAMP tracking data (such as SLR, GPS, DORIS, TDRSS, Tranet Doppler), and PGS7760B, a test solution based on only forty days of CHAMP data. The EGM96S solution is deficient in power above degree 40-45 due to the lack of homogeneous and high-quality global coverage. In contrast, the CHAMP test solution does not lose power at the high degrees. In fact, the upturn in the power spectrum is a signature of aliasing and an indication the CHAMP solutions should be extended beyond degree 90.

An independent altimeter-derived anomaly was used to test the satellite-only geopotential solutions by comparing the discrepancies at degree 70 between the anomalies predicted by these geopotential solutions, and the gravity anomalies derived from ocean radar altimeter data. It was found that for the pre-CHAMP solution, EGM96S, the discrepancy has a variance of 10.19 $mGal^2$, whereas for the CHAMP satellite-only test solution the anomaly discrepancy has a variance of 4.57 $mGal^2$. This single test implies that even a few months of CHAMP data have greater strength than the space geodetic tracking data collected over the previous thirty years of the space age. This conclusion has an important caveat, namely that a CHAMP-only solution will not represent faithfully the resonance to which different satellites may be sensitive, so that the best solution will still require CHAMP data to be merged with other tracking data, e.g. from JASON, ICESAT, STARLETTE and other satellites.

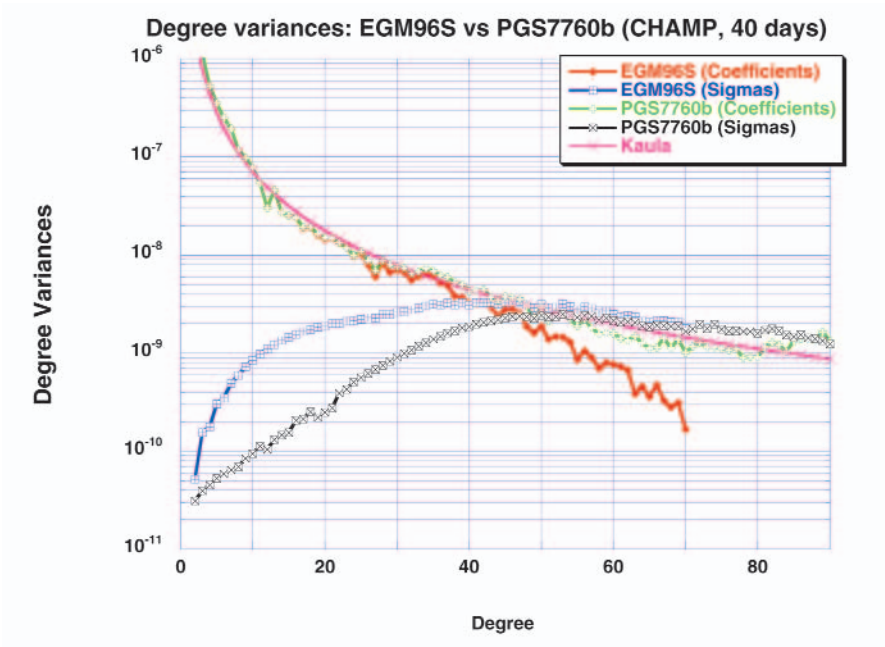

Figure 16: Degree variances for satellite-only geopotential solutions.

Contact: Frank Lemoine, Frank.G.Lemoine@nasa.gov

The NASA Geodetic/Astrometric VLBI Program

The capabilities of Very Long Baseline Interferometry (VLBI) have been developed and continually improved over the past 35 years, and NASA continues to be a major sponsor of the geodetic and spacecraft applications through programs at Goddard Space Flight Center and at the Jet Propulsion Laboratory. It is appropriate that as NASA expands its program in Earth system studies, NASA also continues to take the lead in advancing the space geodetic techniques, which will contribute so significantly to Earth sciences in the coming decades.

VLBI has three important attributes: unique determination of the Celestial Reference Frame (CRF) and the orientation of the Earth in that frame, accuracy, and long-term stability. Only through these VLBI measurements can many of the properties of the Earth's interior be inferred, such as: dynamical oblateness of the core-mantle boundary, magnetic properties of the inner and outer cores, and anelasticity of the mantle. The CRF provides the precise background for deep space navigation of spacecraft and alignment of catalogs at different observing frequencies.

The VLBI definition of the scale of the Terrestrial Reference Frame (TRF), measurement of UT1-UTC, and the long term stability of the reference system and orientation of Earth in space are fundamental requirements for the geodetic measurements by all other techniques. Led by the NASA team, the technological developments that have brought VLBI to its present level of accuracy are the result of international collaboration and support.

Continual technology improvement is the basis of all experimental advances and will provide both better accuracy and more rapid delivery of results. For the global geodetic VLBI program the technology advances have been due to the leadership of the VLBI groups at GSFC and at the MIT Haystack Observatory operating under a NASA contract. The implementation of these projects has been the product of large international collaborations involving many countries and agencies. Current technology emphasis is aimed at two initiatives. The first is the Mark 5 disk-based data

acquisition system, which will benefit the science through better sensitivity while reducing costs and improving reliability. The second is the use of high bandwidth optical fiber communication for real-time VLBI, first demonstrated by the Communications Research Laboratory of Japan.

Mark 4 correlators have been operational at the United States Naval Observatory (USNO), the Max Planck Institute for Radioastronomy (MPIR), the Joint Institute for VLBI in Europe (JIVE), and Haystack for about three years and have now completely replaced all Mark III and Mark IIIA correlators. Over the last year, significant enhancements have been made to Mark 4 correlator software to improve operational flexibility and efficiency. The Mark 4 correlator is now designated as 'mature', but further enhancements are still possible.

The Mark 5 disc-based data system is well along in development and entered field operation in 2002; approximately 20 Mark 5P units have been deployed. In addition, the Mark 5 system was used in a demonstration of ~1 Gbps electronic transmission of VLBI data over an IP network between Haystack Observatory (Westford, MA) and NASA/GSFC, a distance of ~700 km.

Based on the success of the Mark 5 demonstration unit shown in 2001, NASA (under contract with Haystack Observatory) is now undertaking the development of an operational 1 Gbps Mark 5 system with support from other cooperating partners: Bundesamt fuer Kartographie und Geodaesie (BKG, Federal Agency for Cartography and Geodesy, Germany), Korean VLBI Network (KVN), MPIR, JIVE, National Radio Astronomy Observatory (NRAO) and USNO.

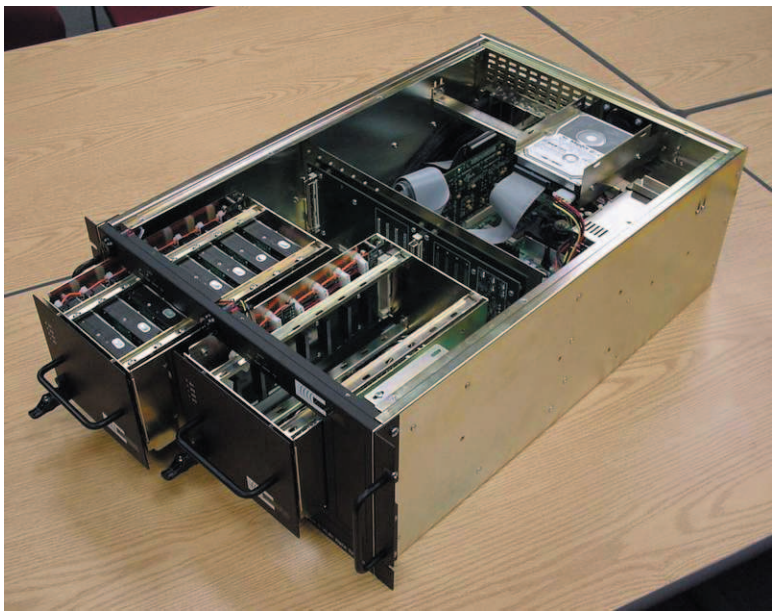

Figure 17. Mark 5 disk-based VLBI data recorder.

e-VLBI Development

NASA and DARPA supported Haystack Observatory to demonstrate 1-Gbps e-VLBI over a standard IP-based network between Haystack Observatory and NASA/GSFC. Part of the network path was over standard U.S. science network infrastructure, where other users share the network links and the data must traverse many routers and switches. One purpose of this test was to determine the real throughput of these networks under stressful shared conditions. Tests between Haystack Observatory and the Westford antenna already demonstrated sustained data rates of ~980 Mbps over standard Gigabit Ethernet links through several switches. The Westford antenna at Haystack Observatory was used in conjunction with the GGAO antenna at NASA/GSFC.

In two tests in October VLBI data were transmitted from both antennas to the Mark 4 correlator at Haystack Observatory for correlation. In the first test the data were first recorded on Mark 5P and then transmitted at ~788 Mbps to Haystack for rebuffering and correlation. In a second test the GGAO data were transmitted real-time to Haystack.

The first intercontinental e-VLBI fringes were achieved between Kashima, Japan and Westford in October buffered on a K5 disk-based recorder in Japan and a Mark 5P at Westford. Data were transmitted in both directions and correlated at both ends with normal results. Although the data rates were only ~1.5 Mbps, the rates should improve substantially in the future. The intention is to seek support to extend Gbps e-VLBI to other sites within the U.S. as well as overseas to Europe. Paths between Hawaii and Washington, DC and between the U.S. and Germany are being organized for further tests.

Contact: Chopo Ma, Chopo.Ma@nasa.gov

International VLBI Service (IVS)

The GSFC Very Long Baseline Interferometry (VLBI) group has been actively involved in initiating and participating in the International VLBI Service for Geodesy and Astrometry (IVS). This aligns with NASA's efforts for the development of partnerships within industry, government and the international community in sharing resources.

The IVS is a service of the International Association of Geodesy (IAG), International Astronomical Union (IAU) and Federation of Astronomical and Geophysical Data Analysis Services (FAGS). The charter and the basis for international collaboration is given by the Terms of Reference (ToR) accepted by IAG and IAU and by the proposals provided by individual agencies in response to the call of participation. IVS is an international collaboration of organizations that operate or support VLBI components.

The IVS inauguration date was March 1, 1999. IVS is tasked by IAG and IAU for the provision of timely, highly accurate products Earth Orientation Parameters (EOPs), Terrestrial Reference Frame (TRF), Celestial Reference Frame (CRF), etc. IVS has no funds of its own and is dependent on the support of individual agencies that responded to the call for participation.

The IVS Coordinating Center is based at GFSC and is operated by NEOS (National Earth Orientation Service), a joint effort for VLBI by the U.S. Naval Observatory and NASA GSFC. The mission of the Coordinating Center is to provide communications and information for the IVS community and the greater scientific community and to coordinate the day-to-day and long-term activities of IVS. GSFC provides the web server for the Coordinating Center. The address is http://ivscc.gsfc.nasa.gov

During 2002, the VLBI group processed and analyzed 164 24-hr geodetic/astrometric sessions and 192 1-hr UT1 Intensive sessions. The 24-hr sessions included the weekly R1 and R4 observations for monitoring of EOP. In addition 15 continuous CONT02 sessions were scheduled in October using Gilmore Creek, Alaska; Kokee Park, Hawaii; Algonquin, Ontario; Westford, Massachusetts; Ny Alesund, Norway; Wettzell, Germany; Hartebeesthoek, South Africa, and Onsala, Sweden. Analysis was begun as the sessions became available from the correlators, and the quality of the data is quite good. These sessions will provide information for high frequency and transient phenomena in Earth orientation and station motions.

Analysis staff collaborated with NRAO and Caltech personnel to perform the astrometric analysis of two new VLBA calibrator survey experiments and determined milli-arcsecond level positions of 276 additional calibrator sources, many of which can be used in geodetic VLBI sessions. A paper with the first 1332 source positions was published. Analysis staff collaborated with USNO, JPL, and NRAO personnel to process and analyze VLBI survey observations at K band

(23 GHz) and Q band (44 GHz). These observations are the beginning of the work to generate a Ka band (34 GHz) catalog to support future spacecraft navigation and to extend the microwave celestial reference frame to other frequencies.

VLBI solutions were used to study ocean loading. Position variations of 40 VLBI stations at 32 tidal frequencies were obtained from analysis of 3 million measurements of group delays from 1980 to 2002. It was found that the estimates of station displacements are generally in a good agreement with the ocean loading computed on the basis of ocean tide models for the main diurnal and semi-diurnal tides. However, discrepancies between VLBI results and all models of ocean loading for K1, K2 and S2 tides exceed both the errors of the VLBI estimates and the errors of ocean loading displacements based on the reported formal uncertainties of ocean tide models. It was found that there is a significant non-tidal signal at diurnal and annual frequencies. Applying a model of hydrological loading reduces the variance of the residual vertical displacements at the annual frequency by 30%.

The large VLBI analysis package Calc/Solve was maintained, upgraded, and distributed to the IVS community bimonthly. The capability to access the NCEP reanalysis weather model and to calculate atmosphere loading was added to the VLBI analysis system. The transfer of the code of Solve from a HP Unix platform to a Linux platform was begun to make the system available to more users.

Contact: Chopo Ma, Chopo.Ma@nasa.gov

Crustal Dynamics Data Information System (CDDIS)

The CDDIS is a dedicated data center supporting the international scientific community as NASA's space geodesy data archive since 1982. This data archive was initially conceived to support NASA's Crustal Dynamics Project. Since the end of this successful program in 1991, the CDDIS has continued to support the science community through NASA's Solid Earth and Natural Hazards program, HQ Code YS. The CDDIS provides easy and ready access to a variety of data sets, products, and information about these data. The CDDIS archive includes Global Positioning System (GPS), GLObal NAvigation Satellite System (GLONASS), Satellite Laser Ranging (SLR), Very Long Baseline Interferometry (VLBI), and Doppler Orbitography and Radiolocation Integrated by Satellite (DORIS) data and products. The specialized nature of the CDDIS lends itself well to enhancement to accommodate diverse data sets and user requirements. Information about the system is available at http://cddisa.gsfc.nasa.gov.

The CDDIS serves as one of the primary data centers for the following services within the International Association of Geodesy (IAG):

International GPS Service (IGS) and its diverse pilot projects and working groups

International Laser Ranging Service (ILRS)

International VLBI Service for Geodesy and Astrometry (IVS)

International Earth Rotation Service (IERS)

International DORIS Service (IDS)

The CDDIS is operational on a dedicated computer facility located in Building 33 at NASA GSFC. This computer facility hosts web sites for the CDDIS, the ILRS, and several other GSFC facilities. The majority of the CDDIS data holdings are accessible through anonymous ftp and the web.

By the end of 2002, users had downloaded over 40 million files, averaging over 250 Gbytes in size each month. Furthermore, nearly 200 users accessed the CDDIS on a daily basis to download data. Nearly ninety countries accessed and downloaded data from the CDDIS last year. Over 120 institutions in over sixty countries supply data to the CDDIS on a daily basis for archival and distribution to the international user community.

CDDIS Activities in 2002

In support of the IGS pilot project on Low Earth Orbiter (LEO) missions, the CDDIS enhanced its archive to include GPS data from flight receivers on-board SAC-C and CHAMP. Data from ICESat and JASON will be archived in 2003. Analysts will retrieve these data to produce precise orbits of these LEO platforms, which will aid in the generation of other products, such as temperature and water vapor profiles in the neutral atmosphere and ionosphere imaging products. The IGS LEO Pilot Project will test the ability of the various components of the IGS infrastructure to support near real-time acquisition, dissemination, and processing of GPS data.

The CDDIS began archiving data from continuously-operated GPS receivers located at or near tide gauge instruments in support of another IGS pilot project, TIGA-PP, or the Tide Gauge Benchmark Monitoring Pilot Project. Analysts using these data will produce time series of coordinates for studying vertical motions of tide gauges and tide gauge benchmarks.

The CDDIS staff assisted in the publication of several ILRS documents, particularly the 2000 and 2001 annual reports and the updated ILRS brochure.

New Thrusts for the CDDIS

Providing funds are available, a new LINUX-based system will be purchased to replace the current UNIX server. This system will be equipped with one or two RAID disk arrays (nearing one TB of on-line disk space) and optionally a dedicated tape backup system.

Website: http://cddisa.gsfc.nasa.gov/cddis_welcome.html

Contact: Carey E. Noll, Carey.E.Noll@nasa.gov

Improved Mapping Functions for Atmospheric Corrections in Satellite Laser Ranging

An accuracy-limiting factor in modern space geodetic techniques, such as the Global Positioning System (GPS), Very Long Baseline Interferometry (VLBI), and Satellite Laser Ranging (SLR), is atmospheric refraction. The atmospheric refraction modeling at radio wavelengths has improved significantly in the last decade, in contrast to that for optical wavelengths, where the standard for data analysis is still the 1970s Marini-Murray refraction model. A better atmospheric refraction model is of great importance in reducing the error budget in SLR measurements in high-precision geodetic and geophysical applications. For example, the study of spatial and temporal variations in the Earth's gravity field, the monitoring of vertical crustal motion, and the prospect of a more robust combination of solutions from different space techniques.

Two new mapping functions (MFs) were developed to better model the elevation angle and observational wavelength dependence of the atmospheric delay for SLR data analysis. The new MFs were derived from ray tracing through a set of data from 180 radiosonde stations globally distributed, for the year 1999, and are valid for elevation angles above 3°. When compared against ray tracing of two independent years of radiosonde data (1997-1998) for the same set of stations, the

MFs reveal sub-millimeter accuracy for elevation angles above 10º, representing a significant improvement over other MFs. This is confirmed in improved data reductions of LAGEOS and LAGEOS 2 SLR data from the Int. Laser Ranging Service (ILRS) global tracking network.

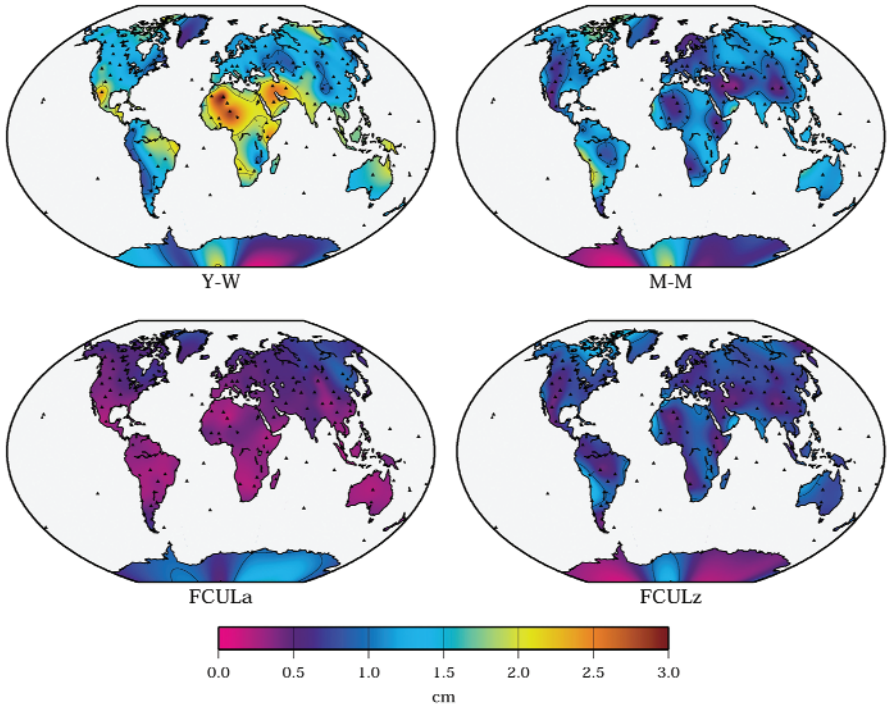

Figure 18. Two-year average r.m.s. differences: model predictions minus ray tracing, at 10 degrees elevation angle. Plots on the left represent MF errors for our new MF "FCUL2000a" and the MF of Yan and Wang; plots on the right represent the combined error of zenith delay modeling (ZD) and MF errors for the Marini-Murray and our model FCUL2000z.

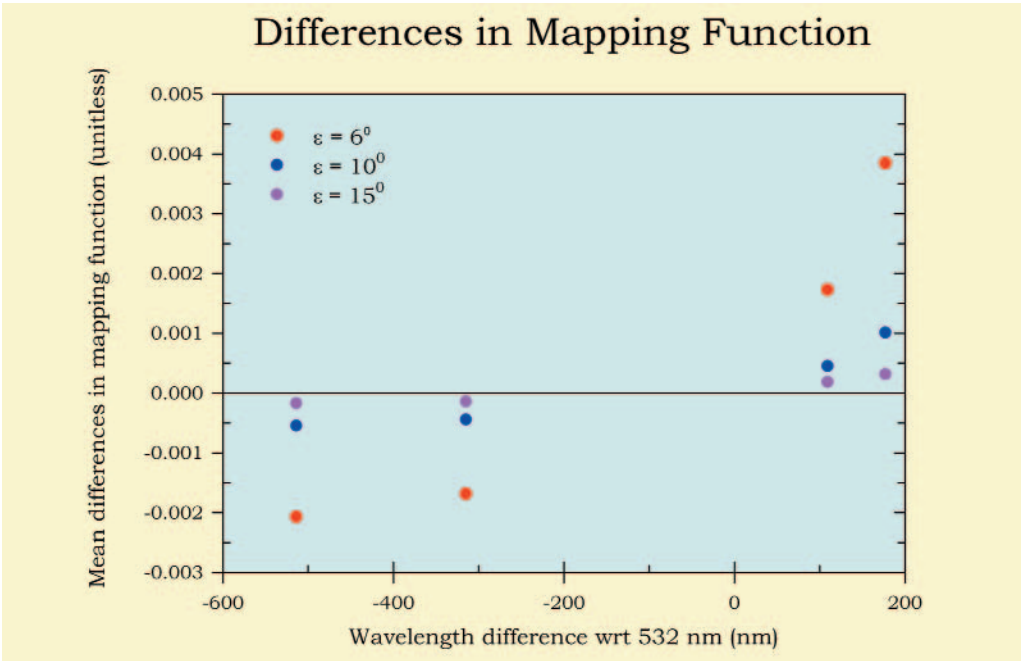

Figure 19. Mean differences in the mapping function scale factor with respect to nominal wavelength of 532 nm. The worst departure is at 355 nm and for a nominal 2.5 m correction, corresponds to 1 cm.

Table 1. RMS for Mapping Functions (e = 10°), in the sense "model minus ray tracing" (cm).

λ	Full models		Mapping functions ONLY		
(nm)	Marini-Murray	FCULz	FCULa	Yan-Wang	Saastamoinen
355	1.77	3.83	0.55	1.72	3.04
423	0.79	0.75	0.46	1.65	2.48
532	1.14	0.82	0.41	1.56	2.16
847	1.05	0.75	0.39	1.56	2.05
1064	0.98	0.62	0.39	1.77	2.06

Reference:

Mendes, V.B., G. Prates, E.C. Pavlis, D. E. Pavlis, and R.B. Langley "Improved mapping functions for atmospheric refraction correction in SLR" Geophysical Research Lett., 29(10), 1414, doi:10.1029/2001GL014394, 2002.

Contact: Erricos Pavlis, epavlis@JCET.umbc.edu

Absolute Earth Scale from SLR Measurements

Since the LAGEOS I satellite was launched in 1976, the systematic instrument error of the best satellite laser ranging observatories has been steadily reduced. Advances in overall system accuracy, in conjunction with improved satellite, Earth, orbit perturbation and relativity modeling, now allows us to determine the value of the geocentric gravitational coefficient (GM) to less than a part per billion (ppb). This precision has been confirmed by observations of the LAGEOS II satellite, and is supported by results from Starlette, albeit at a lower level of precision. When observations are considered from other geodetic satellites orbiting at a variety of altitudes and carrying more complex retro-reflector arrays, consistent measures are obtained of scale, based upon empirically determined, satellite-dependent detector characteristics. The adoption of a value of GM differing by a ppb would result in a difference of a few millimeters in the height definition of a near-Earth satellite. The precision of the estimate of GM from satellite laser ranging has improved by an order of magnitude in each of the last two decades.

The Evolution of Scale Definition

During the 1970s, the determination of the Earth's geocentric gravitational coefficient was independently determined from observations of several interplanetary spacecraft, including the Ranger, Surveyor, Lunar Orbiter, Pioneer, Mariner and Viking flights. The analysis of the first six months of LAGEOS I data was shown on a vertical scale with a full range of 1 km^3/sec^2, corresponding to the sixth decimal digit of GM, and equivalent to about one part per million. The early, decimeter-accuracy LAGEOS observations were included in the development of the GEM-L2 gravity model, most of whose data was collected in the 1970's, when the prevailing scale knowledge was based on the speed of light 299729.5 km/sec. An uncertainty of 0.02 km^3/sec^2 (50 parts per billion) was assigned to the new estimate for GM with a value of 398600.44 km^3/sec^2 after appropriate scaling for the speed of light currently adopted (299729.458 km./sec).

Improvement in Scale Definition

LAGEOS I and II data collected between 1986 and 1992 were used to determine the IERS92 standard. The data collected since 1990 suggested higher estimates of GM with generally better con-

sistency from each LAGEOS satellite. The average value for LAGEOS II was 498600.44187 km^3/sec^2, which was chosen as the most appropriate value from this analysis. The scatter of annual determinations of GM from several other geodetic satellites over a four-year period was found to contribute no absolute scale information, but their scatter provided an indication of overall network consistency for the tracking of these satellites.

Latest Results

In a recent analysis, ten years of data from LAGEOS I and II were combined to simultaneously estimate independent values of GM at monthly interval. The scatter (standard deviations) about the mean of the monthly values shown in Figure 20 gives a realistic error measure of about one-half part per billion, and the formal errors of single estimates give optimistic assessments. The formal errors would hold if the ranging observations were randomly distributed about the orbits at the level of the final residual fit for each satellite. The orbit fits are about 3 cm for LAGEOS I and II and the orbital residuals are not random. The high range residual level is caused by unmodeled Earth, satellite and orbit errors. As these models improve in the future, the associated uncertainty in the scale parameters will be reduced. The inclusion of a more precise pressure measurements yielded a GM value which is about one half ppb higher than the adopted standard which is just within the quoted uncertainty.

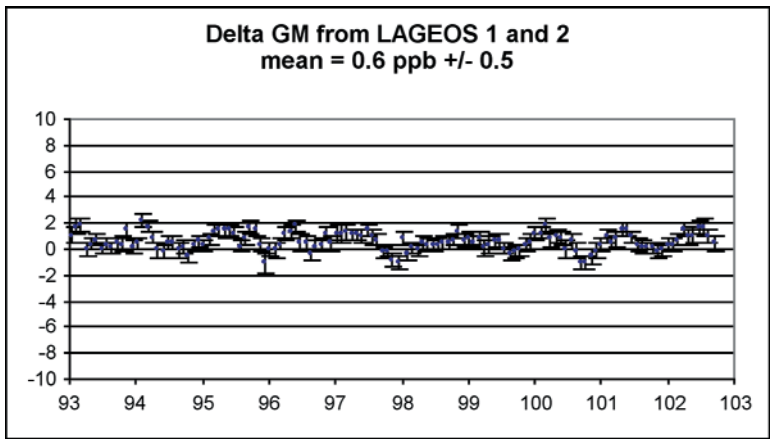

Figure 20. Determination of Scale from a Recent Analysis

Scientific Relevance of Earth Scale Determination:

Satellite geodesy depends on the integrity of the geocentric gravitational coefficient for its definition of scale. An accurate value of the universal gravitational constant times the mass of the Earth (GM) enables us to monitor the behavior of the Earth, as sensed by satellite observations, in an absolute reference frame. Improved orbit scale definition provides an important component to the definition of the geopotential model, and has among its most practical applications a contribution to the refinement of the positioning of altimeter satellites, which carry stringent radial accuracy requirements. This work will help to define the long-term stability of the SLR reference frame and improve the positioning capability of the network. The rate of sea level rise caused by global warming is currently measured over decade time scales with tide gauges, which provide observations relative to the Earth's surface. The scale inherent in laser ranging observations to stable high-altitude satellites enables us to determine accurate geocentric height at the observatories. The work also contributes to the refinement of the positioning of altimeter satellites, which carry stringent radial accuracy requirements in order to define sea level relative to the Earth's center. Furthermore, we anticipate that routine monitoring of Earth processes to which ranging scale is sensitive, such as seasonal and secular variability in Earth albedo, can also provide important indicators of the effects of global change.

Contact: Ronald Kolenkiewicz, Ronald.Kolenkiewicz-1@nasa.gov

Kinematic GPS Activity within the Laboratory for Terrestrial Physics

Kinematic positioning is a technique that takes advantage of the simultaneous visibility of four or more GPS satellites, from anywhere and at any time, to find the position of moving vehicles without knowing their actual dynamics. It is an extremely versatile technique, as exemplified by the topics of recent studies carried out in cooperation with colleagues at other organizations. These include: The Polytechnic University of Catalonia (UPC) (on improving GPS-based navigation with atmospheric models); the Navy's Naval Surface Warfare Center (NSWC) at Dahlgren, the UPC, the University of Alicante, and the University of Tasmania (on the precise location of buoys at sea for satellite altimeter calibration), and the University of Nagoya, and the Japan Hydrographic Department (on sea-floor tectonics).

Low Earth Orbiter (LEO) Trajectory Determination:

Another project is to find a way to use kinematic GPS for precise positioning of LEOs equipped with GPS receivers. Some new ideas are being tested. The most recent is, first to use long-range kinematic GPS (lacking dynamic constraints), and then make an orbit fit (constrained by orbit dynamics) to the resulting trajectory, in order to filter out the kinematic errors. These errors tend to be rather large in satellite trajectories, because both the fast-changing subset of GPS spacecraft in view from the LEO, and the very long baselines between this and the fixed ground stations, together make ambiguity floating imprecise, and ambiguity fixing unreliable. The procedure outlined here requires a relatively small number of ground sites distributed around the world, selected from the much larger set of IGS stations on the basis of their consistently good performance. This method could be useful when processing altimetry and other satellite data requiring good orbit registration. The technique has been implemented almost entirely with software already available at the Branch. It has been tested making two 24-hour orbit estimates for the oceanographic satellite TOPEX/Poseidon, and another two, for the satellite JASON. The estimated orbits agree to better than 5 cm RMS in height and 17 cm in three-dimensional RMS with the NASA Goddard Space Flight Center Precise Orbit Estimates (POE), which are also produced at the Branch (see section on POE). The results are summed up in the Table below (from a paper Colombo, Luthcke, Rowlands, Poulose, and Chin, in the Proceedings of ION GPS 2002). Those POE have been derived exclusively from DORIS Doppler and laser tracking data, so they provide an entirely independent way to verify GPS-based results.

Work continues on improving the purely kinematic solutions. The goal is to use dynamics-free kinematic solutions to check the dynamically determined POEs for systematic errors, to detect problems and, perhaps, help validate the force models used.

Table 2. Departure of Dynamic Orbit Fit from GSFC's POE (Centimeters)

TOPEX

DAY	RSS	dR (RMS)	dR MEAN	Points in Orbit Fit
12/14/93	14.6	3.8	0.2	1801
06/24/95	8.6	1.4	0.2	1766

JASON

DAY	RSS	dR RMS	dR MEAN	SLR RMS	Points in Orbit Fit
08/04/02	15.1	4.5	-0.3	9.9	1242
09/04/02	15.1	4.8	0.1	9.5	1367

Contact: Oscar Colombo, ocolombo@olympus.gsfc.nasa.gov

Global Geophysical Fluids

Application of Core Dynamics Modeling to Geodetic Studies

Earth's outer core is the largest geophysical fluid system (in both volume and mass). Its temporal and spatial variations interact with other geophysical processes and generate global geodynamic changes that can be measured via space geodetic technologies. A well-known example is the length of day (LOD) variation of the Earth. Geomagnetic observations demonstrated that LOD variation on decadal time scales results from exchange of axial angular momentum between the Earth's core and the solid mantle. This core-mantle angular momentum exchange is a product of core-mantle interactions. Therefore, multi-disciplinary studies in geodynamo, geodesy and geomagnetism could help not only interpreting geodetic/geomagnetic observations, but also furthering the understandings of core dynamics.

During 2002, efforts were continued in the application of the MoSST core dynamics "geodynamo" model on dynamics of core-mantle interactions. In addition to complete the research in electromagnetic core-mantle coupling (two papers are in preparation), research was begun in gravitational core-mantle coupling that arises from mantle and outer core density anomalies with two actions. The first is the development of a module to calculate gravity field anomalies of the mantle, and the resultant gravitational torque. The second is a construction of a mantle density anomaly model from seismic observations (reported at EGU/AGU Joint Assembly in Nice, France). In collaborating with recent progress on time-varying gravity measurements (e.g. J_2 series), gravity variation was also analyzed due to core fluid density anomalies with the MoSST model. With various parameters and exclusion of possible effect of mantle deformation due to pressure variation at the Core-Mantle Boundary (CMB) (internal loading), it was found that core fluid density anomalies (due to convection) could contribute to a very complicated time-varying gravity field at the Earth's surface (see Figure 21). In particular, the J_2 component could be as large as 10^{-10}/year, and could partially explain the observational results. Findings suggest that time-varying gravity measurements could also be used in core dynamics studies by providing possible constraints on density variation (and thus buoyancy force) in the fluid outer core, thus opening a new method of detecting dynamics of the Earth's deep interior.

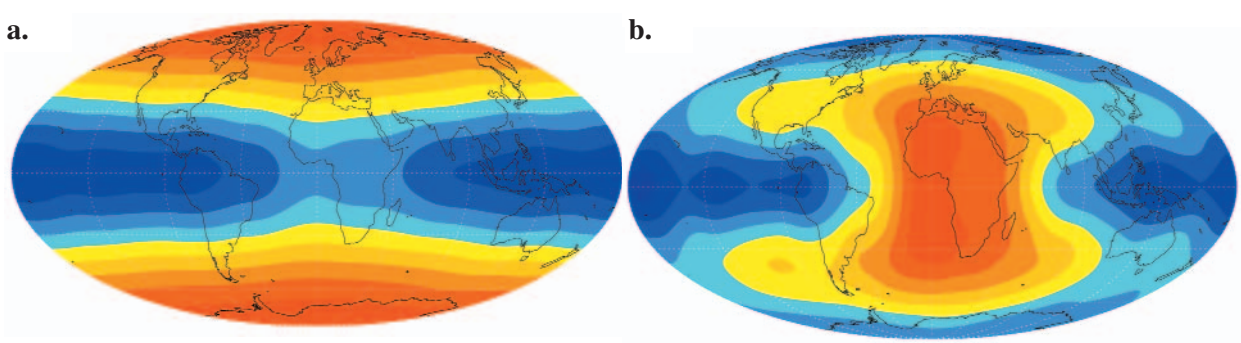

Figure 21. Snapshots of time-varying gravity anomaly (i.e. the departure of the gravity field from the Earth's mean gravity field) at the Earth's surface due to core fluid density variations: (a) the total gravity anomaly that demonstrates a dominant J_2 component, (b) the non J_2 part of gravity anomaly, showing significant spatial variation due to higher order gravity anomalies. The orange and blue colors represent the anomaly above and below the mean field, respectively.

Contact: Weijia Kuang, Weijia.Kuang-1@nasa.gov

Precise Atmospheric Loading Estimates for New Space Gravity Missions.

The new space gravity missions will provide gravity field measurements with unprecedented precision and high spatial resolution. The retrieval of oceanic and hydrological signals from the monthly time-variable gravity field recovered by the GRACE satellites requires a precise knowledge of the atmospheric contributions.

The atmosphere being nearly hydrostatic at low frequencies, the atmospheric thickness is usually neglected and the atmospheric loading is therefore modeled using only the surface pressure and a thin-layer (2-D) assumption. Because of the new requirements in accuracy, this traditional approach is no longer sufficient for deducing atmospheric loading effects and have to model the effects induced by the three-dimensional (3-D) structure of the atmosphere.

The 3-D structure of the air density has been reconstructed from the classical meteorological parameters (pressure, temperature and specific humidity) on a realistic topography provided by meteorological centers such as NCEP (National Center for Environmental Predictions). Using these global meteorological datasets has shown that the differences between the 2-D and 3-D approaches are larger than the expected GRACE sensitivity (Figure 22) up to harmonic degrees of 20-40 (corresponding to wavelengths of 1000-2000 kilometers) and hence should be taken into account.

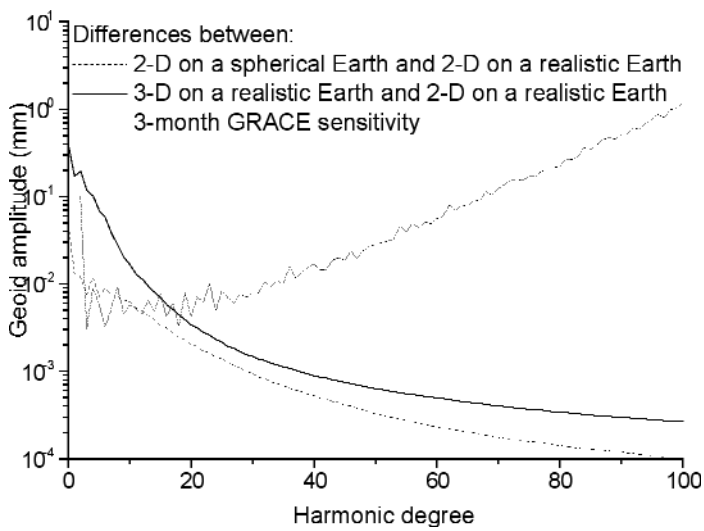

Figure 22. Spectrum of the geoid height RMS differences between the 2-D approximations and 3-D loading, according to NCEP Operational and for April 2002 through June 2002.

Also shown is the 3-D atmospheric loading that is not only required for estimating the high frequency atmospheric contributions on Earth's gravity field variations but also for longer periods for the zonal harmonic coefficients, mainly at annual and semi-annual timescales.

Contact: Jean-Paul Boy, boy@bowie.gsfc.nasa.gov

Crustal Deformation

Earth Anelasticity from Satellite Tracking and Altimetry

The moon and sun raise tides not only in the oceans, but also in the solid Earth. These "Earth tides" have long attracted the interest of geophysicists, partly because they hold the promise of revealing unknown properties of the Earth's deep interior. For example, one long-sought goal has been to determine the anelastic properties of the deep interior. Those properties are known fairly well at seismic frequencies, but not at lower frequencies, so studies of Earth tides, especially those of diurnal and semidiurnal periods, could help close this gap in understanding the Earth's response to large-scale forces. Unfortunately, all previous Earth-tide studies have failed to determine the tidal anelastic effect because the signal is very small and hidden by the much larger ocean-tide signals.

A recent analysis of space geodesy data has now determined the anelastic lag in the Earth tide. This was done by combining satellite tracking data, primarily laser tracking of LAGEOS and other geodetic satellites, with satellite altimeter data, primarily from TOPEX/POSEIDON. The tracking data are senstive to the gravitational effect of tides, while the altimeter data are sensitive to the direct geometric effect. By themselves neither data type can separate the ocean tide from the Earth tide, but combining the two data types allows a clean separation.

Analysis of the principal semidiurnal tide (period 12.4 hours) reveals an Earth tide lag of 0.102°±0.023°, corresponding to a time lag of about 25 seconds between maximum tidal forcing and maximum Earth-tide elevation. This implies a solid-earth Q of about 300.

Similar determinations for other tides will hopefully allow us to determine the variation of Q as a function of frequency, a key property of the Earth's deep interior.

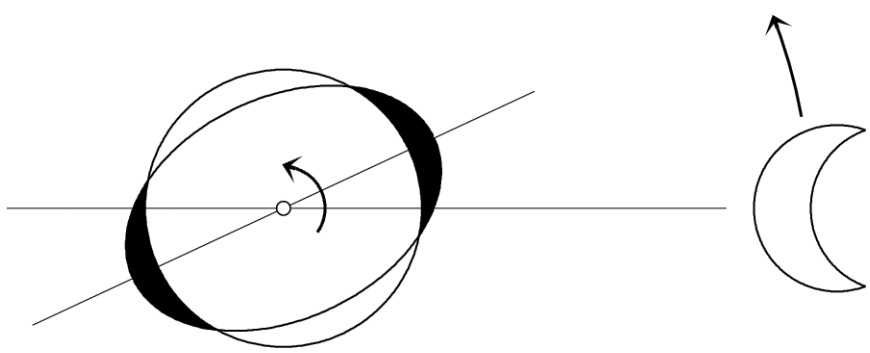

Figure 23. Because of anelasticity the Earth's tidal bulge lags the moon's tidal force, while the Earth's rotation sweeps this lagged bulge ahead of the moon. The lag in the Earth tide has been determined to be about 0.1°. For comparion, the lag in the ocean tide is almost 65° and has hitherto hidden the small Earth-tide.

Reference:

Ray, R. D., R. J. Eanes, and F. G. Lemoine, "Constraints on energy dissipation in the Earth's body tide from satellite tracking and altimetry," Geophysical Journal International, vol. 144, pp. 471-480, 2001.

Contact: Richard Ray, Richard.D.Ray@nasa.gov

Invited Review Summary of South Central Alaska Crustal Deformation

The 1964 Alaska earthquake is the largest known seismic event (moment magnitude, Mw=9.2) to strike North America and the second largest event to occur anywhere in the world within the modern observational era. The region of south central Alaska that was directly affected by this earthquake (i.e. from Cordova to Kodiak Island and Anchorage to well offshore, see Figure 24) lies at the boundary between the converging Pacific and North America tectonic plates. Over the past few decades a tremendous body of scientific information has been developed about the earthquake cycle in this region that has given new insight into how strain is accumulated and released in subduction zones. The temporal and spatial pattern of crustal deformation that has been revealed is far more complex than predicted by extant models of plate boundary zone seismicity. The editors of the series "Advances in Geophysics", have asked Steve Cohen to prepare for publication a comprehensive summary of crustal deformation in southcentral Alaska. The summary is based not only on the decade long observational and modeling study he has carried out, but also on studies from other investigators.

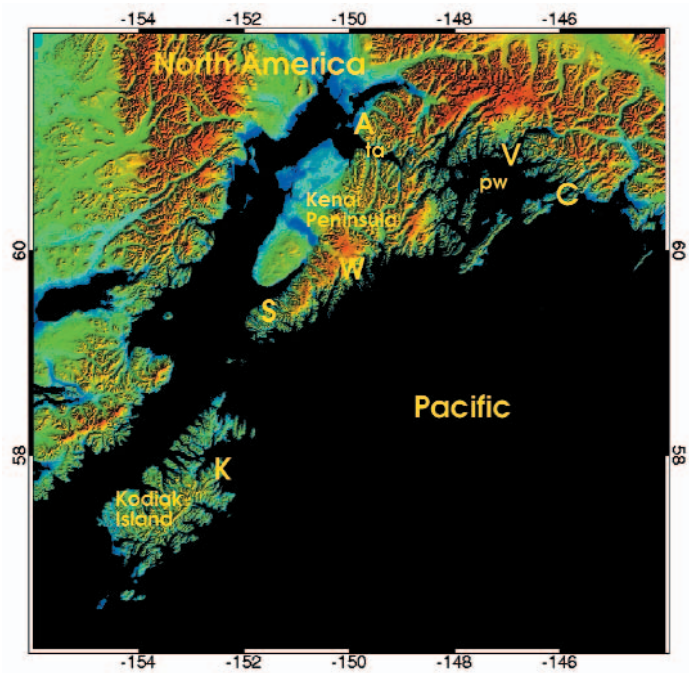

Figure 24. Topographic rendition of Southcentral Alaska. Cities shown by letters are A=Anchorage, C=Cordova, K=Kodiac, S=Seldovia, V=Valdez, W=Seward. Also ta=Turnagain Arm and pw=Prince William Sound.

The available geodetic data is a rich mixture of space age and conventional observations. For the past decade Global Positioning System (GPS) studies of point positions have provided data used to derive estimates of horizontal and vertical crustal velocities. Areas of special concentration have included the Kenai Peninsula, nearby offshore locations, the greater Anchorage area, the Kodiak Island-Katmai region to the southwest, and near Valdez to the east. Prior to the availability of GPS, precision level surveys were undertaken to provide information on vertical motion. Repeated surveys were conducted along the Turnagain Arm, and single epoch measurements are available on the Kenai Peninsula. Tide gauge measurements have been made more or less continuously at a half dozen or more coastal sites. In a few cases, these measurements provide a time series extending back to before the 1964 earthquake. Very Long Baseline Interferometry (VLBI) measurements were made in the late 1980's on Kodiak Island and at a few other sites in Alaska. Recently, a continuously operating GPS station was installed near the tide gauge at Seldovia.

Additional information about crustal movements come from a limited number of triangulation measurements, tsunami records, and geological observations such as changes in the heights of algae and soil depositional changes.

Some of the most significant results from this wealth of data include:

(1) The postseismic uplift in the region that subsided during the earthquake was both rapid and large. Between Anchorage and the Kenai Peninsula the subsidence was as much 2m during the earthquake. However, the cumulative uplift since the earthquake may exceed 1m in some locales (Figure 25). The most rapid uplift was right after the earthquake and may have been as much as 150 mm/yr. Leveling data from the Turnagain Arm suggests that postseismic creep occurred along the down-dip extension of the coseismic rupture plane in the first few years following the earthquake. On the other hand, decreases in the vertical displacement rate at tide gauges on Kodiak Island and Cordova reveal the existence of a much longer-lived transient phenomenon lasting on the order of 1-2 decades. Other tide gauge data suggest that an even longer lived post-seismic process may also be at work.

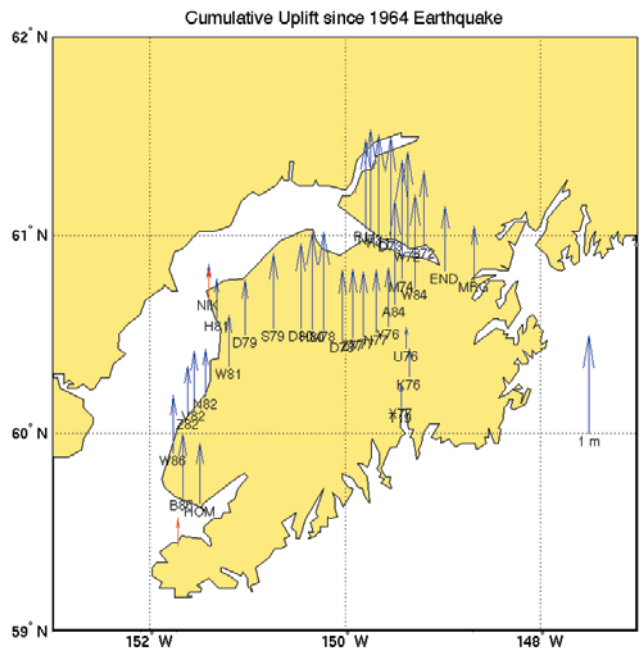

Figure 25. Uplift since 1964 on Kenai Peninsula and adjacent areas. The uplift is plotted relative to a tide gauge station at Seward. The red arrows show uplift as determined from tide gauge observations, the blue arrows show uplift determined by comparing post-earthquake leveling height observations to contemporary GPS vertical position determinations.

(2) There is considerable along-strike (lateral) variability in the contemporary pattern of horizontal deformation. On the eastern Kenai Peninsula, the present-day velocities (relative to stable North America) are as large as 30-40 mm/yr. These are parallel to the direction of relative plate motion, decrease with distance from the plate boundary, and are largely consistent with standard models of strain accumulation along a strongly coupled plate interface. However, in the western Kenai Peninsula, the velocities are directed SSW, i.e. generally in the opposite direction from those on the eastern side of the Peninsula, and have speeds on the order of 20 mm/yr. The pattern of crustal deformation is suggestive of a long-lived or delayed response to the 1964 earthquake, but does not allow for significant contemporary strain accumulation.

(3) There can be sudden changes in the deformation pattern even several decades after the earth-

quake. GPS measurements near Anchorage made prior to 1998 display a velocity pattern similar to those on the Kenai Peninsula and are indicative of strain accumulation. However, the velocities reversed after 1998 and it appears that a “slow earthquake,” with considerable slip, may well have occurred.

Taken as a whole, these observations suggest a complex pattern of plate boundary interactions where the coupling between the overriding and subduction plates not only varies with location but also with time. Thus the models of regional seismotectonics that are required today are much more sophisticated than the simple elastic-frictional or even viscoelastic-frictional models of just a few years ago. Researchers are now developing various numerical models of this crustal deformation that take into account both bulk rock properties and fault rheology, variations in the plate interface geometry, and both plate interface and crustal faulting. The "Advances in Geophysics" article is a comprehensive summary of both the observational information and modeling results from the southcentral Alaska region that will serve as a resource for investigators studying both the Alaskan as well as other subduction zones.

Contact: Steve Cohen, Steven.C.Cohen@nasa.gov

Topography and Surface Change

Puget Sound Lidar Studies

Surface deformation caused by large earthquakes often produces geomorphic features that provide significant constraints on fault locations, sense of motion, and displacement magnitudes. David Harding, a participant in the Puget Sound Lidar Consortium (http://www.pugetsoundlidar.org), is using very high resolution digital elevation data in the Puget Lowland of Washington State to characterize deformation caused by Holocene earthquakes. The elevation data was acquired by airborne laser mapping, a technique that reveals the ground topography beneath the dense temperate rain forest cover of the Pacific Northwest.

At invited talks this year at the Geological Society of America Cordilleran Section annual meeting, the Spring American Geophysical Union meeting, and the Geological Society of Washington, Harding reported on results that define spatial patterns of fault slip that occurred circa A.D. 900 in the Seattle fault zone. This slip was due to a magnitude 7 (or greater, earthquake). Harding used the laser mapping data to measure the elevation of shoreline angles at the landward edge of uplifted and tilted terraces that border Puget Sound (Figure 26). A shoreline angle is a paleo-horizontal marker originally formed at sea level by wave-cut erosion. The terraces define a broad, 5 km wide, asymmetric anticline across the width of the Seattle fault zone, formed by slip on the most northerly, basal thrust.

The terrace offsets on the south limb of the anticline indicate that structural higher thrusts also underwent slip during the earthquake. This study documents that multiple fault strands within the Seattle fault zone are still active and constrains their magnitude and sense of slip during the A.D. 900 earthquake. These results contribute to an improved assessment of the earthquake hazard in the densely populated Puget Sound region.

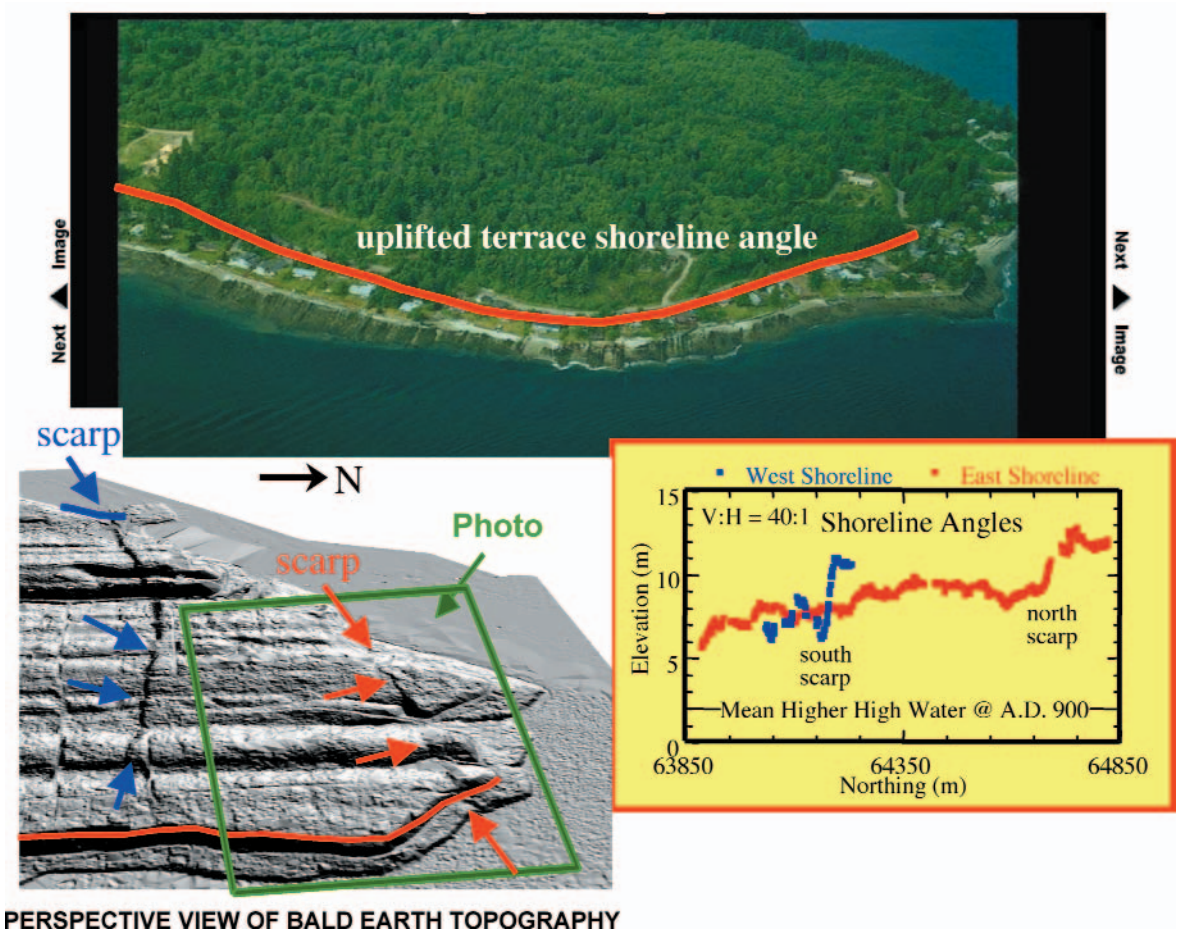

Figure 26. An example of terrace shoreline angle elevation profiles (lower right) measured from laser mapping elevation data (lower left) that reveals the ground topography beneath dense vegetation (the north-south ridges are the result of glacial erosion). The terrace was uplifted by as much as 10 m, tilted to the south, and offset by fault scarps during the A.D. 900 earthquake.

Contact: David Harding, David.J.Harding@nasa.gov

Quantifying Plains Volcanism on the Eastern Snake River Plains and Mars

Basaltic plains style volcanism is a common form of volcanic planetary resurfacing, and is thought to be a significant factor in the volcanic and thermal histories of all of the terrestrial planets (Earth, Moon, Mercury, Mars, and Venus, as well as some of the larger satellites of the Gas giants). Plains volcanism is well illustrated on Earth, with perhaps the textbook example being the Eastern Snake River Plains (ESRP) of Idaho. Volcanic features in the ESRP have erupted through several hundred separate vents, and are characterized by a mix of rift eruptions, low shields that often coalesce, a few cinder cones, and extensive fields of relatively thin lava flows. Commonly the flows were slowly emplaced through systems of channels and lava tubes over rather low regional slopes. The total thickness of the sequence is thought to be a few km, erupted over about 15 million years, with the most recent eruptions within the last few thousand years, and future eruptions possible at wide time intervals.

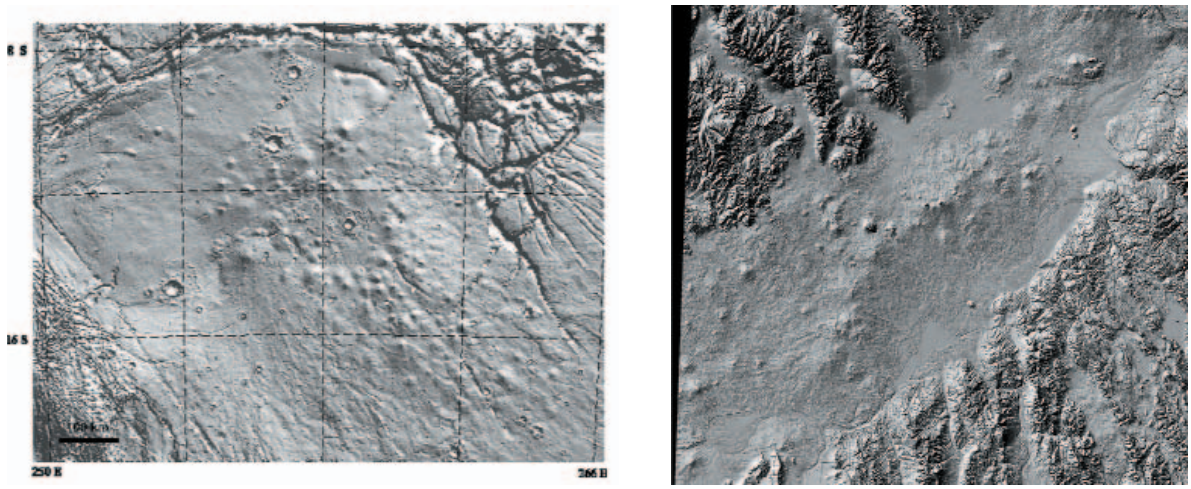

Figure 28. Shaded relief topography for the Syria region of Mars (left) and the Eastern Snake River Plains region of Idaho (right). Both regions show basaltic plains volcanism features, including low shields, flow fields, lava tubes, and rift eruptions.

While this style of volcanism is well known, it is not yet well understood or quantified even though it is important for the understanding of regional terrestrial resurfacing rates, volcanic hazards, and tectonic-volcanic systems relationships. Susan Sakimoto and colleagues Tracy Gregg (SUNY, Buffalo) and Scott Hughes (Idaho State) are engaged in the study, which combines existing remote sensing measurements with higher accuracy field measurements and ground truth to understand the topography and petrology or the ESRP system, and to use that data to constrain eruption types and rates. In parallel with the terrestrial measurement effort, they are characterizing similar regions on Mars, with the expectation that terrestrial results will be directly applicable to the similar martian rate and eruption style questions. The work is in collaboration with the Idaho Space Grant, and is funded through both the NASA Space Grant EPSCoR 2000 program and through the NASA Mars Data Analysis Program.

This past summer, the field season in the ESRP was focused on using GPS receivers to characterize topography profiles across the summit regions of the low volcanic shields as well as across some of the tube and channel fed volcanic flows. The summit regions show some systematic differences in topography that appear to be correlated with the petrology (texture and composition) of the lavas. This may be a direct reflection of the chemical evolution of the contributing magma chamber (e.g. Hughes, et al., 1999, 2001, 2002a, 2002b). The field data combined with remote spectral and topographic data and laboratory compositional and petrological work suggests that the steeper summit regions on many of the basaltic shields are very likely an expression of the slightly more evolved petrology for these shields, and in some cases are diagnostic of the extent of local ground water involvement in the eruption process. The parallel work on the topography of the martian volcanic fields (e.g. Sakimoto et al., 2001, 2002a, 2002b) shows a similar range of summit topography variations for the small shield volcanoes. It is expected that the terrestrial results will help us understand the contributions of local water availability and compositional evolution to topography in the ESRP. It should also have direct applicability to constraining similar questions on the chemical evolution and local water availability for our analogous martian plains volcanism regimes.

These results were presented in a set of paired sessions at the 2002 Fall Geological Society of America meeting in Denver in the session T90. Terrestrial Approaches to Extraterrestrial Problems and Vice Versa. (Sakimoto et al., 2002b, Hughes et al., 2002b).

References:

Hughes, S. S., M. McCurry, et al.. Geochemical correlations and implications for the magmatic evolution of basalt flow groups at the INEEL. Geology, Hydrogeology and Environmental Remediation, Idaho National Engineering and Environmental Laboratory. P. K. Link and L. L. Mink, Geol. Soc. of Am. Special Paper 353, 2002a.

Hughes, S.S., S.E.H. Sakimoto, and T.K.P. Gregg,Plains volcanism in the Eastern Snake River Plain: Quantitative measurements of petrologic contributions to topography with comparisons to Mars, GSA Annual Meeting Abstracts, Paper #77-3, 2002b.

Hughes S.S., R.P. Smith, W.R. Hackett, and S.R. Anderson Mafic volcanism and environmental geology of the eastern Snake River Plain, in Hughes, S.S., and Thackray, G.D., eds., Guidebook to the Geology of Eastern Idaho: Idaho Museum of Natural History, p. 143-168, 1999.

Hughes S.S., P.H. Wetmore, and J.L. Casper Evolution of Quaternary tholeiitic basalt eruptive centers on the eastern Snake River Plain, Idaho, in Bonnichsen, B., White, C., and McCurry M., eds., Tectonic and magmatic evolution of the Snake River Plain volcanic province: Idaho Geological Survey Special Publication, 2000.

Sakimoto, S.E.H., J.B. Garvin, B.A. Bradley, M. Wong, and J.J. Frawley, Small martian north polar volcanoes: Topographic implications for eruption styles, LPSC XXXII, CDROM, abstract #1808, 2001.

Sakimoto, S.E.H., D. Mitchell, S.J. Reidel, and K. Taylor, Small Shield Volcanoes on Mars: Global Geometric Properties and Model Implications for Regional Variations in Eruptive Styles, LPSC XXXIII, CDROM, abstract #1717, 2002.

Sakimoto, S.E.H., S.S. Hughes, T.K.P. Gregg, Plains volcanism on Mars: Topographic data on shield and flow distributions and abundances, with new quantitative comparisons to the Snake River Plain Volcanic Provinces, GSA Annual Meeting Abstracts, Paper #77-2, 2002b.

Contact: Susan Sakimoto, sakimoto@core2.gsfc.nasa.gov

Planetary Geology and Geophysics

Buried Basins on Mars

MOLA data has revealed an abundance of Quasi-Circular Depressions (QCDs) on Mars which have little or no expression in image data. These are most likely buried impact basins, covered versions of the impacts exposed at the surface. An earlier study of more than 600 of these in the lowlands of Mars showed that the crust below the young, smooth plains was as old and likely older than the exposed cratered highlands (Frey et al., 2002). In a paper given at the 2002 Lunar and Planetary Science Conference, Herb Frey showed that these buried lowland basins constrain the lowlands in eastern Mars to have formed in the earliest part of the Early Noachian, the oldest period of martian history (Frey, H., 2002). Further, in at least this part of Mars, the lowlands formed as the result of a giant impact. Though first suggested by George McGill in 1989 to be a giant impact, the Utopia Basin was not universally accepted as a larger version of Hellas or Argyre until MOLA topography showed its full bowl-like shape. Like the rest of the lowlands of Mars, this area has a large number of buried basins superimposed on it (Figure 29). These were shown by H. Frey and co-workers to be of Early Noachian age, meaning the Utopia impact which must pre-date these smaller basins is even older. Since the impact produced the low topography characteristic of this region (and since that imprint has remained intact since the impact), the crustal dichotomy in eastern Mars must date from essentially the earliest part of recorded martian history. Processes other than impact appear to have had little role to play in at least this part of Mars.

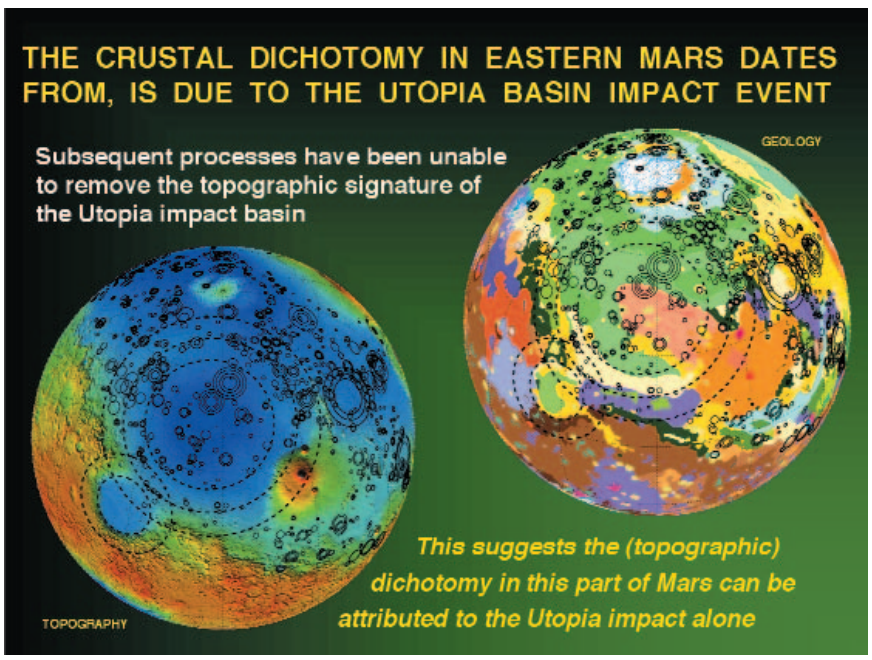

Figure 29. MOLA topography (lower left) and global geology (upper right) with lowland QCDs (mostly buried impact basins) superimposed on it. The large multi-ring structure is the Utopia impact basin, which is overlapped by the Isidis impact basin on its SW side. From Frey, H. 2002a.

Buried basins elsewhere on Mars have also provided evidence for crust older than the Early Noachian. In what started as a science fair project, sophomore Erin Frey of South River High School, working with her father, Herb Frey, found clear evidence for QCDs not visible on images in the oldest and most heavily cratered parts of Mars (Frey and Frey, 2002; Frey, E. et al., 2002). The region to the SE of the ancient Hellas impact basin, about 1.2 million sq km, is mapped as Early Noachian, based on its rugged nature and high density of craters. E. Frey found that there

was a significant population of buried basins in this area, which implies a crust below that is older than the surface. The total cumulative crater density is about 1.6 times that of the visible crater density. These results were presented at the Spring AGU Meeting in Washington by E. Frey (Frey and Frey, 2002) in her first professional paper. H. Frey did a similar study in the other major outcrop of Early Noachian terrain near the slightly younger (but still Early Noachian-age) Isidis impact basin and found similar evidence for an even larger population of buried basins (Frey, E. et al., 2002). Thus it appears what is mapped as Early Noachian material is not primordial crust on Mars dating back to 4.6 billion years ago. Curiously, in both the Hellas and Isidis areas the total crater density, the buried and visible populations together, are nearly the same. They are also very similar to the total crater density for several other Noachian areas (Figure 30).

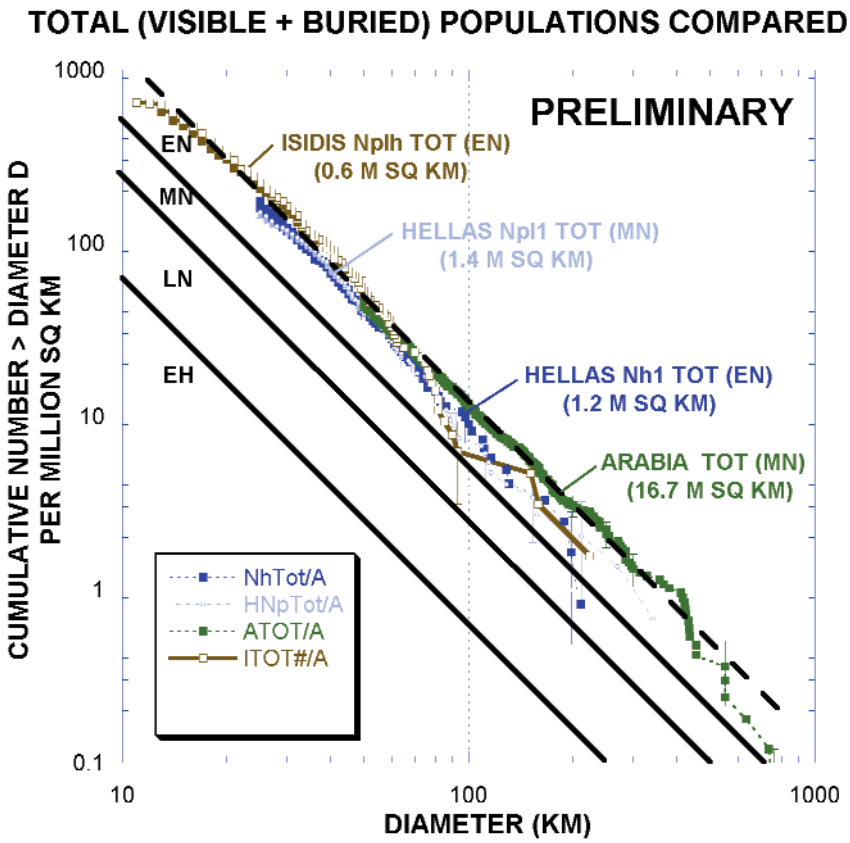

Figure 30. Total (visible + buried) cumulative frequency curves for several Noachian terrains, including a large area in Arabia and areas near the Hellas and Isidis impact basins. Note that all of these seem to show a similar crater retention age. From Frey, E. et al., 2002.

Similar total (visible + buried) crater retention ages for a number of different old units at different places around Mars could be due to crater saturation and might be a limit beyond which we cannot see and cannot date (in terms of impact craters) the buried surfaces. Alternatively, the similar crater retention age could represent a common early crustal age, perhaps of the original crust on Mars.

This work was presented at the Geological Society of America Meeting in Denver, CO (Frey, E., et al., 2002).

References:

Frey, E. L. and H. V. Frey, Evidence for an Earlier Early Noachian on Mars, Spring AGU Paper P32A-01, 2002.

Frey, E.L., H. V. Frey, W. K. Hartmann and K. L. Tanaka, Evidence for Crust Older than the Oldest Surface Units on Mars, GSA Annual Fall Meeting, Paper 26-2, 2002.

Frey H.V. Age and Origin of the Crustal Dichotomy in Eastern Mars, Lunar Planet Sci. Conf. XXXIII, abstract 1680, 2002.

Frey, H.V., J. H. Roark, K. M. Shockey, E. L. Frey and S. E. H. Sakimoto, Ancient Lowlands on Mars, Geophys. Res. Lett. 29, 10.1029/2001GL013832, 2002.

Contact: Herb Frey, Herbert.V.Frey@nasa.gov

Recent Studies of Mars Magnetic Anomalies

Why are some Martian terranes strongly magnetic and some non-magnetic? In a talk at the 33rd Lunar and Planetary Science Conference, Mike Purucker discussed the origin of a terrane, centered at Noachis Terra in the southern highlands, that has no strong magnitude magnetic fields (anomaoies) associated with it, unlike that of nearby terranes. This is enigmatic because the age of the rocks at the surface in the non-magnetic region is not much different from those in the adjacent, strongly magnetic region. Parts of this non-magnetic region are associated with the Argyre and Hellas impact basins, but one or more additional large impacts or thermal events may be necessary to produce such a region absent large-scale fields. Some candidates were suggested based on MOLA topographic data, which is useful for revealing even subtle depressions or basins.

As part of a popular presentation to a technical audience of non-specialists at the Society of Exploration Geophysicists, Purucker reviewed the state of knowledge on possible mineral resources on Mars. In a presentation called “Exploration Geophysics on Mars: A tale of Minerals and Water,” he also suggested the presence of deep concentrations of iron in the Terra Cimmeria and Sirenum regions, and the possible presence of near-surface Cu-Fe sulfides in the Apollinaris Patera region. An online version of the talk is available online at: http://geodynamics.gsfc.nasa.gov/research/purucker/mag_gravity_luncheon.html and a version is being prepared for publication in 'The Leading Edge.'

Contact: Mike Purucker, purucker@geomag.gsfc.nasa.gov

Atmospheric Rotational Effects on Mars Based on the NASA Ames General Circulation Model

The objective of this investigation is to compute and analyze how the atmosphere affects the rotation of Mars, based on outputs from the NASA Ames General Circulation Model (GCM). The model provides surface values of stress and pressure, which serve as inputs to the calculation of topographic (mountain), stress (friction), and gravitational atmospheric torques. The model also provides time series for the moments of inertia of the ice caps due to the condensation and sublimation of CO_2, and a time series for the axial component of atmospheric angular momentum.

The rotational variations of a planet can be analyzed into axial and equatorial components. The axial variations (along the z-axis, which is the rotation axis) are reflected in changes in the length of day (LOD). The equatorial variations (x,y) produce changes in the orientation of the axis of rotation (polar motion). The methodology of planetary rotational investigations can follow the angular momentum approach or the torque approach. The chosen methodology determines the boundaries of the appropriate control volume.

This investigation uses the torque approach to compute axial and equatorial variations in rotation. In this case the control volume includes only the solid body of Mars. The time variable moments of inertia produced by CO_2 condensation and sublimation are taken into account in the axial computations.

The angular momentum approach is used as well to obtain axial variations. The control volume then includes Mars' solid body and its atmosphere. Torques do not appear in this formulation.

Although experience with the Earth system indicates that the angular momentum approach is more reliable to compute LOD variations, the torque approach gives more insight on the mechanisms by which angular momentum is being transferred between the solid body and the atmosphere. Also, pressure and gravitational torques computed are not just the frictional component. Torque results are of interest on their own to ascertain the relative importance of various modes of angular momentum transfer.

In Mars' case the stress torque is the major contributor to the torque budget. This is different from the results obtained from Earth atmospheric models, in which case the ellipsoidal torques (polar flattening, gravitational) have by far the greatest total power magnitude, with the topographic torque ranking third.

The dominance of the frictional stress torque in Mars' budget can be attributed at least in part to the tangential stress dependency on the second power of the surface wind speeds. That is, Mars' less massive atmosphere (by a factor of 50) and the square of the wind speeds combine to produce smaller frictional stresses by a factor of 30, while Mars pressure torques are directly proportional to surface pressures which are 145 times smaller than Earth's. The solution of Liouville's equations provides the changes in Mars' rotation, i.e., changes in LOD and polar motion.

As shown in Figure 31, the polar motion computed from the torque forcing function reaches a maximum of 16.26 mm in the second half of the Martian Northern Hemisphere winter. The rotation pole moves around the axis of figure close to 3 and 1/2 times during the Martian year. Torque-induced annual and semi-annual polar motion is much less than the 21-cm obtained by other investigations from products of inertia due to ice caps offsets.

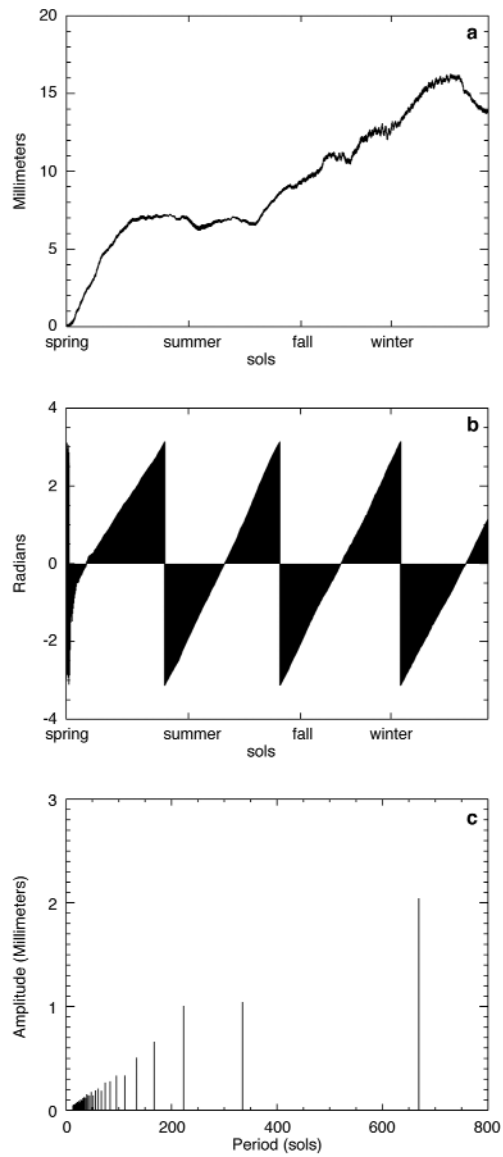

Figure 31. Polar motion due to torque, a) displacement time series, b) phase angle time series, c) displacement power spectrum.

Changes in LOD using the angular momentum approach are 0.187 and 0.136 milliseconds for the annual and semi-annual harmonics. The time series is portrayed in Figure 32. The expected precision of the planned NetLander Ionospheric and Geodesic Experiment (NEIGE) should detect

the main harmonics in the ΔLOD time series. Annual and semi-annual polar motion harmonics induced by atmospheric torque are below the level of NetLander Ionospheric and Geodesic Experiment (NEIGE) detectability. The model used here for the solid body of Mars does not include a liquid core; therefore possible near-diurnal resonances are excluded. We hope to study them in a future work.

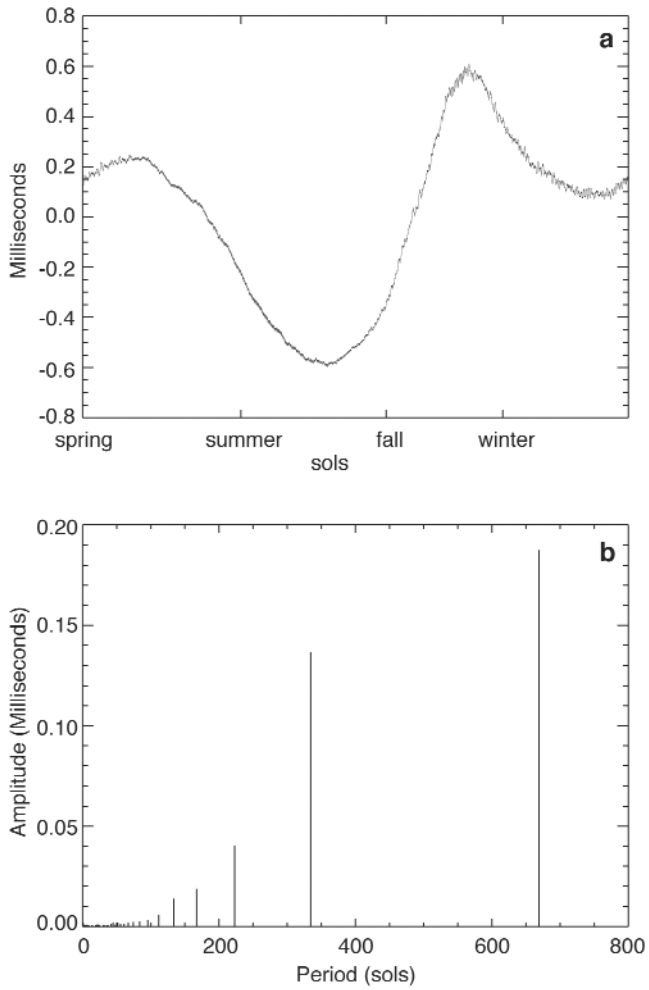

Figure 32. Delta LOD based on sum of axial atmospheric angular momentum and caps' inertia, a) time series, b) power spectrum.

Reference:

Sanchez, B. V., D. D. Rowlands, R. M. Haberle, J. Schaeffer, "Atmospheric Rotational Effects on Mars Based on the NASA Ames General Circulation Model", Journal of Geophysical Research - Planets, accepted January 16, 2003.

Contact: Braulio V. Sanchez, Braulio.V.Sanchez@nasa.gov

Orbital-Rotational-Climatic Interaction

Orbital Noise and Climate Fluctuation

The current debate on the Earth's climate fluctuations, (such as global warming) is driven by the observation of atmospheric concentrations of the greenhouse gases (CO_2 and CH_4). Popular climate models contain high levels of atmospheric carbon dioxide and predict that global greenhouse warming would cause heating in the tropics, but historical fossil isotopic data have indicated cool tropical temperature during greenhouse episodes. This mismatch between observation data and the climate models, known as the cool-tropic paradox, implies that either the data are flawed or we understand very little about the climate models.

Han-Shou Liu and co-workers (Liu, et al., 2002) suggest, from a dynamics point of view, that the common cause of climate and greenhouse-gas fluctuations is the orbital noise in the Earth's system which is distinct from the commonly considered orbital signals in eccentricity and precession. This finding provides a link between orbital noise and climate fluctuations for climate studies. Figure 33 shows calculations of insolation pulsation induced by orbital noise of the Earth's changing obliquity.

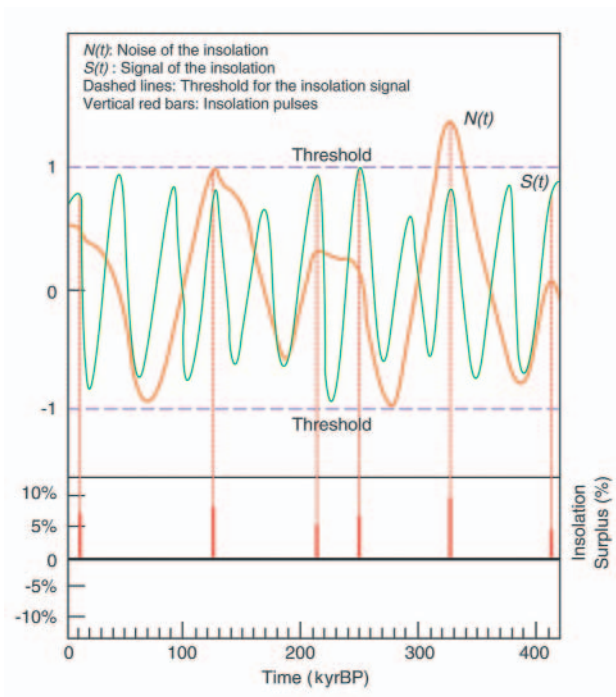

Figure 33. Noise-signal coupling effect on Rubincam's orbital insolation induces pulsation in the incoming solar radiation. The threshold model is derived from the signal to noise mode. The treshold (two horizontal dashed lines) defines the maximum and minimum values of the insolation signal. Time is in kiloyears (kyr) before present (BP).

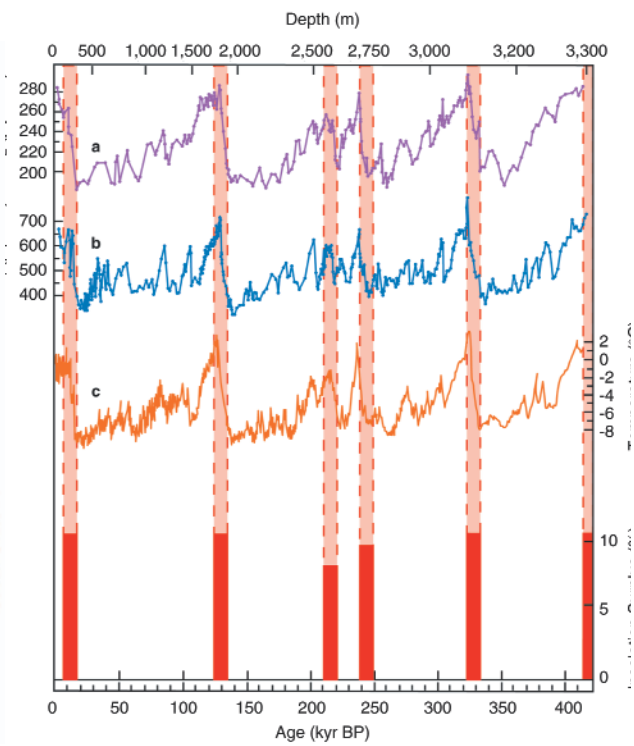

Figure 34. Orbital insolation pulses cause atmospheric concentrations of carbon dioxide and methane and glacial-interglacial temperature changes.

Global greenhouse warming phenomena during the past half million years were the effect and consequence of rapid temperature increases caused by insolation pulsation (Figure 34). In addition, Liu finds that the intensity of the insolation pulsation is dependent on the latitude of the Earth. At high latitude, it provides extreme climate warming conditions for greenhouse-gas concentration. However, it decreases markedly in low-latitude regions, predicting cool tropical temperature during supposed greenhouse episodes.

Reference:

Liu, H.S., R.Kolenkiewicz, and C. Wade, Orbital noise in the Earth system is a common cause of climate and greenhouse-gas fluctuation, Fluctuation and Noise Letters,Vol..2, No.2, 103-110, 2002.

Contact: Han Shou Liu,, Liu@core2.gsfc.nasa.gov

A Spin-Up for Asteroid 951 Gaspra

Gaspra, the first asteroid ever to be photographed up close by a spacecraft, is a small body only 6 km in radius, rotating with a 7 hour period, and orbiting in the asteroid belt at 2.2 AU from the Sun. Gaspra's axial precession period turns out to be nearly commensurate with its orbital precession period. This leads to a resonance condition with huge variations in obliquity (obliquity being the tilt of Gaspra's equator with respect to its orbital plane). How did the asteroid get into this resonance? One way is for the orbit to change over time. However, computing its orbit for the last 3 million years indicates its orbit is highly stable (see Figure 35).

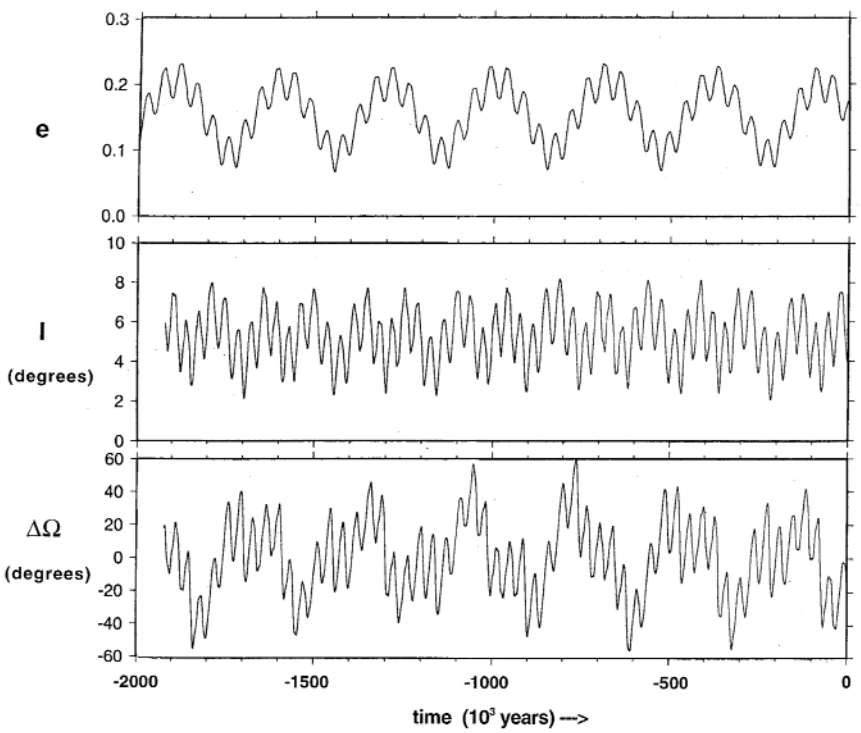

Figure 35. Evolution of the orbit of Gaspara over the last two million years.

A more likely explanation is the YORP effect (Rubincam et al., 2002). YORP stands for Yarkovsky-O'Keefe-Radzievskii-Paddack. In the YORP effect, Gaspra absorbs sunlight and re-

radiates it mostly as heat in the infrared. The infrared photons leaving the surface carry away momentum. By action-reaction, the asteroid receives a slight kick in the opposite direction. It is here the highly shape of Gaspara, known from photographs to be highly irregular, come into play. As shown in Figure 36, the re-radiation causes a net torque on the asteroid, making it spin faster. A change in the spin rate causes the obliquity to change.

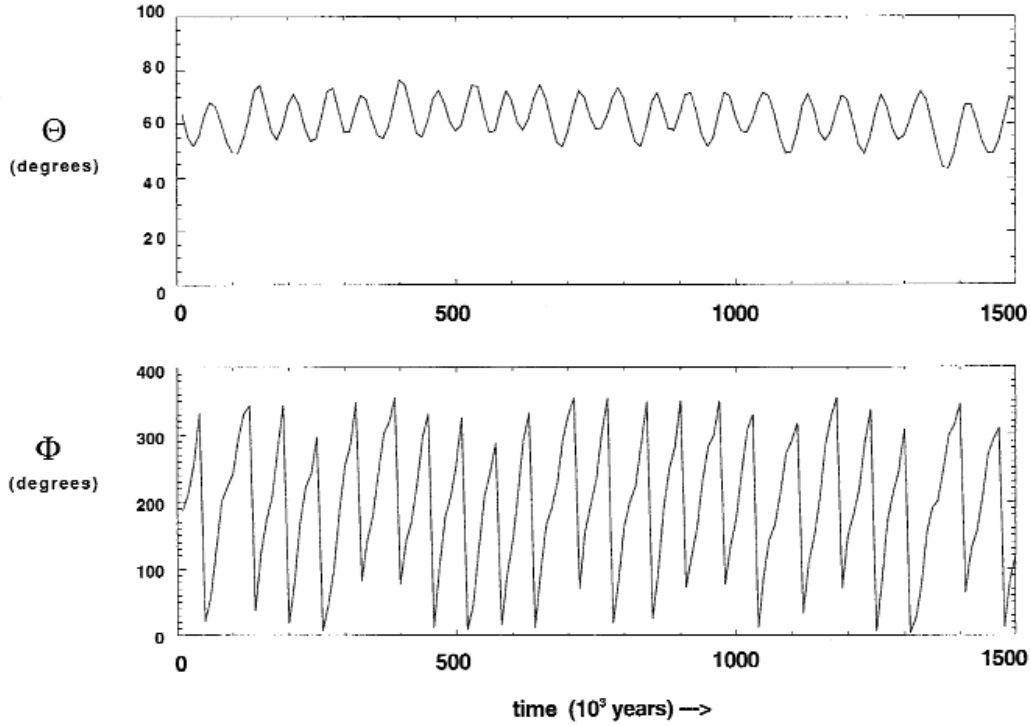

Figure 36. Change in spin and change in obliquity for Gaspra.

It may be that Gaspra started out in a nonresonant state, but evolved into the resonance due to the YORP effect, and has been temporarily trapped there ever since. YORP can alter the spin of small asteroids like Gaspra over hundreds of millions of years, making it competitive with collisions in this regard. Thus YORP may be a major mechanism for altering the spin states of small asteroids and meteorites. These results were published in the September 2002 issue of Journal of Geophysical Research: Planets.

References:

Rubincam, D. P., D. D. Rowlands, and R. D. Ray, Is asteroid 921 Gaspra in a resonant obliquity state with its spin increasing due to YORP?, J. Geophys. Res., 107, 5065, doi:10.1029/2001JE001813, 2002.

Contact: Dave Rubincam, David.P.Rubincam@nasa.gov

Refereed Journal Publications:

Beasely, A. J., **D. Gordon**, A. B. Peck, **L. Petrov**, **D. S. MacMillan**, E. B. Fomalont, and **C. Ma**, The VLBA calibrator survey—VCS1, *Astrophys. J. Sup. Ser.*, *141*, 13-21, 2002.

Cheng AF, Barnouin-Jha O, Prockter L, **Smith, DE**, et al., "Small-scale topography of 433 Eros from laser altimetry and imaging", ICARUS 155 (1): 51-74, 2002

Cohen, S.C. and D.J. Darby, Tectonic plate coupling and elastic thickness derived from the inversion of geodetic data using a steady-state viscoelastic model: Application to southern North Island, New Zealand, *J. Geophys. Res*., 2001JB01687, 2002.

Cox, C. M., and **B. F. Chao**, Detection of a large-scale mass redistribution in the terrestrial system since 1998, *Science*, *297*, 831-833, August 2, 2002.

Cox, C. M., S. M. Klosko, and **B. F. Chao,** Changes in ice-mass balances inferred from time variations of the geopotential observed through SLR and DORIS tracking, in gravity, geoid and geodynamics, M. Sideris ed., IAG Symposia 123, Springer-Verlag, Heidelberg, 2002.

Frey, H.V., J. H. Roark, K. M. Shockey, E. L. Frey and **S. E. H. Sakimoto**, Ancient Lowlands on Mars, *Geophys. Res. Lett*. 29, 10.1029/2001GL013832, 2002.

Fujita, M., **B. F. Chao, B. V. Sanchez**, and T. J. Johnson, Oceanic torques on solid Earth and their effects on Earth rotation, *J. Geophys. Res*., *107*, NO. B8, 10.1029/2001JB000339, 2002.

Heirtzler JR, "The future of the South Atlantic anomaly and implications for radiation damage in space", J ATMOS SOL-TERR PHY 64 (16): 1701-1708, 2002

Hulot G., C. Eymin, **B. Langlais**, M. Mandea, and N. Olsen, Small-scale structure of the geodynamo inferred from Ørsted and MAGSAT satellite data, *Nature*, 416, pp. 620-623, 2002.

Kim, H. R., R. R. B. von Frese, J. W. Kim, **P. T. Taylor** and T. Neubert, Ørsted verifies regional magnetic anomalies of the Antarctic lithosphere, *Geophysical Research Letters*, vol. 29, no. 15, p. 31-33, 2002.

Kletetschka, G., P. J. Wasilewski and **P. T. Taylor**, The role of hematite-limonite solid solution in the production of magnetic anomalies in ground- and satellite-based data, *Tectonophysics*, vol. 347 no. 1-2, p. 167-178, 2002

Kutina, J. and **P. T. Taylor**, Satellite altitude magnetic anomalies-implications for mineral exploration: A review, *Global Tectonics and Metallogeny*, vol. 8, no. 1-2, 2002.

Liu, H. S., R. Kolenkiewicz, and **C. Wade, Jr.,** Orbital noise in the Earth system is a common cause of climate and greenhouse-gas fluctuation, *Fluctuation and Noise Lett. 2,* L101-L108, 2002.

Lowman, P. D., "Exploring Space, Exploring Earth: New Understanding of the Earth from Space Research," Cambridge University Press, 362 p., 2002.

Lowman, P. D., "Exploration Science: A Case History from Earth Orbit," *The Science Teacher*, v. 69, no. 7, p. 24-30, 2002.

Luhmann, J.G., M.H. Acuna, **M. Purucker**, C.T. Russell, and J.G.Lyon, The Martian magnetosheath: how Venus-like?, *Planetary and Space Science*, 50, 489-502, 2002.

Luthcke, S. B., **C. C. Carabajal** and **D. D. Rowlands**, Enhanced geolocation of spaceborne laser altimeter surface returns: parameter calibration from the simultaneious reduction of altimeter range and navigation tracking data, *Journal of Geodynamics*, *34*, 447 – 475, 2002.

McGovern, P., S.C. Solomon, J.W. Head, **D.E. Smith, M.T. Zuber**, M. A. Wieczorek, R.J. Phillips, **G.A. Neumann**, O. Aharonson, Localized gravity/topography admittance and correlation spectra on Mars: Implications for regional and global evolution, *J. Geophys. R*es., 107(E12), 5136, DOI:10.1029/2002JE001854, 2002.

Mendes, V. B., G. Prates, **E. C. Pavlis**, **D. E. Pavlis**, and R. B. Langley "Improved mapping functions for atmospheric refraction correction in SLR", *Geophysical Res. Lett., 29*(10), 1414, doi:10.1029/2001GL014394, 2002.

Pavlis, E. C., "Geodetic Contributions to Gravitational Experiments in Space", Book chapter in *Recent Developments in General Relativity, Genoa 2000*, R. Cianci, R. Collina, M. Francaviglia, P. Fré (eds), Springer-Verlag, Milan, pp. 217-233, 2002.

Pavlis, E. C. and L. Iorio, "The impact of tidal errors on the determination of the Lense-Thirring effect from satellite laser ranging", *International Journal of Modern Physics D*, 11, 4, pp. 599-618, 2002.

Peale SJ, Phillips RJ, Solomon SC, **Smith DE**, et al., "A procedure for determining the nature of Mercury's core", METEORIT PLANET SCI 37 (9): 1269-1283 SEP 2002

Ponte, R. M. and **R. D. Ray**, `Atmospheric pressure corrections in geodesy and oceanography: a strategy for handling air tides,' *Geophysical Research Letters, 29(24),* 6.1-6.4, 2002.

Purucker, M., B. Langlais, N. Olsen, G. Hulot, and M. Mandea, The southern edge of cratonic North America: Evidence from new satellite magnetometer observations, *Geophys. Res. Lett*., 29, 1 August 2002.

Ravat, D., B. Wang, E. Wildermuth and **P. T. Taylor**, Gradients in the interpretation of satellite-altitude magnetic data: an example from central Africa, *Journal of Geodynamics*, vol. 33 no. 1-2, p.131-142, 2002.

Ravat, D., K. Whaler, M. Pilkington, **T. Sabaka and M. Purucker**, Compatibility of high-altitude aero-

magnetic and satellite-altitude magnetic anomalies over Canada, **Geophysics**, 67, 546-554, 2002

Rowlands, D. D,. R. D. Ray, D. S. Chinn and **F. G. Lemoine**, Short-arc analysis of intersatellite tracking data in a gravity mapping mission, *Journal of Geodesy, 76,* 307-316, 2002.

Rubincam, D. P., **D. D. Rowlands,** and **R. D. Ray**, Is asteroid 951 Gaspra in a resonant obliquity state with its spin increasing due to YORP? *Journal of Geophysical Research, 107,* 1-7, 2002.

Sabaka, T.J., N. Olsen and **R.A. Langel**, A comprehensive model of the quiet-time, near-Earth magnetic field: phase 3, *Geophys. J. Int*., 151, 32-68, 2002.

Taylor, P.T. and J.J. Frawley, Satellite-Altitude-Magnetic Data and the Search for Mineral Resources: the Kiruna region of Sweden, *Global Tectonics and Metallogeny*, vol. 8, no. 1-2, 2002

Voorhies, C.V., T.J. Sabaka, and M. Purucker, On magnetic spectra of Earth and Mars, *J. Geophys. Res*., 10.1029/2001/JE001534, 04 June 2002.

Withers, P., R. D. Lorenz and **G. A. Neumann**, Comparison of Viking Lander descent data and MOLA topography reveals kilometer-scale offset in Mars atmosphere profiles, *Icarus,* 159, 259–261, doi:10.1006/icar.2002.6914, 2002.

Zweck, C., J. T. Freymueller, and **S .C. Cohen**, Three dimensional elastic dislocation modeling of the postseismic response to the 1964 Alaska Earthquake, *J. Geophys. Res*., 107(B4), 10.1029/2001JB00409, 2002.

Zweck, C., J. T. Freymueller, and **S. C. Cohen**, The 1964 Great Alaska Earthquake; Present day and cumulative postseismic deformation in the western Kenai Peninsula, *Phys. Earth Planet. Int*., 132, 5-20, 2002.

Conference Proceedings Papers:

Colombo, O. L., **S. B. Luthcke**, **D. D. Rowlands**, **D. Chin** and **S. Polouse**, Filtering errors in LEO trajectories obtained by kinematic GPS with floated ambiguities, *Institute of Navigation International Symposium "GPS 2002"*, Portland, Oregon, September 24-27, 2002.

MacMillan, D. S., L. Petrov, and C. Ma,, Geodetic results from Mark4 VLBI, *IVS General Meeting Proceedings*, 50-54, February 4-7, 2002.

Ma C., D. S. MacMillan, and L. Petrov, Integrating analysis goals for EOP, CRF, and TRF, *IVS General Meeting Proceedings*, 255-259, February 4-7, 2002.

Ma C., D. Gordon, D. S. MacMillan, and L. Petrov, Towards a future ICRF realization , *IVS General Meeting Proceedings*, 355-359, February 4-7, 2002.

Mertikas, S., **E. C. Pavlis**, Th. Papadopoulos, and X. Frantzis Preparatory steps for the establishment of a European radar altimeter calibration and sea-level monitoring site for JASON, ENVISAT and EURO-GLOSS, in Proceedings of the *2001 IAG Scientific Assembly: Vistas for Geodesy in the New Millennium*, of the *International Association of Geodesy*, Budapest, Hungary, September 2-7, 2001, electronic publication (CD), 2002.

Pavlis, E. C. Dynamical determination of origin and scale in the Earth system from satellite laser ranging, in *Vistas for Geodesy in the New Millennium*, proceedings of the 2001 International Association of Geodesy Scientific Assembly, Budapest, Hungary, September 2-7, 2001, J. Adam and K.-P. Schwarz (eds.), Springer-Verlag, New York, pp. 36-41, 2002.

Purucker, M., H. McCreadie, S. Vennerstroem, G. Hulot, N. Olsen, H.Luehr, and E. Garnero, Highlights from AGU's Virtual Session on New Magnetic Field Satellites, *EOS*, 83, 368, August 20, 2002 (with associated CD-ROM).

Laser Remote Sensing and Technology

The Laboratory for Terrestrial Physics contains three organizations which are primarily laser remote sensing and technology oriented - the Geoscience Technology Office, the Space Geodesy and Sensor Calibration Office, and the Laser Remote Sensing Branch.

The **Geoscience Technology Office** develops advanced mission concepts and the associated components and instrumentation required to carry them out. It is composed of personnel with broad experience in the analysis and development of both active and passive optical sensors and often supports the activities of the other two technical organizations within the Laboratory. Under priorities established by Laboratory upper management, the GTO performs advanced mission analyses and simulations, evaluates and selects from among technical options for making a new or improved scientific measurement, identifies the technological "tall poles," develops the enabling hardware and software, performs appropriate field (ground, air, or space) experiments to demonstrate the technology, and works with other Laboratory entities to infuse these new technologies into future ground networks or spaceborne science missions.

The **Space Geodesy Networks and Sensor Calibration Office** manages and operates the NASA Satellite Laser Ranging (SLR) and Very Long Baseline Interferometry (VLBI) Networks in support of global space geodesy and Solid Earth geodynamics. The Office also provides the Earth science research community with a broad range of expertise in calibration and characterization of optical remote sensing instrumentation from the ultraviolet to the near infrared and through all phases of spaceflight.

The **Laser Remote Sensing Branch's** mission is to develop laser remote sensing techniques and instruments for scientific measurements of the Earth and planets. Activities include developing and demonstrating new measurement techniques, conducting experiments, and developing ground-based, airborne, and spaceborne laser sensors (lidars). The Branch's work is usually multidisciplinary, and involves theoretical and experimental activities in applied physics, technology development and instrument engineering. Some activities include planning and participating in scientific field campaigns, analyzing the laser measurement and laser sensor performance, acquiring and interpreting lidar data, and developing lasers, optics, and detector components. The Branch's work often involves collaborations with application scientists within Goddard, at universities or other government laboratories, and with researchers and engineers who specialize in lasers and electro-optics.

The accomplishments of these organizations have been broken down by topic: Spaceborne, Airborne, and Ground-based lidars, Laser Technology R&D, Satellite Laser Ranging, and Calibration.

Spaceborne Lidars

Geoscience Laser Altimeter System (GLAS) on the ICESat Mission

The Geoscience Laser Altimeter System (GLAS) is a new space lidar developed for long-term continuous measurements in Earth orbit [1]. Its design combines an altimeter with 5 cm precision with a laser pointing angle determination system and a dual wavelength cloud and aerosol lidar. GLAS was completed in June 2002, has been integrated with the ICESat spacecraft, and the integrated observatory was delivered to the Vandenberg launch site in the fall of 2002. The ICESat mission successfully launched January 12th, 2003 from a Boeing Delta II rocket into a 590 km altitude circular polar orbit. Photos of the launch are shown in Figure1. The ICESat mission parameters are summarized in Table1. GLAS was developed by NASA-Goddard and is

designed to operate continuously for 3-5 years. The ICESat spacecraft was developed by Ball Aerospace, and it and GLAS utilize data from GPS receivers developed by JPL to determine orbit altitude, position and time.

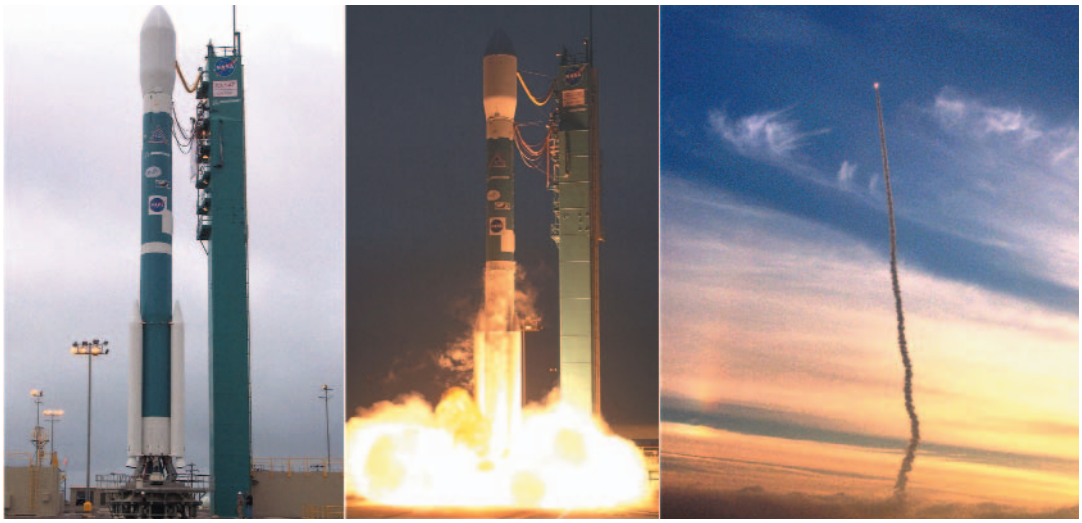

Figure 1. Photos of the launch of ICESat.

Table 1. ICESat Orbit & GLAS Measurements

Orbit altitude	598 km
Orbit inclination	94 degree
Orbit repeat tracks	Within 1 km every 183 days
Ground track spacing	15 km at equator 2.5 km at 80 deg latitude
Post-Processed pointing knowledge	≤ 2 arcsec (all axes)
Position requirements: Radial orbit height Along-track	Post-processing: < 5 cm < 20 cm
Laser measurement direction Off nadir pointing	Nadir viewing (nominal) < 5 degrees
Measurement wavelengths: Surface & cloud tops Atmospheric aerosols	 1064 nm 532 nm
Spot diameter on surface	66 m (e-2 points)
Along-track laser spot Separation	170 m

GLAS measures the range to the Earth's surface with 1064 nm laser pulses as illustrated in Figure 2. Each laser pulse produces a precision pointing measurement from the stellar reference system (SRS) and an echo pulse waveform, which permits range determination and waveform spreading analysis. The single shot ranging accuracy is < 10 cm for ice surfaces with slopes < 2 degrees. Changes in regional ice sheet heights will be determined by comparing successive GLAS measurement sets. GLAS will also measure atmospheric backscatter profiles at both 1064 and 532 nm [2]. The 1064 nm measurements use an analog Si-APD (Avalanche PhotoDiode) detector and measure the height, and profile the backscatter from thicker clouds. The measurements at 532 nm use photon counting detectors, and will measure the vertical height distributions of optically thin clouds and aerosol layers. A series of three ICESat missions are planned, which should dramatically improve our knowledge of the Earth's topography, atmosphere and ice sheets.

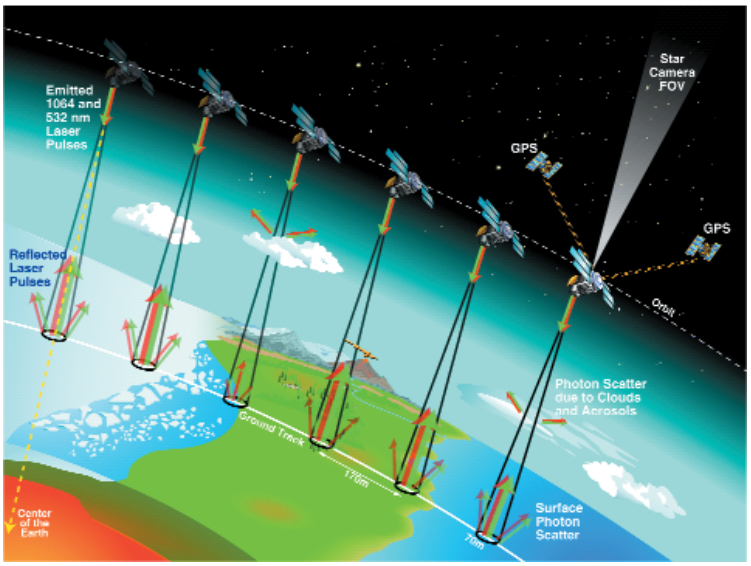

Figure 2: Schematic illustration of the GLAS instrument making measurements from ICESat while orbiting Earth. Graphic by Deborah McLean.

The completed GLAS instrument integrated to the spacecraft is shown in Figures 3a.-c. and its characteristics are summarized in Table 2. Subassemblies include three Q-switched ND:YAG lasers[3], an SRS which measures the pointing angles of each laser firing [4], a 100 cm diameter Beryllium receiver telescope, a 30 pm wide optical filter at 532 nm, and Si APD detectors for 1064 and 532 nm. The subassemblies are mounted on an L-shaped graphite epoxy optical bench. GLAS dissipates heat via 2 radiators, which are shown in Figure 3b and 4.

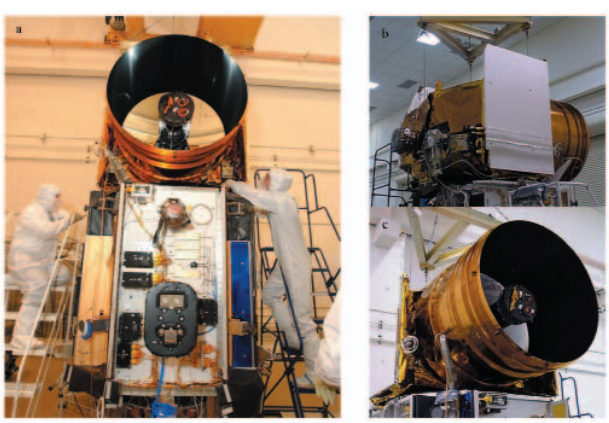

Figure 3. Photos of GLAS integration to spacecraft at Ball Aerospace, Boulder, Colorado. 3a. Shows Instrument mounted on top of spacecraft, 3b. GLAS wrapped with blanketing showing one of two radiators, 3c. View of GLAS 1-meter telescope.

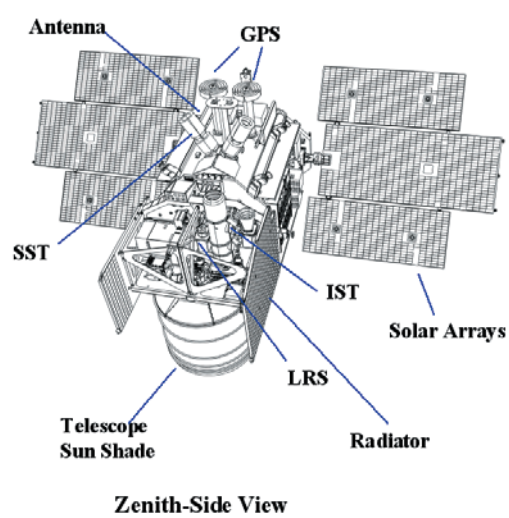

Figure 4. Graphic of Zenith-Side View of ICESat satellite, GLAS plus spacecraft. IST- instrument star tracker, LRS - Laser Reference Sensor, SST- Spacecraft star tracker.

Table 2. GLAS Instrument Specifications

Laser Type	ND:YAG slab, 3 stage Passively Q-switched, Diode pumped
Number of lasers	3 each, one on at any time
Laser firing rate	40 pps
Laser pulse width	5 nsec
Laser Energy	75 mJ 1064 nm 32 mJ, 532 nm
Laser Divergence	110 urad; (exp(-2) pts)
Telescope diameter	100 cm
1064 nm detector	Si APD - analog (2 each)
532 nm detector	Si APD - Geiger (8 each)
Mass	330 kg
Power	300 W average
Instr. Duty cycle	100%
Data rate	~ 550 kbps (uncompress)
Physical size	~ 110 x 140 x 110 cm
Thermal control	Radiators with variable conductance heat pipes

The measurement performance of the completed GLAS instrument was evaluated using several new test instruments called the Bench Check Equipment (BCE). The main GLAS BCE was developed in parallel with GLAS and was used as an inverse altimeter and lidar. It was used to simulate the range of expected optical inputs to the GLAS receiver by illuminating its telescope with simulated background light and laser echoes with known powers and energy levels, widths and delay times. The BCE also allowed monitoring of the transmitted laser energy, the co-alignment of the transmitted laser beam to the receiver line of sight, and performance of the flight science algorithms. A separate BCE was developed to test the angle measurements of the SRS and profile of both the 1064 nm and 532 nm GLAS laser beams. These measurements were evaluated when GLAS was in air, before and after EMI and vibration tests, during and after the thermal vacuum chamber tests, and after delivery to the spacecraft. These measurements will also be used to compare pre-and post-launch performance of the instrument.

References

[1] H.J. Zwally, B. Schutz, W. Abdalati, J. Abshire, C. Bentley, A. Brenner, J. Bufton, J. Dezio, D. Hancock, D. Harding, T. Herring, B. Minster, K. Quinn, S. Palm, J. Spinhirne, R. Thomas, "ICESat's laser measurements of polar ice, atmosphere, ocean, and land," Journal of Geodynamics, Special Issue on Laser Altimetry 34, 405–445, 2002.

[2] J.D. Spinhirne, S.P. Palm, "Space based atmospheric measurements by GLAS" . In: Advances in Atmospheric Remote Sensing with Lidar, , A. Ansmann (Ed.), (Springer, Berlin, 1996) pp.213–217.

[3] R. S. Afzal, J. L. Dallas, A. Lukemire, W.A. Mamakos, A. Melak,, L. Ramos-Izquierdo, B. Schröder, A. W. Yu, " Space Qualification of the Geoscience Laser Altimeter System (GLAS) Laser Transmitters, In: Conference on Lasers and Electro-Optics, OSA Technical Digest, Optical Society of America, Washington, DC, 2002

[4] J.M. Sirota, P.S. Millar, E.A. Ketchum, B. E. Schutz and S. Bae, "System to attain accurate pointing knowledge of the Geoscience Laser Altimeter System, AAS 01-003, PP39-48, 2001.

Contact: James Abshire, James.B.Abshire@nasa.gov

Laser Pointing Angle Measurement for the Geoscience Laser Altimeter

The Geoscience Laser Atlimeter System, GLAS, for the Ice, Cloud, and Land Elevation Satellite (ICESat) mission, will make ice sheet elevation measurements in the polar regions to determine the mass balance of the ice sheets and their contribution to sea level change. In this high precision space based laser altimeter accurate knowledge of the laser beam's pointing angle is critical [1]. The GLAS design incorporates a stellar reference system (SRS) to relate the laser beam pointing angle to the star field to the required accuracy of 7.3 urad (1.5 arcsec). The SRS combines an attitude determination system (ADS) coupled to a 40 Hz laser reference system comprised of two narrow field of view cameras to perform this task.

The overall approach of the SRS is shown in Figure 5. The ADS measures the pointing of the instrument platform with respect to the star field while the laser reference sensor (LRS) samples the laser beam at 10 Hz and measures its alignment with respect to the components of the ADS. The Laser Profiling Array (LPA) measures the spatial profile of the laser beam at 40 Hz. The relative movement between the far field pattern of the GLAS laser beam, a reference source from the star tracker, and an occasional star will be determined. This data combined with the processed ADS data yields the pointing of the laser beam in inertial space.

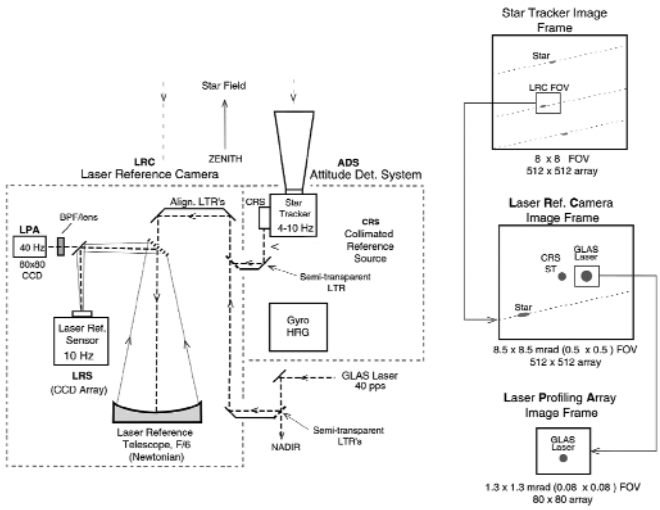

Figure 5. GLAS SRS Conceptual Approach. The GLAS laser beamis coupled into the LRS along with the CRS from the ADS. All optical beams are introduced concentrically through the semi-transparent diagonal mirror of the telescope.

The error budget allotment of the SRS is shown in Table 3. The ADS error component is dervied by combining the performance specifications from the gyro and star tracker with Kalman filtering [2]. Details of the laser reference system error component are listed in the table. This subsystem is the core instrument of the SRS, it combines the laser reference camera (CCD array plus telescope) with coupling optics and reference sources. All components of the LRS system have already been tested, with measured performance listed.

Table 3. SRS Error Budget

Laser Reference System Errors:	urad	arcsec	Comments	
Camera centroid resolution:	0.68	0.14	Laser image centroid	
	0.68	0.14	CRS image centroid	
	0.82	0.17	star image, 80 images through field	
Telescope distortion:	2.42	0.50	mirror deformation & figure uncertainty	
LTR's: internal alignment stability	1.94	0.40	couple to star camera	
	1.94	0.40	couple to glas laser	
	1.70	0.35	couple to glas laser	
ST boresight stability	2.42	0.50		
CRS-ST stability	1.45	0.30		
total LRS RSS error	5.38	1.05	1 sigma	
ADS Errors:	Roll		Pitch	
HD-1003 & HRG SIRU	urad	arcsec	urad	arcsec
1. Attitude Determination	1.45	0.30	1.45	0.30
2. Velocity Aberration	0.16	0.03	0.16	0.03
3. Star Position Accuracy	0.16	0.03	0.15	0.03
4. Ephemeris	0.03	0.01	0.03	0.01
ADS for each axis, (=RSS(2,3,4) +1)	1.68	0.35	1.67	0.35
ADS error (=RSS(roll & pitch))	2.37	0.49	1 sigma	
TOTAL SRS RSS ERRORS	5.61	1.16	1 sigma	

The SRS Bench Check Out Equipment (BCE), shown in Figure 6, was used to calibrate and verify the SRS instrument performance after integration to the main GLAS instrument. The overall thermal performance of the system was then verified during instrument thermal vacuum testing. The BCE incorporates a star field generator and a "ground truth" reference camera. Stars are generated with an array of 16 x 16 pinholes in a chromium coated silica plate. Light is sent to these pinholes by an array of multimode fibers. The light from the star generator is fed directly into the LRS. A large LTR is used to send a sample of the star field to the star tracker and to relay it to a ground reference camera (GRC). The flight laser is simultaneously imaged onto this GRC, which is considered "truth" during performance tests. The camera is capable of recording full images at 40 Hz, thus multiple stars plus the laser can be recorded. The BCE system was kept at constant temperature during performance verification tests, while the instrument was exposed to the full operational temperature range expected in flight. Performance in thermal-vacuum environment was assessed by comparing the infor-

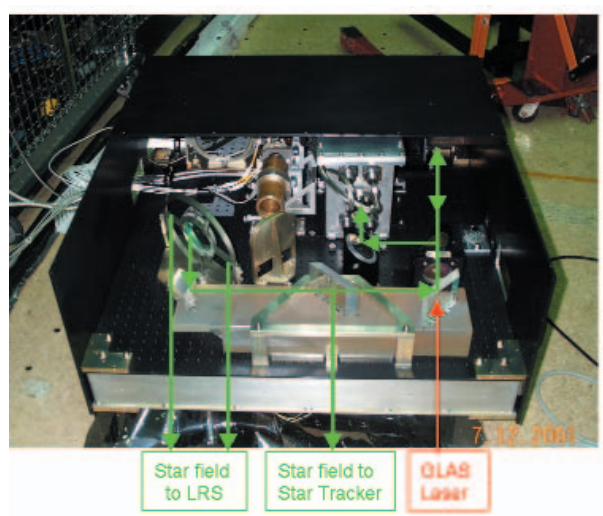

Figure 6. Photo of SRS BCE which stimulates the SRS with a star field and simultaneously measures the GLAS laser and star field with a ground Truth camera.

mation collected in the GRC to that collected by the flight instrument. During instrument thermal vacuum testing, the SRS complied with stability and performance requirements with margin. During spacecraft and instrument commissioning, 29 days after launch, the LRS successfully imaged the GLAS laser beam, the Collimated Reference Source (CRS) and dim stars every fifty seconds. The LRS sensitivity appears to be a factor of five more sensitive than required.

References:

1. Bufton, J.L., Garvin, J.B., Cavanaugh, J.F., Ramos-Izquierdo, L., Clem, T.D. and Krabill, W.B., "Airborne lidar for profiling of surface topography," Opt. Engr., 30:72 (1991).

2. S. Bae and B.E. Schutz, "Laser Pointing Determination Using Stellar Reference system in Geoscience Laser Altimeter System", AAS (00-123) 2000.

Contact: Pamela S. Millar, Pamela.S.Millar@nasa.gov

GLAS Main Bench Checkout Equipment

Testing and calibrating GLAS, and similar lidar systems, is a challenge partly due to the complexity of the expected ground surface echoes and cloud returns, and the stringent test environment. Testing of space instruments takes place in demanding environments such as clean rooms and thermal-vacuum chambers used to simulate on-orbit conditions.

The main Bench Checkout Equipment (BCE) was used to validate the science and engineering specifications of GLAS. This BCE was used to simulate the expected returns for GLAS at 1064 nm and 532 nm and also monitor important instrument parameters such as the laser power, oscillator stability and boresight alignment.

A functional block diagram of the Bench Checkout Equipment (BCE) is shown in Figure 7. It consists of several subsystems: The Altimeter Test System (ATS), the Lidar Test System (LdrTS), the Laser Test System (LsrTS), and the GPS/Timing System. A BCE controller acts as the central data conduit for the BCE subsystems. Two optical targets, a Main and Mini Target are used to optically couple signals into GLAS, perform laser diagnostics and test the boresight alignment of the instrument. The ATS was used to simulate and monitor ground and cloud returns and background at 1064 nm. The LdrTS was used to simulate and monitor ground and aerosol returns and background at 532 nm. The LsrTS was used to perform laser diagnostics. The Timing/GPS System was used to monitor the GLAS oscillator stability and provide a GPS signal to GLAS

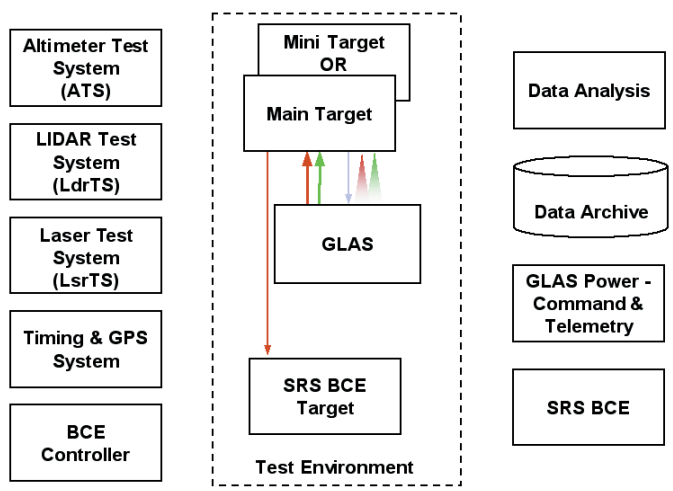

Figure 7. Functional Block Diagram of GLAS Bench Checkout Equipment

and the BCE subsystems. The two optical targets (Main and Mini) were used to retroreflect an attenuated laser beam back into the receiver, sweep the Field of View (FOV) of the 1064 nm detectors using a pair of motorized Risley prisms, and perform laser diagnostics. Additional subsystems were used to provide power, control and telemetry, data archiving, and science data analysis. A separate SRS optical target and BCE were also used to test the performance of the instrument stellar reference system as discussed in the previous section.

Contact: Haris Riris, Haris.Riris.1@gsfc.nasa.gov

Mercury Laser Altimeter (MLA)

The Mercury Laser Altimeter (MLA) is one of the primary instruments on NASA's MErcury Surface, Space ENvironment, GEochemistry and Ranging (MESSENGER) Project, part of the Discovery Program. MESSENGER, the first spacecraft ever to orbit the planet Mercury, will be launched in March 2004 and will enter Mercury orbit in April 2009, after two flybys of Venus and two of Mercury along the way. The flyby and orbital phases of the mission will provide global mapping and detailed characterization of the planet's surface, interior, atmosphere, and magnetosphere.

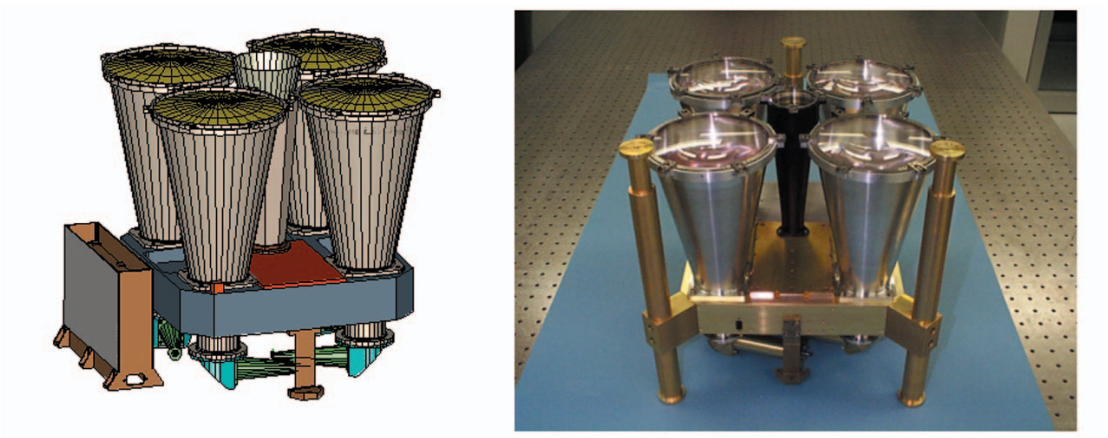

Figure 8: In 2002 MLA has moved from concept to reality. The CDR (critical design review) design is shown at left, and the engineering model is shown at right.

The MLA instrument, shown in Figure 8, is being designed and built as a PI mode instrument by a GSFC instrument team led by the Laser Remote Sensing Branch. The laser, shown in Figure 9, is being designed and built by laser remote sensing branch's Space Lidar Technology Center (SLTC) in College Park, MD, in collaboration with the engineering directorate.

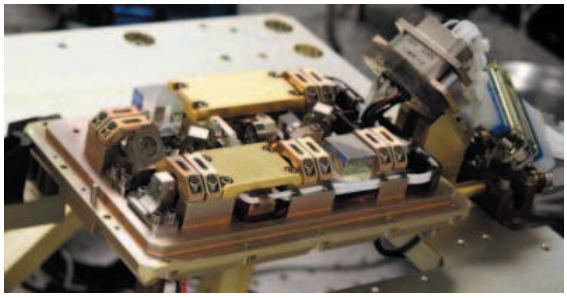

Figure 9: MLA Engineering Model laser has met or exceeded all performance requirements.

In 2002 MLA progressed from concept to reality. In February 2002, MLA successfully completed Critical Design Review (CDR) and was approved for implementation. The remainder of 2002 was spent in fabrication and assembly of engineering models and flight hardware subsystems. As of December 31, 2002, all subsystems have showed performance meeting or exceeding requirements, and the final as-delivered MLA Instrument is expected to show exceptional performance.

MLA was designed primarily to measure the libration, topography, and surface composition of Mercury. The MLA Instrument design leverages heavily from earlier successful developments from the Mars Orbiter Laser Altimeter (MOLA) and GLAS. Like MOLA, the receiver detection threshold is dynamically adjusted real-time via on-board software algorithms to be as low as possible while maintaining a predetermined false alarm rate, which is monitored via a noise counter whose output is fed back to the threshold control loop algorithm.

The MLA structure is constructed entirely of beryllium, with beryllium receiver tubes, laser bench and beam expander, and mounted to the MESSENGER spacecraft deck via three titanium flexures. The power converter assembly is housed in a magnesium chassis that mounts directly to the spacecraft deck.

The optical bandwidth of the MLA receiver, consisting of four transmitting receiver tube assemblies which fibercouple to the SiAPD detector, is 0.8 nm wide FWHM (full-width half maximum) and centered at 1064 nm. The receiver field of view is 400 μrad FWHM.

The laser is a Cr doped Nd:YAG design employing passive Q-switching. The expected output energy is 20 mJ, with an 8 Hz repetition rate and 5 nsec pulse width. Divergence is expected to be less than 50 μrad.

The timing and signal processing employs a unique design based around an APL-supplied "Time-of-Flight" ASIC which will allow superb time resolution, down to 400 ps. MLA has three matched filter pulse capture channels (10, 60, 270 nsec), and will allow detection of return pulse widths from 7-1000 nsec, with up to 15 returns captured per shot.

MLA looks forward to a successful delivery to the MESSENGER Spacecraft in May 2003.

Contact: Xiaoli Sun, Xiaoli.Sun-1@nasa.gov

The Mars Orbiter Laser Altimeter (MOLA) - Radiometry

The Mars Orbiter Laser Altimeter (MOLA) continued operation in its passive radiometry mode, producing near infrared images of Mars. MOLA has now recorded two years of seasonal radiometric changes. The calibration of the receiver responsivity was further refined to account for the unusually cold detector temperature after the external heater was powered off to conserve spacecraft power.

Figure 10 shows a series of MOLA false-color albedo images of Mars polar caps. Colors correspond to ratios of detected (incident) to radiant flux in the range 0-40%. Martian seasons are denoted by the longitude of Sun (Ls): 0° at the start of northern Spring, or equinox, and 180° at the southern equinox. The southern cap (left column) recedes from the start of spring (Ls=180°) to mid-summer (Ls=300°), with a dark interior region thought to represent slab CO_2 ice. The northern polar cap (right column) leaves bright outliers as it contracts. The interval between images is 30° of Ls, or roughly 57 Martian sols. Over the course of a year, roughly 30% of the atmosphere is exchanged between the poles as CO_2 frost accumulates and sublimates.

The investigation into the apparent failure of the clock oscillator was concluded. Extensive tests

were performed on a flight spare unit and a similar failure mode was partially reproduced. Gradual losses in the quartz crystal, and gain reduction due to accumulated space radiation damage to transistors, caused the signal amplitude of the oscillator circuit to vanish or become too low to trigger the CMOS buffer gate.

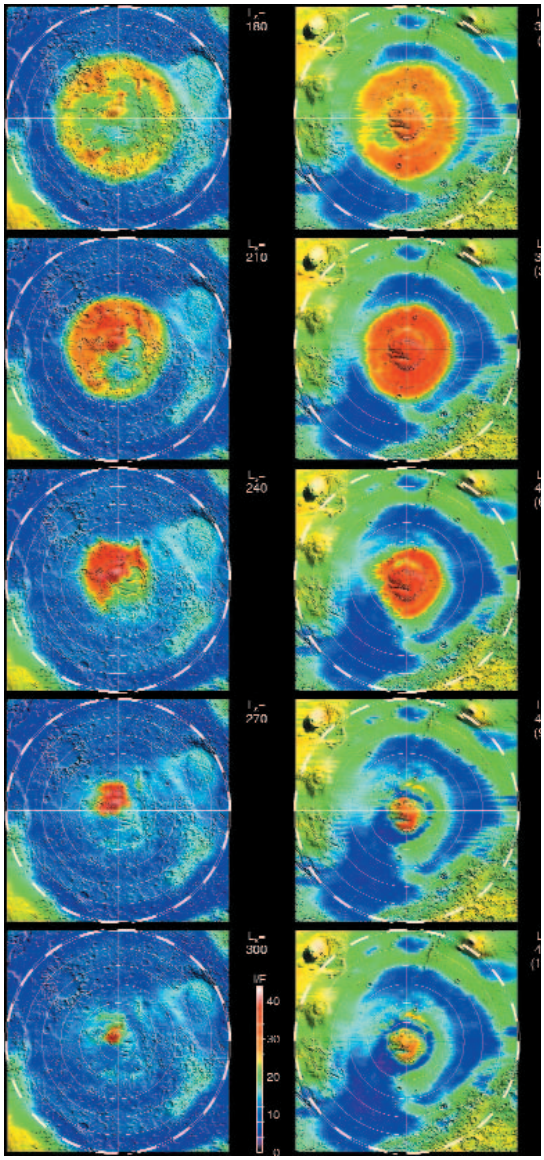

Figure 10. MOLA false-color albedo images of Mars polar caps.

Contact: Dr. Xiaoli Sun, Xiaoli.Sun-1@nasa.gov

Airborne and Ground Based Lidars

Laser Vegetation Imaging Sensor (LVIS) - Airborne Imaging Laser Altimetry

The Laser Vegetation Imaging Sensor (LVIS) is a wide-swath (2 km), full return-waveform, imaging, airborne laser altimeter developed at GSFC for measuring topography (including sub-canopy) and vegetation height and vertical structure. LVIS data has produced some of the best estimates of above-ground biomass in densely forested regions. LVIS has been selected as a part of the LBA project to map ~15,000 km^2 of topography and vegetation structure parameters in the Brazilian Amazon in 2003. The LVIS instrument has recently been redesigned to improve performance and to drastically reduce size, weight and power consumption. The updated instrument has been assembled and tested in the NOAA Cessna Citation jet aircraft. The upgraded LVIS system significantly expands the instrument's capabilities allowing the collection of full return-waveform imaging data at rep-rates exceeding 10 kHz. In addition to the Brazilian flight mission, the LVIS instrument has been selected to map ~3,000 km^2 of topography and vegetation structure parameters at 5 m horizontal resolution in the state of Maryland. Further improvements to the LVIS receiver and scanning systems are planned to increase the swath width to 4 km by the end of 2003.

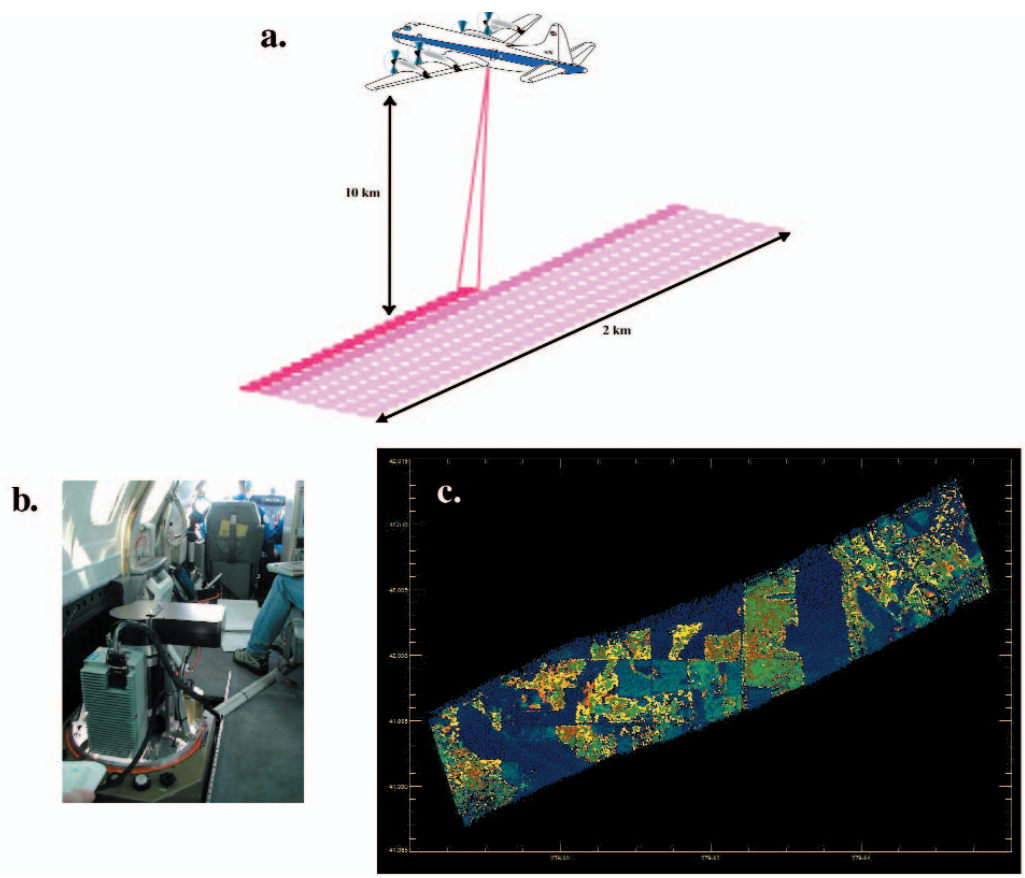

Figure 11. The top graphic (a) illustrates the scan pattern used by LVIS to produce images of topography and vegetation structure from an aircraft. The image on the bottom left (b) shows the compact new LVIS instrument seated in a standard air-photo camera mount in the NOAA Cessna Citation. The graphic on the bottom right (c) is an example swath of vegetation height data from the LVIS instrument.

Contact: Bryan Blair, James.B.Blair@nasa.gov

Airborne Multikilohertz Microlaser Altimeter (Microaltimeter)

The Microaltimeter, developed under NASA's Instrument Incubator Program (IIP), operates at multi-kHz rates from aircraft cruise altitudes with a single pulse energy of a few microJoules (mJ) and a 14 cm diameter off-axis telescope, which is spatially shared by the transmitter and receiver. The final configuration of the system uses a multi-anode metal channel dynode photomultiplier in order to segment the ground image into 16 elements (4x4 pixels). Each of the anodes is input to an independent timing channel so that the altimeter can be operated in a 3D imaging mode. For increased portability between aircraft, the instrument is packaged to fit into a standard Lyca camera mount, which is widely used in airborne experiments.

In September 2002 the final flight experiments were completed over Ocean City, Maryland and Assateague Island, Virginia regions, collecting over 3.3 Gigabytes of data, which represents over 1.5 hours of actual laser ranging to the surface, using a 4 mJ per pulse laser operating at 532 nm. The instrument was flown onboard the Wallops P3B aircraft from an altitude of 3300 m, using a circular scanning wedge to create a ground swath of about 120 m in diameter. With the laser fire rate of 8 kHz, and a scan rate of 10 Hz, the distance between laser footprints was around 50 cm. The flight took place in clear sky conditions during the early afternoon of September 12th, 2002.

The IIP Final Report for the Microaltimeter was delivered in November 2002, containing twelve papers written on various aspects of the project and an Executive Summary. While the IIP part of the Microaltimeter project has now ended, work continues in house on the analysis and validation of the flight data against an existing Digital Elevation Model (DEM) of the region, and EarthData Technologies, LLC will be working with the Microaltimeter ranging data through a Memorandum of Agreement with NASA. As a spin-off to the technology, the next Shuttle Laser Altimeter experiment (SLA03) will make use of the concepts and hardware design of the Microaltimeter.

The following figure shows the work in progress on the post processing. The results are from the May 2001 Microaltimeter flight over buildings in Ocean City from an altitude of 1650 m with the scanner rotating at 10 Hz. The ground swath is roughly 15 m in diameter by 120 m in length, with a vertical dimension of 10 m. The point cloud plot on the left gives the terrain heights from the ground (blue) and the buildings (green, yellow and orange) after post processing of ranging information. The plot on the right is a bar plot of the same data, filling in the gaps between the points by interpolation.

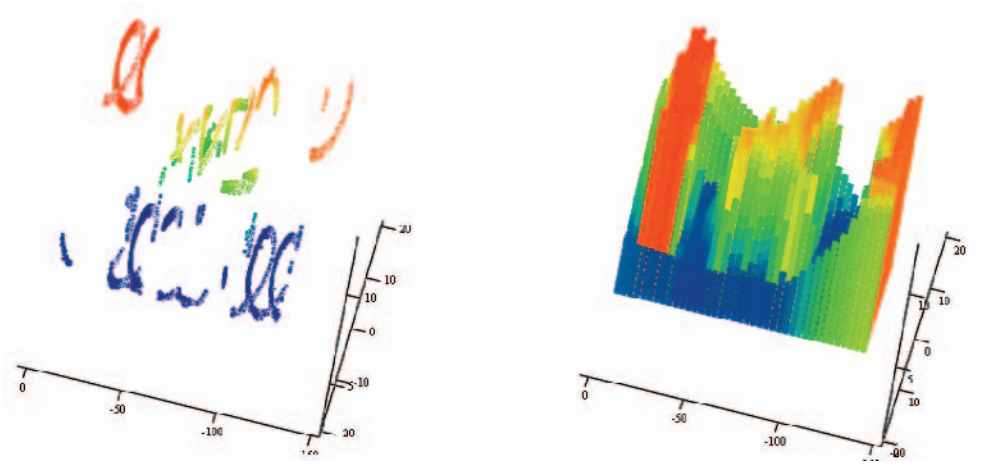

Figure 12. 3D terrain heights of Ocean City buildings from May 2001 Microaltimeter flight ranges. The left plot is a point cloud plot and the right plot is the same data shown as an interpolated bar plot.

Contact: Jan McGarry, Jan.F.McGarry@nasa.gov

Spectral Ratio Biospheric Lidar

The Normalized Difference Vegetation Index (NDVI) and related vegetation indices (VI) rely on the distinctive optical properties (reflectivity and absorption) of chlorophyll containing vegetation. The dominant pigment in plant leaves, Chl a, strongly absorbs visible light (from 0.4 to 0.7 μm) for use in photosynthesis, with blue and red peaks near 0.43 and 0.67 μm. However, the cell structure of the leaves strongly reflects near-infrared light (from 0.7 to 1.2 μm). This transition around 0.7 μm is referred to as the red edge. In general, if there is much less reflected radiation in red wavelengths than in near-infrared wavelengths, then the vegetation is likely healthy and dense whereas if there is little difference in the intensity of the reflected red and near-infrared wavelengths then plant leaves are likely sparse, absent, or dead.

A land-surface lidar that uses spectral reflectance to discriminate living vegetation from non-living sources of surface roughness would have great potential for airborne mapping and for future NASA missions. In particular, Earth-orbiting lidar missions to map biomass carbon and to measure dynamic topography and ecosystem change could yield much more accurate and specific data, if they include vertically-resolved discrimination of the types of surfaces measured. A lidar instrument that actively measures vegetation spectral response, in two narrow wavelength bands on either side of the red edge would also provide unprecedented information for calibration of passively acquired multi-spectral vegetation data (e.g. AVHRR). This is due to the precise pointing capability, narrow laser divergence (i.e., small spot size on the surface) and narrow fields of view possible with lidar instruments. Also, by keeping the two probe wavelengths close to the red edge, the lidar can measure and remove along-path reflectance from atmospheric aerosols. Therefore, any differences in measured spectral reflectance at the two probe wavelengths are due to differences in the surface features and not the atmospheric path. Precursor techniques used fundamental (1064 nm) and doubled (532 nm) Nd:YAG lidar signals or ratios of active near-IR reflectance signals for target discrimination and ranging. Paired wavelengths near the vegetation red edge have not been used in existing lidar systems.

A laboratory demonstration instrument was developed this year, using low power diode lasers operating at 670 and 775 nm. This instrument will be used to show that the underlying measurement concept is feasible. However, the 50-70 mW output power of these lasers is not sufficient to demonstrate the concept from an aircraft or from orbit. And there are currently no space-qualified, high power lasers available at these wavelengths, 670 nm and 775 nm. The most attractive path for scaling transmitter power to that needed for high-altitude airborne platforms and on-orbit applications appears to be frequency doubling the output of rare-earth-doped fiber amplifiers and Raman amplifiers developed for the telecommunications industry (1.2-1.6 μm). These devices and related components have been built for demanding applications, e.g., undersea fiber-optic links, with established reliability.

For FY03 a prototype spectral-ratio biospheric lidar system will be built using robust, commercial-off-the-shelf (COTS) telecommunication components (e.g Er/Yb doped fiber amplifiers, Raman amplifiers) in conjunction with TRL-4 (Technology Readiness Level 4) non-linear optical components for frequency doubling (e.g. periodically poled KTP) generating several watts of laser power at 670 and 775 nm. Active measurements will be demonstrated of vegetation spectral responses, at power levels appropriate for resolving surface types within shadowed canopy volumes and suitable for high-altitude airborne use or possibly, on-orbit systems.

A breakthrough in this area, and work to define a pathway to space, could provide the Laboratory and Goddard with a crucial advantage in competing for future NASA Earth Science missions. The Jet Propulsion Laboratory (JPL) flew a 1550 nm fiber laser as part of the Shuttle Radar Topography mission (SRTM), and work is on-going at several institutions to develop space-based fiber laser communication systems for data down-link. Other R&D funding at GSFC has supported work to adapt telecommunications components for use in space laser transmitters. Related work is developing sub-

systems for column CO_2 measurements (CO_2 Laser Sounder) using some of the same components identified for this proposal (e.g. Distributed Feed Back or DFB laser diodes operating at 1572 nm).

See annual report topic "Fiber Amplifier Power Scaling/Frequency Doubling" J. Rall, this report.

Contact: Jonathan A. R. Rall, Jonathan.A.Rall@nasa.gov

Automatic Weather Station (AWS) Lidar

A ground based, autonomous, low-power atmospheric lidar instrument is being developed at NASA Goddard Space Flight Center. This compact, portable lidar will operate continuously in an insulated enclosure, charge its own batteries through a combination of a small rugged wind generator and solar panels, and transmit its data from remote locations to ground stations via satellite. The goal is to co-locate these instruments at several of the many remote Automatic Weather Station (AWS) sites in Antarctica. The NSF Office of Polar Programs provides support to place weather stations in remote areas of Antarctica in support of meteorological research and operations around the continent. The AWS meteorological data will directly benefit the analysis of lidar data while a network of ground based atmospheric lidar will provide knowledge regarding the temporal evolution and spatial extent of Type Ia polar stratospheric clouds (PSC). These clouds play a crucial role in the annual austral springtime destruction of stratospheric ozone over Antarctica, i.e. the ozone hole. In addition, the lidar will monitor and record the general atmospheric conditions (transmission and backscatter) of the overlying atmosphere which will benefit the Geoscience Laser Altimeter System (GLAS) aboard the recently launched ICESat mission. A conceptual design of the Automatic Weather Station Lidar is shown in Figure 13. A prototype lidar was developed and deployed to the Automated Geophysical Observatory (AGO) P1 in January 1999. AGO Lidar was designed to operate inside the heated AGO enclosure and to consume less than 15 W of power continuously.

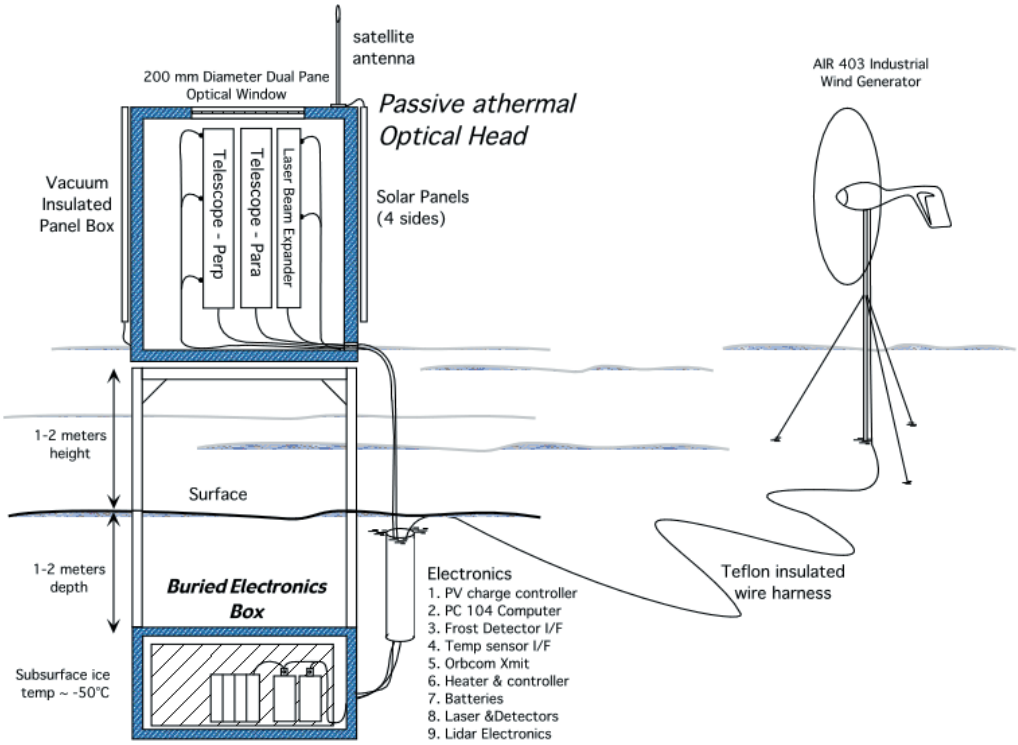

Figure 13. Conceptual design of the Automatic Weather Station Lidar.

Lessons learned from AGO Lidar have influenced the design of the AWS Lidar instrument. A completely autonomous, free-standing approach was adopted. In order to minimize electrical generation and heating requirements, a two-enclosure approach was chosen which simplified the thermal design and thermal management of the instrument. One temperature controlled box containing all of the power dissipating electronics and electro-optics will be buried approximately 1 m below the surface while the other box (not temperature controlled) will be mounted on poles about 1 meter above the surface. This above surface box will contain the fiber-optic coupled, athermal refractive telescopes and the out-going laser beam expander.

The working design of the instrument employs a frequency-doubled, diode-pumped, Nd:YAG microchip laser which is fiber coupled to the outgoing beam expander. However, concurrent work developing high-power, frequency-doubled fiber amplifiers may supersede this approach. (See Annual Report 2002 topic: Fiber Amplifier Power Scaling/Frequency Doubling.) The fiber coupled beam expander used to transmit the outgoing laser energy and the two receiver telescopes, used to sense depolarization of the scattered light, will employ a novel athermal telescope which was designed, built and tested at Goddard Space Flight Center. This fiber-coupled telescope, shown in Figure 14 undergoing temperature testing in an environmental chamber, maintained focus and alignment from –50°C to +30°C, an 80°C temperature range. To increase the effective aperture of the receiver, multiple telescopes can be added.

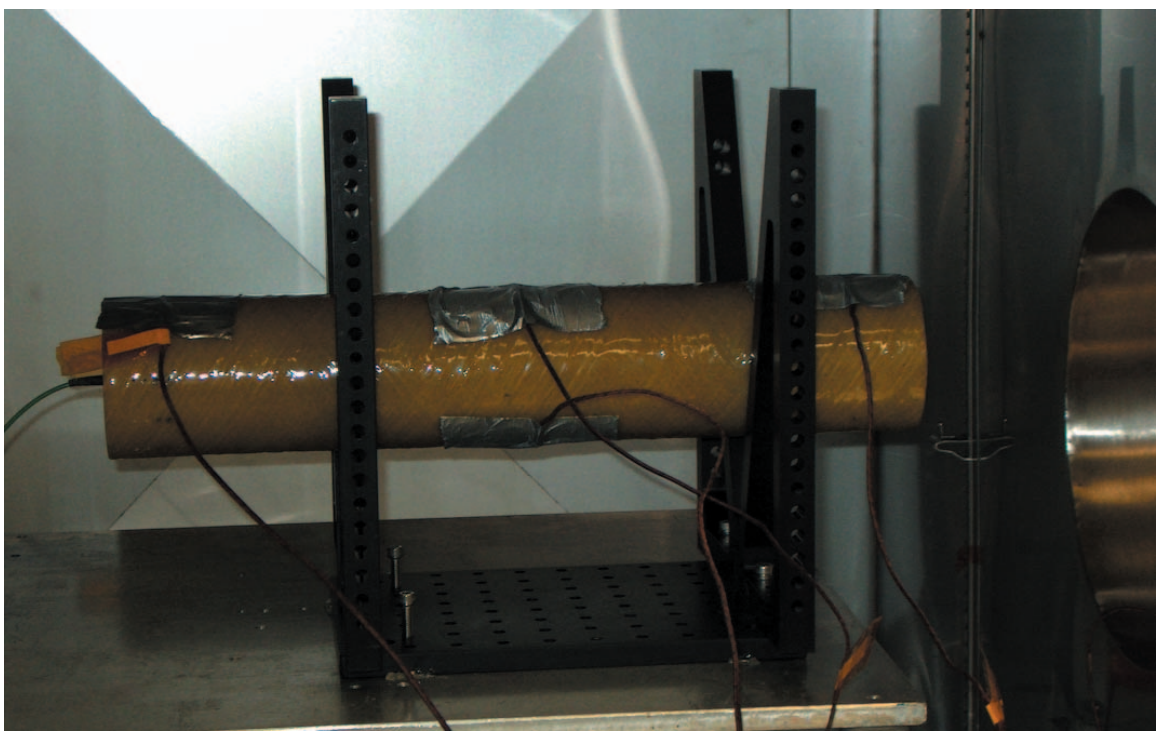

Figure 14. Athermal refractive telescope

To power the lidar instrument and satellite transceiver, storage batteries contained in the sub surface enclosure will be charged by a combination of four 30 W solar arrays and a rugged, 400 W wind generator (Figure 15). The four, 30 Watt solar panels will be mounted on each side of the above surface enclosure to take advantage of the continuous low-elevation solar angle during the austral summer. The small, rugged wind generator will be installed on a guy-stabilized, 3-4 m pole nearby to charge the batteries during the six-month, polar night.

Figure 15. Marine wind generator and solar panels undergoing testing at NASA Goddard Space Flight Center.

The buried box approach takes advantage of the nearly constant subsurface ice temperature of -50°C which greatly simplifies thermal design of the instrument and the excellent insulating properties of the surrounding snow and ice. This box will be heated by a combination of waste heat from the electronics and electro-optics (~10 watts) and an additional heating element to maintain an acceptable operating temperature range. The above surface box will be mounted on four poles augered into the ice. This is to take advantage of the wind-scouring effect that tends to keep smooth, elevated flat surfaces free of ice and snow accumulation and to reduce or eliminate snow drifting/accumulating around the base.

Incremental deployment of AWS Lidar hardware is set to begin during the 2003-2004 summer servicing season.

References:

[1] J. A. R. Rall, J. Cavanaugh, J. Campbell James B. Abshire & James D. Spinhirne, "Automated Geophysical Observatory (AGO) Lidar," Abstract accepted for presenatation at the 2002 International Geoscience And Remote Sensing Symposium (IGARSS), Toronto, Canada June 24-28, 2002.

[2] Holz, J., Directed Studies Paper, "Investigation of an Athermal, Refracting Telescope," August 14, 2002.

Contact: Jonathan A. R. Rall, Jonathan.A.Rall@nasa.gov

Laser Technology R&D

Vegetation Canopy Lidar: VCL Laser Transmitter Development

Work on the Vegetation Canopy Lidar Laser Transmitter (VCL LT), has concentrated on increasing reliability, damage risk reduction and lifetesting. Furthermore, the preparation of clean room assembly laboratories for the LTs and developing semi-autonomous data systems for the lasers during assembly has been pursued. Most recently, our work has centered on a VCL Breadboard model of the Laser Transmitter (VCL BB) in order to identify a micro-damage problem with the AR (anti-reflection) coated surface of the laser slabs. This damage issue, has been resolved and the "trigger" set of conditions have been replicated on the BB. Additionally, the High Efficiency Laser Transmitter (HELT), developed by the American University (AU) team, has been run for > $3x10^9$ shots continuously without damage. This proves the viability of the unstable resonator design for long, unattended operation in space. Finally, a diode-based, single frequency seed laser centered at 1064 nm is under development under an Earth Science Technology Office (ESTO) charter.

VCL Laser Transmitter Research and Development

Slab Micro-burns Investigation

Having solved the primary problems with the laser, we discovered that a LT in the process of being constructed would still exhibit a gradual degradation of power. During our troubleshooting effort, it was discovered that small micro-burns, some even < 1 μm in diameter, could be seen on the AR (antireflection) coating on the laser slab. Figure 16 is a photograph of typical micro-burns on a Nd:YAG slab AR surface, magnified at 100X.

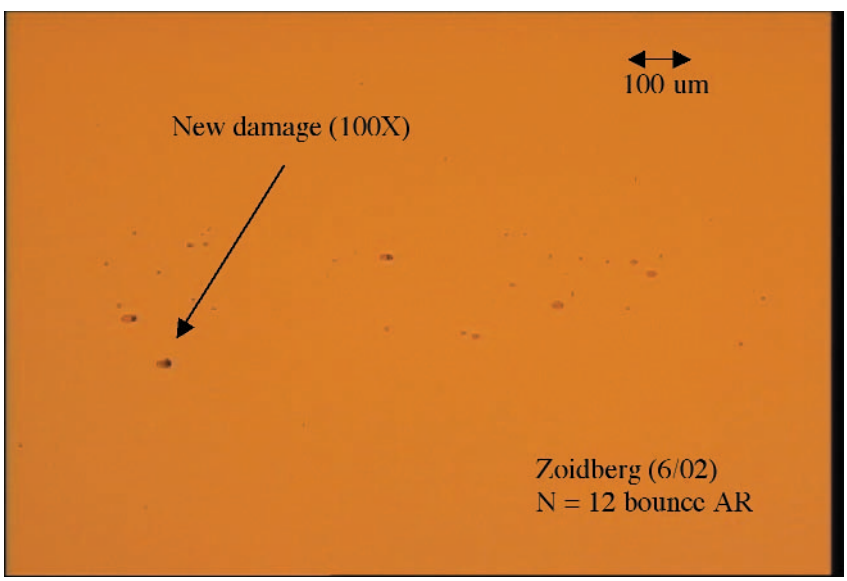

Figure 16: Sample micro-burns on Nd:YAG slab AR surface.

The micro-burns are very small, about 1 μm - 10 μm in diameter and were found in narrow lines, approximately on centerline of the laser beam at the bounce points on the AR coating of the zig-zag slab. The spots are much smaller than the laser beam spot size at the bounce points and propagate (increase) in number and eventually cause a slab to fail. Almost every type of known damage mechanism was thoroughly studied; including contamination, coating quality, coating material, surface quality, surface microfractures, longitudinal mode beating, small scale self focusing,

and others. Each of these potential causes were evaluated and eliminated.

Based on results from a laser simulation software package, GLAD, clipping effects were ruled out, another possible damage trigger, since no effect in the beam profiles or wavefronts were observed. In order to evaluate the intensity fluences, it would be necessary either to work with the LT optical bench outside of the flight laser box or to assemble a laboratory version of the VCL LT. We chose to set-up a breadboard version in a laser R&D laboratory as it provided much more flexibility. In order to accurately quantify any findings and apply them to the LT's, an exact optical replica was made with the breadboard using flight optics, flight optic mounts, and their respective positions.

VCL BB Studies

Studies with the VCL BB were carried out over a period of 6 months. After each change in the cavity parameters, the laser was run at full power for over 16 hours (> 15 million shots) to produce a single data point on performance and damage rate. The slab was inspected and documented. Evidence of micro-burns could be found with an illuminated microscope that employs an encoded translation stage for repeatable inspection precision. In small 1 cm steps, the oscillator cavity was reduced from HELT's configuration of 41cm to the VCL LT fixed length of 37cm. The pump lens to laser diode array (LDA) distance was then changed in several steps as small as +/- 0.001". Figure 17 shows the results of this head variation study.

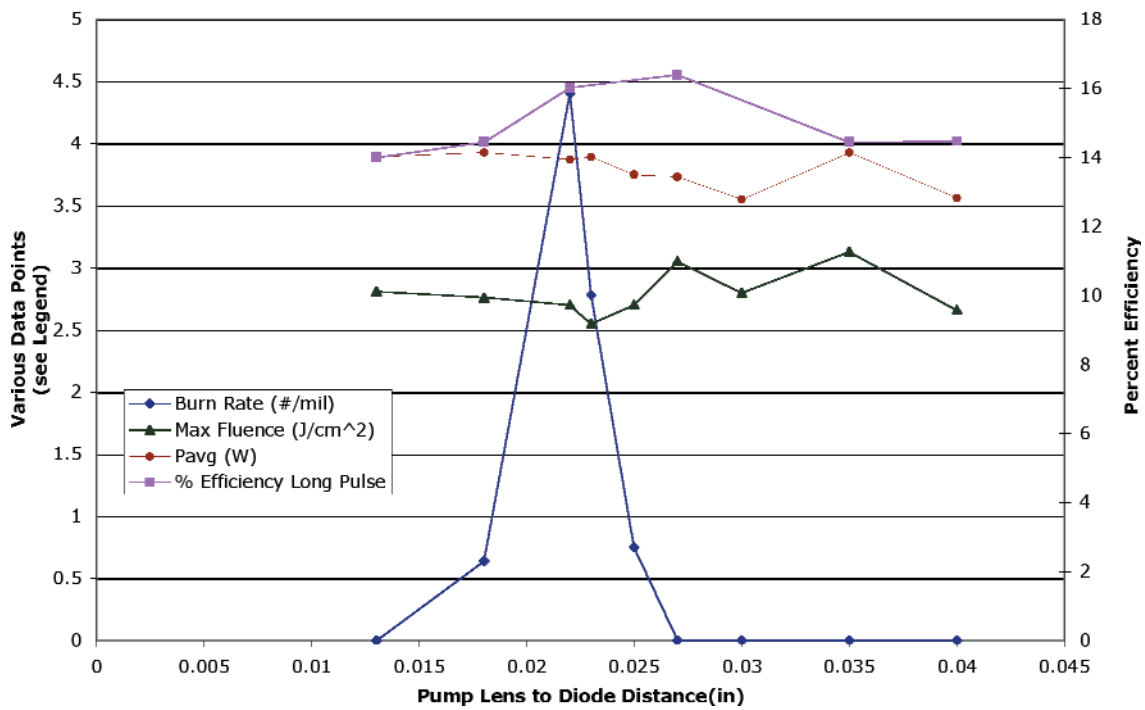

Figure 17. VCL Breadboard Burn Rate Data

Nd:YAG slab damage was present with 4 positions of this pump lens sweep. Upon each of these inspections the total number of new burn locations were cataloged and counted to generate the burn rate plot.

The burn rate vs. pump lens to LDA distance peaks at 0.022" LDA – pump lens spacing. The other data on the graph show that the cavity fluence and optical efficiency change only a small

amount as a function of the pump lens to LDA distance. The cavity loss was adjusted prior to Q-switching in order to provide constant average powers over the course of this experiment. For this reason the efficiency is measured prior to each adjustment. Optical ray trace modeling of the shape and distribution of the pump energy in the slab as a function of the pump lens to LDA distance has been performed in order to identify any correlations with the measured damage peak. Peaking behavior in the pump intensity has been found in models where small filamentary thermal lenses can be produced with individual LDA beams overlapping in the media. It is hypothesized that this effect acts as a damage "trigger" in side pumped head designs. Further work is underway to determine the operational margins in the non-damage settings for this configuration. Figures 18a and 18b show the unfolded and folded assemblies of the VCL BB.

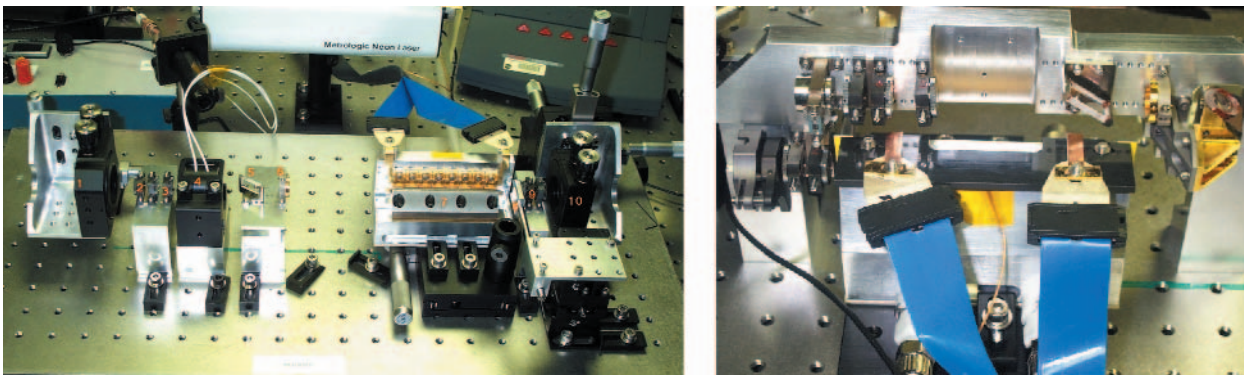

Figure 18a. (at left) Unfolded VCL BB using flight optics, mounts and relative positions (end mirror mounts not shown). Figure 18b. (at right) Folded VCL BB, Q-switch removed, including flight retro.

Final plans for the VCL BB uses a custom optical bench designed to incorporate the 180-degree beam turning "internal-retro". This configuration will be used to find a final optical prescription to be employed in the VCL LT design.

High Efficiency Laser Transmitter (HELT): VCL Lifetest

Features of the HELT laser include an unstable resonator cavity with a Gaussian reflective output coupler designed with the aid of the unstable resonator theory of M. Morin of the Canadian Optics Institute. HELT's pump head is conductively cooled with an optimized design for collimating the pump diode radiation into the zig-zag slab. The VCL BB laser discussed earlier has a head based on this design. The schematic of the basic HELT optical layout is essentially the same as for VCL BB, as this design was adapted by the VCL laser. A near-Brewster cut zig-zag slab is side pumped by 7 four -bar diode arrays of 60 W per bar at up to 70 A drive current.

The unstable resonator consists of an R= 2.5 m concave high reflector (HR) mirror and an R = -2.37 m output coupler. The output coupler is a GRM (graded reflectivity mirror) with a Gaussian reflectivity profile of center reflectivity 63% and $1/e^2$ beam waist of 1.12 mm. Paraxia analysis of this resonator gives beam waists of 1.29 mm and 1.26 mm on the GRM and HR, respectively. The waist in the presence of the slab will be somewhat different due to aperture effects. The geometrical magnification is 1.27 and the total magnification (including diffraction) is 1.40. This magnification is sufficient to reduce the 2nd order mode strength by 50% relative to the TEMoo mode. Further discrimination against higher order modes is provided by the GRM. A thermal lens created in the pump-stripe-dimension of the slab is compensated for by a cylindrical lens of focal length f = -65 cm.

The design of the pump head is significantly different than the VCL LTs. It incorporates 7 four-bar LDAs as compared to VCL (&VCL BB) which have 8 three-bar arrays. Each array is 10 mm

long and the distance between the bars is ~ 0.4 mm. The HELT arrays have a 34% greater emitting area than the VCL head design. Consequently the VCL pump diode illumination is ~ 30% greater in intensity before being collimated with the cylindrical pump lens. The AR coatings on the HELT slab receives lower pump irradiance and pumps a larger volume of the slab for the same input energy. This creates a broader region of inversion density in the slab, promotes a larger lasing beam, and therby reduces the risk of damage from beam irregularities, both spatial and temporal.

A continuous operation lifetest was initiated with the HELT laser in July 2002 in order to determine long term reliability for this design. All operating specifications, such as LDA current, temperature and repetition rate, were held constant and the performance was monitored. Results of this test are illustrated in Figure 4. The run started with 15 mJ of output pulse energy and ended above the end of life requirement of 10 mJ after 2.3 billion laser shots (or one year of operation). The gradual energy loss shown in figure 4 is due to the typical pump diode degradation.

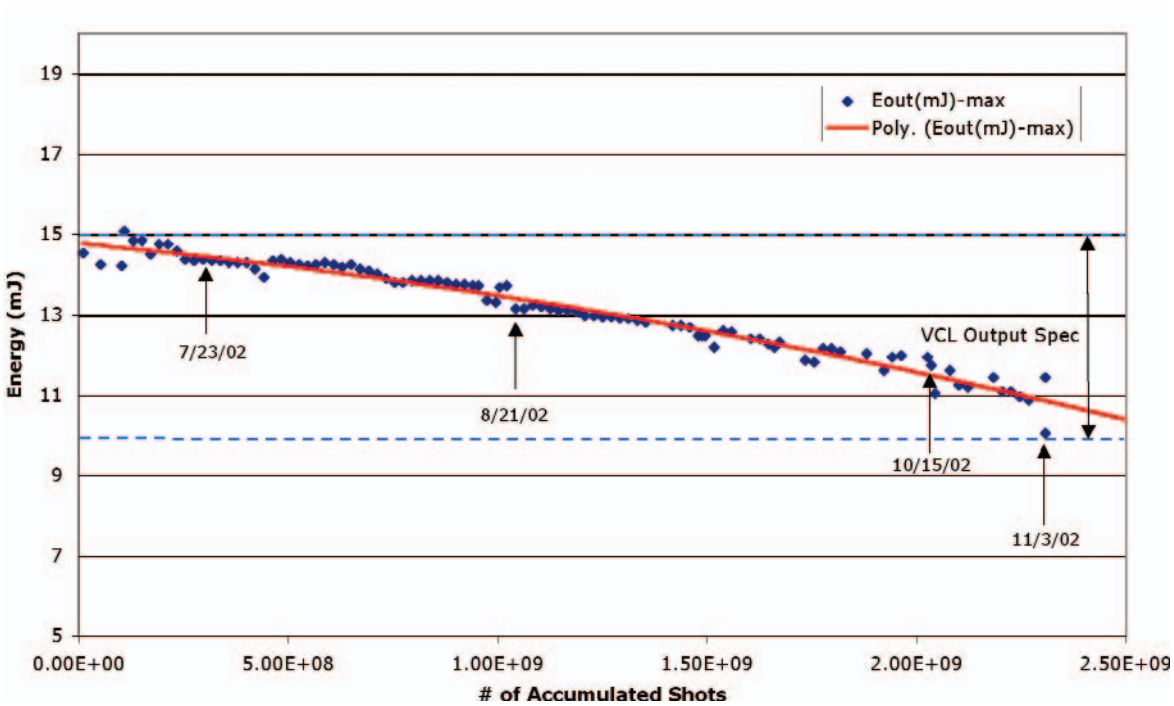

Figure 19. HELT Pulse Energy.

The slab was removed on 7/23/02, 8/21/02, 10/11/02, and 11/3/02 for inspection and no damage was ever found, even under 600x power magnification. The absence of optical damage for a flight laser of this energy and beam quality which has managed a "shot lifetime" of > $2x10^9$ shots is unprecedented. Further, this laser was operated in a normal R&D lab environment, without the benefit of clean room air flow. HELT's LDA pump pulse width has been stepped up from 89us to 105us to increase the pulse energy, and will run for another 2.3 billion shots. As of 01/25/03 HELT has surpassed 3 x 10^9 shots and it should reach 5 x 10^9 shots in April 2003.

Contact: Barry Coyle, Donald.B.Coyle@nasa.gov

Diode Based Single Frequency 1064 nm Laser for Seeding High Power Nd:YAG Lasers

A compact, robust micro laser, wavelength stabilized to 1064.1 nm for use in optically seeding high power Nd:YAG lasers for space lidar applications is under development. Seeding reduces longitudinal mode beating which can damage the optics in a high power laser cavity, greatly reducing its lifetime. The concept of the seed laser is based on stabilizing the output of a standard Fabry-Perot semiconductor laser using optical feedback from a Bragg grating embedded in a KTP waveguide. This design is a proprietary technique developed by AdvR Inc. of Bozeman, MT, the company performing most of the development work. This micro laser is designed as a smaller, more efficient, more robust, less costly replacement for the NPRO (non-planar ring oscillator) Nd:YAG lasers currently used for seeding. The main advantages of a diode based seed laser over the diode pumped NPRO is it requires less components, is inherently more efficient and therefore could potentially cost less.

Brief review and description of progress:

Three of four primary milestones listed have been met in FY02; (1) T\the semiconductor lasers that meet specifications and lifetime have been procured and tested, (2) the KTP Bragg waveguides that will stabilize the semiconductor laser at the proper wavelength for seeding have been fabricated, and (3) a prototype package of the Bragg stabilized laser was delivered to GSFC for seeding experiments. The work is on track for FY03's main task, and 4th milestone, which is to deliver a prototype seed laser ready for vibration and thermal-vac testing by October 2003. This system will come complete with feedback circuitry, fully characterized performance data over temperature, and be optically isolated.

The seeding experiments with the first delivered prototype were successfully performed with the HELT lifetest laser. An improvement in packaging is underway in order to reduce the thermal and mechanical stresses, while retaining ease of alignment. Figure 20 shows the prototype unit prior to assembly.

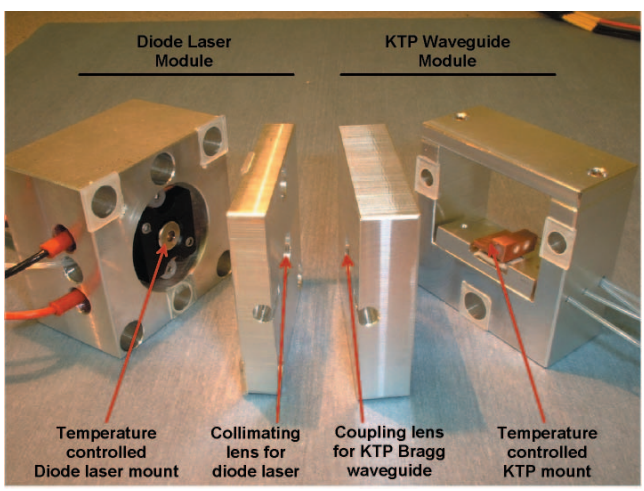

Figure 20. Prototype components of diode seed laser. Each "slice" is approximately 2 inches square. This unit was used to seed HELT lifetest laser in Feb. 2003.

The first delivered prototype package works well in the lab and, to date, has proven to be very temperature insensitive. This compact design is the first effort to house the KTP Bragg stabilized laser in a sealed package with no adjustment knobs for optimum stability. The components are held in aluminum mounts that can be aligned and fixed into place using UV cure epoxy.

Prior to our seed test, the first prototype laser had been running continuously (CW) for a lifetest-for over 50 days. Output power, center wavelength and side mode suppression of the laser was monitored over time and exhibited little or no degradation. A heterodyne technique was used for a high resolution linewidth measurement where two nearly identical lasers are co-aligned and the resultant beat frequency is recorded. Figure 21 shows a measured linewidth of 400 kHz for each laser.

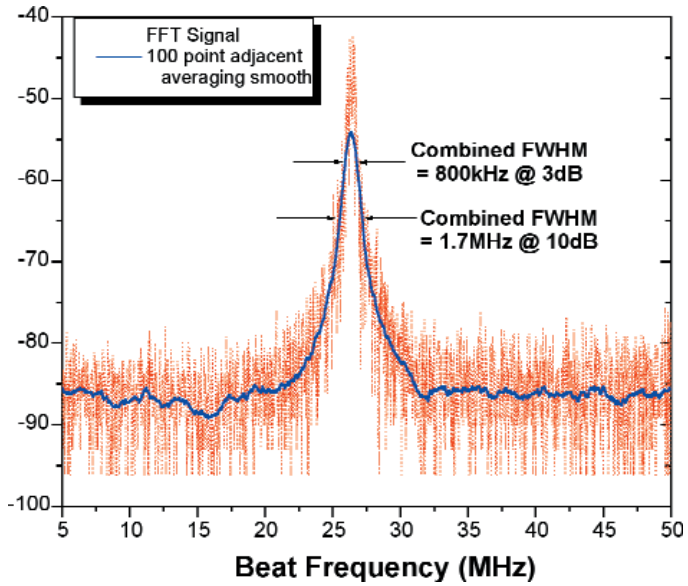

Figure 21. Measured 400 kHz linewidth (800 kHz/2) of 2 identical KTP tuned seed lasers.

Thermal stability of the unit was excellent and no external feedback, thermal, diode drive current, nor KTP voltage was needed to hold seed. The seeding "link" was held continuously for over 5 hours, until we began diode thermal sweeps for characterization purposes. Based on this effort's recent progress, a successful delivery of a flight qualifiable design is expected to be completed by October 2004.

Contact: Barry Coyle, barry@cornfed.gsfc.nasa.gov

One Micron Testbed Program: Laser Risk Reduction

Computer Modeling: Vegetation Canopy Lidar (VCL)

The VCL laser utilizes a Nd^{+3}:YAG zig-zag slab geometry where pump light is coupled into the gain medium through use of a cylindrical undoped YAG lens. Questions arose regarding the distribution of pump light in the slab and if it might be related to optical damage intermittently observed on the slab coatings. To address this issue, the diode array-lens-slab system was modeled using the OptiCAD ray-tracing software. This software not only allows for the design and modeling of optical systems with user-defined individual optical components, but also provides capabilities for the custom design of light sources, including laser diode array (LDA) bars with adjustable performance parameters. Results for the cross-sectional slab pump light distribution for the VCL laser are shown in Figures 22(a) and 22(b) for two different LDA-to-lens distances.

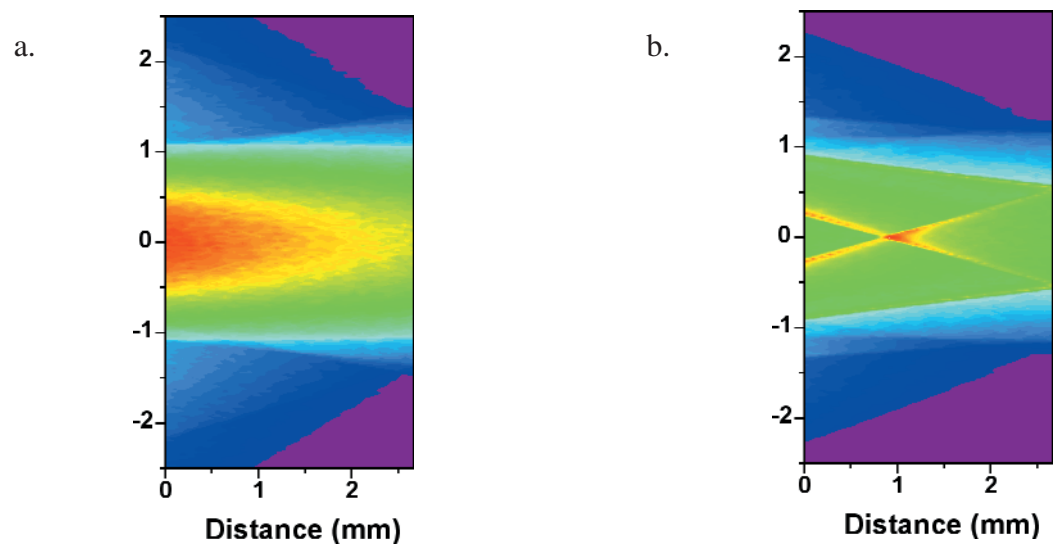

Figure 22: Absorbed energy distribution for diode-to-lens distances of (a) .018" and (b) .035".

At the shorter LDA-to-lens distance, the pump light takes a smooth Gaussian profile across the slab width; however, increasing this distance by only 0.017" (0.43 mm) results in an intraslab focal point roughly 1 mm from the slab input face. Since it has been found that the optical damage observed in VCL is strongly dependent on the position of the pump lens, it may be that such intraslab pump beam focusing plays a significant role. More experimental work is currently underway to examine this possibility.

Another issue with the VCL laser that required attention was possible aperture effects of the intracavity beam by optical components, resulting in the introduction of diffraction rings to the cavity laser mode. To examine this possibility, a code was developed for the physical optics software package GLAD, capable of predicting the transverse cavity mode as well as the phase front of the beam at any point in the oscillator. Figure 23(a) and 23(b) show results for the cavity mode and beam phase front at the slab face. These results indicate that beam clipping at the slab faces does not occur to any significant degree, suggesting diffraction effects are not a likely source of optical damage.

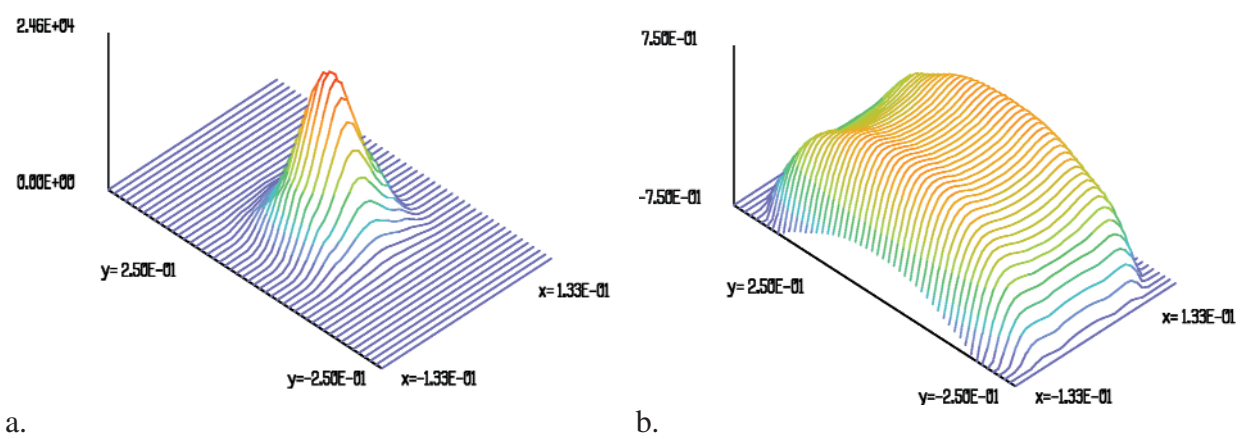

Figure 23: (a) Mode structure and (b) phase front at slab face.

1 μ_ Test Bed

The ability to predict such factors as mode structure, phase distortion, and beam divergence is crucial to the design and optimization of laser systems for the Laser Risk Reduction program. In the interest of testing the accuracy of current modeling methods, computer models for well-characterized oscillators were constructed and matched against empirical data. Two such oscillators chosen for this testing were the MLA and GLAS lasers.

MLA

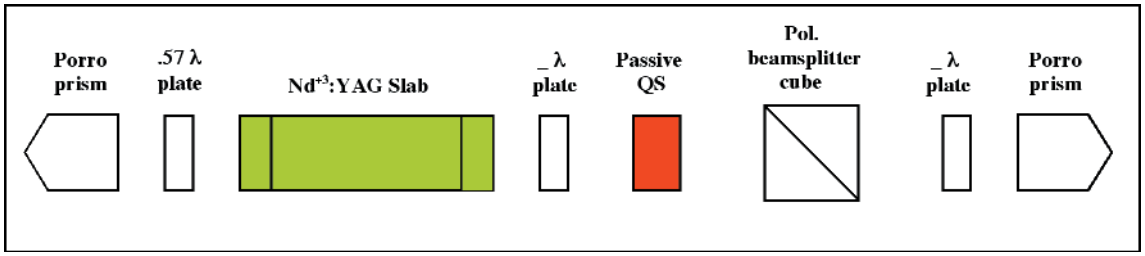

Figure 24: Basic layout of the MLA oscillator.

The quantities of interest for the MLA laser, shown in Figure 24, are the pump light distribution in the slab, intracavity and far-field mode profiles, and beam divergences. First, the distribution of pump light in the slab was investigated. MLA relies on a simple proximity-coupled pump arrangement rather than a pump lens system as in VCL. The cross-section of the OptiCAD-modeled distribution of pump energy for the MLA laser is shown in Figure 25 below:

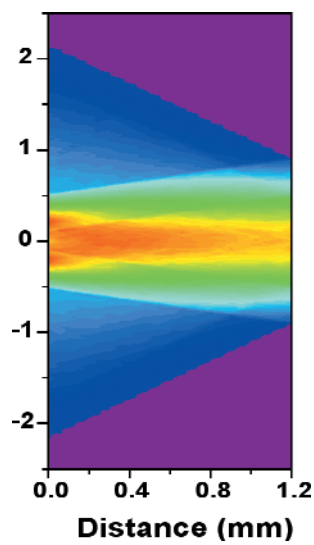

Figure 25: Pump light distribution in MLA slab.

The simulated pump light distribution was then used in a GLAD model to estimate the size and divergences of the output beam. Comparisons of the measured and modeled output beam diameters in the x- and y-dimensions versus distance are shown in Figures 26(a) and 26(b), respectively:

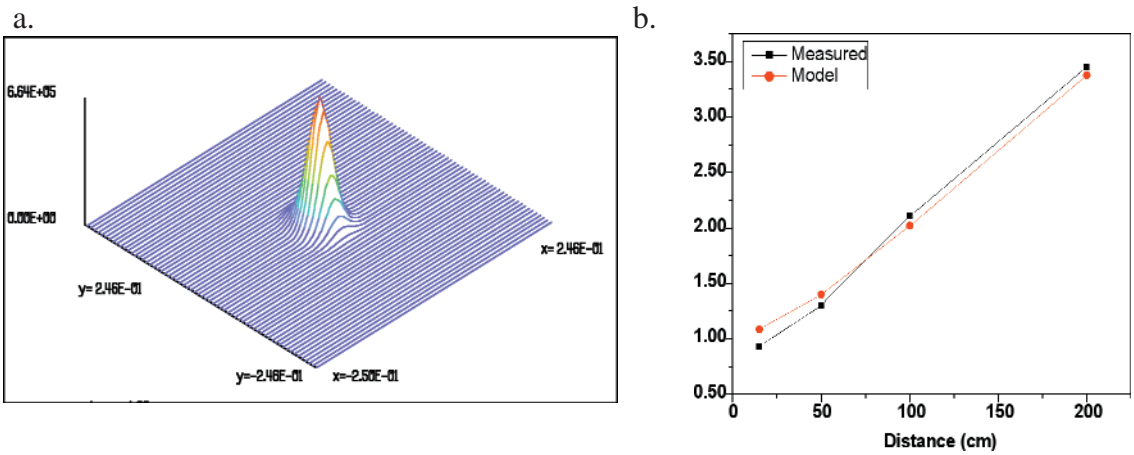

Figure 26: Modeled and measured beam diameters vs. distance for (a) x-dimension and (b) y-dimension.

In addition to providing reliable estimation of the output beam diameter for the MLA oscillator, the GLAD model predicts the x- and y-divergences to be 1.77 mR and 1.79 mR, respectively, as compared to measured values of 1.72 mR for both dimensions.

GLAS

GLAS is another compact, well-characterized passively Q-switched oscillator that provided an opportunity to assay modeling techniques. This laser, illustrated in Figure 27, utilizes a zig-zag slab identical to MLA's, and also makes use of Cr+4:YAG as the saturable absorber material. The major difference between the two systems is that the stimulated radiation is confined in the cavity with a flat 60% output coupler and a 2.5 m HR mirror rather than crossed Porro prisms.

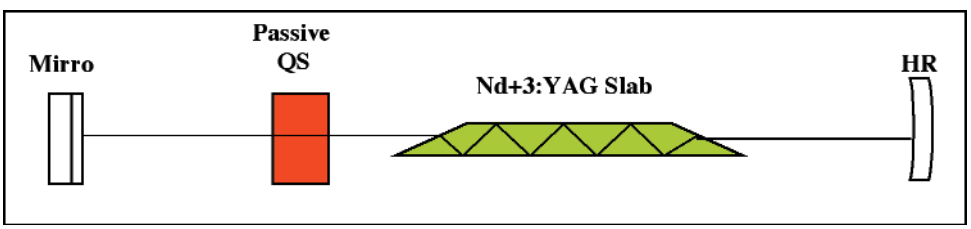

Figure 27: Basic layout of GLAS laser oscillator (no amps shown).

Parameters such as cavity length, pump power, saturable absorber concentration, etc., were estimated from published literature as well as GSFC GLAS documentation and entered into a GLAD code. As was done for MLA, the inversion density distribution in the slab was estimated using OptiCAD. The code calculated ~0.8 mm for the intraslab mode diameter, closely matching the reported value. The model also predicted an output pulse energy of 1.24 mJ as compared to the reported 1.5 mJ. However, the predicted 2.4-3.0 ns pulsewidth underestimates the experimental value of ~4 ns. Example data from the GLAD code is shown in figures 28(a) and 28(b):

a. b.

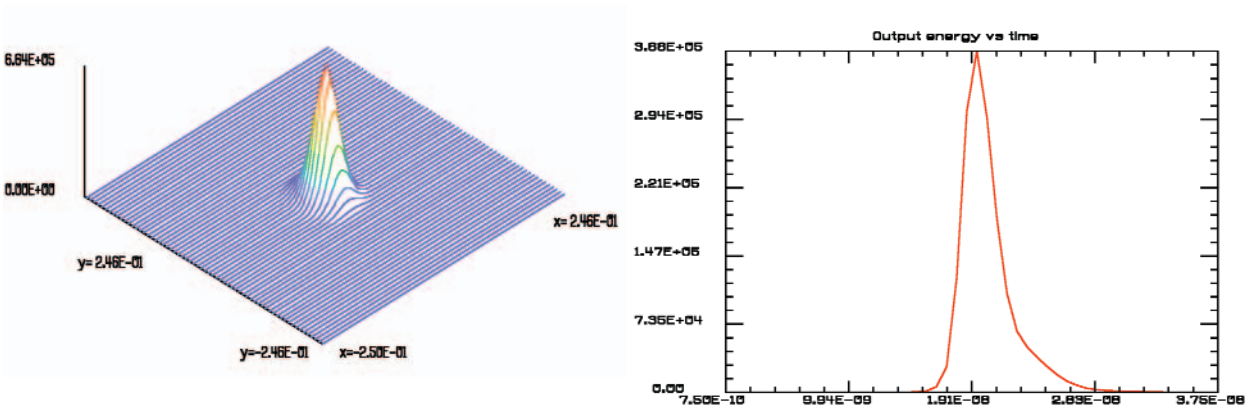

Figure 28: (a) Predicted near-field mode structure and (b) output pulse shape for GLAS laser.

Contact: Barry Coyle, Donald.B.Coyle@nasa.gov

Fiber Amplifier Power Scaling/Frequency Doubling Effort

The Fiber Amplifier Power Scaling/Frequency Doubling effort is a laboratory research project to demonstrate the feasibility of using fiber optic amplifiers as laser sources/transmitters for a variety of Earth science applications. Fiber amplifier-based lasers have many potential advantages for use in space due to their compact, rugged and highly efficient nature. They can address a broad wavelength region in the NIR that can be extended into the visible region using nonlinear, second harmonic generation (i.e. frequency doubling). Atmospheric CO_2 and O_2 can be actively sensed with lasers operating at 1572 nm and 761 nm respectively. Vegetation Index (i.e. chlorophyll content of vegetation) can be estimated using two lasers operating at 660 nm and 785 nm and taking the ratio of reflected laser energy. Currently there are no space-qualified, high power lasers at these wavelengths. Rare earth doped (Ytterbium & Erbium), high power (5-10 W CW) fiber amplifiers are commercially available telecom products.

Literature and web searches were conducted to identify as many academic institutions and industry vendors as possible to accurately establish the state of the art (i.e. Technology Readiness Level or TRL) of high power (10 W CW and >300 kW pulsed) fiber amplifier work and efficient (>50%) non-phase matched second harmonic generation (SHG) of these devices. Research conducted at the Imperial College of London, UK has demonstrated efficient frequency doubling (>40%) of Yb-doped fiber amps to the 3-6 Watt level. More recently, research at the Naval Research Lab in Washington, D.C. has demonstrated pulsed fiber amplifiers at 1064 nm producing 300-kW pulses.

A conceptual design was developed of a frequency-doubled fiber amplifier system based on knowledge gathered from academia and industry. Two parallel approaches have been identified: Rare-earth doped (e.g. Ytterbium (Yb) and Erbium (Er)) fiber amplifiers for "fixed" wavelength (1.0 μm and 1.5 μm) systems and Raman amplification in standard SMF-28 transport fiber for "custom" wavelengths (1.2-1.6 μm). Phase matched SHG was deemed too complicated to ever be elevated to an appropriate TRL for space applications. Therefore, non-critical, quasi-phase matched SHG using periodically-poled non-linear optical crystals was the selected approach. A relatively new material, periodically-poled KTP (PPKTP) was chosen because it offers high conversion efficiency (>50%) and ruggedness as compared to Lithium Niobate.

All the major equipment was procured in FY02 and we will begin assembling the initial demon-

stration experiment in the 2nd quarter of FY03. This will include characterizing the performance of the Er/Yb doped fiber amp with both a CW seed and pulsed seed source and at both the fundamental wavelength, 1570 nm, and frequency doubled to 785 nm. A similar demonstration/characterization will be performed with the 40 dBm Raman Amplifier. Other work that we will address this year includes identifying non-linear processes such as Stimulated Brillouin Scattering (SBS) and Stimulated Raman Scattering (SRS) which become problematic with short (e.g. nanosecond) pulses and high peak powers. Future investigations will explore different methods to mitigate these technical hurdles while ensuring good doubling efficiency and narrow linewidth operation.

References:

[1] Champert, P.A., S.V. Popov, & J.R. Taylor, "3.5 W frequency-doubled fiber-based laser source at 772 nm," Applied Physics Letters, Vol 78, No 17, April 23, 2001.

[2] Di Teodoro F., J.P. Koplow, S.W. Moore, & D.A.V. Kliner, " Diffraction-Limited, 300-kW peak-power pulses from a coiled multimode fiber amplifier, Optics Letters, Vol 27, No. 7, April 1, 2002.

Contact: Jonathan A. R. Rall, Jonathan.A.Rall@nasa.gov

Laser Sounder Technique for Remotely Measuring Atmospheric CO_2 Concentrations

Accurate measurements of tropospheric CO_2 abundance with global-coverage, 300 km spatial and monthly temporal resolution are needed to quantify processes that regulate CO_2 storage by the land and ocean. We are investigating the feasibility of a satellite-borne laser-sounding instrument that would meet these requirements. The laser sounder approach uses the differential absorption technique to accurately measure the atmospheric column abundance. We propose to use three separate laser transmitters to permit simultaneous measurement of 1) CO_2 - at 1570 nm 2) O_2 - at 770 nm and 3) aerosol backscatter - at 1064 nm - in the same atmospheric path. This method greatly reduces the major error sources including interference from other trace gas species (e.g. H_2O), variability in dry air density caused by pressure or topographic changes, the effects of clouds and aerosols in the path and diurnal biases in CO_2 concentration. The laser sounder technique uses the strong reflection from the Earth's surface. This greatly enhances the system feasibility for near term space deployment.

We choose to work at the CO_2 overtone band at 1570 nm that falls within the telecommunication L-band and at 1540 nm (the O_2 A-band at 770 nm =1540 nm/2) in the telecommunication C-band in order to leverage the world-wide industry investment in the associated laser and electro-optic technology. This includes single-frequency DFB laser diodes and high optical power (>10 W average) erbium fiber amplifiers recently space qualified by Lucent.

The active sounding technique has advantages over passive spectrometers in its high (MHz) spectral resolution and stability, the ability to measure at night and in dim-light, a narrow measurement swath, and the ability to simultaneously detect and exclude measurements with clouds or aerosols in the path. For space, the concept is a lidar measuring at nadir in sun-synchronous orbit. Using dawn and dusk measurements make it possible to sample the diurnal variations in CO_2 mixing ratios in the lower troposphere. A 1-m telescope is used as the receiver for all wavelengths. When averaging over 50 seconds, a SNR of ~1500 is achievable for each atmospheric constituent at each on- and off-line measurement. Such a mission can furnish global maps of the lower tropospheric CO_2 column abundance at dawn and dusk. Global coverage with an accuracy of a few ppm with a spatial resolution of ~ 50,000 sq. km appears achievable each month.

Under NASA's ESTO ATI (Earth Science Technology Office Advanced Technology Initiative) program support, we have demonstrated key elements of the CO_2 measurement technique, laser transmitter, photon counting detector. These include measurements of line shapes for CO_2 in an absorption cell using the fiber amplifier transmitter, and measurements at 1570 nm with SNRs of > 500 using a PMT detector. Recently we have made stable CO_2 absorption measurements over a 205m-long open horizontal path using our breadboard sounder instrument [± 1.7% (7 ppm) accuracy with 10 s averaging time], and have obtained good agreement with HITRAN predictions and with simultaneous measurements from an in-situ CO_2 analyzer over several hours.

In addition to this system effort, we have initiated key component development efforts for 1) high-peak-power single-frequency fiber-amplifiers with reduced Stimulated-Brillouin-Scattering (GSFC Internal R&D funds), 2) InGaAs avalanche photodiode photon counting detectors (NASA's ESTO Laser Risk Reduction funds) 3) frequency-doubled erbium-fiber-amplifier based laser transmitters (GSFC Internal R&D).

Contact: James Abshire, James.B.Abshire@nasa.gov

Spaceborne Imaging Laser Altimetry Mission Concept and Technology Development

The Laser Remote Sensing Branch at GSFC is investigating various techniques for implementing an LVIS-like, wide-swath, full-waveform imaging laser altimeter in space. This instrument will enable high accuracy, high resolution full Earth mapping. A concept for a full-Earth imaging laser altimeter mission is being developed for possible launch in 5-10 years. The goal of this mission would be to completely map the topography and vegetation structure of the entire land surface of the Earth including topography beneath dense vegetation, all at < 10 m horizontal resolution. The concept utilizes extremely high rep-rate lasers (75 kHz), a streaming waveform digitizer system for recording the range to the surface and the vertical structure of each pixel, and a novel high-speed, highly accurate laser scanning system. The data set from this system would represent 2 orders of magnitude improvement in vertical accuracy (~ 10 cm), and 1-2 orders of magnitude improvement in horizontal resolution (< 10 m) over existing data. The waveform-based measurement is a proven technology developed specifically for vegetation penetration and novel topographic change detection (including beneath vegetation).

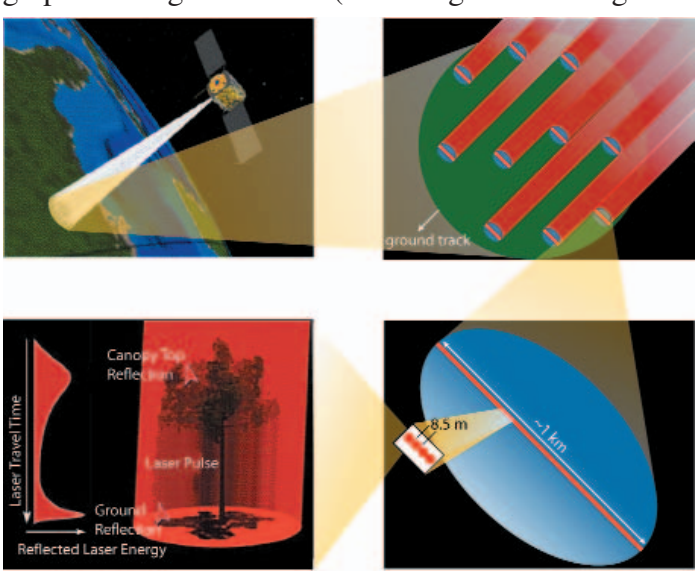

Figure 29. The graphic below illustrates the full-Earth imaging lidar concept. Starting at the upper left and going counter-clockwise: 1) View of the spacecraft nadir swath encompassing a 10 km diameter field-of-view (FOV). 2) 10 km FOV segmented into ten, 1 km mini-swaths. 3) Individual 1km mini-swath consisting of ~120 discrete laser footprints that will be scanned at a high rate across the nadir track of the spacecraft. 4) Last is an illustration of the full return-waveform concept showing the full illumination of the area within each footprint and the resulting return echo that fully characterizes the vertical structure of its topography and vegetation

Contact: Bryan Blair, James.B.Blair@nasa.gov

Investigation of Bose-Einstein Condensates for Advanced Gravity Gradiometer Designs

Measurements of the gradient in the gravity field of the Earth from orbit provides a powerful investigative tool for global geophysical effects. Deep ocean currents, the seasonal bulk redistribution of the atmosphere, and water storage and transport (i.e. in underground aquifers and deep ice sheets) are some of the many phenomena that produce gravitational effects that can be studied with orbiting gradiometers.

Recent developments in ultra-cold matter have resulted in the creation of a new state of matter, Bose-Einstein condensates. These condensates are small clouds of gas at nanoKelvin temperatures. These temperatures can be reached without cryogenics by the clever use of lasers. At these temperatures the atoms in the gas cloud display interference patterns which are strongly influenced by gravity. A brief investigation has concluded that a matter interferometer based on these condensates may permit the construction of gravity sensors orders of magnitude more sensitive than any prior technique.

Without the need for cryogenics it is possible to envisage a satellite-based gradiometer that could have a long lifetime. Such an instrument would permit Earth studies over a multi-year baseline.

This work specifically targets the design of an orbital (zero-g) instrument that might enable a future gravity sensing mission. The first objective is to analyze the potential performance of new, in-house, gravity gradiometer designs via computer simulations. Next is to identify the geophysical phenomena that would become observable with the increased sensitivity of these cold-atom interferometer designs. These studies will be used to seed new instrument/mission proposals.

Key technology elements needed to establish a starting point for Goddard research into these condensates are being identified. The goal of this effort is to investigate the design of spaceflight versions of the existing laboratory subsystem elements such as atomic vapor ovens, magneto-optical traps, and evanescent-wave atom mirrors.

Contact: David Skillman, David.R.Skillman@nasa.gov

Satellite Laser Ranging

NASA Satellite Laser Ranging (SLR) Network

Satellite Laser Ranging (SLR) is a fundamental measurement technique used by the NASA Space Geodesy Program to support both national and international programs in Earth dynamics, ocean and ice surface altimetry, navigation and positioning, and technology development. NASA built the five trailer-based Mobile Laser Ranging Stations (MOBLAS) that have remained in operation at fixed sites for over fifteen years. Two highly compact Transportable Laser Ranging Systems (TLRS), built by NASA, also remain in operations. The University of Hawaii and the University of Texas continue to operate the two high performing Observatory SLR systems at their respective Universities. The University of Texas system also has lunar ranging capability.

NASA has continued its successful partnerships with the Australian Surveying & Land Information Group (AUSLIG) in Yarragadee, Australia (MOBLAS-5); the South African National Research Foundation/Hartelbeesthoek Radio Astronomical Observatory (HRAO) in Hartelbeesthoek, South Africa (MOBLAS-6); and the University of French Polynesia/CNES in Tahiti, French Polynesia (MOBLAS-8). Under these partnerships, NASA continues to provide the SLR system, training, engineering support, and spare parts to maintain operations. The host country provides the site, local infrastructure, and the operating crew. NASA has begun discussing a partnership agreement with the Indian Space Research Organization (ISRO) located in Bangalore, India for the operations of TLRS-4.

The NASA SLR Network has been fully operational in the field for over twenty years. During this time, the Network has seen many modifications and upgrades to maintain system operations and more importantly, to increase data quantity and quality. Through a declining budget, NASA continues to ensure system operations and performance are maintained at the highest level. During the last two years, the MOBLAS, TLRS, MLRS (University of Texas SLR system), and HOLLAS (University of Hawaii SLR system) have received both hardware and software changes to maintain and enhance system operations. Upgrades were made to the timing subsystem, the receiver subsystem, the laser subsystem, the communications subsystem, the mount subsystem, and the processing software for the NASA SLR Network.

In summary, the NASA Network still consists of nine NASA operated, partner operated and University operated stations covering North America, the west coast of South America, the Pacific, South Africa, and Western Australia. The NASA SLR Network continues to provide over 40% of the total data volume in the International Laser Ranging Service (ILRS) as well as the most precise sub-cm accuracy ranging data.

Table 4. NASA Satellite Laser Ranging Network

Location	SLR System	Operating Agency
Monument Peak, California	MOBLAS-4	Mission Contractor (HTSI)
Greenbelt, Maryland	MOBLAS-7	Mission Contractor (HTSI)
Mount Haleakala, Maui, Hawaii	HOLLAS	University of Hawaii
Fort Davis, Texas	MLRS	University of Texas at Austin
Arequipa, Peru	TLRS-3	Universidad Nacional de San Agustin
Yarragadee, Australia	MOBLAS-5	Australian Surveying & Land Information Group
Hartebeesthoek, South Africa	MOBLAS-6	National Research Foundation
Tahiti, French Polynesia	MOBLAS-8	University of French Polynesia/CNES
Bangalore, India *	TLRS-4	Indian Space Research Organization (ISRO)

* Preliminary Discussions underway

Contact: David Carter, David.L.Carter@nasa.gov

International Laser Ranging Service

The ILRS was established in 1998 as an official service of the International Association for Geodesy (IAG). The ILRS collects, merges, analyzes, archives, and distributes Satellite Laser ranging (SLR) and Lunar Laser Ranging (LLR) observation data sets of sufficient accuracy to satisfy the objectives of a wide range of scientific, engineering, and operational applications and experimentation. The basic observable is the precise time-of-flight of an ultrashort laser pulse to and from a satellite, corrected for atmospheric delays. These data sets are used by the ILRS to generate a number of fundamental data products, including: centimeter accuracy satellite ephemerides, Earth orientation parameters, three-dimensional coordinates and velocities of the ILRS tracking stations, time-varying geocenter coordinates, static and time-varying coefficients of the Earth's gravity field, fundamental physical constants, lunar ephemerides and librations, and lunar orientation parameters. As such, the ILRS provides fundamental data to support the International Terrestrial Reference Frame (ITRF) and the International Earth Rotation Service (IERS). The ILRS consists of several operational elements: tracking stations, operational centers, analysis centers, data centers, and a central bureau.

ILRS Governing Board

The Governing Board is responsible for the general direction of the ILRS. It defines official ILRS policy and products, determines satellite tracking priorities, develops standards and procedures, and interacts with other services and organizations. There are sixteen members of the board; elections for the next two-year term of the ILRS Governing Board were held in mid-2002. Table 5 shows the current members of the board.

Table 5. ILRS Governing Board (as of October 2002)

Hermann Drewes	Ex-Officio, CSTG President	Germany
Michael Pearlman	Ex-Officio, Director ILRS Central Bureau	USA
Carey Noll	Ex-Officio, Secretary, ILRS Central Bureau	USA
Werner Gurtner	Appointed, EUROLAS, Governing Board Chairperson	Switzerland
Giuseppe Bianco	Appointed, EUROLAS	Italy
David Carter	Appointed, NASA	USA
Jan McGarry	Appointed, NASA	USA
Ben Greene	Appointed, WPLTN	Australia
Hiroo Kunimori	Appointed, WPLTN, Missions WG Coordinator	Japan
Bob Schutz	Appointed, IERS Representative to ILRS	USA
Graham Appleby	Elected, Analysis Representative	UK
Ron Noomen	Elected, Analysis Representative	The Netherlands
Wolfgang Seemueller	Elected, Data Centers Representative	Germany
Peter Shelus	Elected, Lunar Representative	USA
Georg Kirchner	Elected, At-Large Representative	Austria
Ulrich Schreiber	Elected, At-Large Representative	Germany

Working Groups

The ILRS has established five Working Groups to help formulate policy and provide technical expertise. The Missions Working Group routinely reviews current tracking priorities and campaigns, and develops recommendations on new requests for tracking support. During 2002, the Missions Working Group coordinated support for ADEOS-II (environmental monitoring), GRACE (gravity field studies), JASON (ocean surface topography), and ENVISAT (follow-on to ERS for climate research). In 2002, the Data Formats and Procedures Working Group reviewed the user requirements for SLR full-rate data and established procedures for transmitting and archiving these data as well as processing two-color laser ranging data. This working group continues to sponsor two study groups, one on determining necessary modifications to the current

satellite predictions format and a second on atmospheric refraction models used in SLR analysis. The Networks and Engineering Working Group completed work on gathering system information into consistent site-specific log files and compiled this information into a spreadsheet for ease of use by the analysis community. The Analysis Working Group held two workshops in 2002. These meetings focused on benchmarking and pilot projects designed to assess the current state of the SLR analysis community and eventually develop standard ILRS products such as daily X/Y pole and length-of-day values for the IERS. During 2002 the Signal Processing Ad Hoc Working Group continued to work on improved center-of-mass corrections and signal processing techniques for the many satellites currently tracked by SLR.

Tracking Network

In 2002, three stations were approved by the ILRS Governing Board for membership in the ILRS tracking network: the optical station located at the Naval Research Laboratory in Washington D.C., a system located at the Astronomical Observatory of Ivan Franko National University of Lviv, Ukraine, and the refurbished system at the Communications Research Laboratory in Koganei (near Tokyo), Japan. Furthermore, the TIGO (Transportable Integrated Geodetic Observatory) system became operational in Concepción, Chile in May 2002 and has become a key component of the continued effort to strengthen SLR coverage in the southern hemisphere. The addition of these stations expands the operational ILRS network to over forty systems as shown in Figure 32.

Figure 30. Current ILRS Network

Missions

During 2002, the ILRS provided operational tracking of over thirty targets, including passive geodetic (geodynamics) satellites, Earth remote sensing satellites, navigation satellites, engineering missions, and lunar reflectors. The Governing Board recently approved the tracking of two new missions, ICESat, in support of precise orbit determination (POD) for the altimeter and validation

of the GPS instrument, and the National Polar-orbiting Operational Environmental Satellite System (NPOESS), a 2013 mission, for POD. Four previously approved missions, ADEOS-II, GRACE, JASON, and ENVISAT were launched and successfully tracked by the ILRS network during 2002. Continued tracking of both ADEOS-II and ICESat will be coordinated with the sponsoring agencies because of optical sensitivity of on-board instruments. The METEOR-3M mission requested emergency satellite tracking by the ILRS network due to the failure of the on-board GLONASS receiver to provide sufficient POD for the SAGE-II instrument. The ILRS supported two intensive tracking campaigns in 2002: ETALON and Reflector; tracking priorities for these satellites were elevated in order to increase data yield. Analysts requested additional tracking of the two ETALON satellites in order to study Earth orientation and low order, low degree harmonics of the gravity field. The Reflector satellite was a novel approach to investigate satellite dynamics using a distributed array.

ILRS Central Bureau

The Central Bureau continued development of a new website for the ILRS which became operational in May 2002. In addition to a complete content review, this new website provides easier information retrieval through breadcrumbs and a navigation bar as well as an upgraded search engine. A bibliography of articles relevant to SLR was completed and installed in the website. Staff conducted a thorough review and implementation of site documentation for all stations in the ILRS network. The Central Bureau also coordinated the publication of the 2000 and 2001 editions of the ILRS Annual Report series. A revised brochure highlighting key areas of interest in the ILRS website was compiled and published in September 2002. The central bureau also arranged various meetings of the service and working groups at the April European Geophysical Society (EGS) assembly and the October laser ranging workshop.

Meetings

The ILRS was a co-sponsor, with NASA and the Smithsonian Center for Astrophysics, of the 13th International Workshop on Laser Ranging, held in Washington D.C. during the week of October 7, 2002. The workshop was a very successful venue for the exchange engineering and scientific information with the intent to improve the scientific product of laser ranging. Over 160 colleagues attended the five-day event which covered such topics as scientific achievements, station performance evaluation and operational issues, target design, timing devices, system calibration, atmospheric correction, detectors, technology development, automation and control systems, and advanced systems and techniques.

The 7th and 8th ILRS General Assembly meetings were held in April and October 2002, in conjunction with the EGS Spring Meeting in Nice, France and the 13th International Workshop on Laser Ranging in Washington D.C., respectively. Both meetings were well attended and allowed the ILRS to present current status and obtain feedback on operational issues from the international community. Meetings of the Governing Board and Working Groups were also held during these time periods.

Web site: http://ilrs.gsfc.nasa.gov

Contact: Carey Noll, Carey.E.Noll@nasa.gov

SLR2000 Autonomous Satellite Laser Ranging Station

Next generation NASA Satellite Laser Ranging (SLR) systems will be replications of the SLR2000 system currently under development at the Goddard Geophysical and Astronomical Observatory (GGAO) in Greenbelt, Maryland. The SLR2000 is a fully autonomous, eye-safe, sub-centimeter precision ranging instrument capable of tracking a wide range of cube corner equipped satellites up to 20,000 km altitude. Satellite range is determined by measuring round trip time-of-flight accurate to a few picoseconds, applying system calibration offsets and correcting for atmospheric refraction. Scientific applications include maintenance of terrestrial reference frames, precision orbit determination, geophysics, gravity studies, fundamental physics, and global time transfer. The SLR2000 is operated in an eye -safe fashion by reducing the single pulse energy to 135 mJ per pulse at the exit port while filling the whole 40 cm telescope with the transmit beam. The current NASA Mobile Laser Ranging Stations (MOBLAS) transmit an average power of about 500 mw in making 5 measurements per second. By comparison, the SLR2K has an average transmitted power of only 270 mw. While firing at a 2 KHz rate SLR2K will make 10 to 100 times more range measurements per second than a MOBLAS system. This is accomplished by the efficient use of receive photons in the range measurement in operating at the single photoelectron signal level.

SLR2K SYSTEM PARAMETERS

Laser:	**Diode pumped Nd:YAG**
Fire rate:	**2 KHz**
Pulse Energy:	**135 ujoules/pulse**
Beamwidth:	**10, 40 arcsec (exit port)**
Detector:	**Photek quadrant MCP PMT**
Gain:	**3.E6**
QE:	**13% @ 532 nm**
Active area:	**12 mm diameter**
Image size:	**6 mm**
Receiver:	**4 independent channels**
Field of view:	**10, 40 arcsec**
Discriminator:	**Phillips Scientific 708**
TIU:	**HTSI 1.5 ps Event Timer**
Risley prisms:	**0-30 arcsec point ahead**
T/R Switch:	**Polarization (passive)**
Telescope:	**OSC 40 cm off-axis**
Pointing system:	**Xybion Ax/El gimbal**
Tracking error:	**~ arcsec RMS both axes**
Command rate:	**50 Hertz**

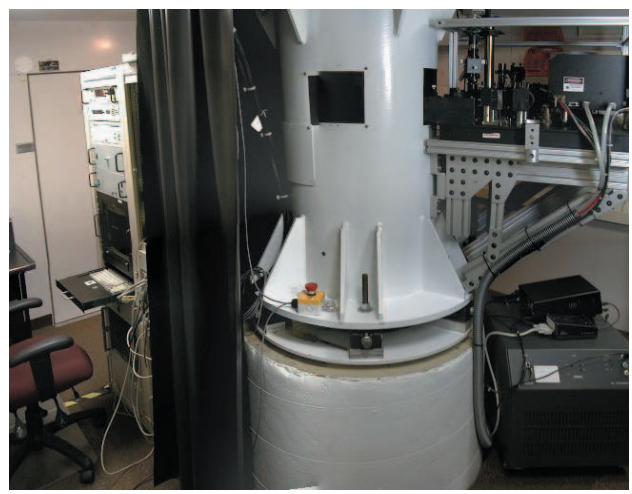

Figure 31. SLR2000 system specifications (left) and photo of the shelter interior (right).

Progress on the SLR2000 project has been held up the past year with two major problems identified and corrected in the 40-cm off-axis telescope. Image quality expected to be better than 2 arcseconds was typically only 18 to 20 arcseconds. This was found to be caused by a shift in the position of the primary mirror in its holding cell. The second problem involved an internal fold mirror of the telescope with insufficient angular adjustment. Both problems have been corrected and work continues on system check out and verification. The laser transceiver table has been installed and optical alignments for both gimbal and telescope are being conducted. Visual star calibrations will begin in early CY03 with visual satellite tracks and laser tracking by the end of CY03.

Contact: Tom Zagwodzki, Thomas.W.Zagwodzki@nasa.gov

Calibration

EOS Calibration

The Earth Observing System (EOS) is a decadal, international multi-satellite program in global remote sensing of the Earth. As such, EOS is and will continue to be the fundamental source of satellite data on the earth and its environment into the 21st century. The overall goal of the EOS mission is to advance the scientific understanding of the entire earth system and its changes on a global scale through the development of a deeper understanding of the components of that system and their interactions. In order to achieve those goals, EOS has and will continue to produce global, long-time series, remote-sensing data sets from multiple instruments on several satellite platforms. The correct interpretation of scientific information from these data sets requires the ability to discriminate between on-orbit changes in the instruments and changes in the earth physical processes being monitored. The ability to make this distinction depends crucially on the calibration of the instruments with respect to a set of recognized physical standards or processes, the careful characterization of the instruments' performance at the subsystem and system levels, the cross-calibration of the instruments, and the post-launch validation of the instruments fundamental radiance and reflectance products.

Code 920.1 provides technical and administrative support to the EOS Project Science Office in the calibration of satellite, airborne, and ground-based instruments. This includes coordinating and participating in satellite instrument reviews, participating in algorithm theoretical basis document (ATBD) reviews, coordinating and participating in measurement assurance programs (MAPS) with the assistance of the National Institute of Science and Technology (NIST), and providing over-arching technical guidance in the EOS lunar photometry project underway at the United State Geological Survey in Flagstaff, Arizona.

Instrument Reviews and Workshops

In 2002, the EOS Calibration program, operating within Code 920.1, participated in and/or coordinated a number EOS instrument and mission-level reviews and workshops. These reviews included the following:

•Solar Radiation and Climate Experiment (SORCE) Instrument Pre-ship Review; Laboratory for Atmospheric and Space Physics; University of Colorado; Boulder, Colorado; February 21-22, 2002.

•High Resolution Dynamics Limb Sounder (HIRDLS) Calibration Working Group Meeting; Oxford University; Oxford, United Kingdom; July 10-11, 2002.

•Solar Radiation and Climate Experiment (SORCE) Observatory Pre-ship Review; Orbital Sciences Corporation; Dulles, Virginia; October 21, 2002.

•Multi-angle Imaging SpectroRadiometer (MISR) Calibration Review; Jet Propulsion Laboratory; Pasadena, California; October 22, 2002.

•Workshop on Satellite Instrument Calibration for Measuring Global Climate Change; University of Maryland; College Park, Maryland; November 12-14, 2002.

Aperture Round-robin and Instrument Measurement Comparison in Support of the Measurement of Total Solar Irradiance

The concept for an aperture area comparison involving representatives from the solar irradiance

measurement community was formulated at the May 2000 Calibration Workshop for the Total Irradiance Monitor (TIM) held at the University of Colorado's Laboratory for Atmospheric and Space Physics (LASP). In 2002, the comparison was initiated and is being coordinated by the National Institute of Standards and Technology (NIST) Optical Technology Division and the EOS Project Science Office at NASA Goddard. The NIST Optical Technology Division has expertise in the metrology of aperture area as applied to radiometry. The goals of the comparison are to provide an independent determination of the area of circular apertures that have heritage with solar irradiance determinations, thus providing a measurement of the reproducibility, and to use this information to evaluate discrepancies in determinations of the solar constant. Participants in the aperture area comparison include the World Meteorological Organization (WMO), the Royal Meteorological Institute of Belgium, the Jet Propulsion Laboratory (JPL), and the Laboratory for Atmospheric and Space Physics (LASP) University of Colorado.

The EOS Calibration program has coordinated discussions on measurement comparisons between the TIM and the Active Cavity Radiometer Irradiance Monitor (ACRIM). The TIM was launched on January 25, 2003 on EOS SORCE. ACRIM instruments have provided a 20 year data record of total solar irradiance measurements. Currently, the ACRIM III instrument launched on December 20, 1999 on EOS ACRIMSAT and the VIRGO suite on SOHO are providing total solar irradiance data. Both the TIM and ACRIM instrument teams agreed that the first and primary comparison of TIM to ACRIM and other TSI-measuring instruments will be on-orbit in mid 2003. The participants also agreed that if those on-orbit comparisons between TIM and ACRIM do not agree to within the ACRIM measurement uncertainty of 0.2%, then ground-based and shuttle-based comparison of the instruments will be warranted. Those comparisons would be coordinated by the EOS Calibration program.

Robotic Lunar Observatory Calibration

The Robotic Lunar Observatory (ROLO) funded by the EOS Project Science Office and located at USGS in Flagstaff, Arizona, has developed a spectral irradiance model of the Moon while accounting for the effects of lunar libration, phase, and spacecraft location. This lunar irradiance model can be used as an effective on-orbit reference to compare current calibrations of orbiting satellite instruments. In an effort to establish an absolute radiometric scale to the ROLO lunar observations, NASA's Code 920.1, NIST, and the University of Arizona have teamed with USGS to fully characterize the ROLO telescope/detector systems. This effort began in early 2002 and will culminate in mid 2003 by using a NIST calibrated collimated source to measure the ROLO small angle scatter and system level radiance response.

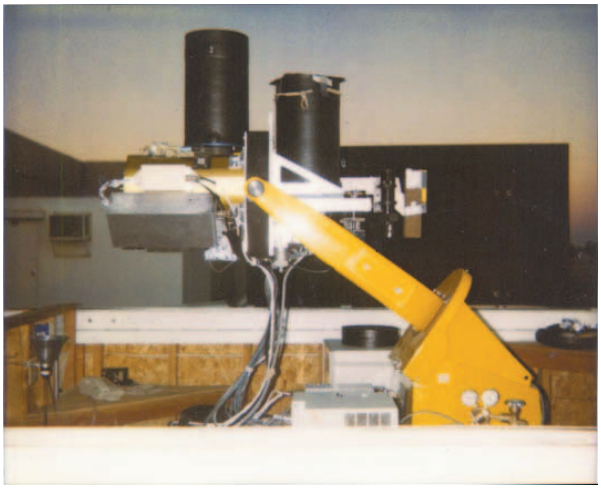

Figure 32. The ROLO visible/near infrared and shortwave infrared telescopes located at USGS in Flagstaff, Arizona.

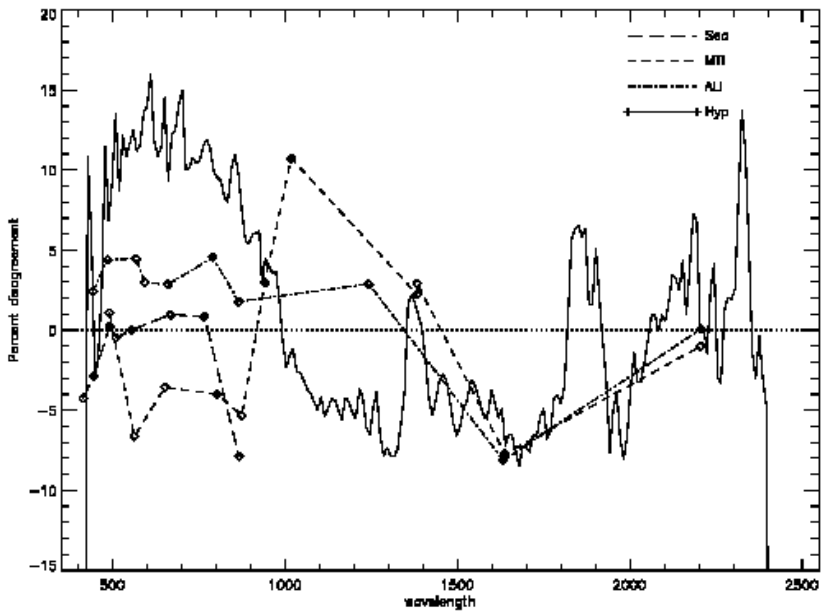

Figure 33. The lunar irradiance model produced by the ROLO project enables the on-orbit calibrations of remote sensing instruments to be compared. The lines on this plot represent the % deviation of the calibration of the Sea-viewing Wide Field-of-view Sensor (SeaWiFS), Multispectral Thermal Imager (MTI), Adavanced Land Imager (ALI), and Hyperion instruments from the ROLO model.

Contact: Jim Butler, James.J.Butler@nasa.gov

Diffuser Calibration Facility (DCaF)

The Diffuser Calibration Facility (DCaF) has operated within Code 920 since May 1993. The facility is a class 10,000 cleanroom containing a unique, state-of-the-art, out-of-plane optical scatterometer. This scatterometer is capable of measuring the bi-directional scatter distribution function (BSDF is a term which includes bi-directional reflective and transmissive distribution function measurements (i.e. BRDF and BTDF)) of transmissive or reflective, specular or diffuse optical elements and surfaces in addition to granular, powdered, or liquid samples. The facility is considered a secondary standards calibration facility with measurements directly traceable to the Spectral Trifunction Automated Reflection Radiometer (STARR) located at the National Institute of Standards and Technology (NIST) in Gaithersburg, Maryland. BSDF measurements are made at any incident and scatter angle above or below a sample. The scatterometer employs incoherent and coherent monochromatic light sources. The incoherent source is a xenon arc lamp and 0.25 m Czerny-Turner monochromator. The current operating wavelength range of this source is 230 to 900 nm with an adjustable bandwidth between 4 and 10 nm. The coherent sources include He/Ne lasers at 543.5, 594.1, 612.0, and 632.8 nm and a He/Cd laser at 325.4 nm. The scatterometer is capable of polarized or unpolarized measurements using all sources. The sample stage can support samples up to 12 inches on a side and weight up to 10 lbs. Samples can also be rastered for reflectance or tranmittance uniformity. Scatterometer receivers include uv-sensitive and visible silicon photodiodes and photomultiplier tubes. The data acquisition electronics include programmable preamps matched to each detector and a programmable dual channel lock-in amplifier. The scatterometer is completely automated and data is displayed in real time. In year 2002, the facility commissioned an 8 degree directional/hemispherical reflectance measurement capability for diffuse reflective samples. This measurement complements and validates the alternative approach of integrating BRDF over the complete scattering hemisphere of a sample to determine hemispherical scatter.

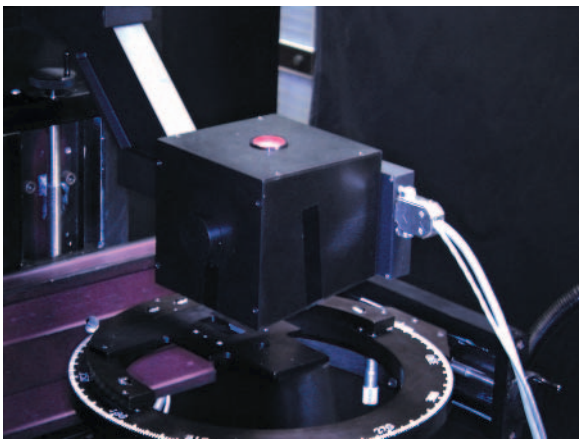

The measurement uncertainty of DCaF BSDF measurements is 0.7% (k=1), and agreement between absolute BSDF measurements made by the DCaF and by NIST on identical samples is 1% or better over the complete wavelength and angular operating ranges of the scatterometer. The measurement uncertainty of DCaF 8 degree directional/hemispherical measurements is 0.2% (k=1) over the complete operating wavelength range.

Figure 34. Integrating sphere/detector attachment to the scatterometer permits the direct measurement of 8 degree directional hemispherical scatter from optical surfaces.

In calendar year 2002, the facility installed an imaging microscope for sample inspection, and commissioned a materials solar exposure capability designed to mimic the on-orbit degradation of optical surfaces.

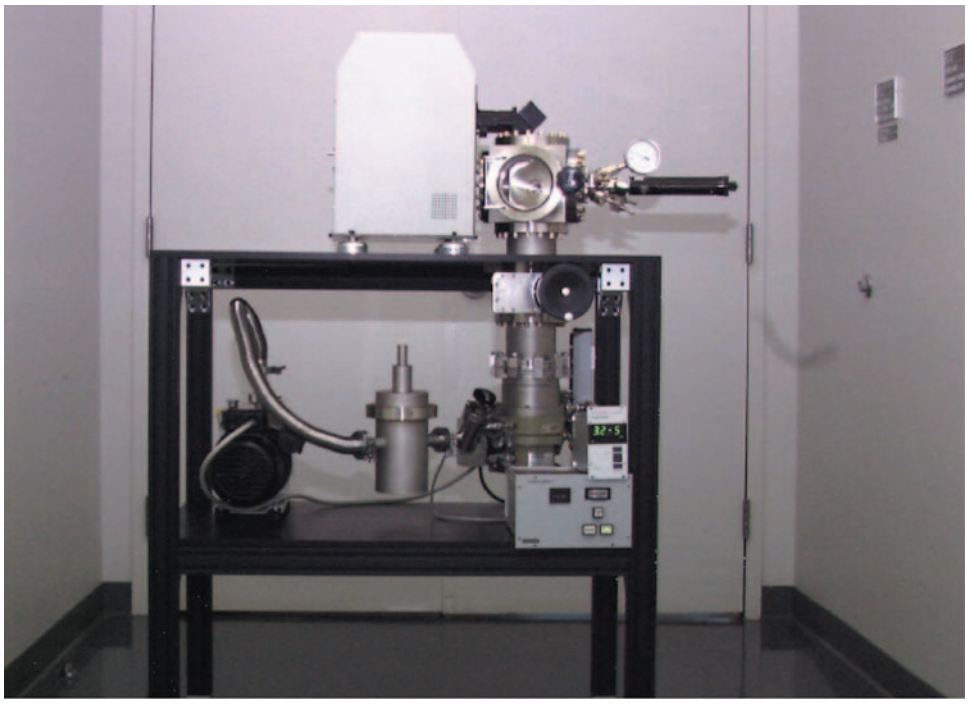

Figure 35. The Diffuser Calibration Facilities materials testing capability enables the controlled exposure of optical components to solar and contamination environments experienced on-orbit. Pre- to post-exposure changes in the optical properties of the components are measured on the facility scatterometer.

Since 1993, the DCaF has literally made tens of thousands of scatter measurements for flight and non-flight projects from both the government and private sectors. In calendar year 2002, the

DCaF provided scatter measurements to the following flight and non-flight projects in accordance with established flight and deployment schedules.

NASA SIMBIOS Calibrations:

In April and June of 2002, NASA's Sensor Intercomparison and Merger for Biological and Interdisciplinary Oceanic Studies (SIMBIOS) project became a new customer of the DCaF. In support of this project, the DCaF made BRDF measurements of three Spectralon diffusers used in the calibration of ocean color validation instruments. These measurements were made at 5 wavelengths between 400 and 900nm, at normal incidence, and over scatter angles of 42 to 48 degrees. One of the three samples was raster scanned to determine its BRDF uniformity.

Stereo COR-1 and COR-2 Calibrations:

The COR-1 project in the Solar Physics Branch was a repeat customer of the DCaF in 2002. The DCaF successfully measured the BTDF of 10 opal glass samples at normal illumination using a He/Ne laser at 632.8 nm and over a range of in- and out-of-plane scatter angles. The COR-1 project used these DCaF results in the evaluation of candidate opal glass diffusers for on-orbit flat-fielding of the COR-1 detector array. In addition to the opal glass samples, the DCaF used the He/Ne laser source to measure the BTDF of two neutral density filters for the COR-1 project.

The related COR-2 project was a new DCaF customer in 2002. The DCaF measured specular scatter from a highly polished aluminum mirror and glass sample. These measurements were made using the facility He/Ne laser at 632.8 nm and the monochromator-based source at 632.8 nm and 700 nm. The samples were illuminated normally and scatter was measured over a ±80 degree angular range. These results were used in evaluating the ability of aluminum mirrors and glass to act as heat rejection optics in the COR-2 instrument.

NASA Stennis Tarp Calibrations:

The DCaF made an extensive series of BSDF measurements for NASA's Stennis Commerical Remote Sensing Program Office on 4 tarp samples used in the vicarious calibration of commercial satellite sensors. The samples were measured at 485, 550, 633 (i.e. laser and monochromatic sources), and 800 nm over a large range of incident and scatter elevation and azimuthal angles. The effect of tarp weave orientation with respect to incident illumination and reflected scatter was quantified. The 8 degree directional hemispherical reflectance of the tarps was also measured at the aforementioned 4 wavelengths.

Mars Regolith Simulant BRDF Measurements:

In an effort to illustrate the versatility of the DCaF scatterometer, a granular sample of Mars Regolith Simulant from Johnson Space Center (JSC). The JSC MARS-1 sample is the < 1 mm diameter fraction of weathered volcanic ash from Pu'u Nene, a cinder cone on the island of Hawaii, which has been repeatedly cited as a close spectral analog to the bright Mars regions. This sample was measured from 250 to 900 nm over a range of incident and scatter angles from 0 to ±60 degrees. The sample reflectance was measured up to ±10 degrees out-of-plane and its 8 degree directional/hemispherical reflectance was quantified over the 250 to 900 nm wavlength range.

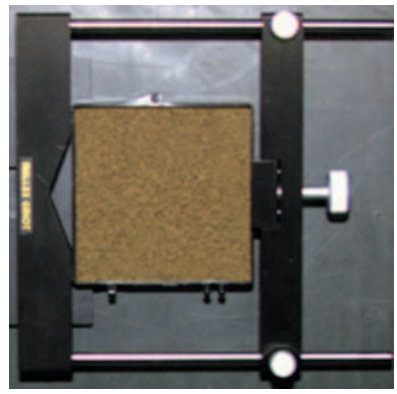

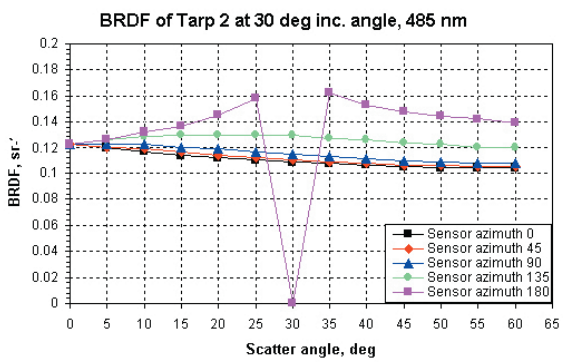

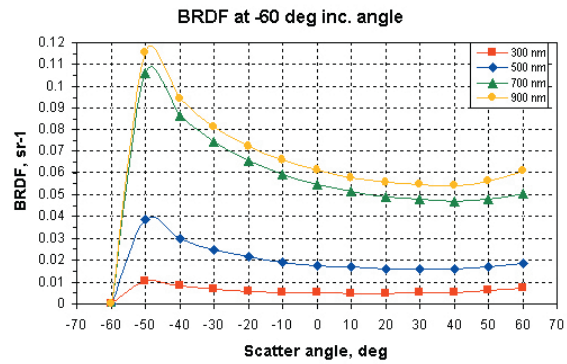

Figure 3. NASA's Stennis tarp (left) and NASA's JSC Mars simulated regolith sample 1 (right) images and BRDF results. The optical scatter from these un-conventional, different sample types is easily measured by the DCaF scatterometer.

Future Work:

In 2003, a scatterometer measurement capability from 1.0 micron to 2.5 microns using laser and monochromatic sources will be commissioned. In addition, work on improving the near-specular measurement of mirrors, designing and implementing an innovative, high precision, non-invasive sample alignment method, and designing and adding a controlled contaminant introduction system to the materials exposure capability will continue.

Contact: Jim Butler, James.J.Butler@nasa.gov

Calibration Facility

Figure 39, a photograph of "Hardy" together with its power supply and data collection console, is the largest (1.8 m diameter) and most intense of our sources. A ring of tungsten halogen lamps inside the source, behind the wire harness visible in Figure 34, is driven by a set of DC power supplies, with the current stabilized to better than ± 0.01%. This level of stabilization is necessary to reduce the corresponding changes in spectral radiance at the most sensitive wavelength (400 nm) to less than ± 0.1%. Barium sulfate paint, containing a small amount of polyvinyl alcohol as a binder, coats the interior surfaces of the source. This material is highly reflecting at wavelengths below 1μm, resulting in a large number of diffuse reflections for those photons emitted from the lamp filaments that successfully exit through the source aperture. Consequently, spectral radiance uniformity across the 25 cm diameter exit aperture is better than ± 0.2% for wave-

lengths below 1 μm, and is almost as uniform at higher wavelengths.

Sources are calibrated approximately every month relative to a NIST standard irradiance lamp. This procedure is necessary to offset slow degradation in radiance output caused by aging of the lamps within the source and the barium sulfate paint (usually a few percent per annum). With the wealth of supporting information collected on temperature, humidity, lamp voltages and lamp usage times, etc., we hope to build a predictive ability for identifying lamps and other components in the early stages of failure and to forecast changes in spectral radiance.

The Calibration Facility maintains several sources, each intended for a particular range of activities. Our 1.2 m diameter hemisphere source ("Laurel") is particularly useful when large diameter exit apertures are required, or when laboratory space is limited. Laurel has been used, for example, to assess the uniformity of response of the EPIC camera system on the Triana spacecraft. This work, completed in 2000, required an unusually large source diameter of over 45 cm. Another popular source, identified as "Slick", uses internal plates of polytetrafluoroethylene (PTFE) to scatter light emitted by the lamp filaments. PTFE is preferable to barium sulfate in that it contains negligible amounts of water and it has a higher reflectivity beyond a wavelength of 1μm. Occasionally the sources themselves travel to sites around the world. In recent years Calibration Facility staff and equipment have advanced NASA field programs in Portugal, Brazil, Japan and Canada, as well as many American states.

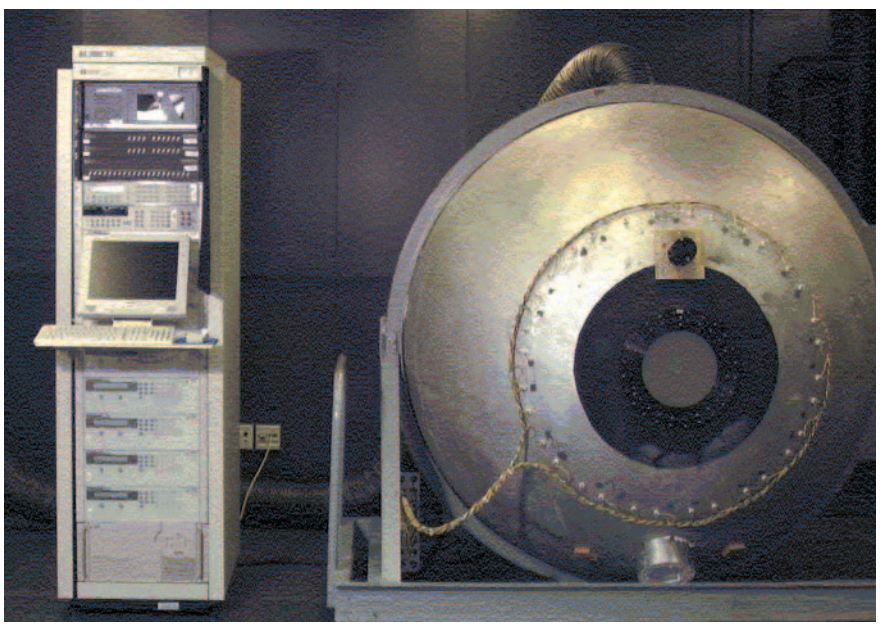

Figure 39. "Hardy", a calibration source.

The Calibration Facility usually houses its radiance sources in class M 5.5 clean rooms, implying that the density of airborne particles with a diameter of 0.5μm or greater is less than $10^{5.5}$, or 353,000 per cubic meter. The clean room air within the sources is further controlled in temperature and humidity.

The Calibration Facility's primary source calibration instrument is an Optronic Laboratory model 746 monochromator with an integrating sphere irradiance collector (746/ISIC). The 746/ISIC is calibrated in irradiance response prior to each measurement using a 1000 W quartz-halogen standard irradiance lamp that is traceable to NIST irradiance standards, and in wavelength using conventional line source lamps and lasers. Using silicon photodiode and lead sulfide detectors, the 746/ISIC transfers the irradiance calibration from the standard lamp to the sphere source being

measured. Knowledge of the aperture areas of the sphere under test and the ISIC collection sphere coupled with a measurement of the distance between the two apertures enables the radiance of the sphere source to be calculated. In the visible/near infrared wavelength region from 400 nm to 1000 nm, the 746/ISIC obtains data in 10 nm steps with a bandwidth of 10 nm. In the short-wave infrared wavelength region from 1000 nm to 1600 nm, data is obtained every 20 nm with a bandwidth of 20 nm. In the wavelength region from 1600 nm to 2500 nm, data is obtained every 20 nm with a bandwidth of 40 nm.

Although the primary customers of the Calibration Facility directly support the EOS Project, anyone interested in using the Calibration Facility is encouraged to contact our group. Provided the proposed work advances NASA's interests, we will be delighted to provide calibration services on a time-available basis and negotiable cost. Our website address is www.spectral.gsfc.nasa.gov, which we share with the Diffuser Calibration Facility. Further details, including source spectral radiance uncertainty estimates, were contained in the annual report for 2001.

Achievements in 2002:

The Environmental Control System (ECS) was installed and successfully tested in March 2002. The ECS dries and cools the air within "Hardy", shortening the warm-up time of the source and increasing the stability of spectral radiance within water vapor bands. The Temperature and Humidity Monitoring System (THMS) was also completed in March. Temperature and humidity data from critical points within the source system are now routinely recorded into the data system whenever the lamps inside the source are illuminated.

A paper describing monitoring and stability results was presented at SPIE's 9th International Symposium on Remote Sensing, Crete, Greece.

In May 2002 the electronics and software for the rebuilt Calibration Transfer System (CTS 750) was completed, and work began on characterizing it and comparing its performance with the operational system (known as the CTS 746 system).

Code 900 used the Calibration Facility during the year to calibrate a large number of Cimel sun photometers returned to GSFC for calibration from AERONET sites around the world. GSFC radiometers such as the Cloud Absorption Radiometer (CAR), Sensor Integration and Modeling for Biological Agent Detection (SIMBAD) radiometers from the SIMBIOS program, and several spectrometer systems and sources associated with the Landsat and MODIS projects were either calibrated or had their calibration compared with independent standards during the year, and calibration work associated with the second SIMBIOS Radiometric Intercomparison (SIMRIC-2) was performed.

The MErcury Surface, Space ENvironment, GEochemistry and Ranging mission (MESSENGER) includes the Mercury Laser Altimeter (MLA). MLA's out-of-field stray light was measured in the Calibration Facility in September, and found to be within 20% of the theoretical worst-case value.

Spectrometers from NASA's Langley Research Center and the University of Maryland were calibrated during the year, and several sources were calibrated at NASA's Ames Research Center (ARC) at the request of ARC. NASA's Wallops Flight Facility requested and received calibration support for one of their sources.

Contact: Peter Abel, Peter.Abel-1@nasa.gov

Refereed Journal Publications:

Degnan, J.J., ”A conceptual design for a spaceborne 3D imaging lidar”, J. e&i Elektrotechnik und Informationstechnik, Vol. 4, pp. 99-106, 2002.

Degnan, J.J., “Photon-counting multikilohertz microlaser altimeters for airborne and spaceborne topographic measurements”, J. Geodynamics, Special Issue on Laser Altimetry, Vol. 34, pp.503-549, 2002.

Degnan, J.J., “Asynchronous laser transponders for precise interplanetary ranging and time transfer”, J. Geodynamics, Special Issue on Laser Altimetry, Vol. 34, pp. 551-594, 2002.

Drake, J. B., R. Dubayah, D. B. Clark, R. G. Knox, **J. B. Blair**, M. A. Hofton, R. L. Chazdon, R. L. Weishampel, and S. Prince, Estimation of tropical forest structural characteristics using large-footprint lidar, Remote Sensing of Environment, 79: 305-319, 2002.

Drake, J. B., R. Dubayah, R. Knox, D. B. Clark, and **J. B. Blair**, Sensitivity of large-footprint lidar to canopy structure and biomass in a neotropical rainforest, Remote Sensing of Environment, 81:378-392, 2002.

Hofton, M. A. and **J. B. Blair**, Laser altimeter return pulse correlation: A method for detecting surface topographic change, Journal of Geodynamics, 34:477-489, 2002.

Hofton, M. A., **L. E. Rocchio, J. B. Blair** and R. Dubayah, Validation of vegetation canopy lidar sub-canopy topography measurements, Journal of Geodynamics, 34:491-502, 2002.

Mallama A.J. and **J.J. Degnan**, “A thermal infrared cloud mapper for observatories”, Publications of the Astronomical Society of the Pacific”, Vol. 114, pp.913-917, 2002

Zwally, H.J., B. Schutz, W. Abdalati, **J. Abshire**, C. Bentley, A. Brenner, **J. Bufton**, J. Dezio, D. Hancock, **D. Harding**, T. Herring, B. Minster, K. Quinn, S. Palm, J. Spinhirne, R. Thomas, “ ICESat’s laser mreasurements of polar ice, atmosphere, ocean and land,” Journal of Geodynamics, Vol 34, 405-445, 2002.

Proceedings Papers, NASA Technical Reports, etc.

Abshire, J.B., X. Sun, **E.A. Ketchum, P.S. Millar, H. Riris**, “Geoscience Laser Altimeter System (GLAS) for the ICESat Mission, “ IEEE IGARSS-02 conference, paper xx, Toronto Canada, June 24-28, 2002.

Andrews, A. E., "CO_2 Measurements from Space: Possibilities and Possible Pitfalls," Carbon Data Assimilation Workshop, National Center for Atmospheric Research, Boulder, CO 20-31 May 2002.

Andrews, A. E., J. F. Burris, **J. B. Abshire**, M. A. Krainak, **H. Riris, X. Sun**, **G. J. Collatz**, "A Ground-Based Profiling Differential Absorption LIDAR System for Measuring CO2 in the Planetary Boundary Layer" Carbon Cycle Science: The North American Carbon Program" special session of the Fall 2002 Meeting of the American Geophysical Union, San Francisco, California, 6-10 December 2002.

Butler, J.J., P.Y. Barnes, E.A. Early, C. van Eijk-Olij, A.E. Zoutman, S. van Buller-Leeuwen, and J.G. Schaarsberg, "Comparison of Ultraviolet Bidirectional Reflectance Distribution Function (BRDF) Measurements of Diffusers Used in the Calibration of the Total Ozone Mapping Spectrometer (TOMS)", Proceedings of the 9th International Symposium on Remote Sensing, Agia Pelagia, Crete, 2002..

Carter, D., "System Upgrades of the NASA SLR Network", Proceedings of the 13th International Workshop on Laser Ranging, October 7-11,2002, Washington, D.C.

Georgiev, G. and **J.J. Butler**, "Bidirectional Reflectance Distribution Function and Hemispherical Reflectance of JSC Mars-1," SPIE Proceedings on Surface Scattering and Diffraction for Advanced Metrology II, Seattle, Washington, 2002.

Degnan, J.J., "SLR2000: Progress and Future Applications", Proceedings of the 13th International Workshop on Laser Ranging, October 7-11,2002, Washington, D.C.

Degnan, J.J.,"Optimization of the Correlation Range Receiver Parameters in SLR2000", Proceedings of the 13th International Workshop on Laser Ranging, October 7-11,2002, Washington, D.C.

Mallama, A., **J. J. Degnan**, F. E.Cross, J. M. Mackenzie, "Infrared Sky Camera -- The Production Mode", Proceedings of the 13th International Workshop on Laser Ranging, October 7-11,2002, Washington, D.C.

McGarry, J., T. Zagwodzki, J.J. Degnan, "SLR2000 Closed Loop Tracking with a Photon-Counting Quadrant Detector", Proceedings of the 13th International Workshop on Laser Ranging, October 7-11, 2002, Washington, D.C.

McGarry, J., J. Cheek, A. Mallama, R. Ricklefs, A. Mann, M. Perry, J. Horvath, R. Barski, "SLR2000 Software: Current Test Results and Recent Developments", Proceedings of the 13th International Workshop on Laser Ranging, October 7- 11, 2002, Washington, D.C.

Meister G, **P. Abel**, R. Barnes, J. Cooper, C. Davis, M. Godin, D. Goebel, G. Fargion, R. Frouin, D. Korwan, R. Maffione, C.McClain, S.McLean, D. Menzies, A. Poteau, J.Robertson, J. Sherman, "The first SIMBIOS Radiometric Intercomparison (SIMRIC-1), April - September 2001", NASA/TM-2002-210006, March 2002.

Marketon J., **Peter Abel, James J. Butler**, Gilbert R. Smith, John W. Cooper, "Integrating sphere source monitoring and stability data", SPIE 9th International Symposium on Remote Sensing, Crete, Greece, 2002.

Patterson, D., **J. McGarry**, "Overview of Data for the SLR2000 Tracking Mount", Proceedings of the 13th International Workshop on Laser Ranging, October 7-11,2002, Washington, D.C.

Sun, X. and **J.B. Abshire**, "Performance of a breadboard lidar receiver at 1570nm for remotely sensing atmospheric CO2 concentrations," *Conference on Laser and Electro-Optics (CLEO),* May 20-24, 2002, Long Beach, CA, Paper CFF3.

Education/Public Outreach

The Laboratory for Terrestrial Physics' Education and Public Outreach Program supports exploration and discoveries of Earth and Planetary Science through a wide-ranging outreach program to the general public. The Program is a comprehensive resource for research conducted by the Laboratory and promotes scientific literacy and awareness of Earth and Planetary Science. The Laboratory's Program aligns with NASA's education objectives to enhance educator knowledge and preparation, develop supplementary curricula, forge new education partnerships and support all levels of students. Several of the Laboratory's premier Educational and Public Outreach projects came to fruition in 2002, including:

- GLOBE (Global Learning and Observation to Benefit the Environment)
- Baltimore Student Sun Photometer Network (BSSN)
- IMAGERS (Interactive Multimedia Adventures for Grade School Education Using Remote Sensing)
- Earth as Art
- Earth as History
- MOLA: Models of Earth and Mars Topography for Classroom Use
- Classroom Activity Development
- Website Development

The Global Learning and Observation to Benefit the Environment Program (GLOBE)

Scientists in the Biospheric Sciences Branch worked throughout 2002 with the GLOBE program. Their work included the development of student protocols, outreach activities, and the use of GLOBE student data for Earth Science research. The GLOBE Program is a worldwide network of K-12 students, teachers, and scientists working together to study and understand the global environment (http://www.globe.gov). GLOBE is a cooperative effort, led in the United States by a Federal interagency program supported by NASA, NSF, EPA and the U.S. State Department, in partnership with colleges and universities, state and local school systems, and non-government organizations. Internationally, GLOBE is a partnership between the United States and 100 other countries. Over one million primary and secondary students in more than 12,000 schools and more than 20,000 GLOBE-trained teachers have taken part in the program as of December 2002, and those numbers continue to grow!

GLOBE students make observations and measurements that have been developed by research scientists on the soils, hydrology, land cover, phenology, and atmosphere at or near their schools. The GLOBE Protocols have students characterizing the soils at their site by horizon, and provide data on soil color, structure, texture, consistence, roots, rocks, carbonates, pH, particle size distribution, fertility, and bulk density. In addition, students collect soil temperature and soil water measurements. In the Atmosphere Protocol, students collect data daily on cloud type and cover, precipitation, precipitation pH, and current, maximum and minimum air temperature. For Land Cover, a Modified UNESCO (MUC) land cover classification is obtained as well as qualitative and quantitative biometric measurements (tree height and circumference, grass biomass, canopy

cover, and ground cover). The Phenology Protocol directs the students to observe the timing of bud burst and other growth milestones of local vegetation. In the Hydrology Protocol, students make weekly measurements of transparency, water temperature, dissolved oxygen, pH, electrical conductivity, salinity, alkalinity, and nitrate at a local water body.

Upon joining the GLOBE program, each school receives a 15 km by 15 km Landsat sub-image of their particular area. Using the Land Cover Protocol, students classify the imagery according to vegetation type and characteristics for "ground truth" purposes. Using GPS receivers, students determine the latitude and longitude and collect other metadata about their study sites. Students then report their data through the internet to the GLOBE data archive, and scientists use these data in their research.

As part of the GLOBE project, Dr. Elissa Levine developed the student protocols and learning activities for soil characterization that are part of the GLOBE soil investigation. These are available as part of the Teacher's Guide on the GLOBE web page (www.globe.gov). Dr. Levine and her team within the Biospheric Sciences Branch have also developed educational materials and web resources. They perform training sessions and other outreach functions for the educational community, and use the GLOBE student data for their Earth Science research. In one study, GLOBE student data for soil, atmosphere, land cover, and GPS are being used to parameterize and validate a biophysical Earth system simulation model (GAPS). GAPS (General Purpose Simulation Model of the Atmosphere-Plant-Soil System) is a menu-driven model that simulates soil, plant, and atmospheric processes (e.g. evapotranspiration, soil water flow, plant water uptake) using a choice of algorithms and robust graphical display of output. As an example, soil characterization data, as well as land cover, climate, and GPS data collected by GLOBE students from Reynolds High School, Greenville, Pennsylvania, USA, were used to parameterize GAPS. The model simulated daily soil moisture content by horizon at the Reynolds site for 1997 through 2000. The students' soil moisture data were then used to validate model simulations. In the validation exercise, the optimal simulation scenario for GLOBE data was chosen based on the best fit of the GLOBE data to model results. Results of this study demonstrate that GLOBE student data could provide an important source of input and validation information for simulation models such as GAPS and improve our understanding of the Earth system (Figure 1). Similar simulations are being performed using data from other GLOBE schools in different biomes.

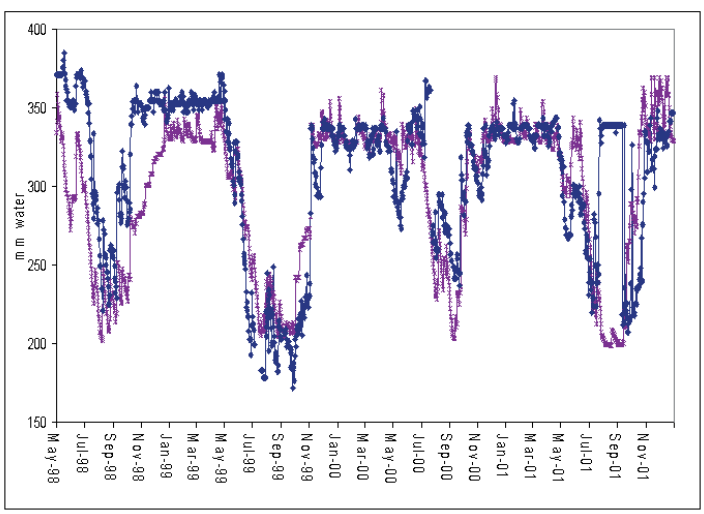

Figure 1. Comparison of the simulated and actual soil moisture content in the root zone (90 cm) (Reynolds HS, Greenville, PA, USA)

In another research project, Dr. Levine and her team compared recent GLOBE soil and water pH data with the same data collected by USEPA in the early 1980's as part of the Direct Delayed Response Program (DDRP) to determine trends in soil and water pH over the last 2 decades. This research proj-

ect focused on the DDRP data collected from the Woods Lake watershed in the Adirondack region of New York State and the Northville Central GLOBE School in Northville, New York.

Dr. Levine, Dr. Dan Kimes, and the GLOBE Soil Team also continue to investigate the relationship between soil color and other soil and ecosystem properties using GLOBE student data worldwide. In order to find the most robust model for this comparison, complex modeling techniques such as neural networks are being used. Results from this project will help scientists to better understand concepts related to soil development as well as how to use soil color as an indicator of other soil and environmental conditions (e.g. carbon content, fertility, water content, etc.).

Detailed papers describing these research projects are on the GLOBE web site (www.globe.gov).

Contact: Dr. Elissa Levine, Elissa.Levine@nasa.gov

Baltimore Student Sun Photometer Network (BSSN)

The "Baltimore Student Sun Photometer Network" (BSSN) is an education project, related to Dr. Elissa Levine's Baltimore Asthma studies. It is funded through a grant from the Director's Discretionary Fund (DDF) at Goddard Space Flight Center. The BSSN project provides students in 20 schools throughout the Baltimore City area with hand-held sun photometers and breath peak-flow meters. These students are making daily measurements of atmospheric aerosols and cloud cover in order to relate the presence of particulates (which have been strongly correlated with asthma) to lung function on a real time basis. In addition, the student measurements will provide the first local scale characterization of particulates which will be used to validate the measurements of the Aeronet Sun photometer (located on top of the Maryland Science Center in Baltimore and part of an International network of instruments measuring particulates in the atmosphere). Results are submitted daily by students via the internet where they are stored, and can be viewed at the project website (http://bssn.gsfc.nasa.gov). Learning materials and other information are also available for students and teachers use at this website. Information from this unique project will also be fed in to our data base to increase our understanding of pediatric asthma in the Baltimore region and help improve predictive capabilities.

Contact: Dr. Elissa Levine, Elissa.Levine@nasa.gov

The IMAGERS (Interactive Multimedia Adventures for Grade School Education Using Remote Sensing) Program

Also coming to fruition in 2002, the IMAGERS Program is NASA's comprehensive Earth science education resource for the introduction of remote sensing and satellite imagery to children in grades K-8. The Program is comprised of two multimedia web sites: "The Adventures of Amelia the Pigeon" and "The Adventures of Echo the Bat". The objective of IMAGERS is to captivate children at an early age in Earth science through multimedia adventures.

"Echo the Bat" and "Amelia the Pigeon" have two major components: (1) an interactive web site with a multimedia adventure game; and (2) an activity guide with lesson plans and reproducible hands-on activities. The interactive web sites engage children, while the supplemental materials enable educators to introduce the concepts through hands-on activities in the classroom. Applying this methodology, parents and teachers are able to teach Earth science using remote sensing imagery via identification of land use, exploration of featured habitats, and changes in the environment.

"The Adventures of Echo the Bat", originally developed in 1998, was the inaugural project of the IMAGERS Program. The web site follows Echo as he migrates through various habitats in Arizona and teaches students to understand about light and the electromagnetic spectrum as a foundation for remote sensing. The Adventure offers a directed and investigative approach to how land features look from space, what the colors mean in a satellite image, and how to identify habitats using false color. These fundamental concepts behind remote sensing science are reinforced in the classroom with a teacher's guide for grades 5-8.

Following the success of the web site, an Echo the Bat picture book was released in 2001. The book tells the story of Echo's adventure in Arizona to children grades K-4, through the introduction of the five basic concepts of understanding satellite imagery: perspective, shape, pattern, color, and texture. The book also contains an activity guide, which reinforces these concepts with hands-on activities for the classroom.

The IMAGERS project saw major expansion in 2002 with the completion of the Echo the Bat expansion to Arizona State Parks, and the launch of the Amelia the Pigeon website and teacher's guide. These two milestones, outlined below, played a crucial role in expanding the IMAGERS program to a national audience.

In the summer of 2002, Echo the Bat project was expanded again and introduced to a broader audience through an informal education project with Arizona State Parks. Located in three different geographic regions of Arizona, each location features an interactive information display, accompanied by an activity sheet. The general public (adults and children) visiting these locations are introduced to the local habitat through satellite imagery. Each of these locations have trained education specialists who interact daily with visitors and school groups and introduce the benefits of studying the environment from space.

"The Adventures of Amelia the Pigeon" was launched in the fall of 2002. The Amelia Project is the second interactive IMAGERS web site with multimedia components to engage the K-4 audience and illustrate Earth science concepts. The Pigeon Adventure presents science concepts through metaphors and analogies that relate to inner-city life. The use of a pigeon as the vehicle for the web site provides a metaphor familiar to inner-city children, and Amelia is utilized to introduce the concept of perspective. Through aerial photography created by Pigeon cameras, the web site focuses on the benefits of a bird's eye view. Throughout the interactive adventure portion of the web site, aerial and satellite imagery are used to demonstrate the advances of remote sensing through the century. Amelia the Pigeon presents new insights into habitats as she explores the urban environment of New York City.

Figure 2. Scenes from The Adventures of Amelia the Pigeon. The water color artwork, at left, was done by Jean Masetti.

To learn more about these exciting projects and the IMAGERS Program at NASA, visit the IMAGERS web site: http://www.imagers.gsfc.nasa.gov/

Contact: Ginger Butcher, ginger@ltpmail.gsfc.nasa.gov

Earth as Art

To gain wider recognition of the public value of the Landsat Program, administered jointly by USGS and NASA, the Satellite Systems Branch at the USGS EROS Data Center created an exhibit of 41 framed Landsat images that were selected on the basis of their aesthetic appeal. These images use the visceral avenue of art to convey the thrilling perspective on the Earth that Landsat provides. With vivid colors woven into amazing natural patterns, the images connect the public audience to science and technology in basic, almost instinctive ways that differ from other kinds of Education and Public Outreach (EPO) programs.

The initial public response to these images at the local level was so positive and immediate, the decision was made in 2002 to collaborate on extending their influence to a national scale. USGS staff from the Land Remote Sensing Program and EPO specialists from NASA Goddard Space Flight Center met on March 22, 2002 to discuss possibilities for collaborating on a pilot EPO program for the exhibit. From this meeting, the USGS/NASA team developed the pilot program entitled Landsat: Earth as Art.

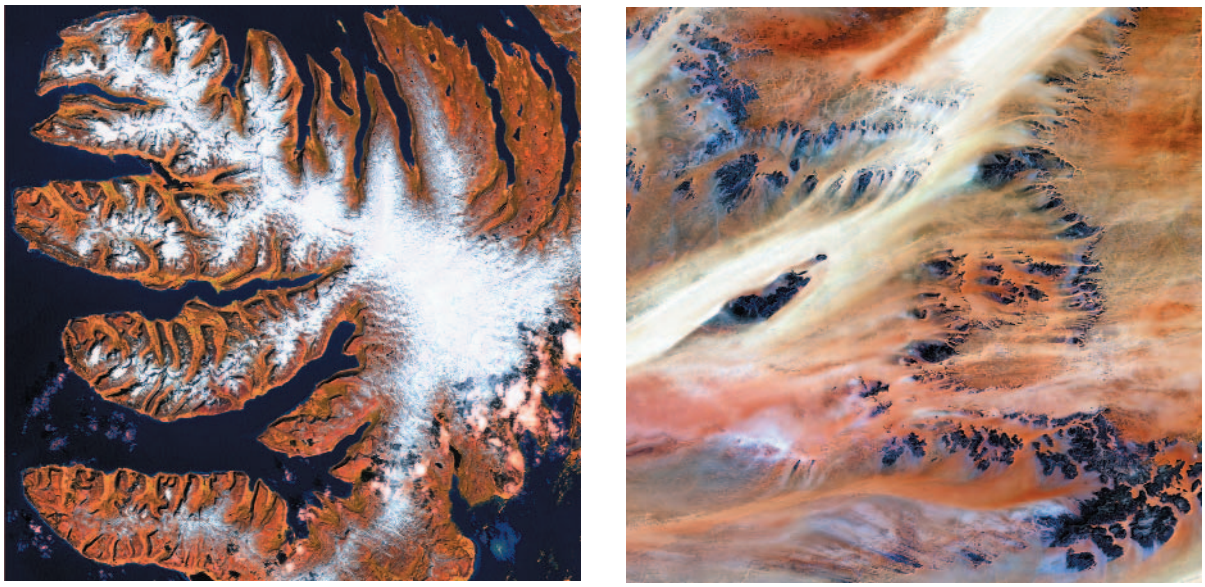

Figure 3. Two Landsat Earth as Art images. (Left) The West Fjords in Iceland. (Right) The Terkezi Oasis in Chad, Africa.

The USGS/NASA EPO team launched Landsat: Earth as Art with a display of a complete set of 41 images in two locations (Library of Congress, and a Science Center in South Dakota affiliated with USGS). A third set of the 41 images were also displayed on a rotational basis at the NASA Headquarters and the NASA Goddard Space Flight Visitors Center. By piloting the images as exhibits in a small number of places, the USGS/NASA team enabled the collection of varied feedback that will allow a decision to be made on expansion of the Earth as Art Program to a national level. The objectives of the Earth as Art pilot exhibits were:

- to increase public appreciation of the USGS/NASA Landsat Program

• to increase the public's general level of knowledge and understanding of viewing Earth from the perspective of space

• to increase public awareness of remote sensing technology

• to introduce teachers and students to the Landsat Program

The pilots also established contacts for development of possible partnerships in future expanded efforts. Currently planned for 2003 are four additional exhibit locations in different regions of the country (Salt Lake City, Utah; Albequerque, New Mexico; Roanoke, Virginia; Lincoln, Nebraska).

Figure 4. The Landsat 7- Earth as Art exhibit at: (left) NASA Headquarters and (right) the Library of Congress.

In conjunction with the pilot exhibits launched in 2002, the Earth as Art web site was developed and placed online. Proving to be a rapid international success, the Earth as Art web site has reached millions of students, teachers, and people of all ages worldwide. From the international success of this new web site, an exhibit was launched in Tel Aviv, Israel in late 2002. To learn more about this exciting program and to view Earth as Art images, visit the Earth as Art website: http://landsat.gsfc.nasa.gov/earthasart/

Contact: MK Richardson, mkrichardson@ltpmail.gsfc.nasa.gov

Earth as History

On the heels of the success of the Earth as Art Program, the concept for a new program known as Earth as History was developed in 2002. A collaborative project in which major federal agencies will publicize the value of maps, aerial photography, and satellite imagery for the study of history, the Earth as History Program is still in the development stages. The intended audience of this program is the general public, educators, and students of all ages.

Historical research and the study of history can both benefit when satellite imagery, aerial photography, and maps serve as source material. While many scholars, students, and teachers understand the value of historical maps, in general they tend to appreciate aerial photography and satellite imagery less as tools in historical research.

While it is true that aerial photography and satellite imagery are relative newcomers compared to traditional maps, both forms of earth observation have recorded the world during a very pivotal time in history…the twentieth century. Aerial photography has been a viable technology with a well-defined scientific foundation since approximately 1920. Satellite imagery became a major tool in 1972 with the launch of ERTS, the first of today's Landsat platforms.

To commence the Earth as History Program, an educational World Wide Web site and exhibits will be launched in 2003. The goal of the program (both via the web site and exhibits) will be to illustrate the ways in which the three geographic technologies illuminate historical studies.

Initially, the theme of urbanization and forces that shape cities will take the audience on journeys of exploration through historical maps, aerial photographs, and satellite images. In its first phase, the project will feature the growth of four American urban areas: New York, St. Louis, Las Vegas, and Honolulu. The cities of Rome, Cairo, Lima, and Tokyo will be utilized to represent international urbanization.

Earth as History web sites and exhibits will include reproductions of maps, aerial photographs, and satellite images. Short narrative texts, captions, and diagrammatic maps will support the images and place each in context. This interpretive material will contribute basic themes about forces that shape urban change.

Earth as History funding will be sought in the future to:

(1) develop lesson plans, activities, and curriculum support that will help educators incorporate the material from the web sites and exhibits into classroom activities;

(2) create multiple copies of the exhibits, which can travel to schools, libraries, museums, and other educational and cultural institutions.

Contact: Jeannie Allen, allen@ventus.gsfc.nasa.gov

MOLA: Models of Earth and Mars Topography for Classroom Use

"Exploring Planetary Topography in the Classroom Using 3-Dimensional Models" is the title of a Director's Discretionary Fund proposal won by John Keller of Code 691 and four Code s921 co-investigators in 2002. Susan Sakimoto, Stephanie Stockman, Jim Roark and Herb Frey provided expertise in Earth and Mars geology, use of MOLA and Earth-based topographic data, and educational outreach using planetary analogs. Keller generated a number of example models for display at both the DDF presentation and at the Fall Geological Society of America (GSA) meeting. Figure 6 shows one such set of models, for the volcano comparison between Olympus Mons (Mars) and the Hawaiian Islands on the Earth, as shown in Figure 5. The vertical exaggeration is the same for both models, in this case, 7x the horizontal scale. The huge volume of Olympus Mons is greater than the volume of the Hawaiian Islands combined.

The DDF proposal is to develop teacher kits and lesson plans around comparative features on the two planets. These will include volcanoes, rift canyons, large river systems, polar caps, and other structures which permit discussion of the measurement and use of topographic data in understanding geologic processes, and how those processes can be similar or different on different planets. The models and lesson plans will be tested out in classrooms by teachers in Sakimoto's course "Teaching the Solar System" in the Spring of 2003 at Johns Hopkins University.

Keller is an expert in the production of plastic models of spacecraft parts and planetary surface features. The same plastic extrusion device obtained to support mission development work can

be used to make 3-dimensional models of volcanoes, river valleys, impact craters and other features - provided a really good topography data set exists. MOLA (Mars Orbiting Laser Altimeter) has provided such data for Mars and comparable data exists for many parts of the Earth. So it is possible to make high accuracy topographic maps of surface features of interest. Figure 5 shows such views for the large Valles Marineris rift canyons of Mars compared to the East African Rift Valleys on Earth, and the largest volcano on Mars compared with the Hawaiian Islands. But flat views, even in perspective, do not fully convey the volumetric aspects of such objects. This is where models, like those of volcanoes at the right, can be useful.

The models were displayed at the Fall meeting of the Geological Society of America Meeting (GSA) by the Planetary Geology Division, of which Sakimoto is president. At the GSA, a visually impaired undergraduate took advantage of the models (below). The models were displayed at the Geological Society of America meeting in Denver, CO. Being 3-dimensional and solid allows exploration of the topography by touch for those who cannot see.

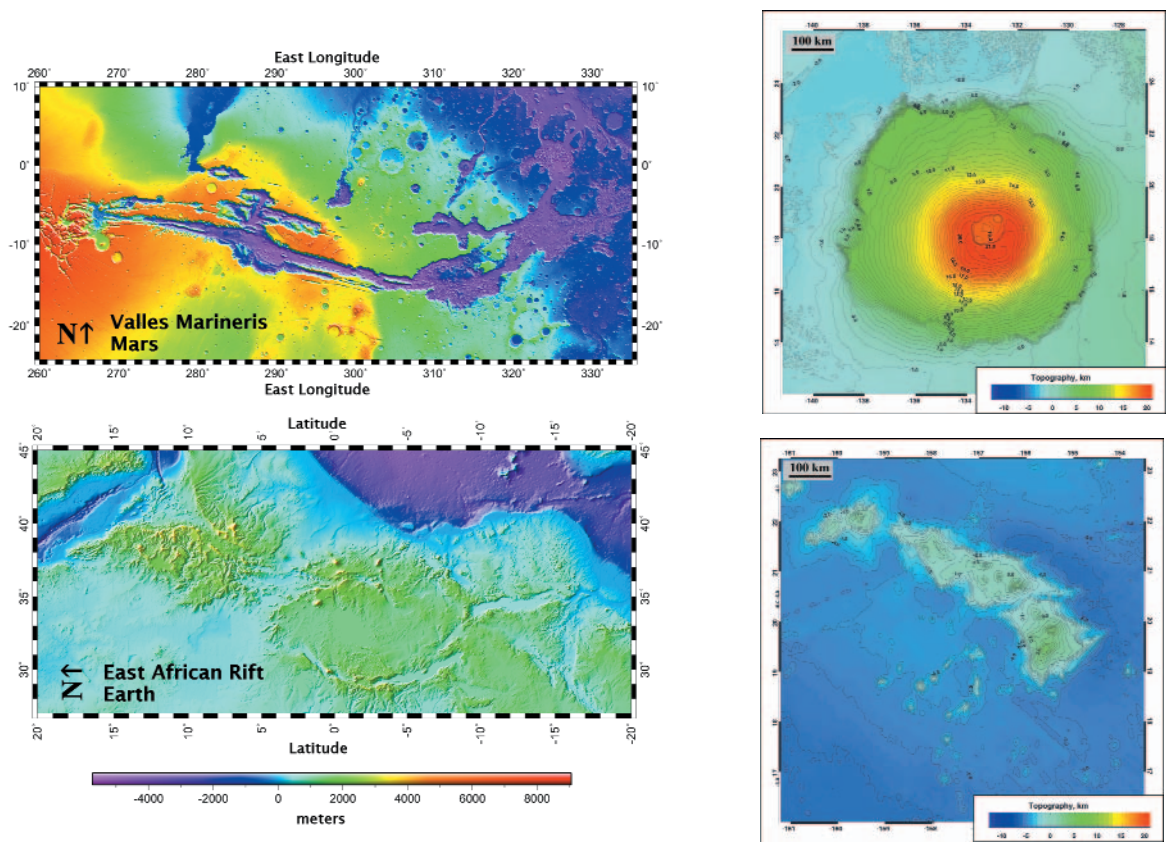

Figure 5. Topographic renditions of the Valles Marineris rift canyons on Mars (upper left) compared to the East African Rift Valley systems on Earth (lower left) at the same spatial scale and with the same topographic scale. The martian canyons are much, much deeper. On the right are compared the largest volcano on Mars, Olympus Mons (upper right), with the Hawaiian Islands on Earth (lower right).

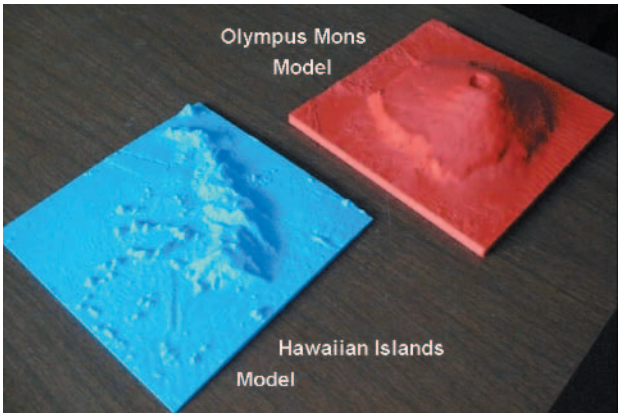

Figure 6. Models of volcanoes on Earth (Hawaiian Islands in blue, lower left) and on Mars (Olympus Mons, in red, upper right). The models have the same spatial scale and the same vertical exaggerations (here, 7x horizontal). Each is about 8 inches on a side.

Contact: Herbert Frey, Herbert.V.Frey@nasa.gov

Classroom Activity Development

In conjunction with several of the EPO Program projects highlighted above, classroom activities were developed in 2002 to further expand the educational value of programs where appropriate. Specifically, the following classroom activities were developed and are due to be launched in 2003:

• *Bumpy, Wrinkled, Smooth: How Our Earth Looks from Space*. A supplemental activity to the Echo the Bat Web site, this activity can be used in both formal and informal education mediums for grades K-4.

• *Number to Pictures: How Satellite Images are Created*. A supplemental activity to the Echo the Bat Web site, which can be used in both formal and informal education mediums for grades 5-8.

• *Global Tectonic Activity Map litho*, highlights a new global plate tectonic map from Dr. Paul Lowman's research with a classroom activity.

• *Finding Impact Craters with Landsat.* This classroom activity is a demonstration for grades 5-8 on the understanding of the role of impact events in shaping the Earth. Students write a series of guidance questions for a field expedition to determine whether or not a given landform is an impact crater.

• *An Introduction to Remote Sensing and Landsat,* covering fundamental ideas about remote sensing and its applications; where remote sensing fits in the curriculum; investigations that students can carry out with remote sensing; how Landsat's multispectral instrument works; and how teachers can use Landsat in the classroom. Currently available as a PowerPoint presentation on http://landsat.gsfc.nasa.gov

For more information on Landsat's classroom activities please contact: Stephanie Stockman, stockman@core.gsfc.nasa.gov

Website Development

Expanded greatly in 2002, the Laboratory for Terrestrial Physics' web site continues to grow today. A "one-stop" resource for all the Lab's activities, this web site has continued to prove to be a key element in the EPO Program. The crucial role of the Lab's web site in the success of EPO Programs such as Landsat: Earth as Art cannot be overstated. As educational and outreach programs continue to expand, the further development of the web site will continue to allow EPO Programs and products to reach a global audience. In 2003, look for an updated and streamlined web site of resource materials, articles on recent scientific research, more classroom activities, and the utilization of established public and private sector web sites to promote the Lab's achievements. Visit our sites listed below to learn more:

Laboratory for Terrestrial Physics (LTP) Main Page: http://ltpwww.gsfc.nasa.gov/

LTP Education and Public Outreach (EPO) Main Page: http://ltp-education.gsfc.nasa.gov/

Contact: Maggie Masetti, mmasetti@ltpmail.gsfc.nasa.gov

Other Projects

Additionally, the following EPO projects currently under development commenced in 2002:

• New Laboratory for Terrestrial Physics Brochure: A new Laboratory brochure for public outreach is being developed to highlight current projects, past achievements, and resources available.

• Documentary: Currently under production, this documentary highlights the developmental stages of the MESSENGER Mission. Ongoing project that will continue until launch date in March 2004

• GLAS and MOLA Websites: New websites are under development that incorporate and present the Lab's research to a general public audience. These sights are being developed for user friendly navigation for resource and educational information. These web sites will be available in the Spring of 2003: http://glas.gsfc.nasa.gov and http://mola.gsfc.nasa.gov.

For more information on the Laboratory's EPO Program please contact: MK Richardson, mkrichardson@ltpmail.gsfc.nasa.gov

Acknowledgements

The Laboratory for Terrestrial Physics would like to recognize its members for their hard work and accomplishments. This report is proof of the outstanding work they do.

We'd like to thank the Goddard, national, and international communities for their contributions and collaborations with us. We'd like to especially recognize the Massachusetts Institute of Technology (MIT), Scripps Institute of Oceanography, the University of Maryland (UMD) College Park and Baltimore campuses, and the Earth Resources Observation Systems (EROS) Data Center (EDC) for their collaborative efforts.

We would like to thank all who took time from their busy schedules to contribute to this report, especially the Branch Heads and their teams. Special thanks to Charlie Schnetzler for organizing the publications and for sharp eyes while editing. Our thanks go out to the Branch and Office secretaries and administrators.

Thanks go to Maggie Masetti who organized, complied, formatted, edited, and did the layout of the report. Thanks to MK Richardson whose editorial expertise and hard work helped the text of the report to flow smoothly.

Appendix 1 - Acronyms

AERONET	Aerosol Robotic Network
ALI	Advanced Land Imager
APD	Avalanche photodiode
AVHRR	Advanced Very High Resolution Radiometer
BARC	Beltsville Agricultural Research Center
BioSAR	Biological Synthetic Aperture Radar
BKG	Bundesamt fuer Kartographie und Geodaesie
BSDF	Bi-directional Scatter Distribution Function
BRDF	Bi-directional Reflectance Distribution Function
CCD	Charged Coupled Device
CCRS	Canadian Center for Remote Sensing
CDDIS	Crustal Dynamics Data Information System
CF	Calibration Facility
CIESIN	Center for International Earth Science and Information Network
CHAMP	CHAllenging Mini-Satellite Payload
CMB	Core-Mantle Boundary
DAAC	Distributed Active Archive Center
DCaF	Diffuser Calibration Facility
DFB	Distributed FeedBack
DLR	Deutsche Zentram Fur Luftund Raumfahrt
DMSP/OLS	Defense Meteorological Satellite Programs Operation Linescan System
DORIS	Doppler Orbitography and Radiopositioning Integrated by Satellite
DSN	Deep Space Network
EDC	EROS Data Center
ENVISAT	ENVIronmental SATellite
EO-1	Earth Observing One (satellite)
EOS	Earth Observing System
EPSCoR	Experimental Program to Stimulate Competitive Research
EROS	Earth Resources Observing System
ERS	European Remote Sensing Satellite
ESA	European Space Agency
ESE	Earth Science Enterprise
ESSP	Earth System Science Pathfinder
ETM +	Enhanced Thematic Mapper Plus
FAME	Full-sky Astrometric Mapping Explorer
FWHM	Full Width Half Maximum
GFO	GEOSAT Follow-On
GGFC	Goddard Geophysical Fluids Center
GIMMS	Global Inventory Mapping and Monitoring Studies
GIS	Geographic Information System
GLAS	Geoscience Laser Altimeter System
GLONASS	Global'naya Navigatsionnay Sputnikovaya Sistema (Global Navigation Satellite System)
GOFC/GOLD	Global Observation of Forest and Land Cover Dynamics
GPS	Global Positioning System
GRACE	Gravity Recovery And Climate Experiment
GSFC	Goddard Space Flight Center
HSI	HyperSpectral Imager
IAG	International Association of Geodesy
IDS	International DORIS Service
IEEE	Institute of Electric & Electronics Engineers
IERS	International Earth Rotation Service

IGS	International GPS Service
ILRS	International Laser Ranging Service
INDOEX	Indian Ocean Experiment
IVS	International VLBI Service for Geodesy and Astrometry
JIVE	Joint Institute for VLBI in Europe
KTP	Potassium (K) Titanate (Ti) Phosphate (P)
KVN	Korean VLBI Network
LAI	Leaf Area Index
LBA	Large-Scale Biosphere-Atmosphere Experiment in Amazonia
LCLUC	Land-Cover Land-Use Change
LDCM	Landsat Data Continuity Mission
LDOPE	Land Data Operational Product Evaluation
LEO	Low Earth Orbiter
LLR	Lunar Laser Ranging
LTP	Laboratory for Terrestrial Physics
MBLA	Multi Beam Laser Altimeter
MCST	MODIS Characterization Support Team
MFF	Medusae Fossae Formation
MGS	Mars Global Surveyor
MISR	Multi-angle Imaging SpectroRadiometer
MLA	Mercury Laser Altimeter
MLL	Mixed Layer Lidar
MOBLAS	Mobile Laser Ranging Stations
MOC	Mars Orbiter Camera
MODAPS	MODIS Adaptive Processing System
MODIS	Moderate Resolution Imaging Spectroradiometer
MOPITT	Measurements Of Pollution In The Troposphere
MOSST	MOdular, Scalable, Self-consistent, Three-dimensional
MPIR	Max Planck Institute for Radioastronomy
NCEP	National Center for Environmental Predictions
NDVI	Normalized Difference Vegetation Index
NEIGE	NetLander Ionospheric and Geodesic Experiment
NOAA	National Oceanic and Atmospheric Administration
NPOESS	National Polar-orbiting Operational Environmental Satellite System
NPP	NPOESS Preparatory Project
NRAO	National Radio Astronomy Observatory
NRL	Naval Research Laboratory
NTIA	National Telecommunications and Information Administration
OMI	Ozone Measuring Instrument
ORNL	Oak Ridge National Lab
POD	Precision Orbit Determination
PRIDE	Puerto Rico Dust Experiment
RAID	Redundant Array of Inexpensive Disk
RASL	Raman Airborne Spectroscopic Lidar
RVF	Rift Valley Fever
SAFARI	Southern Africa Regional Science Initiative
SAVE	Southern Africa Validation of EOS (SAVE
SAR	Synetic Aperture Radar
SeaWifs	Sea-viewing Wide Field-of-view Sensor
SDP	Scientific Data Purchase
SLA	Shuttle Laser Altimeter
SLR	Satellite Laser Ranging
STARSHINE	Student Tracked Atmospheric Research Satellite for Heuristic International Networking Experiment

STRI	Smithsonian Tropical Research Institute
TEC	Total Electron Content
TOPEX	Ocean TOPography EXperiment
TOMS	Total Ozone Mapping Spectrometer
TRF	Terrestrial Reference Frame
USDA	United States Department of Agriculture
UNFAO	United Nations Food and Agriculture Organization
USGCRP	U.S. Global Change Research Program
USNO	United States Naval Observatory
USUHS	Uniformed Services University of the Health Sciences
VCL	Vegetation Canopy Lidar
VHF	Very High Frequency
VLBI	Very Long Baseline Interferometry

Appendix 2 - Grants, Contracts, Co-operative Agreements

The Laboratory for Terrestrial Physics has many efforts that involve sources of information, areas of study, and co-operations housed within, and external to, the physical confines of the Laboratory.

Grants are generally established with colleges and universities. The Laboratory has established grants or contracts totaling nearly $36M with 54 institutions of higher education, involving nearly 200 students and professors. Among those institutions involved are:

University of Alabama
University of Alaska
University of Arizona
Auburn University
Boston University
Bowie State University
Brown University
University of California
California Institute of Technology
University of California, Berkeley
University of California, Irvine
University of California, Los Angeles
University of California, San Diego
University of California, Santa Barbara
Calvin College
University of Colorado
Columbia University
Cornell University
University of South Florida
Florida State University
University of Hawaii
Harvard University
University of Indiana
Johns Hopkins University
Louisiana State University

University of Maryland, Baltimore Campus
University of Maryland, College Park
University of Massachusetts
Massachusetts Institute of Technology
University of Miami
University of Michigan
Michigan State University
University of Missouri
University of Montana
University of Nevada, Reno
University of New Hampshire
State University of New York
University of North Carolina
Northwestern University
Oregon State University
Pennsylvania State University
University of Pittsburgh
Rochester Institute of Technology
South Dakota State University
Stanford University
University of Texas
University of Utah
University of Virginia
University of Washington
Central Washington University
University of Wisconsin

The Laboratory is responsible for grants with 3 commercial industries:

G. O. Logic
Analytical Imaging and Geophysics LLC
AER, inc.

The Laboratory holds cooperative agreements with 11 institutions, with over 30 people involved:

U.S. Department of Agriculture
UNSA (Peruvian Space Agrncy)
Desert Research Institute
Environmental Protection Agency
U.S. Geological Survey
Marine Biological Laboratory
National Center for Atmospheric Research
National Oceanic and Atmospheric Administration
Scripps Institute of Oceanography
Smithsonian Institution
Woods Hole Oceanographic Institute

Additionally, performance-based contracts are held with a number of commercial service providers. Among these are: General Sciences Corp., Global Science and Technology, Honeywell Technology Solutions, NVI, Raytheon, Science Systems and Applications, Inc., and Sigma Research.

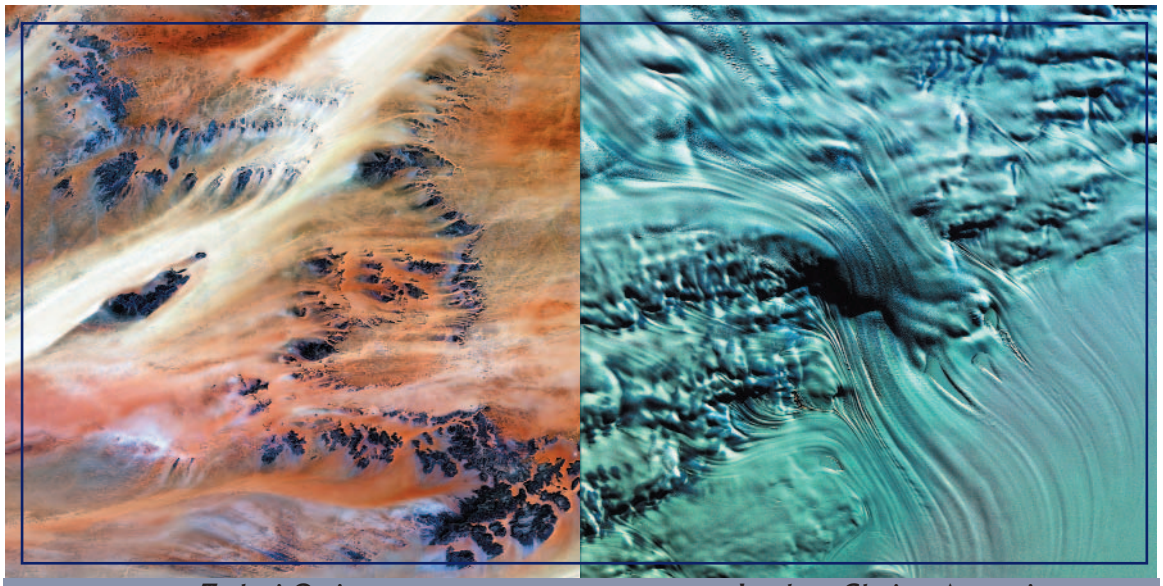

Terkezi Oasis

Lambert Glacier, Antarctica

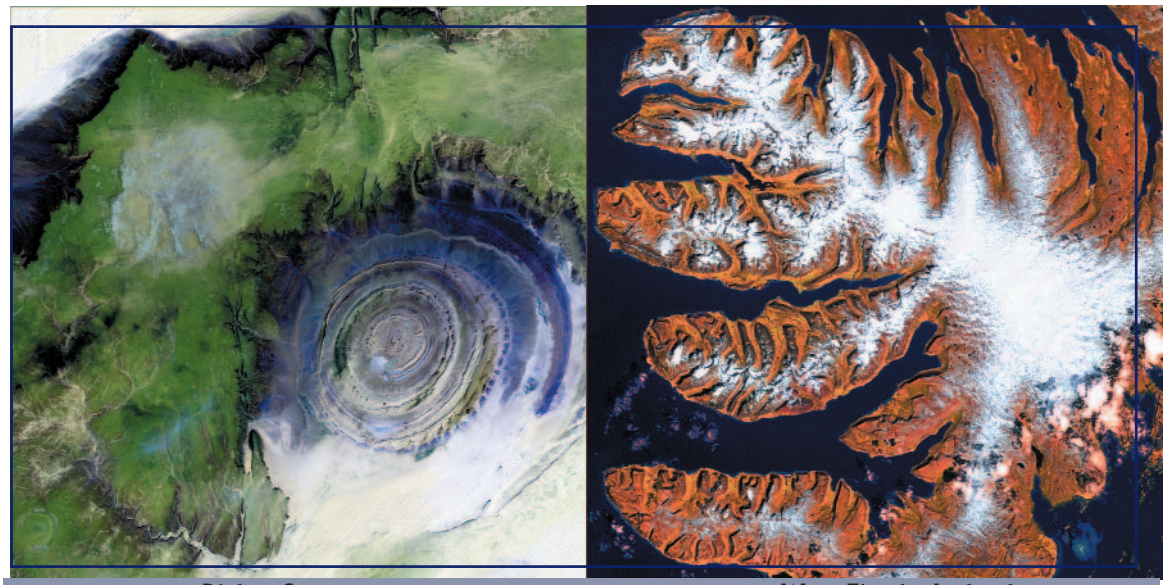

Richat Structure

West Fjords, Iceland

NP-2003-5-550-GSFC